INSTITUTE FOR FUSION STUDIES

DOE/ET-53088-528 IFSR #528-Review

Percolation, Statistical Topography, and Transport in Random Media

M.B. Isichenko
Institute for Fusion Studies
The University of Texas at Austin
Austin, Texas 78712

December 1991

THE UNIVERSITY OF TEXAS

AUSTIN

PERCOLATION, STATISTICAL TOPOGRAPHY, AND TRANSPORT IN RANDOM MEDIA *

M.B. Isichenko
Institute for Fusion Studies
The University of Texas at Austin
Austin, Texas 78712

Abstract

A review of classical percolation theory is given, with an emphasis on novel applications to statistical topography and turbulent diffusion. Statistical topography involves the geometrical properties of the iso-sets (contour lines or surfaces) of a random potential $\psi(\mathbf{x})$. For rapidly decaying correlations of ψ, the iso-potentias fall into the same universality class as the perimeters of percolation clusters. The topography of long-range correlated potentials involves many length scales and is associated either with the correlated-percolation problem or with Mandelbrot's fractional Brownian reliefs. In all cases, the concept of fractal dimension is particularly fruitful in characterizing the geometry of random fields. The physical applications of statistical topography include diffusion in random velocity fields, heat and particle transport in turbulent plasmas, magnetoresistance in inhomogeneous conductors with the Hall effect, and many others. A geometrical approach to studying transport in random media, which captures essential qualitative features of the described phenomena, is advocated.

*To be submitted to *Reviews of Modern Physics.*

Contents

I. INTRODUCTION

A. General

The percolation problem describes the simplest possible phase transition with nontrivial critical behavior. The pure geometrical nature of this transition and its compelling application to diverse physical problems have drawn the attention of many researchers and the percolation theory is well reviewed (Shante and Kirkpatrick, 1971; Essam, 1972; Kirkpatrick, 1973; Stauffer, 1979; Essam, 1980; Zallen, 1983; Stauffer, 1985; Kesten, 1982; Deutscher *et al.*, 1983; Shklovskii and Efros, 1984; Sokolov, 1986). The general formulation of the percolation problem is concerned with elementary geometrical objects (spheres, sticks, sites, bonds, etc.) placed at random in a d-dimensional lattice or continuum. The objects have a well-defined connectivity radius λ_0 and two objects are said to communicate, if the distance between them is less than λ_0. One is interested in how many objects can form a cluster of communication and, especially, when and how the clusters become infinite. The control parameter is apparently the density n_0 of the objects (their average number per unit volume), or the dimensionless filling factor $\eta = n_0\lambda_0^d$. The *percolation threshold*, $\eta = \eta_c$, corresponds to the minimum concentration at which an *infinite cluster* spans the space. Thus the percolation model exhibits two essential features: critical behavior and long-range correlations near the critical value of the control parameter η.

This model is relevant for a number of transport problem in disordered media, which exhibit critical behavior, such as the electron localization (Anderson, 1958; Ziman, 1969) and hopping conduction in amorphous solids (Shklovskii and Efros, 1984; Zallen, 1983). Other applications of percolation theory may concern the spreading of disease in a garden or, say, the critical concentration of bribe-takers to impede the normal functioning of a government.

Not only critical phenomena can be associated with the percolation model. Consider,

for example, the diffusion of a passive tracer in a two-dimensional, steady, incompressible random flow

$$\mathbf{v}(x,y) = \nabla\psi(x,y) \times \hat{\mathbf{z}} \,, \tag{1.1}$$

where $\psi(x,y)$ is a random stream-function. The streamlines of this flow are the contours of ψ. The geometry of the streamlines is associated with the geometry of percolation clusters as follows. Let us call "objects" the regions where $\psi(x,y)$ is less than a specified constant level h. If $z = \psi(x,y)$ is imagined to be the elevation of a random landscape and h designates the level of flooding, then the objects are the lakes. Two neighboring lakes "communicate" if they merge into a bigger lake, which is a "cluster." So the contours $\psi(x,y) = h$ present the coastlines of the lakes, that is, the envelopes of the clusters. The control parameter of this percolation problem is the level h which assumes that at some critical level, $h = h_c$, the lakes form an infinite ocean and among the contours $\psi(x,y) = h_c$ there is at least one infinitely long.

Flow (1.1), however, includes streamlines lying at all levels, and its transporting properties show no critical behavior in the only relevant control parameter (Péclet number)

$$P = \frac{\psi_0}{D_0} \,, \tag{1.2}$$

which is the ratio of the root-mean-square stream-function ψ_0 and the molecular diffusivity D_0 of the tracer. Nevertheless, if the Péclet number is large, $P \gg 1$, the transport shows long correlation because the tracer particles advected along very large streamlines diffuse from these lines to more typical short-closed lines very slowly and hence provide a significant *coherent* contribution to the turbulent diffusivity D^*. The larger the Péclet number, the longer and narrower the bundles of streamlines which dominate the effective transport in the considered flow. Under definite constraints, the effective diffusivity scales as (Isichenko *et al.*, 1989)

$$D^* \simeq D_0 P^{10/13} \,, \quad P \gg 1 \,, \tag{1.3}$$

where the exponent 10/13 is expressed in terms of the critical exponents of two-dimensional percolation theory.

The effective diffusion in a random flow presents an example of a long-range correlated phenomenon without critical behavior. The critical exponents of the percolation transition enter the result because the large value of the control parameter ($P \gg 1$) picks up a near-critical (in the sense of the contour percolation) set of streamlines dominating the effective transport. Unlike the transport processes occurring *on* the percolation clusters (Aharony, 1984; Orbach, 1984; Rammal, 1984; O'Shaughnessy and Procaccia, 1985a, 1985b; Havlin and Ben-Avraham, 1987; Hans and Kehr, 1987; Harris, 1987), the motion along the incompressible streamlines involves transport *around* the percolation clusters.

The appearance of formula (1.3) leaves little hope for its derivation using a regular perturbation theory method in solving the advective-diffusive equation

$$\frac{\partial n}{\partial t} + \mathbf{v}\nabla n = D_0 \nabla^2 n \tag{1.4}$$

for the tracer density n. Instead, geometrical arguments can be used to reduce the advective-diffusive problem to the problem of random contours whose critical behavior is not amenable to any kind of a perturbation analysis but is well described in terms of percolation theory.

The problem of critical phenomena (Domb *et al.*, 1972-1987) belongs among the most difficult in nonlinear physics. This is well manifested in the fact that several decades separate Boltzmann-Gibbs statistical mechanics and the first solution of the Ising model by Onsager (1944). After Wilson (1971a, 1971b, 1975) introduced the renormalization-group technique to the theory of phase transitions, the number of solvable critical models rapidly increased (Ma, 1976; Baxter, 1982). Some of the analytical results on percolation criticality were obtained relatively recently (den Nijs, 1979; Saleur and Duplantier, 1987).

The value of the available results on critical behaviors is grossly increased by the *universality of critical exponents* describing the behavior of the order parameter and of other

physical quantities near the critical point. Universality implies that the set of critical exponents is structurally stable, that is, does not change under a small perturbation of the model itself, provided that the perturbation does not introduce long correlations that decay slower than some algebraic function. This universality leads to the possibility of new applications of critical phenomena theory that might go far beyond the phase transition problems in statistical physics.

This paper concentrates on applications such as the processes of transport in classical random media including turbulent flows or inhomogeneous conductors. Many problems of this kind are reduced to the statistical properties of contours (isolines) of random potentials studied in the framework of *statistical topography.* In the simplest case of a potential characterized by a single scale of length, and a rapidly decaying correlation function, the statistical topography problem is mapped onto the simplest percolation problem delivering all necessary characteristics of the long-range contour behavior. For the case of algebraic behavior in the random potential correlator, the topography involves essentially many length scales, but still can be studied using a renormalization-type technique hinged on the knowledge of the monoscale-percolation exponents.

B. Fractals

An essentially geometrical approach to studying transport processes requires a concise characteristic of random fields. The fractal dimension serves such a characteristic. Introduced originally by Hausdorff (1918) and Besicovitch (1929), the concept of fractional, or generalized dimension was first used in fairly abstract mathematical studies on number theory (Besicovitch, 1935a, 1935b; Good, 1941). The fractal dimension was introduced in a physical context by Mandelbrot (1975a, 1977, 1982, 1983), whose works generated a widespread interest in fractal geometry (Pietronero and Tosatti, 1986; Paladin and Vulpiani, 1987; Peitgen and Saupe, 1988; Feder, 1988; Voss, 1989). Fractal dimensions were reported for numerous

environmental data (Burrough *et al.*, 1981) and even for space-time (Zeilinger and Svozil, 1985). The most sensible physical applications of fractals are concerned with turbulence (Mandelbrot, 1975b; Procaccia, 1984; Sreenivasan and Meneveau, 1986; Constantin *et al.*, 1991; Benzi *et al.*, 1991), chaotic attractors (Kaplan and Yorke, 1979; Mori, 1980; Farmer *et al.*, 1983; Grassberger and Procaccia, 1983), and critical phenomena (Suzuki, 1986), including transition to chaos in classical systems (Jensen *et al.*, 1985). Of course, there are many others (Mandelbrot, 1983; Feder, 1988).

The original Hausdorff-Besicovitch definition of the "dimensional number" D of a set of points F imbedded in a d-dimensional space is as follows. Let F be divided into the subsets $U_1, U_1, \ldots$ having the diameters (maximum linear size measured in the d-space) $\lambda_1, \lambda_2, \ldots$, respectively. Denote by $U(F,\lambda)$ the set of all possible divisions of the set F with $\lambda_i \leq \lambda$. Then the "exterior s-dimensional measure" $M_s(F)$ is defined as

$$M_s(F) = \lim_{\lambda \to +0} \inf_{U(F,\lambda)} \sum_i \lambda_i^s \,. \tag{1.5}$$

Finally, if $M_s(F) = 0$ for $s > D$, and $M_s(F) = \infty$ for $s < D$, then D is the "dimensional number," or the "fractional dimension" of F.

Another definition of D, which is due to Kolmogorov (1958) and known as capacity, is

$$D = -\lim_{\lambda \to +0} \frac{\log N_\lambda}{\log \lambda} \,, \tag{1.6}$$

where the *covering number* N_λ is the minimum number of d-dimensional cubes of side λ needed to cover the set F. The Hausdorff-Besicovitch and Kolmogorov definitions of D are equivalent, except for completely pathological cases that are of no physical interest (Young, 1982). The parameter D satisfies evident inequalities $0 \leq D(F) \leq d$ and $D(F') \leq D(F)$, if $F' \subset F$, and can in principle take on arbitrary fractional (and even irrational) value, such as $\log 8/\log 3 = 1.893\ldots$ for the Sierpinski carpet shown in Fig. 1. For "well-behaved" sets, *F 1* the dimension D equals the topological dimension, which is an integer, such as $D = 0$ (set

of isolated points), $D = 1$ (a smooth curve), $D = 2$ (a smooth surface), and $D = 3$ (a region of finite volume). Mandelbrot (1982) proposed the term "fractals" for the sets whose dimensional number D is greater than the topological dimension and less than the dimension d of the encompassing space. For this case, Mandelbrot coined the term "fractal dimension" for D.

The most appealing property of fractals is their self-similarity, or scaling, meaning that some parts of a whole are similar, after rescaling, to the whole. For example, the upper left square comprising one nineth the area of the Sierpinski carpet (Fig. 1) can be magnified three *F 1* times to reproduce the original carpet. This is an example of an exact self-similarity. For fractals involving a random element, one speaks about a statistical self-similarity, meaning equivalent, after the proper rescaling, statistical geometrical distributions characterizing a part and the whole fractal. Examples of random fractals are the trajectory of a particle pursuing Brownian motion ($D = 2$, see Fig. 2) and the infinite cluster near the percolation *F 2* threshold ($D = 91/48$ for $d = 2$ and $\simeq 2.50$ for $d = 3$).

It is important to note that virtually no real physical object qualifies for the formal definition of a fractal involving a nontrivial (that is, lying between the topological and the ambient dimension) Hausdorff-Besicovitch dimension (1.6). Instead, *physical fractals* can be defined as geometrical objects having a sufficiently wide *scaling range* $[\lambda_{\min}, \lambda_{\max}]$ specifying the length scales of a self-similar behavior. As soon as the ratio $\lambda_{\max}/\lambda_{\min}$ becomes much larger than unity, one can speak about a fractal. Specifically, in the scaling range, the covering number N_λ behaves proportional to λ^{-D}. If one restricts oneself to the area of the size $\lambda_{\max}$ equal to the upper limit of the scaling range, then the covering number $N_{\lambda_{\max}}$ is apparently of the order of one, hence

$$N_\lambda \simeq \left(\frac{\lambda_{\max}}{\lambda}\right)^D , \qquad \lambda_{\min} < \lambda < \lambda_{\max} . \tag{1.7}$$

Expression (1.7) replaces the more mathematical definition (1.6) of the fractal dimension D

and is actually used in the computation of D using box-counting algorithms (Feder, 1988). Furthermore, definition (1.7) generalizes the Hausdorff-Besicovich definition (which corresponds to the limiting case $\lambda_{\min} = 0$) in that the fractal dimension can also characterize the long-scale behavior. For example, an infinite percolation cluster at the percolation threshold is self-similar in the scaling range $[\lambda_0, \infty]$, where λ_0 is the size of communicating objects (Kapitulnik *et al.*, 1984). In fact, a percolation cluster is one of the most popular models of a fractal. The long-correlated properties of virtually all critical phenomena implies a statistical self-similarity in a diverging scaling range, which makes fractal geometry quite a suitable language to describe phase transitions (Suzuki, 1986).

In general, $\lambda_{\max}$ in (1.7) can be replaced by a smaller variable radius, $a \leq \lambda_{\max}$, and putting $\lambda = \lambda_{\min}$ we obtain the *radius-mass relation*

$$M(a) \simeq \left(\frac{a}{\lambda_{\min}}\right)^D , \qquad a > \lambda_{\min} , \tag{1.8}$$

where the center of the circle of radius a lies on the fractal and it is assumed that the mass covered by a $\lambda_{\min}$-sized box is unity.

Using formula (1.7), one can measure the fractal dimension of curves (topological dimension 1) by a compass. Let λ be the compass step. Then the measured length is

$$L(\lambda) = \lambda N_\lambda \simeq \lambda \left(\frac{\lambda_{\max}}{\lambda}\right)^D \propto \lambda^{1-D} . \tag{1.9}$$

The observation that there is no "actual" length of a coastline, meaning that the result (1.9) depends on the accuracy λ, became one of the stimuli for introducing the concept of fractals (Mandelbrot, 1967; 1975b).

Normally, different definitions of the fractal dimension yield the same result. One, however, should be cautious with *self-affine* fractals, that is, those reproducing themselves after rescaling which is different in different directions. Usually, the distance in such systems is measured in different directions by quantities of different physical dimensionality, such as

time and length. For the fractal dimension to be meaningful, one has to switch to nondimensional variables, a procedure that involves using some units of measure (seconds, centimeters, etc.). Hence the scaling range of self-affine fractals may depend on the units used. A further complication is that, for self-affine fractals, the "box-counting dimension" (Eq. (1.7)) and the "compass dimension" (Eq. (1.9)) may be different (Mandelbrot, 1985). One example of a self-affine fractal is the graph $\{t, B_H(t)\}$ of a fractional Brownian function $B_H(t)$, whose definition and properties are discussed in Sec. III.B. While the box-counting (Hausdorff-Besicovitch) dimension of the fractional Brownian graph equals $2 - H$ $(0 < H < 1)$, its compass dimension is $1/H$ $(1/2 < H < 1)$ (Mandelbrot, 1985).

In table I we depict fractal dimensions and scaling ranges of some geometrical objects discussed in this paper. Notice that the same objects can have different values of fractal dimension in different scaling ranges. *T I*

To calculate the fractal dimension of more complicated objects involving cross-sections of fractals by a plane or by a line or the intersection of several fractals, a simple formula can be used. Consider two fractals, F_1 and F_2, with the fractal dimensions D_1 and D_2 respectively, in a d-dimensional cube with the edge a. According to Eq. (1.7), the covering number of F_i is $N_\lambda(F_i) \simeq (a/\lambda)^{D_i}$. If all the cube is divided into boxes with the size λ, then F_i intersects the following fraction of boxes:

$$p_\lambda(F_i) = N_\lambda(F_i)\left(\frac{\lambda}{a}\right)^d \simeq \left(\frac{\lambda}{a}\right)^{d-D_i} . \tag{1.10}$$

Suppose that there is no correlation in the position of F_1 and F_2, then we find the fraction $p_\lambda(F)$ of λ-boxes covering the intersection $F = F_1 \cap F_2$:

$$p_\lambda(F) = p_\lambda(F_1)p_\lambda(F_2) \simeq \left(\frac{\lambda}{a}\right)^{2d-D_1-D_2} . \tag{1.11}$$

Comparing (1.11) with the relation $p_\lambda(F) = N_\lambda(F)(\lambda/a)^d \propto (\lambda/a)^{d-D}$ we find the fractal dimension of the intersection (Mandelbrot, 1984)

$$D = D_1 + D_2 - d . \tag{1.12}$$

A corollary of the intersection rule (1.12) concerns the cross-sections of fractals by regular shapes. Let $D_2 = d - 1$ be the dimension of a plane in the space ($d = 3$) or of a line in the plane ($d = 2$). Then the fractal dimension of the cross-section is unity less than that of the fractal F_1:

$$D = D_1 - 1 \ . \tag{1.13}$$

A generalization of the intersection rule (1.12) for the case of N independent intersecting fractals reads

$$D = D_1 + \ldots + D_N - (N-1)d \ . \tag{1.14}$$

Of course, formulas (1.12)–(1.14) are valid as long as $D > 0$, otherwise the intersection is essentially empty. The scaling range of the intersection of several fractals is the intersection of individual scaling ranges unless one of the fractals is self-affine. For example, the self-affinity of the fractional Brownian graph ($D = 2 - H$) leads to an upper bound on its scaling range (see table I), which depends on the unit of measure. This bound can be lifted by a cross-section: The fractional Brownian zero-set ($D = 1 - H$) is a self-similar fractal in an unbounded scaling range. *TI*

Among the most intensively studied fractal objects are the chaotic, or "strange" attractors that present a generic invariant set for dissipative dynamical systems with the dimension of the phase-spase $d \geq 3$. The first example of such attractor was studied by Lorenz (1963). The motion on the attractor is characterized by (a) the sensitive dependence of the trajectory behavior on initial conditions, that is, exponentially diverging neighboring orbits, and (b) exponentially shrinking phase-space volume. In terms of the characteristic Lyapunov exponents (Lichtenberg and Lieberman, 1983), $\Lambda_1 \geq \Lambda_2 \geq \ldots \geq \Lambda_d$, which describe the growth rates of the edges of an infinitesimal phase-space hypercube, this means that $\Lambda_1 > 0$, whereas $\sum_{i=1}^{d} \Lambda_i < 0$. Kaplan and Yorke (1979) conjectured that the fractal dimension of a

chaotic attractor be given by the simple formula

$$D = j + \sum_{i=1}^{j} \Lambda_i / |\Lambda_{j+1}| \,, \tag{1.15}$$

where j is the maximum integer for which $\sum_{i=1}^{j} \Lambda_i > 0$. Young (1982) showed that formula (1.15) is exact for $d = 3$. Notice that one of the Lyapunov exponents of a dynamical system is necessarily zero (in the direction of the phase-space flow) that leads to further simplification of the Kaplan-Yorke formula for $d = 3$ ($\Lambda_1 > 0 = \Lambda_2 > \Lambda_3$; $|\Lambda_3| > \Lambda_1$):

$$D = 2 + \Lambda_1 / |\Lambda_3| \,, \tag{1.16}$$

Thus the fractal dimension of a chaotic attractor in a system with three degrees of freedom lies between 2 and 3, because the chaotic behavior ($\Lambda_1 > 0$) of self-avoiding orbits is not possible on manifolds with the dimension two or less.

The concept of fractal dimension decribes only geometrical, or static properties of self-similar objects. The characterization of dynamical properties of fractals, such as the fraction of time spent by a particle in a given subset of an attractor (Grassberger, 1983b), the relative intensity of energy dissipation in turbulence (Frish and Parisi, 1985), or the relative intensity of passive scalar gradients in chaotic advection (Ott and Antonsen, 1988), involves a continuous set of exponents (Hentschel and Procaccia)

$$D_q(F) = \frac{1}{q-1} \lim_{\lambda \to 0} \frac{\log \sum_{i=1}^{N_\lambda} p_i^q}{\log \lambda} \,. \tag{1.17}$$

Here p_i ($\sum_i^{N_\lambda} p_i = 1$) is the corresponding "relative importance" called probability measure, or mass density, of the subset $U_i(\lambda) \subset F$ contained inside the i-th covering cube with the edge λ. In the limit $q \to 0$ expression (1.17) becomes the fractal dimension (1.6). For a "homogeneous fractal," whose parts are equally important, the probability measure is constant, $p_i \equiv N_\lambda^{-1}$, and the generalized dimension D_q equals the fractal dimension $D(F)$ for all q.

The set F can be represented as a union of a continuous family of subsets F_α each being a fractal of the fractal dimension $f(\alpha) \leq D(F)$, and characterized by the singularity of the probability measure $p_i(\lambda) \propto \lambda^\alpha$. The generalized dimension D_q is ralated to the α-singularity dimension $f(\alpha)$ as (Jensen *et al.*, 1985; Halsey *et al.*, 1986)

$$D_q(F) = \frac{1}{q-1} \min_\alpha [q\alpha - f(\alpha)] \ . \tag{1.18}$$

The continuously changed generalized dimension D_q and the corresponding function $f(\alpha)$ present the mathematical formalism of the theory of *multifractals* (Paladin and Vulpiani, 1987; Feder, 1988). The self-similarity property of multifractals is more complicated than that of homogeneous fractals and is described in terms of *multiscaling* (Jensen *et al.*, 1991).

In this paper, we are primarily concerned with homogeneous fractals, such as percolating streamlines of an incompressible random flow. The streamlines are homogeneous fractals due to the Liouville theorem applied to the Hamiltonian equations of tracer particle motion.

II. PERCOLATION

In this section a brief review is given of lattice and continuum percolation theories with an emphasis on the universality of critical behavior. In the long run, this universality enables the success in applying percolation theory to a number of problems, which seem to be very far from the original one introduced by Broadbent and Hammersley (1957). An incomplete list of problems, to which percolation theory has been applied, includes hopping conduction in semiconductors (Seager and Pike, 1974; Shklovskii and Efros, 1984), gelation in polymers (de Gennes, 1979a), electron localization in disordered potentials (Ziman, 1969; Thouless, 1974; Ziman, 1979), random intergrain Josephson contacts in high-T_c superconductors (Gurevich *et al.*, 1988), gas-liquid transition in colloids (Safran *et al.*, 1985), permeability of porous rocks (Thompson *et al.*, 1987), plasma transport in stochastic magnetic fields (Kadomtsev and Pogutse, 1979; Yushmanov, 1990; Isichenko, 1991b), turbulent diffusion (Gruzinov *et al.*, 1990), epidemic processes (Grassberger, 1983a), and forest fires (MacKay and Jan, 1984).

The goal of this section is not to compete with major reviews on percolation theory (Shante and Kirkpatrick, 1971; Essam, 1972; Kirkpatrick, 1973; Stauffer, 1979; Essam, 1980; Zallen, 1983; Stauffer, 1985; Kesten, 1982; Deutscher *et al.*, 1983; Shklovskii and Efros, 1984; Sokolov, 1986) but rather to serve as a precursor to further discussion. We also supplement earlier review articles by covering recent analytical and numerical results related to hull exponents, correlated percolation, and continuum percolation.

In this section, we focus primarily on the geometrical properties of percolation clusters that are described by the so-called *static* exponents. A variety of *dynamic* properties of percolation clusters including conduction and random walks on clusters, their elastic properties, etc., are given lesser discussion. Review of the dynamics of percolation clusters and of other fractals is given in Aharony (1984), Orbach (1984), Rammal (1984), Havlin and Ben-Avraham (1987), Hans and Kehr (1987), and Harris (1987).

In Sec. A the simplest conceptual problem of random percolation on a periodic lattice is discussed and a review of the exponents of critical behavior near the percolation threshold is given. The scaling theory of percolation clusters, which relates different percolation exponents, is outlined in Sec. B. The universality of critical exponents, that is, their insensitivity to the geometry of the underlying lattice is discussed in Sec. C. Correlated percolation is reviewed in Sec. D. In Sec. E we discuss different formulations of the continuum percolation problem, which are free from lattice constraints.

A. Lattice percolation and the geometry of clusters

This new kind of a mathematical problem was motivated by the question of percolation of a fluid through a porous medium or a maze, thus resulting in the term "percolation problem." Broadbent and Hammersley, the founders of the percolation theory, coined the term "percolation" as opposed to the term "diffusion." According to Broadbent and Hammersley (1957), if diffusive processes involve a random walk of a particle in a regular medium, then percolation processes involve a regular motion (e.g., fluid or electric current flow) through a random medium. The simplest problem of this kind can be formulated as follows. Given a periodic lattice embedded in a d-dimensional space, and the probability p for each site of the lattice to be "occupied" (and hence with the probability $1-p$ to be "empty"), what is the distribution of resulting clusters over sizes and other geometrical parameters? A cluster means (by definition) a conglomerate of occupied s sites, which communicate via the nearest-neighbor rule (Fig. 3). In percolation theory special attention is given to the *percolation threshold*, $p = p_c$, *F 3* at which an *infinite cluster* spans the lattice. Besides this *site percolation*, one can introduce the idea of *bond percolation*, with clusters of connected conducting bonds (Fig. 4). The *F 4* bonds are conducting with the probability p and, correspondingly, blocked with the probability $1 - p$. The site- and the bond-percolation problems are very similar to each other. There also exists a hybrid site-bond formulation of the percolation problem (Heermann and

Stauffer, 1981). To be specific, we discuss percolation theory mainly on the example of the site problem.

Statistically, one can describe the cluster distribution by the cluster density $n_s(p)$, which is the number of clusters including exactly s occupied sites, per unit volume. It is convenient to choose the unit volume, which corresponds to one site of the lattice. For sufficiently small s, the density $n_s(p)$ can be calculated in a straightforward way by simply counting the number of permissible configurations ("lattice animals") of a cluster (de Gennes *et al.*, 1959; Sykes and Essam, 1964a; Sykes and Glen, 1976; Sykes *et al.*, 1976a, 1976b, 1976c; Essam, 1980). These expressions for $n_s(p)$ are polynomial functions of p. For example, a cluster consisting of a single site on a two-dimensional square lattice means the occupancy of the site (probability p) and the emptiness of the four nearest neighbors (probability $(1-p)^4$). Hence, $n_1(p) = p(1-p)^4$. Analogously, $n_2(p) = 2p^2(1-p)^6$, $n_3(p) = 2p^3(1-p)^8 + 4p^3(1-p)^6$, etc. For higher s, the calculation of $n_s(p)$ becomes menacingly cumbersome and is best done on computer (Martin, 1974).

The percolation problem would be somewhat tedious, were the cluster distribution a smooth function of the probability p, as suggested by the above series expansions for finite s. The central point of the theory is that, for each of lattice, there exists a *critical probability* p_c, $0 < p_c < 1$, at which an infinite cluster definitely (i.e., with the probability one) appears. The existence of this critical transition — the percolation threshold — is heuristically evident from the following argument. For $p = 1-\varepsilon$, $0 < \varepsilon \ll 1$, the percolation to infinity through occupied sites cannot be destroyed by removing a small fraction ε of sites (Fig. 3(c)). On *F 3c* the other hand, for small $p \ll 1$, it is clearly exponentially improbable to percolate to a large distance a through occupied sites, hence, for $a \to \infty$, the probability of finding such a cluster tends to zero. Thus, for $p \ll 1$, there is no infinite cluster (Fig. 3(a)). This indicates *F 3a* the existence of a critical probability p_c (Fig. 3(b)), which, roughly speaking, is "of the order *F 3b* of 1/2."

The value of the critical probability p_c depends on the dimension of space d, the kind of problem (site or bond), and the type of lattice. In two dimensions, p_c can be calculated exactly for some lattices (Sykes and Essam, 1963, 1964b). The critical probabilities of certain lattices can be simply related to each other. Suppose there exists a one-to-one correspondence between the bonds of two lattices A and B. Suppose further that, if a bond on lattice A is conducting, then the corresponding bond on lattice B is blocked, and visa versa. If, under such convention, the percolation through lattices A and B are mutually excluding, then these two latices are said to be *matching*, or *dual*: A=B*. Geometrically, the corresponding bonds of matching lattices "cut each other" (see Fig. 5). The simplest examples of matching *F 5* lattices are triangular (T) and honecomb (H); the square lattice (S) is self-matching: S=S*. The critical probabilities of matching lattices are complementary:

$$p_c(\mathrm{A}, b) + p_c(\mathrm{A}^*, b) = 1 \ , \tag{2.1}$$

where "b" means the bond-problem. It immediately follows that the critical probability for the two-dimensional square lattice is

$$p_c(\mathrm{S}, b) = 1/2 \ . \tag{2.2}$$

One can similarly introduce matching between bond- and site-lattices. For example, the sites of the triangular lattice match the bonds of the square lattice (Fig. 5(c)), hence *F 5c*

$$p_c(\mathrm{T}, s) = 1 - p_c(\mathrm{S}, b) = 1/2 \ . \tag{2.3}$$

For matching bond problems on triangular and honeycomb lattices, Sykes and Essam (1963, 1964b) found an additional exact relation for critical probabilities based on the star-triangle overlapping property. This relation yields

$$1 - 3p_c(\mathrm{T}, b) + p_c^3(\mathrm{T}, b) = 0 \ , \tag{2.4}$$

hence

$$p_c(\mathrm{T}, b) = 1 - p_c(\mathrm{H}, b) = 2\sin(\pi/18) \ . \tag{2.5}$$

In the three-dimensional case, no percolation threshold is known exactly, and only numerical data are available. Table II shows the values of p_c for the simplest lattices. At *T II*
first glance, there is no apparent rule describing the values of the critical probabilities p_c for different lattices. An approximate rule, however, was found by Scher and Zallen (1970), who noticed that, for each dimension, there exists an invariant, which is almost independent on the type of lattice. This invariant, $\phi_c = fp_c$, is the critical fraction of space occupied by the spheres (discs in 2D) of the bond-length diameter, positioned in the occupied sites of the lattice. The quantity f is called the filling factor of the lattice and denotes the volume fraction occupied by mutually touching spheres positioned at each site. The critical space occupation probability equals $\phi_c = 0.44 \pm 0.02$ in two, and $\phi_c = 0.154 \pm 0.005$ in three dimensions.

The decrease of the critical probability with increasing dimension d is easily understood. For example, 2D bond clusters on a square lattice (S) are nothing more than a planar cross-section of 3D bond clusters on a simple cubic lattice (SC) at the same probability p. Even though all 2D clusters are finite ($p < p_c(\mathrm{S}, b) = 0.5$), they can belong to an infinite 3D cluster communicating via the third dimension ($p > p_c(\mathrm{SC}, b) \simeq 0.248$). The lattice filling factor f is also smaller for higher dimensions: $f(\mathrm{S}) = \pi/4, \quad f(\mathrm{SC}) = \pi/8$.

A more fundamental difference between two- and three-dimensional percolation is that in 3D one can introduce two nontrivial critical probabilities, $p_c \equiv p_{c1} < p_{c2}$. Let us call the clusters of occupied sites (or conducting bonds) "black." The second critical probability p_{c2} specifies the threshold of percolation through "white" clusters of vacant sites (or blocked bonds) corresponding to the occurance probability $1 - p$. Since the black and the white percolation problems are identical, we conclude that $p_{c2} = 1 - p_{c1}$.

In two dimensions, simultaneous percolation through both black and white clusters is impossible unless these clusters may cross each other (as is the case for bonds on a triangular lattice). This is well manifested in that the critical percolation probabilities p_c are not less

than 1/2 (with the mentioned exception for the triangle bonds; see table II). For $p_c > 1/2$ *T II* (square sites, honeycomb sites and bonds) and $1 - p_c < p < p_c$, there is percolation through neither black nor white clusters.

In three dimensions, one generally has $p_c < 1/2$ (see table II) so that $p_{c1} < p_{c2}$. The *T II* presence, at $p_{c1} < p < p_{c2}$, of both black and white infinite clusters reflects the existence of different nonintersecting, isotropic paths to infinity. (This is why freeway overpasses are made three-dimensional.) The difference between two and three dimensions becomes especially distinct for percolation in the continuum (Sec. E).

The cluster density $n_s(p)$ accounts only for finite-size clusters. The infinite cluster is characterized by the density $P_\infty(p)$, which denotes the probability for a given site to belong to the infinite cluster. (Sometimes $P_\infty(p)$ is defined as the conditional probability for a given *occupied* site to belong to the infinite cluster. These two definitions of $P_\infty(p)$ differ by the factor of p, which is unimportant for the critical behavior near $p = p_c$.) It can be shown (Kikuchi, 1970; Newman and Schulman, 1981) that, in two or three dimensions, there exists either exactly one (for $p \geq p_c$) or no (for $p < p_c$) infinite cluster. The sum of all the probabilities for a given site to belong to either a finite-size cluster or the infinite cluster must equal p (the probability to be simply occupied):

$$\sum_{s=1}^{\infty} s\, n_s(p) + P_\infty(p) = p\ . \tag{2.6}$$

In the subcritical case, $p < p_c$, $P_\infty(p)$ is identically zero. For $p > p_c$, $P_\infty(p)$ is positive, consequently, in the vicinity of the percolation threshold, the function $P_\infty(p)$ is non-analytic. There is extensive numerical evidence of the power dependence

$$P_\infty(p) \propto (p - p_c)^\beta \theta(p - p_c)\ , \quad |p - p_c| \ll 1\ , \tag{2.7}$$

where $\theta(x)$ is the Heaviside step function. The exponent β is one of the standard set of *critical exponents* $\alpha, \beta, \gamma, \ldots$ (Domb *et al.*, 1972-1987) that govern the behavior of different

quantities near the critical point:

$$\widehat{S}_p \sum_{s=1}^{\infty} n_s(p) \propto |p - p_c|^{2-\alpha} , \tag{2.8a}$$

$$\widehat{S}_p \sum_{s=1}^{\infty} s\, n_s(p) \propto (p - p_c)^{\beta} , \tag{2.8b}$$

$$\widehat{S}_p \sum_{s=1}^{\infty} s^2\, n_s(p) \propto |p - p_c|^{-\gamma} , \tag{2.8c}$$

$$\widehat{S}_H \sum_{s=1}^{\infty} s\, n_s(p_c) e^{-Hs} \propto H^{1/\delta} , \tag{2.8d}$$

$$\xi(p) \propto |p - p_c|^{-\nu} . \tag{2.8e}$$

In Eqs. (2.8), the operator $\widehat{S}_x$ denotes the main singular (as a function of x) part of the subsequent expression. Specifically, this operator yields zero when applied to an analytic function. "Singular" in this context means a function that is either discontinuous or has a discontinuous derivative of some order at $p = p_c$. All expressions (2.8) assume $|p - p_c| \ll 1, \quad 0 < H \ll 1$. Equation (2.8b) is a direct consequence of Eqs. (2.6) and (2.7). The quantity $\xi(p)$ in Eq. (2.8e) is the so-called *correlation*, or *coherence length*, which is a characteristic size of the cluster distribution (see Sec. B). This is not an average radius of percolation clusters (the average linear size is of the order of the lattice period as small clusters still dominate) but rather a maximum size, above which the clusters are exponentially scarce. The correlation length $\xi(p)$ is also the upper bound of the scaling range where percolation clusters behave self-similarly and hence may be characterized by a fractal dimension (Stanley, 1977, 1984; Margolina *et al.*, 1982; Kapitulnik *et al.*, 1984). Equivalently, the correlation length separates an algebraic behavior of a cluster correlation function (Shklovskii and Efros, 1984) from its exponential decay.

Table III summarizes the percolation critical exponents. These exponents depend only *T III* on the dimension of the space but not on the type of lattice and the kind of percolation

problem (see Sec. C). As discussed in the Sec. B, phenomenological (scaling) arguments can be used to derive relations between the critical exponents entering Eqs. (2.8), so that only two of them are left to be calculated from first principles. The choice of these two "basic" exponents is relative; we will consider the correlation length exponent ν and the infinite cluster density exponent β as the basic percolation exponents. In two dimensions ($d = 2$), these indices are known analytically (den Nijs, 1979; Pearson, 1980; Baxter, 1982), namely, $\nu = 4/3$ and $\beta = 5/36$. For $d = 3$, only numerical estimates are available: $\nu \simeq 0.90$ and $\beta \simeq 0.40$ (see table III). *T III*

In the analogy, which can be drawn between the percolation problem and magnetic phase transitions (Stauffer, 1979), the sums on the left-hand sides of Eqs. (2.8) can be regarded as free energy (2.8a), spontaneous magnetization (2.8b), susceptibility (2.8c), and magnetization (2.8d) in the external field H. In these terms, the probability difference $p - p_c$ corresponds to the temperature difference $T_c - T$, so that subcritical (finite) clusters present a "high-temperature" (disordered) phase, and the supercritical infinite cluster spans the space to form a "low-temperature" (ordered) phase. Hence the infinite cluster density $P_\infty(p)$ plays the role of the order parameter of the percolation phase transition (Kikuchi, 1970).

Generally, the lattice percolation problem can be placed among other discrete lattice phase transition models, such as the Ising (1925) model, the q-state Potts model (Potts, 1952; Nienhuis *et al.*, 1979), the n-vector model $O(n)$ (Stanley, 1968; Nienhuis, 1982), and others (Baxter, 1982). The Ising model, which was historically the first analytically solved phase-transition model, is the particular case of $O(n)$ for $n = 1$ and also of the q-state Potts model for $q = 2$. The percolation problem corresponds to a proper limit of the Potts model for $q \to 1$ (Fortuin and Kasteleyn, 1972).

In two dimensions, there is a powerful technique for the calculation of various critical exponents. This technique is based on the representation of the "Coulomb gas" introduced, in its most convenient form, by Kadanoff (1978). A review of the results obtained with this

method can be found in Nienhuis (1984).

Another approach for possibly exact evaluation of critical exponents in two dimensions is based on the conformal invariance technique (Polyakov, 1970; Belavin *et al.*, 1984; Dotsenko and Fateev, 1984; Saleur, 1987). This method predicts a discrete series of "permissible" fractal dimensions (Kac, 1979; Larsson, 1987).

$$d_f = (100 - x^2)/48 \,, \tag{2.9}$$

where x is an integer. Speculating on the correspondence between various objects (e.g., clusters and their subsets) and conformal fields, one can pick up a conformal dimension (2.9) closest to a numerical value and claim an exact result (Larsson, 1987). All analytically known fractal dimensions associated with 2D percolation clusters and random walks belong to this list of "magic numbers" (see table IV). *T IV*

In cases when analytical results were not available, the most accurate estimates for critical probabilities and critical exponents were obtained using the series expansion method (Sykes and Essam, 1964a; Sykes *et al.*, 1976a, 1976b, 1976c; Adler *et al.*, 1990). The idea of the method (Domb and Sykes, 1960) is to present diverging sums, such as the one in Eq. (2.8c), in the form of series in p (low-density expansion) or $1 - p$ (high-density expansion), using the lattice animal enumeration. The critical behavior is then studied by locating the nearest singular point of the series on the real positive axis of p.

The critical exponents introduced above are usually referred to as *static* exponents, because they characterize only the geometry and distribution of clusters. Percolation clusters are usually used for modelling such physical objects as amorphous solids (Zallen, 1983), composite materials (Garland and Tanner, 1978), porous rock (Thompson *et al.*, 1987), polymers (de Gennes, 1979b), etc. In studying various physical properties of such media (conductivity, elasticity, permeability, etc.), the corresponding properties of percolation networks are described in term of *dynamic* exponents. The simplest problem of this kind associated with

the appearance of an infinite cluster is the problem of long-range conductance in a random resistor network (Kirkpatrick, 1973; Skal and Shklovskii, 1974; Shklovskii and Efros, 1984; Havlin and Ben-Avraham, 1987; Harris, 1987). For bond percolation where each "conducting" bond has a fixed resistance of unity, while "blocked" bonds have an infinite resistance, the large-scale behavior of the system undergoes a sharp transition from an insulator ($p < p_c$) to a conductor ($p > p_c$). Near the percolation threshold, the long-range direct-current conductivity $\sigma_{\rm dc}$ has a singularity of the form

$$\sigma_{\rm dc} \propto (p - p_c)^{\mu} \theta(p - p_c) \; . \tag{2.10}$$

The conductivity exponent μ is one of the dynamic exponents. The value of $\mu \simeq 1.3$ is relatively well established for two dimensions. In the three-dimensional case, the computation is more expensive and reported results are more controversial, $\mu = 1.7 - 1.9$ (see table III). *T III*
The processes of ac conductivity in random resistor network are described by a set of new exponents studied theoretically by Bergman and Imry (1977) and Hui and Stroud (1985) and experimentally by Yoon and Lee (1990).

The critical exponents α, β, γ, δ, and ν characterize the distribution of clusters. For many applications, the structure of an individual cluster is also important. Let us introduce for brevity some terms characterizing the geometry of a percolation cluster. We will call s, the number of sites belonging to the cluster, the "cluster mass" and a, the maximum linear size of the cluster, the "cluster diameter," or simply the "size." (Notice that some authors refer to the number of sites s as the "size." Sometimes, the "mean cluster size" is defined as the ratio of sums on the left-hand side of Eqs. (2.8c) and (2.8b). We will not follow this notation.) The mass s and the size a of a large cluster are related by $s(a) \propto a^{d_c}$, which is a direct consequence of the radius-mass relation (1.8) for a fractal. The fractal dimension d_c does not depend on the cluster size. What changes with the probability p, or with the size a, is the scaling range, which is $[\lambda_0, a]$ for a finite cluster and $[\lambda_0, \xi(p)]$ for the infinite one.

The fractal dimension d_c of a percolation cluster can be expressed through other exponents. To establish this relation, let us notice that the density $P_\infty(p)$ of the infinite cluster is its mass to volume ratio $M(a)/a^d$ at $a \gg \xi(p)$. Writing this relation at the lower limit of its applicability, $a \simeq \xi(p)$, we find $M(\xi(p)) \simeq \xi^d(p)P_\infty(p)$. On the other hand we have $M(a) \simeq (a/\lambda_0)^{d_c}$ for $\lambda_0 < a < \xi(p)$. Using this radius-mass relation on the upper limit $a = \xi(p)$, and Eqs. (2.7), (2.8e) we conclude (Kapitulnik *et al.*, 1984)

$$d_c = d - \frac{\beta}{\nu} . \tag{2.11}$$

Notice that in the early work by Stanley (1977), who proposed to describe near-critical percolation clusters by an "effective dimension," an incorrect expression for the dimension was given ($d_p = d - 2\beta/\nu$). Thus, the fractal dimension d_c of a percolation cluster is always smaller than the dimension d of the ambient space, due to numerous "holes" in the cluster. In two dimensions, $d_c = 91/48 \simeq 1.90$; for $d = 3$, $d_c \simeq 2.5$ (see table III). *T III*

For the problem of electrical conductivity of a random network and other dynamic properties, another object is relevant — the "backbone" of an infinite percolation cluster. The conductivity problem is more convenient to describe in terms of bond percolation. The backbone is defined as the network of unblocked connected bonds, through which one can go to infinity by at least two non-intersecting paths (Fig. 6). In other words, the backbone is a set *F 6* of bonds, through which electric current would flow, were a voltage applied to the cluster at infinitely remote electrodes. The rest of the cluster is referred to as a collection of "dead," or "dangling ends." A dangling end can be disconnected from the cluster by cutting a single bond.

Similar to the fractal dimension d_c of the whole cluster, one can introduce the backbone fractal dimension d_b. This exponent was determined numerically by Herrmann and Stanley (1984), who found $d_b = 1.62 \pm 0.02$, for $d = 2$, and $d_b = 1.74 \pm 0.04$, for $d = 3$. The inequality $d_b < d_c$ means that almost all the mass of a large cluster is concentrated in its dangling ends.

The closest conformal dimension (2.9) to the 2D d_b value is (at $x = 5$) $25/16 \simeq 1.56$, which lies slightly beyond the reported statistical error. This discrepancy questioned the universality of the "magic numbers" (2.9) (Larsson, 1987).

The backbone, in turn, can be devided into multiply-connected paths (Harris, 1983). For example, the singly-connected bonds bear all the current flowing through the cluster, hence these bonds are sometimes called "red" (Stanley, 1984; another term for this object – "cutting bonds"). Coniglio (1981) found that the fractal dimension of the set of red bonds is simply related to the correlation length exponent ν : $d_{rb} = 1/\nu$. In two dimensions, $d_{rb} = 3/4$, which corresponds to the conformal dimension (2.9) at $x = 8$. The red bonds are present only in the "incipient" infinite cluster, that is, the infinite cluster at $p = p_c$. The backbone of a supercritical infinite cluster ($p > p_c$) has a network-like structure and, since the hole sizes in the network are bounded from above by a finite correlation length $\xi(p)$, the singly-connected (and generally, finitely-connected) bonds do not exist.

From the viewpoint of conduction, a percolation backbone behaves as a multifractal, where the natural measure of fractal inhomogeneity is the Ohmic dissipation density (Paladin and Vulpiani, 1987).

The minimum-distance path connecting two remote points on a near-critical cluster was invoked for the model of "growing clusters" (Alexandrowicz, 1980; Stanley, 1984; Grassberger, 1985). The minimum, or chemical path has the fractal dimension $d_{\min} \simeq 1.1$. If this object corresponds to a conformal field, the Larsson (1987) conjecture that $d_{\min} = 17/16$ may be valid, which is the closest conformal dimension (at $x = 7$) to the numerical data (see table III). *T III*

Another geometrical characteristic of a cluster is its outer perimeter, or the "hull" L_h defined as the number of empty sites that (a) are adjacent to the cluster sites and (b) can be related to infinity via a chain of empty sites connected as either nearest or next-to-nearest neighbors. The hull may also be presented as a continuous line of the length L_h ($d = 2$), or

a surface of the area L_h ($d = 3$), enveloping the cluster from outside (see Fig. 7). Without restriction (b) one would have the full (outer and inner) perimeter, which scales directly proportional to the cluster mass s (Reich and Leath, 1978). In two dimensions, the outer and the inner perimeters are topologically disconnected and the external hull mass L_h is much less than the cluster mass s. This leads to the existence of a nontrivial, for $d = 2$, hull exponent d_h, which is the fractal dimension of the hull. The hull measure L_h is expressed through its size a as follows: *F 7*

$$L_h \propto a^{d_h} . \tag{2.12}$$

The hull exponent in two dimensions was computed by Ziff (1986), who found $d_h = 1.750 \pm 0.002$ (see also data in table III). Sapoval *et al.* (1985) and Bunde and Gouyet (1985) argued on a similarity between diffusion fronts and percolation hulls that led to the heuristic conjecture for the hull exponent: *T III*

$$d_h = 1 + 1/\nu = 7/4 , \quad d = 2 . \tag{2.13}$$

Later analytical study of Saleur and Duplantier (1987) confirmed result (2.13) from the first principles.

The properties of an internal hull, that is, of a line enveloping an internal hole in the cluster, are very similar to those of the external hull. Indeed, an internal hull can be considered as the external hull of a complimentary cluster of vacant sites (probability $1 - p$) that fills up a hole in the original cluster.

One can introduce hull critical exponents analogously to those associated with clusters themselves. For example, the beta exponent β_h is defined similarly to Eq. (2.11), $d_h = d - \beta_h/\nu$, $\nu_h \equiv \nu$. The values $\beta_h = 1/3$, $\gamma_h = 2$ for $d = 2$ suggest that percolation hulls are more simple objects than underlying percolation clusters and are of independent significance. Weinrib and Trugman (1985) showed that percolation hulls are associated with a special kind of random walk called a "smart kinetic walk" (SKW) which can be generated with no regard

to clusters (Ziff *et al.*, 1984; Ziff, 1986, 1989). Other importance of percolation hulls lies in their ability to model the fronts of diffusion-limited aggregation (Meakin and Family, 1986) and contour sets of random functions (see Sec. E).

Grossman and Aharony (1986, 1987) found that properties of external perimeters of percolation clusters can be drastically changed by only a slight modification if the perimeter definition. They defined another, "unscreened," or "accessible" perimeter as the set of empty sites neighboring the occupied cluster sites and related to infinity through a chain of empty nearest neighbors only (in contrast to the "natural" hull definition allowing also for next-to-nearest-neighbors in the chain). The unscreened perimeter can be presented as the "hull of the hull" (see Fig. 7). The numerical result $d_u = 1.37 \pm 0.03$ (Grossman and Aharony, 1986) for the unscreened perimeter of a 2D percolation cluster was strongly different from the prediction of Eq. (2.13). A similar result for the modified perimeter, $d_u = 1.343 \pm 0.002$, was reported by Meakin and Family (1986). *F 7*

Saleur and Duplautier (1987) noticed that a "natural" hull, or a smart kinetic walk with the fractal dimension $d_h = 7/4$ is equivalent to a self-avoiding walk (SAW) at the Θ point describing a collapse transition of a polymer chain in a solvent (de Gennes, 1979a), which is an unstable tricritical point (Levine and Sarbach, 1985; Duplantier and Saleur, 1987). The Grossman-Aharony modification of the hull definition corresponds, in these terms, to an increase in the repulsive interaction of the polymer chain that drives its fractal dimension to the standard excluded-volume SAW value $d_{\mathrm{SAW}} = 4/3$ (Nienhuis, 1984).

In three dimensions, due to the multi-connected topology of the external boundary of a cluster, it was conjectured (Stauffer, 1979; Sokolov, 1986; Gouyet *et al.*, 1988; Strenski *et al.*, 1991) that the external hull comprises a finite fraction of the net cluster perimeter, hence the fractal dimensions of the cluster and of its hull are the same:

$$d_h = d_c = d - \beta/\nu \ , \quad d = 3 \ . \tag{2.14}$$

B. Scaling and distribution of percolation clusters

Percolation clusters belong to the class of random physical fractals (Gefen *et al.*, 1981; Mandelbrot and Given, 1984; Kapitulnik *et al.*, 1984). Here "random" is an opposite to "deterministic," which describes such regular structures as the Sierpinski carpet (Fig. 1). *F 1*
Unlike deterministic fractals, percolation clusters are not exactly but only statistically self-similar. "Physical," meaning an opposite to "mathematical," implies a finite range of this self-similarity. For a separate finite cluster, the scaling range is $[\lambda_0, a]$, where λ_0 is the period of the lattice and a is the size of the cluster. For the distribution of all clusters, the range of self-similarity is $[\lambda_0, \xi(p)]$ and at $p = p_c$ this range becomes infinite.

Given the "basic" exponents ν, which governs the behavior of the coherence length ξ (2.8e), and the infinite cluster density exponent β, the remaining critical exponents entering Eqs. (2.8) can be obtained phenomenologically, using scaling, or self-similarity arguments. To do so, we first find the asymptotics of the cluster density $n_s(p)$ for $s \gg 1$. Suppose $|p - p_c| \ll 1$, so that $\xi(p) \gg \lambda_0$. Let us call clusters of linear size lying between a and $2a$ the "a-clusters." Since there is no characteristic scale between λ_0 and $\xi(p)$, the density N_a of a-clusters (their number per unit volume) must behave algebraically with a, which is the only kind of dependence without a characteristic scale: $N_a \simeq (\lambda_0/a)^x$, $\lambda_0 < a < \xi(p)$. On the other hand, on scales $\lambda > \xi(p)$, the self-similarity is changed by the statistical uniformity in the cluster distribution that means that the $\xi(p)$-clusters have a density of approximately $\xi^{-d}(p)$. Thus x must equal the space dimension d and we find

$$N_a = C_1\, a^{-d}\,, \quad \lambda_0 \ll a \ll \xi(p)\,, \tag{2.15}$$

where C_1 is a coefficient of the order of unity. The distribution (2.15) implies a dense packing of a-clusters in space, for each $a \in [\lambda_0, \xi(p)]$. For $a > \xi(p)$, the algebraic dependence (2.15) is changed by an exponential decay (Stauffer, 1985). Notice that formula (2.15) is valid for both under- and supercritical cases. At $p > p_c$, the finite clusters lie in the holes inside

the infinite cluster, where the correlation length $\xi(p)$ is the maximum size of the hole. In other words, if the cluster size essentially exceeds the correlation length, this means that this cluster is almost surely infinite.

The density of a-clusters (2.15) enables us to calculate the distribution of clusters over masses. For the given size a, a-clusters have typically the mass $s(a) \simeq (a/\lambda_0)^{d_c}$, hence

$$N_a \simeq \sum_{s=s(a)}^{2s(a)} n_s \simeq s(a) n_{s(a)} \ . \tag{2.16}$$

Eqs. (2.15) and (2.16) lead to the following expression for the density of s-clusters:

$$n_s = C_2 \cdot s^{-\tau} \ , \ 1 \ll s \ll s(\xi) \ , \tag{2.17}$$

with the exponent (Stauffer, 1979)

$$\tau = 1 + \frac{d}{d_c} = \frac{2\nu d - \beta}{\nu d - \beta} \ . \tag{2.18}$$

The expression

$$s(\xi) = \left(\frac{\xi(p)}{\lambda_0} \right)^{d_c} = |p - p_c|^{-1/\sigma} \tag{2.19}$$

is the characteristic mass of the largest finite cluster, where

$$\sigma = \frac{1}{\nu d_c} = \frac{1}{\nu d - \beta} \ . \tag{2.20}$$

Known the distribution of clusters over masses (2.17), it makes no difficulty to calculate the rest of critical exponents defined in Eqs. (2.8). The result is

$$\alpha = 2 - \nu d \ , \quad \gamma = \nu d - 2\beta \ , \quad \delta = \frac{\nu d}{\beta} - 1 \ . \tag{2.21}$$

If one is interested in the cluster distribution both in the scaling region, $1 < s < s(\xi)$, and in the region of exponentiation decay, $s > s(\xi)$, a more general formulation of the self-similar distribution may be used. Stauffer (1979) gives the universal scaling in the form

$$n_s(p) = s^{-\tau} f\left((p - p_c) s^{\sigma}\right) \ , \quad |p - p_c| \ll 1 \ , \quad s \gg 1 \ , \tag{2.22}$$

where the universal function $f(z)$ is finite for $z \to 0$ and falls off exponentially for $|z| \to \infty$. Expression (2.22) is a generalization of our simple argument.

C. The universality of critical behavior

A fundamental concept in the physics of phase transitions is the universality of critical exponents. This concept reduces the enormous number of different models to a few universality classes, whose sets of critical indices are to be calculated and tabulated. This happy circumstance by no means implies that the calculation of the exponents is easy. In a sense, it is the job for the whole physics of critical phenomena (Domb *et al.*, 1972-1987). In these terms, the percolation problem belongs to one of the simplest universality classes, which is usually called the *universality class of random, or uncorrelated percolation.* It was established that the critical exponents ν and β, as well as all others, do not depend on the kind of the lattice (e.g., square, triangular, etc.) and the kind of the percolation problem (site or bond). The only "crude" parameter that affects the value of the exponents is the dimension d of the ambient space. This statement has been confirmed on a vast variety of numerical experiments and is not subject to any serious doubt. (About a partial violation of universality in continuum models see Sec. E.)

There may be seen a certain analogy between the universality of critical behavior in lattice models and the universal behavior of singularities of differentiable mappings studied in the framework of the catastrophe theory (Poston and Stewart, 1978; Arnold, 1983). In both cases the corresponding power exponents are structurally stable, that is, are unchanged under a small perturbation in the lattice model or the mapping, respectively. A principle difference between critical phenomena and universal catastrophes is that the critical exponents describe *long-range* (in real physical space) correlated behavior, whereas the catastrophe theory deals with the nonanalytical expansion of the inverse (with respect to the original differentiable mapping) *near* the singular point.

The property of the universality complies with the long-range self-similarity of percolation clusters. On spatial scales much longer than the lattice period λ_0, the fine texture of the

lattice is "invisible" and thus cannot affect the long-range scaling properties of clusters near the percolation threshold. This argument suggests that one may consider the percolation problem on an irregular lattice, or even without any lattice, and to expect the same critical behavior as in regular-lattice models. This leads to the idea of continuum percolation (Sec. E) that exhibits critical properties similar to those of the lattice percolation problem.

Not only lattice may be changed but also the rules of the game on it. Kertész *et al.* (1982) studied the percolation model with restricted valence. In this model, the number of occupied nearest neighbors of a site should not exceed the valence v; otherwise, the occupation of the site is prohibited. If v equals the coordination number of the lattice, the percolation is unrestricted. It was found that, while the percolation threshold depends on v, the correlation length exponent ν is invariant.

One may also test the patience of the universality in other manners. For example, the definition of the connectivity can be changed from the nearest-neighbor rule to the next-to-nearest neighbor, etc. The exponents of this *long-range percolation* studied by Quinn *et al.* (1976) and Hoshen *et al.* (1978) did not show any noticeable difference from those of the nearest-neighbor percolation. So much more surprising were the numerical results of Meakin and Family (1986) and Grossman and Aharony (1986, 1987) reporting the fractal dimension d_u of the external perimeter of a 2D percolation cluster, unambiguously less than $d_h = 7/4$, under only a slight modification in the definition of the perimeter (see Sec. A). This observation led Grossman and Aharony to assume a hierarchy of hull fractal dimensions depending on the definition of the hull. Saleur and Duplantier (1987) ruled out this possibility by arguing that only two perimeter exponents are possible, $d_h = 7/4$ (for the "natural hull" – SKW) and $d_u = 4/3$ (for the "unscreened perimeter" – SAW). This conjecture appears to recover (although a more sophisticated) concept of universality.

Into the same class of universality may fall problems of quite a different nature. Alexandrowicz (1980) proposed a model of a "critically branched self-avoiding walk" (CBSAW), which

belongs to the universality class of random percolation, meaning that some of the CBSAW critical characteristics scale similarly to those of percolation clusters. Such an ansatz appeared to be quite useful for the computation of clusters. In a similar sense, we will refer the contours of certain random potentials to the universality class of random percolation, meaning the same long-range scaling properties of the contours as those of the percolation hulls (see section III).

The term "uncorrelated percolation" is not accidental. Introducing gradually growing long-range correlations between sites or bonds, one will ultimately drive the percolation problem out of the boundaries of its uncorrelated universality class.

D. Correlated percolation

The standard formulation of the lattice percolation problem assumes independent occupation of sites characterized by the only parameter – the probability p. This simplified model does not take into account possible correlations which are present in most applications of interest. To allow for correlations, one can characterize the system by in infinite set of random variables θ_i, which are unity at occupied sites (i is the site nimber) and zero at vacant sites. The average value of θ_i is the occupation probability, $\langle\theta_i\rangle = p$. If θ_i are independent, then the standard ("random") percolation model is recovered. In general, the site correlations are characterized by the occupation correlation function

$$c_\theta(\mathbf{x}_i - \mathbf{x}_j) = \langle\theta_i\,\theta_j\rangle - p^2\ . \tag{2.23}$$

For the percolation model to be viable, the critical behavior should be insensitive to short-range correlations, when the correlation function (2.23) falls off sufficiently fast (say, exponentially) at large distance $|\mathbf{x}_i - \mathbf{x}_j| \to \infty$. Harris (1974) studied the effect of short correlations on the cluster scaling in the model of a phase transition with randomly fluctuating local critical temperature. He derived the following criterion of the irrelevance of the

fluctuations:

$$\nu > 2/d \ . \tag{2.24}$$

Using expression (2.21), the Harris criterion (2.24) can be equivalently written as $\alpha < 0$. The idea of this result is that a long-range, near-critical cluster behavior is determined by the occupation probability $p_\xi = \langle \theta_i \rangle_\xi$ averaged over the size of the order of the correlation length $\xi(p)$. The fluctuation of p_ξ can be estimated using the standard "$N^{-1/2}$ rule" where $N \propto \xi^d$ is proportional to the number of sites in a box with the size ξ_p: $\delta p_\xi / p_\xi \propto \xi^{-d/2}$. If we now require that δp_ξ be less than the critical proximity $|p - p_c| \propto \xi^{-1/\nu}$, then we arrive at inequality (2.24). As this criterion is fulfilled in any dimension (see table III), *T III* we conclude that short-range correlations do not drive the percolation problem from its standard universality class. In a more general context, the Harris criterion (2.24) determines the condition of the irrelevance of short-range "quenched" disorder for critical behavior (Weinrib and Halperin, 1983).

The critical behavior, however, can drastically change for *correlated percolation*, when the occupancy of different sites are long-range correlated. Mathematically, this is expressed in a slow (e.g., algebraic) decay of the correlation function (2.23). One such example is the Ising model where the probabilities are proportional to the Boltzmann factor $\exp(-E/T)$ with the energy E determined self-consistently from the resulting distribution of sites (Coniglio *et al.*, 1977; Penrose *et al.*, 1978). This analogy is straightforward only in two dimensions, where the critical points of the magnetic and the percolation transition are the same (in 3D they are different).

In another approach to correlated percolation (Weinrib, 1984) the occupation probabilities p_i are considered random numbers defined by their average $\langle p_i \rangle = p$ and the correlation function

$$c_p(\mathbf{x}_i - \mathbf{x}_j) = \langle p_i \, p_j \rangle - p^2 \ . \tag{2.25}$$

So this formulation involves a two-step process: first, random p_i are drawn for each site, then the site occupancy is generated according to the probabilities p_i : $\theta_i = \theta(p_i - r)$, where r is a random variable uniformly distributed in $[0,1]$ and $\theta(x)$ is the Heaviside step-function. Substituting the expression for θ_i into Eq. (2.23) we conclude that the two correlation functions are the same: $c_\theta(\boldsymbol{\rho}) = c_p(\boldsymbol{\rho}) \equiv c(\boldsymbol{\rho})$.

It is believed that, although insufficient for a complete characterization of the distribution of p_i, the two-point correlation function $c(\boldsymbol{\rho})$ contains enough information to determine the critical behavior. For an algebraically decaying correlation, $c(\boldsymbol{\rho}) \propto \rho^{2H}$, $H < 0$, the criterion of universality can be obtained analogously to the Harris criterion (2.24). Here, the fluctuation of the ξ-scale-averaged occupation probability p_ξ is calculated as

$$\delta p_\xi = \left(\left\langle (p_i - p)^2 \right\rangle_\xi \right)^{1/2} \propto \left(\xi^{-d} \int_0^\xi c(\rho) \rho^{d-1} d\rho \right)^{1/2} \propto \xi^H \ , \tag{2.26}$$

and instead of (2.24) we obtain the following criterion of the irrelevance of correlations:

$$H < -1/\nu \ . \tag{2.27}$$

For a slower fall-off of the correlation function, $-1/\nu < H < 0$, the percolation problem becomes essentially correlated. In this case, the critical behavior becomes different, in particular, the exponent ν is replaced by a new one (Weinrib and Halperin, 1983; Weinrib, 1984),

$$\tilde{\nu}(H) = -1/H > \nu \ , \quad -1/\nu < H < 0 \ . \tag{2.28}$$

Here the tilde distinguishes the correlated percolation exponent from that of the uncorrelated percolation. Result (2.28) corresponds to the threshold proximity $|p - p_c|$ balanced by the probability fluctuation (2.26).

Isichenko and Kalda (1991b) have used a heuristic scale-separation method to conjecture that beta exponent of correlated percolation is the same as in random percolation,

$$\tilde{\beta}(H) \equiv \beta \ , \quad -1/\nu < H < 0 \ . \tag{2.29}$$

The same method applied to the 2D hull exponent evaluation leads to the result (see Sec. III.E)

$$\tilde{d}_h(H) = 1 + (1-H)(d_h - 1)\frac{\nu}{\nu+1} = \frac{10-3H}{7}\ , \quad d = 2\ , \quad -1/\nu < H < 0\ , \qquad (2.30)$$

The correlated hull exponent (2.30) is identified with the fractal dimension of a contour line of a random function with an algebraic covariance. As a three-dimensional hull has the same fractal dimension as the cluster, we conclude analogously to (2.14) that

$$\tilde{d}_h(H) = \tilde{d}_c(H) = d - \tilde{\beta}(H)/\tilde{\nu}(H) = 3 + \beta H\ , \quad d = 3\ , \quad -1/\nu < H < 0\ . \qquad (2.31)$$

The correlated percolation exponents are given in table V. For correlated percolation, *T V* the same scaling arguments are valid as those used in the random percolation problem. In particular, one can calculate other correlated exponents, $\tilde{\alpha}$, $\tilde{\gamma}$, $\tilde{\delta}$, using relations similar to (2.21). Notice that formula (2.13) for the hull exponent cannot be simply generalized for the correlated percolation problem, as well as for higher dimensions. Relations (2.13) and (2.30) are not consequences of scaling arguments but rather first-principle results.

E. Continuum percolation

Although the lattice formulation of the percolation problem is very convenient for both analytical and numerical studies, most natural disordered systems lack perfect lattice structure and require a different approach. The universality of percolation critical exponents well stands moderate violence such as introducing short-range correlations or changing the type of lattice within the same dimensionality. This invokes the idea that the very existence of a lattice is not necessary. The *continuum percolation problem* has various formulations, among which the following three are the most popular.

(a) In the *problem of voids*, or "Swiss-cheese" model (Halperin *et al.*, 1985), equally-sized or size-distributed spherical voids are placed at random in a uniform transport medium (Fig. 8). The spherical holes are allowed to overlap with one another. At a critical value *F 8*

of the hole-volume fraction, the infinite cluster of the underlying medium ceases to exist, and the system fails to support any transport or exhibit a mechanical rigidity. The "Swiss-cheese" model may be appropriate to describe transport and elastic properties of porous media.

(b) In the *problem of spheres*, or "inverted Swiss-cheese" model, also known as the *problem of random sites* (Skal and Shklovskii, 1973; Pike and Seager, 1974), the roles of the two different media are switched: The spheres support the transport and the substrate does not (Fig. 9). One may introduce a "hard core" to model an "excluded volume" repulsive interaction between the spheres (Gawlinski and Redner, 1983; Balberg, 1987). Such interaction is nothing more than a short-range correlation, which can shift the percolation threshold but clearly leaves the critical exponents intact. At a critical filling factor, $\eta = (4/3)\pi nr^3$ for $d = 3$, and $\eta = \pi nr^2$ for $d = 2$ (n is the density and and r the radius of the spheres or discs), the overlapping spheres form an infinite cluster and the system is able to support a long-range current. It was found that the critical parameter equals $\eta_c \simeq 1.1$ in two, and $\eta_c \simeq 0.35$ in three dimensions (see table V). The percolation threshold η_c is only slightly changed by the interaction of spheres (Pike and Seager, 1974; Bug *et al.*, 1985). The fraction ϕ of volume occupied by randomly overlapping objects is less than η (and of course $\phi < 1$) and is determined by the formula (Shante and Kirkpatrick, 1971)

F 9

T V

$$\phi = 1 - \exp(-\eta) \,, \tag{2.32}$$

which is valid in the limit of a large number of objects. The model of random sites was used to describe hopping conduction in doped semiconductors (Shklovskii and Efros, 1984) and phase transitions in ferromagnetics (Abrikosov, 1980).

(c) In the *potential model*, a smooth random function $\psi(\mathbf{x})$ is considered, and one is interested in the geometry of regions where $\psi(\mathbf{x}) \leq h$ =const (see Fig. 10). This model was invoked for the processes of localization of quasi-classical electrons (Ziman, 1969; Zallen and

F 10

Scher, 1971) where $\psi(\mathbf{x})$ is the potential created by disordered impurities and h is the energy of an electron. The inequality $\psi(\mathbf{x}) \leq h$ specifies the classically allowed area for the electron. Above a critical energy level $h = h_c$, a connected subset (cluster) of the allowed region stretches to infinity, and electrons can conduct electric current, otherwise, on a macroscopic scale, the system behaves like an insulator. The potential model is also relevant for the quantized Hall effect (Trugman, 1983). To describe critical levels of the potential continuum model, Zallen and Scher (1971) used the compelling image of a "flooded landscape," where $\psi(x, y)$ denotes the elevation of the Earth's relief and h the water level, so that the inequality $\psi(x, y) \leq h$ describes the flooded area. At sufficiently low h, one clearly has "ponds" and "lakes" in an infinite land (Fig. 10(a)), whereas at higher level there will be localized islands *F 10a* in an infinite ocean (Fig. 10(c)). The specific of two-dimensional geometry implies the *F 10c* impossibility of the simultaneous existence of both land and marine paths to infinity for a generic isotropic landscape. This leads to the existence of a sharp transition at $h = h_c$ from percolating land to percolating ocean, when the last infinite land path disappears and the first infinite see path is conceived. Thus at this critical level $h = h_c$ there does exist an infinite coastline — a contour of the potential $\psi(x, y)$ (Fig. 10(b)). For a random function *F 10b* $\psi(\mathbf{x})$, which is statistically equivalent to $-\psi(\mathbf{x})$ (without any loss of generality we may put the average $\langle\psi(\mathbf{x})\rangle = 0$), the sign-symmetry leads to the critical level $h_c = 0$ and the volume-occupation fraction $\phi_c = \int_{-\infty}^{h_c} P(\psi)d\psi = 1/2$, where $P(\psi)$ is the distribution function of $\psi(\mathbf{x})$ (Zallen and Scher, 1971). This result is due to the unique value of the percolation level in two dimensions. In three-dimensional case, there may exist simultaneous percolation through "3D land" and "3D ocean," since the topology of space admits non-intersecting, statistically isotropic paths to infinity. So one may introduce two percolation levels, $h_{c1}(\equiv h_c)$ and h_{c2}, such that for $h < h_{c1}$ there is percolation only through "land" (i.e., the region $\psi(\mathbf{x}) > h$), for $h > h_{c2}$ only through "sea" ($\psi(\mathbf{x}) < h$), and in the interval $h_{c1} < h < h_{c2}$ the "sea" and the "land" percolate simultaneously. For a sign-symmetric distribution of $\psi(\mathbf{x})$, one has

$h_{c1} = -h_{c2} \neq 0$ (Shklovskii and Efros, 1984).

Zallen and Scher (1971) proposed to use instead of the level h the fraction of "wet" volume,

$$\phi = \phi(h) = \int_{-\infty}^{h} P(\psi)d\psi \ , \tag{2.33}$$

where $P(\psi)$ is the probability distribution function of the random potential. The critical area fraction, $\phi_c = 1/2$, which is the case for a 2D sign-symmetrical (i.e. $P(\psi) = P(-\psi)$) potential, is somewhat higher than the critical space occupation probability for lattices (Scher and Zallen, 1970), ϕ_c(2D lattice) $= 0.44 \pm 0.02$. Unlike the critical level h_c, the three-dimensional value of $\phi_c \simeq 0.15$ (Zallen and Scher, 1971) is much more universal with respect to particular models of the potential. This quantity turned out to be very close to the corresponding lattice critical volume-fraction, ϕ_c(3D lattice) $= 0.154 \pm 0.005$. Skal *et al.* (1973) confirmed this conjecture by calculating ϕ_c for several different Gaussian 3D potentials, which all gave very close results: $\phi_c = 0.17 \pm 0.01$. The percolation thresholds of continuum models are summarized in table VI. *T VI*

It was established (Pike and Seager, 1974; Geiger and Stanley, 1982; Elan *et al.*, 1984) that static exponents describing the geometrical properties of continuum clusters near the percolation threshold are the same as for lattice models in the same dimension. The dynamic exponents, on the contrary, were found to be not universal, varying from one continuum model to another. (There does exist the universality of the transport exponents within the subclass of lattice models.) Feng *et al.* (1987) explained the universality of static exponents and the nonuniversality of dynamic exponents using mapping of continuum models onto irregular-lattice models.

The Swiss-cheese model is mapped onto the bond percolation on a lattice whose bonds are the boundaries of the Voronoi polyhedra constructed around the voids (Elan *et al.*, 1984). A bond is blocked if the corresponding pair of voids are overlapping (Fig. 8). In the inverted *F 8* Swiss-cheese model, the sites of the equivalent lattice lie in the centers of the spheres (Fig. 9). *F 9*

The mapping of the potential model onto a lattice was proposed by Ziman (1969) and, more explicitly, by Weinrib (1982). In these constructions, the sites are associated with the local minima of $\psi(\mathbf{x})$, and the bonds come through saddle points connecting two valleys (Fig. 10(d)). Then the contour lines are the external and internal perimeters of the bond *F 10d* percolation clusters on the equivalent (irregular) lattice. Two neighboring flooded valleys form a connected lake if the water level h exceeds the elevation ψ_s of the mountain pass (saddle) between them. So the inequality $\psi_s < h$ means that the bond coming through the saddle is conducting, whereas at $\psi_s > h$ it is blocked: $\theta_i = \theta(h - \psi_s(\mathbf{x}_i))$. The bond probability $p(h) = \langle \theta_i \rangle$ is then given by

$$p(h) = \int_{-\infty}^{h} P_s(\psi_s) d\psi_s \ , \tag{2.34}$$

where $P_s(\psi_s)$ is the distribution function of saddle point elevations. Similarly, the bonds on the equivalent lattice for the potential $-\psi(\mathbf{x})$ connect maxima of $\psi(\mathbf{x})$ and come through its saddles. In two dimensions, through a non-degenerate saddle point come only two (mutually perpendicular) steepest descent lines, hence the equivalent lattice of $-\psi(\mathbf{x})$ matches that of $\psi(\mathbf{x})$ (see Fig. 10(d)). In the case of a statistically sign-symmetric potential $\psi(\mathbf{x})$ when the *F 10d* critical probabilities of these two lattices are the same, we obtain $p_c = 1/2$, hence $h_c = 0$.

Gruzinov *et al.* (1990) used an approach where one starts from a degenerate, periodic potential $\psi(\mathbf{x})$ and then the degeneracy is lifted by a small random perturbation (Fig. 11). *F 11* This procedure maps the potential continuum problem onto the standard regular-lattice percolation.

The existence of these mappings clearly explains the universality of static critical exponents in the absence of long correlations in the potential $\psi(\mathbf{x})$. In Sec. III.C we show that the criterion for the universality of critical behavior in the potential continuum model is a sufficiently fast decay of the correlator,

$$C(\boldsymbol{\rho}) = \langle \psi(\mathbf{x} + \boldsymbol{\rho}) \psi(\mathbf{x}) \rangle = O(\rho^{-1/\nu}) \ . \tag{2.35}$$

For the power behavior $C(\rho) \propto \rho^{2H}, \quad -1/\nu < H < 0$, the continuum potential model is mapped onto the correlated percolation problem (Sec. D).

Regarding the dynamic characteristics, their universality may break, even at universal static exponents, due to broadly varying "strengths of the bonds" resulting from the mapping. Consider, for example, the Swiss-cheese model. Random overlapping of voids leads to randomly varying widths of "necks" (bonds) passing between three neighboring spherical holes (Fig. 8(b)). The probability distribution of the neck widths remains finite for the *F 8b* width tending to zero, hence the equivalent lattice resistor network has a broad (power-law) distribution of the bond resistances, in contrast to the standard lattice problem where each resistance is either zero or one. This state of affairs leads to a possible change in transport exponents (Sen *et al.*, 1984; Halperin *et al.*, 1985; Bunde *et al.*, 1986; Lubensky and Tremblay, 1986; Machta *et al.*, 1986). Feng *et al.* (1987) analyzed the bond strengths and found that, in all three two-dimensional continuum models, the conductivity exponent μ is the same as in a standard lattice model, whereas in the 3D Swiss-cheese model μ exceeds its lattice counterpart. The inverted Swiss-cheese model and the potential model preserve the universal (lattice) value of the conductivity exponent μ in three dimensions. A similar analysis was done for the elasticity and permeability exponents.

Due to the diversity of various continuum models, of which we discussed only simplest ones, the concept of the universality in continuum has a broader sense. Here, the universality means the invariance of critical exponents with respect to gradually changed parameters of the random ensemble (voids, potentials, etc.), provided that these parameters lie within well-defined boundaries of the corresponding universality class. In other words, the critical exponents are piecewise constant functions of the parameters of the model. In these terms, the correlated percolation is not universal because its critical exponents (2.27)–(2.30) continuously depend on the parameter H. One may call such a behavior a "continuous universality class."

Another approach to the concept of universality can be suggested that does not deal with an ensemble. Instead, a particular realization of, say, potential $\psi(\mathbf{x})$ can be considered and the corresponding critical indices introduced. Thene the potential is infinitesimally perturbed by a smooth perturbation, whose correlator decays sufficiently fast, and the new critical exponents are determined. If for any such perturbation the exponents remain *exactly the same*, then the initial potential $\psi(\mathbf{x})$ is said to be structurally stable. The concept of structural stability is the central one in the catastrophe theory (Poston and Stewart, 1978; Arnold, 1978, 1983). In various applications, one is usually concerned with not an ensemble of random potentials, but rather with a unique, but *generic* realization, if there are no special reasons for the potential to be degenerate in one way or another. The intuitive notion of "generic" corresponds to the well-formalized concept of "structurally stable."

For a structurally unstable (degenerate) function, critical behavior may be different. Trugman and Weinrib (1985) proposed an interesting example of continuous percolation for the potential $W(\mathbf{x}) = [\psi(\mathbf{x}) - h_0]^2$, where h_0 equals the critical level of $\psi(\mathbf{x})$. Such a system exhibits an exotic behavior: Its percolation threshold is zero in terms of both the critical level h_c and the critical volume fraction ϕ_c, and the exponents are different from those of the universality class of random percolation. The "$\phi_c = 0$" potential $W(\mathbf{x})$ is structurally unstable: any mismatch of h_0 from the critical level of $\psi(\mathbf{x})$ drives the problem to the universality class of standard percolation.

In summary, the continuum percolation problem treats the connectivity properties of randomly distributed objects that has much in common with the lattice percolation. Specifically, the contour lines and surfaces of a random potential are associated with the hulls of percolation clusters. In the next section, we discuss the statistics of contours in more detail. For various applications, one may also be interested in the geometry of more complicated objects such as the regions occupied by level contours with diameters of the given order a, regardless of the level h. These issues will be discussed in the framework of a more general

statistical topography, for which the continuum percolation should be regarded a prerequisite.

III. STATISTICAL TOPOGRAPHY

The term "statistical topography" was introduced by Ziman (1979) for the theory of the shapes of random fields, with a special emphasis on the contour lines and surfaces of a random potential $\psi(\mathbf{x})$. One of the first studies on this subject was undertaken by Rice (1944, 1945), who was basically concerned with random functions of one variable, in respect with the noise effect on telephone transmission. For Gaussian noise amplitude $\psi(t)$, Rice derived the expected frequency of the crossings $\psi(t) = h$, for a given sensitivity threshold h. Longuet-Higgins (1957a, 1957b, 1957c, 1957d) generalized Rice's approach for a two-dimensional random function $\psi(x, y)$ and applied its topographic properties to the specks and twinkles on a random water surface (Longuet-Higgins, 1960a, 1960b, 1960c). The statistics of contour lines was also invoked for studying the information contents of two-dimensional images, for example, in television (Swerling, 1962). A mathematical survey of the statistical topography of Gaussian random fields was given by Adler (1981).

The most compelling example of the statistical topography is presented by the diverse and whimsical patterns of natural coastlines and islands. The geographical considerations inspired Mandelbrot (1967) to introduce the concept of fractals. After enjoying a considerable descriptive success, this approach gained a predictive force with introducing the "fractional Brownian functions" (Mandelbrot 1975b; Berry and Hannay, 1978; Berry and Lewis, 1980). These functions possess a power Fourier spectrum in a wide range of wavelengths. In turbulent media, such fields are usually described by Kolmogorov-type spectra (Zakharov, 1984). In particular, this kind of spectrum for gravity waves leads to fractal water surfaces (Stiassnie *et al.*, 1991).

Another approach to the problem of the statistical topography has been developed, without any apparent connection with the information theory, environmental studies, or turbulence, in the solid-state-physics community (Ziman, 1969; Zallen and Scher, 1971; Skal and

Shklovskii, 1973), on the basis of the (continuum) percolation theory. Study of the electronic structure of disordered materials motivated the "monoscale" percolation approach since both the crystalline lattice and known concentration of impurities suggest a well-defined characteristic scale of the problem. Ziman (1969) was the first to draw attention to the isosurfaces of random potentials that embrace classically accessible regions for the electron motion in a disordered potential. General as the correspondence principle between the quantum and classical mechanics might seem, there is, however, no apparent relation between this quasi-classical localization and the intrinsically quantum effect of the Anderson localization of the electron wave-function (Anderson, 1958; Thouless, 1974). An exclusion appears to be a two-dimensional electron gas in a strong magnetic field (Trugman, 1983) experimentally realized with a metal-oxide-semiconductor field-effect transistor (MOSFET) (Prange and Girvin, 1990). This system has drawn much attention in the last decade since the discovery of the quantized Hall effect (von Klitzing *et al.*, 1980).

More classical effects, whose behavior depends on random isolines, include anomalous diffusion in turbulent plasmas (Kadomtsev and Pogutse, 1979; Isichenko, 1991b; Isichenko and Horton, 1991) and the magnetoresistance of inhomogeneous plasmas and semiconductors (Dreizin and Dykhne, 1972; Isichenko and Kalda, 1991a).

The investigation of transport processes in some random media requires detailed information of the distribution of random contours, whereas the random potential often possesses many length-scales. The percolation approach has been combined with the multiscale spectral description in Isichenko and Kalda (1991b) where a heuristic method of the "separation of scales" was used to develop the statistical topography of power-spectrum random functions.

This section is organized as follows. In Sec. A the spectral and correlation properties of random functions are described and a discussion is given of the behavior of Gaussian random fields. In Sec. B the fractional Brownian approach is presented. In Sec. C we briefly return

to monoscale reliefs to more generally restate their topographic properties related to the percolation problem. Section D is devoted to the continuum problem of "graded percolation" corresponding to a monoscale potential with a small average gradient. In Sec. E the approach of the separation of scales is described in the context of the multiscale statistical topography. In Sec. F the statistical properties of the separatrices of random potentials are discussed.

A. Spectral description of random potentials and Gaussianity

Discussing a random potential $\psi(\mathbf{x})$, we should be more specific and determine what exactly is random in ψ and what is not. Since we are particularly interested in the spatial geometry of the potential, the first idea is to characterize ψ by a correlation function (covariance)

$$C(\boldsymbol{\rho}) = \langle \psi(\mathbf{x})\psi(\mathbf{x}+\boldsymbol{\rho}) \rangle \ , \tag{3.1}$$

or by a delta-variance,

$$\Delta(\boldsymbol{\rho}) \equiv \left\langle [\psi(\mathbf{x}) - \psi(\mathbf{x}+\boldsymbol{\rho})]^2 \right\rangle = 2\,[C(0) - C(\boldsymbol{\rho})] \ . \tag{3.2}$$

Here the angular brackets denote averaging over the statistical ensemble of ψ. It is assumed that expressions (3.1) and (3.2) do not depend on $\mathbf{x}$, that is, the random potential $\psi(\mathbf{x})$ is stationary. For stationary random fields, the ensemble-average is the same as the space-average (over $\mathbf{x}$) for almost any realization of ψ (the ergodicity property). "For almost any" means "with the probability one."

For a general random field, the two-point correlation function (3.1) is insufficient to completely characterize the statistical ensemble. For a comprehensive information about $\psi(\mathbf{x})$ one needs to know the whole sequence of the three-point, four-point, etc., correlation functions. For a Gaussian random potential, on the contrary, all properties of the ensemble can be extracted from the average $\langle \psi(\mathbf{x}) \rangle$ and the correlator $C(\boldsymbol{\rho})$. A standard approach is to use the Fourier expansion as first principle and to consider the Fourier components $\psi_{\mathbf{k}}$ to be independent random variables. Suppose the function $\psi(\mathbf{x})$ to be periodic with a

sufficiently large period $\mathcal{L}$ along each coordinate axis in a d-dimensional space. Then the Fourier series expansion,

$$\psi(\mathbf{x}) = \sum_{\mathbf{k}} \psi_{\mathbf{k}}\, e^{i\mathbf{k}\mathbf{x}} \,, \tag{3.3}$$

is taken over the wavevectors $\mathbf{k}$ lying in the nodes of a d-dimensional simple cubic lattice with the period $k_{\mathcal{L}} = 2\pi/\mathcal{L}$. Suppose the following statistical properties of the Fourier harmonics:

$$\langle \psi_{\mathbf{k}} \rangle = 0 \,, \quad \langle \psi_{\mathbf{k}} \psi_{\mathbf{k}'} \rangle = P_{\mathbf{k}} \delta_{\mathbf{k}+\mathbf{k}'} \,. \tag{3.4}$$

We will focus primarily on the case when the spectral density $P_{\mathbf{k}}$ is an isotropic power function inside a wide wavenumber range $[k_m, k_0]$,

$$P_{\mathbf{k}} \equiv \left\langle |\psi_{\mathbf{k}}|^2 \right\rangle = k_{\mathcal{L}}^d\, A k^{-\gamma} \,, \quad k_{\mathcal{L}} \ll k_m < k < k_0 \,, \tag{3.5}$$

and $P_{\mathbf{k}}$ falls out sufficiently fast outside this interval. It is convenient to divide the scaling range $[k_m, k_0]$ into $\log_2(k_0/k_m)$ octaves and to represent the "multiscale" potential $\psi(\mathbf{x})$ as a sum of "monoscale" functions,

$$\psi(\mathbf{x}) = \sum_{\lambda_i = 2^i \lambda_0} \psi_{\lambda_i}(\mathbf{x}) \,, \tag{3.6}$$

where the λ-component $\psi_\lambda(\mathbf{x})$ is defined by the partial sum

$$\psi_\lambda(\mathbf{x}) = \sum_{\frac{1}{2} < |\mathbf{k}|\lambda < 1} \psi_{\mathbf{k}}\, e^{i\mathbf{k}\mathbf{x}} \tag{3.7}$$

and represents a function with a single characteristic length λ. Then the Fourier ($\mathbf{k}$-) spectrum (3.5) corresponds to the "λ-spectrum"

$$\psi_\lambda \equiv [\psi_\lambda(\mathbf{x})]_{\rm rms} = \left(\sum_{\frac{1}{2} < |\mathbf{k}|\lambda < 1} P_{\mathbf{k}} \right)^{1/2} \,. \tag{3.8}$$

Replacing the sum in Eq. (3.8) by integral according to the usual rule $\sum_{\mathbf{k}} \to k_{\mathcal{L}}^{-d} \int d\mathbf{k}$, we obtain

$$\psi_\lambda = A_1\, \lambda^H \,, \quad \lambda_0 \ll \lambda \ll \lambda_m \,, \tag{3.9}$$

$$H = \frac{(\gamma - d)}{2} , \tag{3.10}$$

$$A_1 = \left[A\, S_d \frac{(2^{2H} - 1)}{2H} \right]^{1/2} , \tag{3.11}$$

where $\lambda_0 \equiv k_0^{-1}$, $\lambda_m \equiv k_m^{-1}$, and the numerical factor S_d equals 1 (for $d = 1$), 2π (for $d = 2$), or 4π (for $d = 3$).

The representation of the λ-spectrum (3.7)–(3.9) is convenient because the potential covariance (3.1) and the delta-variance (3.2) are expressed through the exponent H in a universal way for each dimension d. Using Fourier expansion, expression (3.1) is rewritten as

$$C(\boldsymbol{\rho}) = 2 \sum_{\mathbf{k}} P_{\mathbf{k}}\, e^{i\mathbf{k}\boldsymbol{\rho}} . \tag{3.12}$$

The integral over $\mathbf{k}$ corresponding to the sum in (3.12) converges on both limits (so that we may put $k_m = 0$, $k_0 = \infty$ without significant change in result), if $-(d+1)/4 < H < 0$ ($d = 1, 2,$ or 3). Then we have

$$C(\boldsymbol{\rho}) = \zeta_d\, A \rho^{2H} , \quad \lambda_0 \ll \rho \ll \lambda_m , \tag{3.13}$$

where

$$\zeta_1 = 2\Gamma(-2H)\cos\pi H , \quad \zeta_2 = \frac{\pi\Gamma(-H)}{2^{2H}\,\Gamma(1+H)} , \quad \zeta_3 = -\frac{2\pi^2}{\Gamma(2H+2)\sin\pi H} , \tag{3.14}$$

and Γ denotes the Euler gamma function. Similarly, the series for the delta-variance,

$$\Delta(\boldsymbol{\rho}) = 2 \sum_{k} P_{\mathbf{k}}(1 - e^{i\mathbf{k}\boldsymbol{\rho}}) , \tag{3.15}$$

converges insensitive to k_m and k_0 for $0 < H < 1$ and equals

$$\Delta(\boldsymbol{\rho}) = \eta_d\, A \rho^{2H} , \quad \lambda_0 \ll \rho \ll \lambda_m , \tag{3.16}$$

with the numeric coefficients

$$\begin{aligned} \eta_1 &= \frac{2\pi}{\Gamma(2H+1)\sin\pi H} , \quad \eta_2 = \frac{\pi\,\Gamma(1-H)}{2^{2H-1}\,H\,\Gamma(1+H)} , \\ \eta_3 &= \frac{2\pi^2}{(2H+1)\Gamma(2H+1)\sin\pi H} . \end{aligned} \tag{3.17}$$

Thus, the correlation function is a convenient spectral characteristic for negative H, whereas for $0 < H < 1$ the delta-variance turns out to be more convenient.

A random potential defined by Fourier series (3.3) with independent random Fourier components $\psi_{\mathbf{k}}$ belongs to the important class of Gaussian random functions. Indeed, according to the *Central limit theorem*, a sum of a large number of independent random variables is distributed with the Gaussian probability distribution function

$$P(\psi) = (2\pi\,\psi_0^2)^{-1/2}\,\exp\left(-\frac{(\psi - \langle\psi\rangle)^2}{2\psi_0^2}\right)\,, \tag{3.18}$$

where ψ is the value of the potential at a fixed point $\mathbf{x}$. The Gaussian distribution (3.18) is completely defined by two parameters: the expectation $\langle\psi\rangle$ and the variance $\psi_0^2 \equiv \langle(\psi - \langle\psi\rangle)^2\rangle$. Gaussian random variables have the nice feature of additivity: A sum of several Gaussian random variables is also Gaussian with both the expectation and the variance being the sum of the expectations and the variances of the constituents, respectively. Furthermore, the joint probability distribution of several Gaussian random variables ψ_i, $i = 1, \ldots, n$, is given by the *multivariate Gaussian distribution* (Adler, 1981)

$$P(\psi_1, \ldots, \psi_n) = (2\pi)^{-n/2}(\det\, C_{ij})^{-1/2}\,\exp\left(-\frac{1}{2}\sum_{i,j=1}^{n}(\psi_i - \langle\psi_i\rangle)\,C_{ij}^{-1}\,(\psi_j - \langle\psi_j\rangle)\right)\,, \tag{3.19}$$

where

$$C_{ij} = \langle(\psi_i - \langle\psi_i\rangle)\,(\psi_j - \langle\psi_j\rangle)\rangle \tag{3.20}$$

is the covariance matrix, and C_{ij}^{-1} denotes the element of the inverse matrix. Notice that the multivariate Gaussian distribution (3.19) is completely determined by the first- and second-order moments of the participating variables, that is, by the expectations $\langle\psi_i\rangle$ and the covariance matrix C_{ij}. Specifically, a stationary Gaussian random field $\psi(\mathbf{x})$ is completely defined by its average (without loss of generality put $\langle\psi\rangle = 0$) and its correlation function (3.1). Given $C(\boldsymbol{\rho})$, we can simply calculate the two-point probability density $P(\psi_1, \psi_2|\mathbf{x}_1, \mathbf{x}_2)$, which quantity is defined through the probability $P(\psi_1, \psi_2|\mathbf{x}_1, \mathbf{x}_2)d\psi_1 d\psi_2$ for the potential

value $\psi(\mathbf{x}_1)$ to be within the interval $[\psi_1, \psi_1+d\psi_1]$ simultaneously with $\psi(\mathbf{x}_2) \in [\psi_2, \psi_2+d\psi_2]$. Substituting $\psi_1 = \psi(\mathbf{x}_1)$, $\psi_2 = \psi(\mathbf{x}_2)$ into Eqs. (3.19)–(3.20) we have

$$P(\psi_1, \psi_2|\mathbf{x}_1, \mathbf{x}_2) = \frac{1}{2\pi\sqrt{\psi_0^4 - C^2(\boldsymbol{\rho})}} \exp\left(-\frac{\psi_0^2(\psi_1^2+\psi_2^2) - 2C(\boldsymbol{\rho})\psi_1\psi_2}{2(\psi_0^4 - C^2(\boldsymbol{\rho}))}\right) , \qquad (3.21)$$

where $\boldsymbol{\rho} = \mathbf{x}_1 - \mathbf{x}_2$ and the variance $\psi_0^2 = C(0)$. In the limiting cases $\rho \to 0$ $(C(\boldsymbol{\rho}) \to \psi_0^2)$ and $\rho \to \infty$ $(C(\boldsymbol{\rho}) \to 0)$, expression (3.21) reduces to

$$P(\psi_1, \psi_2|\mathbf{x}_1, \mathbf{x}_2) = \begin{cases} P(\psi_1)\,\delta(\psi_1 - \psi_2) , & \rho \to 0 , \qquad (3.22a) \\ P(\psi_1)P(\psi_2)\left(1 + \dfrac{\psi_1\psi_2}{\psi_0^4}C(\boldsymbol{\rho}) + \ldots\right) , & \rho \to \infty . \qquad (3.22b) \end{cases}$$

Equation (3.22a) corresponds to the identical distribution of ψ_1 and ψ_2, ones the points $\mathbf{x}_1$ and $\mathbf{x}_2$ become the same, whereas (3.22b) implies asymptotically independent distribution of ψ_1 and ψ_2 in the limit of infinitely remote (uncorrelated) points $\mathbf{x}_1$ and $\mathbf{x}_2$. Three-point and higher probability densities can be calculated in quite a similar manner.

Analogously, one can calculate individual and joint distributions of various random quantities, such as the elevation ψ, the slope $\boldsymbol{\nabla}\psi$, etc. Differentiating Eq. (3.1) with respect to $\boldsymbol{\rho}$, we obtain

$$\left\langle \psi^2(\mathbf{x}) \right\rangle = C(0) , \quad \langle \psi(\mathbf{x})\boldsymbol{\nabla}\psi(\mathbf{x}) \rangle = \frac{\partial C(0)}{\partial \boldsymbol{\rho}} , \quad \langle \nabla_i\psi(\mathbf{x})\nabla_k\psi(\mathbf{x}) \rangle = -\frac{\partial^2 C(0)}{\partial\rho_i\partial\rho_k} . \qquad (3.23)$$

Expressions (3.23) can be used to calculate the expected measure $M_d(h)$ of the iso-set $\psi(\mathbf{x}) = h$ per unit volume. In d dimensions, the iso-set is characterized by a $(d-1)$-dimensional measure: the number of crossings $\psi(x) = h$ for $d = 1$, the total length of the contours $\psi(x, y) = h$ for $d = 2$, and the total area of the isosurfaces $\psi(x, y, z) = h$ for $d = 3$. Quantity $M_d(h)$ equals the modulus of $\boldsymbol{\nabla}\psi(\mathbf{x})$ averaged over the joint distribution of ψ and $\boldsymbol{\nabla}\psi$ at the given level $\psi = h$ (Rice, 1944, 1945; Longuet-Higgins, 1957a; Swerling, 1962):

$$M_d(h) = \langle |\boldsymbol{\nabla}\psi| \rangle_{\psi=h} \equiv \int |\boldsymbol{\nabla}\psi| P(h, \boldsymbol{\nabla}\psi) d\boldsymbol{\nabla}\psi , \qquad (3.24)$$

where $P(\psi, \nabla\psi)$ is the joint probability distribution function of ψ and $\nabla\psi$ at the same point $\mathbf{x}$. Using formulas (3.19)–(3.20) for the isotropic case $C(\boldsymbol{\rho}) = C(\rho)$, we obtain

$$P(\psi, \nabla\psi) = \frac{1}{(2\pi)^{(d+1)/2}\psi_0\psi_0'^d} \exp\left(-\frac{\psi^2}{2\psi_0^2} - \frac{(\nabla\psi)^2}{2\psi_0'^2}\right) , \tag{3.25}$$

where

$$\psi_0'^2 = -(1/d)C''(0) \tag{3.26}$$

is the variance of each component of $\nabla\psi$. Averaging $|\nabla\psi|$ over distribution (3.25) at $\psi = h$, we find the average frequency of the h-level crossings (Rice, 1944, 1945),

$$M_1(h) = \frac{1}{\pi\psi_0}\sqrt{-C''(0)} \exp\left(-\frac{h^2}{2\psi_0^2}\right) , \tag{3.27}$$

and the average total length of isolines $\psi(x, y) = h$ per unit area (Longuet-Higgins, 1957a; Swerling, 1962),

$$M_2(h) = \frac{1}{2\sqrt{2}\psi_0}\sqrt{-C''(0)} \exp\left(-\frac{h^2}{2\psi_0^2}\right) . \tag{3.28}$$

The knowledge of the correlation function $C(\boldsymbol{\rho})$ is sufficient to calculate other average characteristics, such as the number of the saddle points, maxima, and minima of $\psi(\mathbf{x})$. Rice (1944) derived the average number of maxima and minima in one dimension. The distribution of minima of a 3D Gaussian random potential was calculated by Halperin and Lax (1966) in respect of the low-energy density of states of the Schrödinger equation with a disordered potential. Weinrib and Halperin (1982) investigated the density (per unit ψ interval) of saddles, maxima, and minima of the intensity of a 2D laser speckle field, which was modelled by a complex Gaussian random variable.

Regarding the topological characteristics of iso-sets of Gaussian random fields, their investigation is a much more difficult task. Swerling (1962) established certain inequalities for the number of connected contours pieces comprising the iso-set $\psi(x, y) = h$. Some other characteristics are given in Adler (1981). As discussed in Secs. C–E, percolation theory

presents a powerful tool for studying more subtle topological properties of level lines and surfaces.

Returning to the spectral description of random fields, notice that a decreasing power spectrum (3.9) with $H < 0$ implies a finite variance ψ_0^2 of the potential within an arbitrarily large period $\mathcal{L}$, so that the above results for Gaussian fields apply. A positive exponent H, which is the case for the Earth's relief, corresponds to an infinite variance of ψ for $\lambda_m \to \infty$. Nevertheless, this kind of profile may be treated locally using the delta-variance $\Delta(\rho)$, which is the subject of the next subsection.

B. Brownian and fractional Brownian reliefs

The Brownian motion of a particle due to the thermal agitation of molecules in ambient medium is the simplest natural example of a random process. The velocity of the Brownian motion, $d\mathbf{B}(t)/dt = \mathbf{v}(t)$, can be approximated on a macroscopic time scale t as a "white noise," that is, a Gaussian random function with zero mean and the covariance

$$\langle v_i(t) v_j(t') \rangle = 2D\, \delta_{ij} \delta(t - t') \ , \tag{3.29}$$

where D is a molecular diffusion coefficient. Then the coordinate of the Brownian particle, $\mathbf{B}(x) = \int_0^t \mathbf{v}(t')dt'$, is also Gaussian with the average $\langle \mathbf{B}(t) \rangle = 0$ and the covariance $\langle B_i(t) B_j(t') \rangle = 2D\, \delta_{ij} \min(t, t')$. Notice that $\mathbf{B}(t)$ is not a stationary random process because its correlator is not a function of $(t - t')$. The delta-variance (3.2), however, is a function of $(t - t')$ and hence can serve a better characteristic of this process.

The Brownian motion is a convenient starting point in generating various random fields. *A Brownian (line-to-line) function* $B(x)$ is, by definition, a random function whose increments are Gaussian with zero mean and the variance

$$\left\langle [B(x_1) - B(x_2)]^2 \right\rangle = b^2 \, |x_1 - x_2| \ . \tag{3.30}$$

The Brownian graph $\{x, B(x)\}$ (see Fig. 12(b)) is a fractal with the fractal dimension $D =$ *F 12b*

3/2. Indeed, a parcel of this graph corresponding to the abscissa interval $[x_1, x_2]$ is covered by N_λ boxes with the size λ, where

$$N_\lambda \simeq \frac{x_2 - x_1}{\lambda} \frac{[B(x+\lambda) - B(x)]_{\rm rms}}{\lambda} \propto \lambda^{-3/2} , \quad \lambda < b^2 . \tag{3.31}$$

The inequality displayed in Eq. (3.31) requires that the root-mean square increment $B(x + \lambda) - B(x)$ be larger than λ in order to accommodate many covering squares. At larger scales, $\lambda \gg b^2$, the second factor in (3.31) must be substituted by unity leading to the fractal dimension $D = 1$ (see table I). *T I*

One can similarly define a *Brownian surface*, which is the graph of a *Brownian plane-to-line function* $B(x, y)$ being a Brownian line-to-line function of each of its arguments (Fig. 13(b)). In a straightforward analogy to the above calculation, the fractal dimension of *F 13b* the 2D Brownian relief can be shown to be $D = 5/2$, which, of course, complies with the cross-section rule (1.13), as a Brownian graph is a vertical (e.g., y =const) cross-section of a Brownian surface. Another cross-section of the Brownian surface can be done by a horizontal plane $B(x, y) = h$ = const, with the same result for the fractal dimension, $D = 3/2$, of the iso-set $B(x, y) = h$ (Fig. 14(b)). *F 14b*

As the value $D = 3/2$ appreciably overestimated the measured fractal dimensions of natural coastlines, the Brownian surface model of the Earth's relief was rejected, and a generalization of the Brownian random function was introduced — a *fractional Brownian line-to-line function* $B_H(x)$ (Mandelbrot and Van Ness, 1968). The fractional Brownian line-to-line function $B_H(x)$ is, by definition, a Gaussian random process with zero mean and the delta-variance

$$\left\langle [B_H(x_1) - B_H(x_2)]^2 \right\rangle = b^2 \, |x_1 - x_2|^{2H} , \quad 0 < H < 1 . \tag{3.32}$$

According to Eq. (3.16), this function has a λ-spectrum $(B_H)_\lambda \propto \lambda^H$ in an infinite scaling range ($\lambda_0 = 0$, $\lambda_m = \infty$). A *fractional Brownian surface*, or a plane-to-line function $B_H(x, y)$

is defined substituting x_1 and x_2 by corresponding vectors in definition (3.32). The ordinary Brownian function $B(x)$ is a particular case ($H = 1/2$) of its fractional generalization: $B(x) = B_{1/2}(x)$. The fractional Brownian graph ($H \neq 1/2$; see Fig. 12(a,c)) and the standard Brownian graph ($H = 1/2$; Fig. 12(b)) look qualitatively similar differing only by the degree of irregularity, which decreases for increasing H. A measure of this irregularity can serve the graph fractal dimension D. Similarly to calculation (3.31), one finds $D = 2 - H$, in the scalinig range $\lambda < b^{1/(1-H)}$. The same fractal dimension, but in an infinite scaling range, refers to the horizontal cross-section (iso-set) of fractional Brownian surface $z = B_H(x, y)$, whose own fractal dimension is clearly a unity greater, $D = 3 - H$ ($\lambda < b^{1/(1-H)}$). For a random potential with the delta-variance given by Eq. (3.32) and $H \leq 0$, the graph $\{x, B_H(x)\}$ attains the maximum allowed fractal dimension $D = d = 2$, meaning the dense filling of the (x, y) plane by the short-scale oscillations of the potential (Fig. 12(d)). Still, the fractal dimension of a connected contour piece of such function (Fig. 14(d)) is nontrivial (see Sec. E).

F 12ac *F 12b* *F 12d* *F 14d*

Another object associated with the function B_H is a *fractional Brownian trail* $\mathbf{x} = \mathbf{B}_H(t)$, where each component of $\mathbf{B}_H(t)$ is an independent fractional Brownian function of time. The fractal dimension of the trail imbedded in a d-dimensional space is given by the formula (Mandelbrot, 1983)

$$D = \min(1/H, d) \; . \tag{3.33}$$

For $H = 1/2$ (standard Brownian motion) $D = 2$, which well explains the finite probability of the return of a random walker to the starting point in two dimensions and the zero return probability in three dimensions (cf. Rammal, 1984).

The fractional Brownian function $B_H(x)$ can be generated by its Fourier spectrum (as done in Figs. 12-14), or can be obtained directly from $B(x)$ with the help of a fractional differentiation (for the "antipersistent" case $H < 1/2$) or fractional integration (for the "persistent" case $H > 1/2$): $B_H(x) = \hat{I}^{H-1/2} B(x)$. The Riemann-Liouville fractional integral of

F 12-14

the order α is given by the operator (Ross, 1975)

$$\widehat{I}^{\alpha} f(x) = \frac{1}{\Gamma(\alpha)} \int_0^{\infty} x'^{\alpha-1} f(x-x')dx' , \quad 0 < \alpha < 1 . \tag{3.34}$$

Substituting f by df/dx in the integrand yields the fractional differentiation of the order $1-\alpha$.

The model of a fractional Brownian surface $z = B_H(x,y)$ was used to model the Earth relief (Mandelbrot, 1975b; Berry and Hannay, 1978). The fractal dimension $D = 2 - H$ of the iso-set $B_H(x,y) = h$ predicts the distribution of islands, that is, their number with the size of the order of a, which is essentially the covering number:

$$N_a \propto a^{-D} . \tag{3.35}$$

This distribution fits the empirical number-area rule, or the Korčak (1938) law, which states the numbers of islands with the area above A to scale as A^{-k}, at $k = 2D = 2(2-H)$. The Earth average value $k \simeq 0.65$ corresponds to a fractional Brownian relief with $H \simeq 0.7$.

Thus, the fractional Brownian approach makes it possible to link the relief spectrum with the fractal dimension of the whole iso-set $B_H(x,y) = h$ and with the distribution of islands. However, the fractal dimension of a separate (connected) coastline, a measurable quantity, remains beyond this approach (Mandelbrot, 1983, p. 272). The distribution function of various contours (regardless of the level h) over size remains also unpredicted. These and other issues have to be addressed with the help of a less phenomenological (more "microscopic") approach, and therefore we return to percolation theory.

C. Topography of a monoscale relief

In Sec. II.E we have seen that the iso-set $\psi(\mathbf{x}) = h$ of a random potential behaves like the system of both external and internal perimeters of percolation clusters on a lattice generated by the stationary points (minima, maxima, and saddles) of the potential ψ. Since any physically reasonable random function has finite correlations, the bond probability (2.33)

on the equivalent lattice cannot be considered independent one bond from another, even though the potential $\psi(\mathbf{x})$ has a single characteristic length λ_0. Therefore, the percolation network corresponding to the iso-potentials $\psi(\mathbf{x}) = h$ should be suspected of being long-range correlated, in the sense as described in Sec. II.D. Let us designate by "monoscale uncorrelated," or simply "monoscale," such a potential that generates clusters falling into the universality class of random percolation.

To establish the criterion for a potential $\psi(\mathbf{x})$ to be monoscale, let us calculate the correlation function (2.25) of the bond-probabilities (2.34). To do so, we use the two-point potential probability distribution function $P(\psi_1, \psi_2|\mathbf{x}_1, \mathbf{x}_2)$, and analogously to Eq. (2.34) write

$$\langle p_1(h)p_2(h)\rangle = \int_{-\infty}^{h} d\psi_1 \int_{-\infty}^{h} d\psi_2 \, P(\psi_1, \psi_2|\mathbf{x}_1, \mathbf{x}_2) \; . \tag{3.36}$$

Let us suppose that $\psi(\mathbf{x})$ is Gaussian so that the two-point probability distribution function is given by Eq. (3.21). In the long-range limit, $\rho \equiv |\mathbf{x}_1 - \mathbf{x}_2| \gg \lambda_0$, substituting expression (3.22b) into Eq. (3.36) yields the bond-probability correlation function,

$$c(\boldsymbol{\rho}) \equiv \langle p_1(h)p_2(h)\rangle - p^2(h) = P^2(h)C(\boldsymbol{\rho}) \; , \tag{3.37}$$

which scales directly proportional to the potential covariance $C(\boldsymbol{\rho}) = \langle \psi(\mathbf{x})\, \psi(\mathbf{x} + \boldsymbol{\rho})\rangle$. Notice that for this particular result the Gaussianity of $\psi(\mathbf{x})$ is not essential. According to criterion (2.27), the correlations are irrelevant for sufficiently fast decay of the probability covariance, $c(\rho) = O(\rho^{-1/\nu})$. In terms of the potential correlator $C(\boldsymbol{\rho})$, this criterion reads

$$C(\boldsymbol{\rho}) = O(\rho^{-1/\nu}) \; , \quad \rho \gg \lambda_0 \; . \tag{3.38}$$

So we infer that the potential $\psi(\mathbf{x})$ with the power spectrum $\psi_\lambda \propto \lambda^H$, $\lambda > \lambda_0$, can be considered as monoscale uncorrelated, if $H < -1/\nu$. In two dimensions, this inequality yields $H < -3/4$, whereas for $d = 3$ the upper H limit of uncorrelated behavior is $-1/\nu \simeq -1.1$. The contours of such potentials behave like the hulls of uncorrelated percolation clusters.

Accordingly, the topography of a *monoscale correlated* potential, that is, a function with spectrum (3.9) where $-1/\nu < H < 0$ and $\lambda_m \to \infty$, is related to the correlated percolation problem. This criterion is valid in any dimension. Other details are dimensionality-dependent.

1. Two dimensions

Known the scaling properties of percolation clusters, the topography of a monoscale uncorrelated potential can be described in a similar manner using the scaling properties of percolation perimeters. At this point, however, one must recall the fickle nature of the 2D cluster perimeter, whose fractal dimension is subject to change between the natural value $d_h = 7/4$ and the unscreened value $d_u = 4/3$ under a moderate change of the perimeter definition (Grossman and Aharony, 1986). In the "flooding" terms, the perimeters of the first (natural) kind correspond to the coastlines of islands with gulfs whose width may be less than λ_0. The second kind of perimeter arises when one dams all narrow straits, i.e., those with the width less than λ_0. Since nothing prevents a contour line from coming arbitrarily close to itself (this is the case near a saddle point, when the contour lies close enough to the corresponding separatrix), we conclude that the natural hull (not unscreened perimeter) is the proper image of a contour line.

Let us formulate the basic topographic properties of a monoscale (λ_0) relief $\psi(x, y)$ with the variance ψ_0^2, using the statistics of 2D percolation clusters (Sec. II).

(i) Each level line $\psi(x, y) = h$ is closed with the probability one.

(ii) There exists exactly one unclosed isoline (corresponding to the external perimeter of an incipient infinite cluster), which lies at a critical level $h = h_c$. Specifically, for a sign-symmetric (e.g., Gaussian with $\langle\psi\rangle = 0$) potential, the critical level is zero: $h_c = 0$.

(iii) The number of connected contours $\psi(x,y) = h$ with diameter in the octave $[a, 2a]$ per unit area is given by

$$N_a = \begin{cases} \text{const}\, a^{-2} , & \lambda_0 \ll a \ll \xi_h , \\ \text{exponentially small} , & a \gg \xi_h , \end{cases} \tag{3.39}$$

where the correlation length equals

$$\xi_h = \lambda_0 \left(\frac{|h - h_c|}{\psi_0} \right)^{-\nu} . \tag{3.40}$$

The correlation length exponent $\nu = 4/3$.

(iv) A separate contour piece of ψ with the diameter $a \gg \lambda_0$ is a fractal curve with the scaling range $[\lambda_0, a]$ and the fractal dimension (hull exponent) $d_h = 7/4$, so that the length of the line scales as

$$L(a) \simeq \lambda_0 \left(\frac{a}{\lambda_0} \right)^{d_h} . \tag{3.41}$$

(v) A continuum cluster (connected region where $\psi(x,y) < h$) of a large linear size a has the fractal dimension $d_c = d - \beta/\nu = 91/48$ in the scaling range $[\lambda_0, a]$ ($[\lambda_0, \xi_h]$ for an infinite cluster). For $|h - h_c| \ll \psi_0$, the infinite continuum cluster occupies the area fraction

$$P_\infty = \text{const} \left(\frac{h - h_c}{\psi_0} \right)^{\beta} \theta(h - h_c) , \tag{3.42}$$

where $\beta = 5/36$.

For the completeness of the topography of a 2D monoscale random relief, we derive the expression for the distribution function $F(a)$ of all contours of $\psi(x,y)$ over their size a. Let us define $F(a)$ as the fraction of area covered by the contour lines with diameters in the interval $[a, 2a]$, whatever be their level h.[1]

[1]The dimensionless distribution function $F(a)$, which relates the area fraction to the octave of scales, is here more convenient than a standard distribution function $f(a) \simeq F(a)/a$ yielding the infinitesimal probability $f(a)da$ to find a contour of a linear size in the interval $[a, a + da]$.

First, consider a wider set of contours with diameters $[a, \infty]$. This region may be constructed starting with the contours of the diameter a and adding to them the embracing contours as shown in Fig. 15. This "dressing procedure" begun with an arbitrary initial contour *F 15* will ultimately lead to the infinite isoline, which is unique. Therefore, the set of contours bigger than a is a connected web-like region with holes of the size a and smaller (Fig. 16). Let us *F 16* call this region the "a-web." Since, according to (iii), the contours with diameter greater than a should have the level sufficiently close to the critical level, $|h - h_c| \lesssim h(a) = \psi_0(a/\lambda_0)^{-1/\nu}$, the width of the a-web is estimated as

$$w(a) \simeq \lambda_0 \left(\frac{a}{\lambda_0}\right)^{-1/\nu} , \quad a > \lambda_0 . \tag{3.43}$$

The a-web is a fractal set in a scaling range of $[\lambda_0, a]$ with the fractal dimension $d_h = 7/4$. Indeed, in the limit $a \to \infty$, the web degenerates into the single unclosed isoline of $\psi(x, y)$, whose fractal dimension is d_h and the scaling range is $[\lambda_0, \infty]$.

The fraction of area occupied by the a-web can be calculated as

$$\Phi(a) \simeq \frac{L(a)w(a)}{a^2} \simeq \left(\frac{\lambda_0}{a}\right)^{2-d_h+1/\nu} , \quad a > \lambda_0 . \tag{3.44}$$

The distribution function $F(a) = \Phi(a) - \Phi(2a)$ is clearly of the same order of magnitude. Using the numerical values of the exponents, we obtain the level-averaged distribution of contour sizes (Gruzinov *et al.*, 1990)

$$F(a) \simeq \frac{\lambda_0}{a} , \quad a > \lambda_0 . \tag{3.45}$$

To imagine what the set of contours of diameters $[a, 2a]$ looks like, subtract the $2a$-web from the a-web. The result will be a disconnected set consisting of connected "a-cells" with both the cells' width and the gaps between the cells given by the characteristic quantity $w(a)$ (see Fig. 17). *F 17*

2. Three dimensions

The monoscale topography of a three-dimensional potential differs from the 2D case in that there exist two different critical levels, h_{c1} and h_{c2}, whose difference is of the order of the potential amplitude, $h_{c2} - h_{c1} \simeq \psi_0$ (see Sec. II.E). If the level h satisfies $h < h_{c1}$ or $h > h_{c2}$, the isosurfaces of $\psi(x, y, z)$ are all closed but may be multiconnected (that is, have "handles"). The iso-set $\psi(x, y, z) = h$ at $h_{c1} < h < h_{c2}$ consists of many closed parts and only one (because of the unicity of an infinite cluster) open surface. According to Eq. (2.15), the number of isosurfaces with linear size between a and $2a$ per unit volume scales as $N_a \simeq a^{-3}$, for $\lambda_0 < a < \xi_h$, and is exponentially small for finite $a > \xi_h$. The correlation length is given by expression

$$\xi_h = \frac{\lambda_0}{\psi_0} \max\left(|h - h_{c1}|^{-\nu}, |h - h_{c2}|^{-\nu}\right) , \tag{3.46}$$

where $\nu \simeq 0.9$. If h is close to one of the critical levels, the correlation length is large, $\xi_h \gg \lambda_0$, and there arises a scaling range of self-similarity. The fractal dimension d_h of an isosurface is equal to the cluster fractal dimension, $d_h = d_c = 3 - \beta/\nu \simeq 2.50$, whose scaling range is $[\lambda_0, a]$ for the closed isosurface, and $[\lambda_0, \xi_h]$ for the open one. Specifically, the isosurface area $S(a)$ scales with the diameter a lying in the scaling range as

$$S(a) \simeq \lambda_0^2 (a/\lambda_0)^{d_h} . \tag{3.47}$$

Regarding the distribution function $F(a)$ of isosurfaces over size, it can be concluded that a finite fraction of space is covered by open surfaces ($h_{c1} < h < h_{c2}$). This fraction of volume can be accounted for by "$F(\infty)$," which is (roughly) of the order of one half. The distribution of finite-size isosurfaces can be found similarly to Eq. (3.44),

$$F(a) \simeq \frac{L(a)w(a)}{a^3} \simeq \left(\frac{\lambda_0}{a}\right)^{3-d_h+1/\nu} = \left(\frac{\lambda_0}{a}\right)^{\frac{\beta+1}{\nu}} , \quad a > \lambda_0 . \tag{3.48}$$

Substituting the numerical value of the exponents, $\nu \simeq 0.9$, $\beta \simeq 0.4$, we find that $F(a)$ scales approximately as $a^{-1.6}$.

Topographic properties of monoscale potentials also apply to monoscale correlated potentials ($-1/\nu < H < 0$ and $\lambda_m = \infty$) if exponents ν, d_h, β, etc., are substituted by corresponding H-dependent exponents (2.27)–(2.30) of the correlated percolation problem. This issue is addressed in more detail in Sec. E.

D. Monoscale relief on a gentle slope

In the previous subsection we discussed the level lines and surfaces of random potentials with finite variance. One may also be interested in the topography of a "tilted relief," that is to say, of a random function with an average gradient, which is too small to destroy local hills and valleys but clearly dominates the long-range topographic behavior.

This problem can be relevant, for example, for the quantized Hall effect characterized by extremely low dissipative components of the conductivity tensor (Trugman, 1983). In a two-dimensional electron gas imbedded in the magnetic field $\mathbf{B}$ directed parallel to the z axis, the electrons are localized near the lines of constant electric potential $\varphi(x, y)$, or, in other words, drift in crossed electric and magnetic fields with the velocity $\mathbf{v} = c\mathbf{E} \times \mathbf{B}/B^2$ (Laughlin, 1981). The radius of electron localization near the iso-potentials is $l = (\hbar c/eB)^{1/2}$, which is the electron gyroradius corresponding to the energy $\hbar\omega_B/2$ of the lowest Landau level, where $\omega_B = eB/mc$ is the gyrofrequency. If the background electric field $\mathbf{E}_0 = -\nabla\varphi_0(x, y)$ is created by a statistically uniform impurity distribution, the iso-potentials of φ_0 are closed: an average electric current is absent. When the system is embedded into an external uniform electric field $\mathbf{E}_1$, $E_1 \ll E_0$, an average (Hall) electric current emerges, which is carried along the open isolines of the perturbed potential $\varphi(x, y) = \varphi_0(x, y) - \mathbf{E}_1\mathbf{x}$. This highly simplified model assumes essentially individual electron motion. A similar topographic problem of a tilted relief arises in the essentially collective classical Hall effect in high-temperature pulsed plasmas (Chukbar and Yankov, 1988; Kingsep *et al.*, 1990), where the electric current must flow along the level lines of a two-dimensional plasma density.

In this section, we discuss the topography of a monoscale uncorrelated relief on a gentle slope in some detail, also because this problem also serves as an auxiliary one in the approach of "separated scales" (Sec. E).

Following the model of $\mathbf{E} \times \mathbf{B}$ electron drifts along random equipotentials, it is convenient to represent the isolines of a potential $\psi(x, y)$ as the streamlines of a two-dimensional incompressible flow,

$$\mathbf{v}(x, y) = \boldsymbol{\nabla}\psi(x, y) \times \hat{\mathbf{z}} \, . \tag{3.49}$$

where $\hat{\mathbf{z}}$ denotes a unit vector in the z-direction. In this representation, $\psi(x, y) = -c\varphi(x, y)/B$ is the stream-function of the flow.

Let $\mathbf{v}(x, y)$ be the sum of a monoscale (λ_0) flow $\mathbf{v}_0(x, y) = \boldsymbol{\nabla}\psi_0(x, y) \times \hat{\mathbf{z}}$ and a small uniform component, $\mathbf{v}_1 = v_1\hat{\mathbf{x}}$:

$$\mathbf{v}(x, y) = \mathbf{v}_0(x, y) + \mathbf{v}_1 \, . \tag{3.50}$$

This corresponds to the stream-function

$$\psi(x, y) = \psi_0(x, y) + v_1 y \, . \tag{3.51}$$

Since the potential $\psi_0(x, y)$ is bounded, $\mathbf{v}_0(x, y)$ has zero mean: (almost) any streamline is closed and there is no long-range fluid flux. When a uniform component $\mathbf{v}_1$ is imposed, an average flux arises in the x-direction. Therefore, some fraction of streamlines must open to produce channels carrying this flux (Fig. 18(a)). For very small $\varepsilon = v_1/v_0 \ll 1$, $v_0 \equiv$ *F 18a*
$[v_0(x, y)]_{\text{rms}}$, the perturbation cannot clearly affect the absolute value of the velocity in the channels. Hence, the smallness of $\mathbf{v}_1$ is only manifested in that the channels are narrow (the width $\delta_\varepsilon \ll \lambda_0$) and well separated (the characteristic distance between them $\Delta_\varepsilon \gg \lambda_0$) (Zeldovich, 1983; Trugman, 1983). Given the characteristic velocity v_0 in the channels, the average flux $\mathbf{v}_1$ can be estimated as $v_0\,\delta_\varepsilon/\Delta\varepsilon$, hence

$$\frac{\delta_\varepsilon}{\Delta_\varepsilon} = \varepsilon \, . \tag{3.52}$$

The transverse (with respect to $\mathbf{v}_1$) walk Δ_ε of an open streamline lying in the channels can be found from the argument of "graded percolation" (Trugman, 1983; Sapoval *et al.*, 1985; Bunde and Gouyet, 1985). The idea of this argument is that local behavior of clusters $\psi(x,y) < h$ is the same as for the unperturbed potential $\psi_0(x,y)$, however, the local critical level h_c becomes slowly dependent on y together with the average value of the potential:

$$h_c(y) = h_c(0) + v_1 y \ . \tag{3.53}$$

Let us consider an open level line of potential (3.51) and put the origin on this line. On relatively small scales, namely, for $|y| \ll \Delta_\varepsilon$, the line does not "feel" the average gradient of $\psi(x,y)$ and behaves like an open isoline of the unperturbed function $\psi_0(x,y)$. According to properties (ii) and (iii) of monoscale level contours (Sec. C), the level h of the considered isoline is close to the local critical level: $h \simeq h_c(0)$. Walking in this unperturbed manner, the isoline explores different regions where the critical level (3.53) becomes different from h. According to (iii), this makes the line try to close, in other words, to return back to the region $y \simeq 0$. So the unclosed level line of the tilted relief (3.51) is restrained to walk in a strip parallel to the x-axis (Fig. 18(b)). The characteristic width of such wandering Δ_ε is *F 18b* determined as the self-consistent correlation length ξ_h (3.40):

$$\Delta_\varepsilon = \lambda_0 \left(\frac{|h_c(0) - h_c(\Delta_\varepsilon)|}{\psi_0} \right)^{-\nu} \ . \tag{3.54}$$

Substituting Eq. (3.53) into Eq. (3.54), we find the slope-generated correlation scale

$$\Delta_\varepsilon = \lambda_0 \varepsilon^{-\nu/(\nu+1)} = \lambda_0 \varepsilon^{-4/7} \ , \quad d = 2 \ . \tag{3.55}$$

This scale determines the maximum diameter of closed contours on the tilted relief. The width of the channels is then found from Eq. (3.52):

$$\delta_\varepsilon = \lambda_0 \varepsilon^{1/(\nu+1)} = \lambda_0 \varepsilon^{3/7} \ . \tag{3.56}$$

So we conclude that the contours of a monoscale uncorrelated relief on a gentle slope behave in a nonperturbed manner on scales below Δ_ε. In other words, the contours of $\psi_0(x,y)$

with diameter $a < \Delta_\varepsilon$ are "robust" with respect to the perturbation, whereas the "fragile" contours with $a > \Delta_\varepsilon$ open to form a network of percolating channels. So this network is topologically similar to the Δ_ε-web shown in Fig. 17. (Unless an individual percolating line is plotted, it is hard to tell the direction of the mean flow from the appearance of the channel network.) As expected, the channel width (3.56) is consistent with the Δ_ε-web width (3.43): $\delta_\varepsilon = w(\Delta_\varepsilon)$. *F 17*

Results (3.55)–(3.56) can be extended to level lines of a 2D monoscale correlated relief ($-1/\nu < H < 0, \quad \lambda_m = \infty$) on a gentle slope. To do so, we substitute the uncorrelated percolation exponent $\nu = 4/3$ by its correlated counterpart $\tilde{\nu}(H) = -1/H$, so that

$$\Delta_\varepsilon = \lambda_0 \varepsilon^{1/(H-1)} , \quad -3/4 < H < 0 ; \tag{3.57}$$

$$\delta_\varepsilon = \lambda_0 \varepsilon^{H/(H-1)} , \quad -3/4 < H < 0 . \tag{3.58}$$

Now we consider the three-dimensional case. Due to the openness of a finite fraction of the isosurfaces $\psi_0(x, y, z) = h$, which takes place at $h_{c1} < h < h_{c2} \quad (h_{c2} - h_{c1} \simeq \psi_0)$, the efect of a small average slope is not so pronounced as in two dimensions. The topology of open surfaces is, nevertheless, changed. Consider a surface $\psi_0(x, y, z) + v_1 z = h$, $\varepsilon \equiv v_1 \lambda_0 / \psi_0 \ll 1$. This surface can span only in a layer parallel to the (x, y) plane with the width

$$\Delta_\varepsilon = \lambda_0 / \varepsilon , \quad d = 3 , \tag{3.59}$$

where the local level $h_0(z) = h - v_1 z$ of $\psi_0(x, y, z)$ lies between the critical levels h_{c1} and h_{c2}.

E. Multiscale statistical topography

The standard rercolation theory seems to be inapplicable to describe the statistical topography of "scaleless" random fields, such as those characterized by a power spectrum $\psi_\lambda \propto \lambda^H$. The applicability of percolation theory, nevertheless, is recovered by the observation that "scaleless" is virtually the same as "multiscale." The idea of the *separation of scales*

(Isichenko and Kalda, 1991b) is to decompose a multiscale field into a series of monoscale fields. Namely, we consider the potential

$$\psi(\mathbf{x}) = \sum_{\lambda_i} \psi_{\lambda_i}(\mathbf{x}) \ , \tag{3.60}$$

where $\psi_{\lambda_i}(\mathbf{x})$ are monoscale (λ_i) functions with the amplitudes

$$\psi_\lambda \equiv [\psi_\lambda(\mathbf{x})]_{\rm rms} = \psi_0 \left(\frac{\lambda}{\lambda_0}\right)^H \ , \tag{3.61}$$

and the sum in Eq. (3.60) is taken over a geometrical progression of scales

$$\lambda_i = \lambda_0, \ \mu\lambda_0, \ \mu^2\lambda_0, \ldots, \lambda_m; \ \mu \gg 1 \ . \tag{3.62}$$

To be more exact, the components in series (3.60) must be written as

$$\psi_\lambda(\mathbf{x}) = \left(\frac{\lambda}{\lambda_0}\right)^H \psi_0 \left(\frac{\lambda_0}{\lambda}\mathbf{x}\right) \ , \tag{3.63}$$

where $\psi_0(\mathbf{x})$ is a monoscale (λ_0) random potential with ψ_0^2 variance, whose new realizations are taken for each λ in formula (3.63). In the Gaussian case with independent Fourier harmonics, $\psi_\lambda(\mathbf{x})$ is given by Eq. (3.7).

The statistical topography of potential (3.60)–(3.62) with strongly separated scales is analytically tractable in terms of a recursive percolation analysis, where each subsequent term in series (3.60) is considered locally a "gentle slope" imposed on the previous term. The final results for the "correct" potential (3.6) (that is, with $\mu = 2$) is obtained extrapolating the results for the "incorrect" potential with $\mu \gg 1$ to the marginally applicable limit $\mu = 2$. This method shares a common spirit with the renormalization group technique (Wilson, 1975) but is technically different. It is emphasized that the method of separated scales is poorly based, especially regarding the limit $\mu \to 2$. A partial excuse is given by fact that all predictions of the theory of fractional Brownian functions are recovered by the method of separated scales, which also yields new results inaccessible by the fractional Brownian approach. These new results may have to be checked numerically and/or experimentally.

1. Two dimensions

For a two-dimensional potential $\psi(x,y)$, we introduce an incompressible flow $\mathbf{v} = \nabla\psi(x,y) \times \hat{\mathbf{z}}$, whose multiscale features can be described similarly to Eq. (3.60):

$$\mathbf{v}(\mathbf{x}) = \sum_{\lambda_i} \mathbf{v}_{\lambda_i}(\mathbf{x}) \ . \tag{3.64}$$

Then the stream-function spectrum (3.61) corresponds to the velocity spectrum

$$v_\lambda = v_0 \left(\frac{\lambda}{\lambda_0}\right)^{H-1} \ . \tag{3.65}$$

For $H > 1$, the long-scale components of the flow are more intensive than the short scales, therefore, the streamline behavior is dominated by the largest scale λ_m. Thus the topography of the power-spectrum random function with $H > 1$ is essentially the same, as for the monoscale uncorrelated λ_m-potential $\psi_{\lambda_m}(x,y)$. This remains clearly true in the limit $\mu = 2$.

The case $H < 1$ is more interesting. Here, the flow component $\mathbf{v}_{\lambda_0}(\mathbf{x})$ dominates the absolute value of the velocity field, and $\mathbf{v}_{\lambda_1}(\mathbf{x})$ may be considered a weak ($\varepsilon = v_{\lambda_1}/v_{\lambda_0} = (\lambda_1/\lambda_0)^{-(1-H)} \ll 1$) and quasihomogeneous (because $\lambda_1 \gg \lambda_0$) perturbation of $\mathbf{v}_{\lambda_0}(\mathbf{x})$. According to the results of Sec. D, this perturbation leaves most streamlines of $\mathbf{v}_{\lambda_0}(\mathbf{x})$ nearly intact but "quasi-opens" some of them, that is, makes them walk around the direction of $\mathbf{v}_{\lambda_1}(\mathbf{x})$ in the strips of width (3.55):

$$\Delta_{01} = \lambda_0 \left(\frac{\lambda_1}{\lambda_0}\right)^{(1-H)\frac{\nu}{\nu+1}} \ . \tag{3.66}$$

For $H < -1/\nu$, the expression for Δ_{01} becomes formally larger than $\lambda_1 = \lambda_0\mu$. This means that the assumption of the local homogeneity of the perturbation $\mathbf{v}_{\lambda_1}(\mathbf{x})$ is wrong. In other words, the perturbation turns out to be too small to appreciably affect the pattern of the streamlines. Thus in this case the topography of the relief $\psi(x,y)$ is essentially the same as for the monoscale potential $\psi_{\lambda_0}(\mathbf{x})$. Notice that the same inequality (2.26) (see also Eq. (3.38) is the criterion for the irrelevance of correlations and hence for the membership of the potential $\psi(\mathbf{x})$ in the universality class of random percolation.

In this way, we arrive at the "essentially multiscale" case

$$-\frac{1}{\nu} < H < 1 \,, \tag{3.67}$$

where a nontrivial *interaction of scales* must take place implying an essential dependence of the topographic properties on all scales, that is, on the form of the potential spectrum.

In terms of separated scales, inequality (3.67) implies $\lambda_0 \ll \Delta_{01} \ll \lambda_1$, justifying the assumptions of both the weakness and the quasi-homogeneity of the perturbation $\mathbf{v}_{\lambda_1}(\mathbf{x})$. In this limit, the fraction of area covered by the streamlines with diameter of the order of λ_1 is given by Eq. (3.44) with $a = \Delta_{01}$:

$$F(\lambda_1) \simeq \left(\frac{\lambda_0}{\Delta_{01}}\right)^{2-d_h+1/\nu} = \left(\frac{\lambda_1}{\lambda_0}\right)^{-(1-H)\frac{1+\nu(2-d_h)}{\nu+1}} \,. \tag{3.68}$$

Indeed, once a streamline has reached the displacement Δ_{01}, it becomes quasi-open, that is, walks in the Δ_{01}-strip whose axis follows a streamline of $\mathbf{v}_{\lambda_1}(\mathbf{x})$. The latter is typically closed on the diameter λ_1.

The fractal properties of an open isoline depend on the length scale. In the inertial range $[\lambda_0, \Delta_{01}]$, the effect of the slope is unessential and the fractal dimension of the curve is $d_h = 7/4$. On scales between Δ_{01} and λ_1, the strip is almost straight, meaning the fractal dimension unity in the corresponding scaling range. So the length of the streamline within the displacement λ_1 is given by

$$L(\lambda_1) \simeq \lambda_0 \left(\frac{\Delta_{01}}{\lambda_0}\right)^{d_h} \frac{\lambda_1}{\Delta_{01}} \simeq \lambda_0 \left(\frac{\lambda_1}{\lambda_0}\right)^{1+(1-H)(d_h-1)\frac{\nu}{\nu+1}} \,. \tag{3.69}$$

Now, consider the next-order perturbation of the velocity field, $\mathbf{v}_{\lambda_2}(\mathbf{x})$. It has the same effect on the streamlines of $\mathbf{v}_{\lambda_1}(\mathbf{x})$ as that of the λ_1-component of the flow on the lines of $\mathbf{v}_{\lambda_0}(\mathbf{x})$. So we find that the lines of $\mathbf{v}_{\lambda_1}(\mathbf{x})$, which are already the guidelines for the Δ_{01}-strips, become, in their turn, constrained (if long enough) into Δ_{12}-strips following the streamlines of $\mathbf{v}_{\lambda_2}(\mathbf{x})$ (see Fig. 19). The expressions for Δ_{12}, $F(\lambda_2)$, and $L(\lambda_2)$ differ from *F 19*

those in Eqs. (3.66), (3.68), and (3.69) by only a replacement of λ_1 by λ_2. This argument can be repeated for longer scales, up to λ_m. Generally, we obtain the following expressions for the distribution function of the multiscale level lines over the diameter λ,

$$F(\lambda) \simeq \left(\frac{\lambda}{\lambda_0}\right)^{-(1-H)\frac{1+\nu(2-d_h)}{\nu+1}} = \left(\frac{\lambda}{\lambda_0}\right)^{-4(1-H)/7}, \quad \lambda_0 < \lambda < \lambda_m , \tag{3.70}$$

and for the length of a contour exercising the displacement λ,

$$L(\lambda) \simeq \lambda_0 \left(\frac{\lambda}{\lambda_0}\right)^{D_h}, \quad \lambda_0 < \lambda < \lambda_m , \tag{3.71}$$

where the fractal dimension of a separate contour line is

$$D_h(H) = 1 + (1-H)(d_h - 1)\frac{\nu}{\nu+1} = \frac{10-3H}{7} . \tag{3.72}$$

The transition to a smooth spectrum limit ($\mu = 2$) implies simply the omission of subscripts of λ in Eqs. (3.70) and (3.71) and λ treatment as a continuum variable. Notice that, in the region of its applicability determined by inequalities (3.67), the fractal dimension (3.72) of a multiscale isoline satisfies the inequality

$$1 < D_h < d_h = 7/4 , \tag{3.73}$$

where the maximum value is attained in the monoscale uncorrelated limit $H = -1/\nu = -3/4$.

In the super-long-scale limit, $\lambda > \lambda_m$, the topography is again governed by the monoscale features of the λ_m-component of the potential $\psi(\mathbf{x})$ (see Eq. (3.45)), hence the distribution function falls off somewhat more rapidly than (3.70):

$$F(\lambda) \simeq \left(\frac{\lambda_0}{\lambda_m}\right)^{4(1-H)/7} \frac{\lambda_m}{\lambda}, \quad \lambda > \lambda_m . \tag{3.74}$$

A contour with the diameter $a \gg \lambda_m$ has fractal dimension (3.72) in the scaling range $[\lambda_0, \lambda_m]$ and the fractal dimension $d_h = 7/4$ in the range $[\lambda_m, a]$. It follows that the length of such contour is determined by

$$L(a) \simeq \lambda_0 \left(\frac{\lambda_m}{\lambda_0}\right)^{D_h} \left(\frac{a}{\lambda_m}\right)^{d_h}, \quad a > \lambda_m . \tag{3.75}$$

Analogously to Eq. (3.44), the distribution function $F(\lambda)$ may be represented in the general form

$$F(\lambda) = \frac{L(\lambda)w(\lambda)}{\lambda^2} , \tag{3.76}$$

where $w(\lambda)$ is the characteristic width of the connected set of contours with diameters λ to 2λ (the λ-cell). Using Eqs. (3.70), (3.71), (3.72), and (3.75), we obtain the width of the cell,

$$w(\lambda) = \frac{\lambda^2 F(\lambda)}{L(\lambda)} \simeq \begin{cases} \lambda_0 \left(\dfrac{\lambda}{\lambda_0}\right)^H , & \lambda_0 < \lambda < \lambda_m , \quad (3.77a) \\ \lambda_0 \left(\dfrac{\lambda_m}{\lambda_0}\right)^H \left(\dfrac{\lambda}{\lambda_m}\right)^{-1/\nu} , & \lambda > \lambda_m . \quad (3.77b) \end{cases}$$

The behavior of the isoline fractal dimension (3.72) and the contour distribution function (3.74) does not depend qualitatively on the sign of the spectral exponent H, provided that inequality (3.67) takes place. However, the appearance of the vertical (Fig. 12) and the horizontal (Fig. 14) cross-sections of multiscale surfaces suggests a qualitative difference in the topography of the reliefs with $H > 0$ and $H < 0$. This difference lies in the fractal dimension D of the whole iso-set $\psi(x, y) = h$ (Fig. 14). According to Eq. (3.16), for $0 < H < 1$ the random function $\psi(x, y)$ in the scaling range $[\lambda_0, \lambda_m]$ may be considered a fractional Brownian plane-to-line function and hence,

F 12
F 14
F 14

$$D = 2 - H , \quad 0 < H < 1 . \tag{3.78}$$

The same result can be obtained using the method of separated scales (Isichenko and Kalda, 1991b). For $H = 0$, the iso-set $\psi(x, y) = h$ becomes dense in the plane (x, y): $D = 2$. For $H < 0$, D cannot exceed the ambient space dimension $d = 2$, hence

$$D = 2 , \quad H < 0 . \tag{3.79}$$

Result (3.79) agrees with the finite measure (3.28) of the iso-set of a Gaussian random function with finite variance. For $H > 0$, such measure would tend to zero at $\lambda_m \to \infty$ because $D < 2$.

Thus there is a qualitative difference between the case of a fractional Brownian relief ($0 < H < 1$) and the case of the correlated percolation ($-1/\nu < H < 0$). However, expression (3.72) for the fractal dimension D_h holds in both limits. On the one hand, D_h is the fractal dimension of a connected contour piece on a fractional Brownian relief, where $1 < D_h < 10/7$. On the other hand, $D_h = \tilde{d}_h$ is identified with the hull exponent of a 2D correlated percolation cluster, where $10/7 < D_h < 7/4$.

It is interesting to note that the appearance of formula (3.72) implies a corollary for the correlated percolation exponent $\tilde{\nu}(H)$. The arguments used in deriving (3.72) can be repeated for the case when one starts with the correlated percolation problem corresponding to an exponent H' such that $-1/\nu < H' < H < 0$, and adds stronger correlations (H) using the procedure of the separation of scales. In this way, we arrive at result (3.72), where d_h and ν are substituted by the correlated exponents $\tilde{d}_h(H') \equiv D_h(H')$ and $\tilde{\nu}(H)$, respectively:

$$D_h(H) = 1 + (1 - H)[D_h(H') - 1]\frac{\tilde{\nu}(H')}{\tilde{\nu}(H') + 1}, \quad -1/\nu < H' < H < 0 . \tag{3.80}$$

Putting in Eq. (3.80) $H' = H$, we recover the formula $\tilde{\nu}(H) = -1/H$ as a necessary consistency condition.

2. Three dimensions

We wish to repeat the saparation-scale argument for a three-dimensional random potential $\psi(x, y, z)$. For this purpose we use expression (3.59) for the "walk" width of an isosurface subject to a small average potential gradient. Then instead of Eq. (3.66) we have

$$\Delta_{01} = \lambda_0 \left(\frac{\lambda_1}{\lambda_0}\right)^{1-H}, \quad \lambda_0 \ll \lambda_1 . \tag{3.81}$$

For the method to work, we must have $\Delta_{01} \ll \lambda_1$, which is the case only for $0 < H < 1$. In this case we can calculate the area $S(\lambda_1)$ of the isosurface contained in a λ_1-sized box similarly to Eq. (3.69). The difference, however, is that in the scaling range $[\lambda_0, \Delta_{01}]$ the isosurface fractal dimension is $D = 3$, because its level is far from the critical levels of $\psi_{\lambda_0}(x, y, z)$. In the scaling range $[\Delta_{01}, \lambda_1]$ we have $D = 2$ as the isosurface of $\psi_{\lambda_0}(\mathbf{x}) + \psi_{\lambda_1}(\mathbf{x})$ follows a smooth isosurface of $\psi_{\lambda_1}(\mathbf{x})$. Hence we have

$$S(\lambda_1) \simeq \lambda_0^2 \left(\frac{\Delta_{01}}{\lambda_0}\right)^3 \left(\frac{\lambda_1}{\Delta_{01}}\right)^2 \simeq \lambda_0 \left(\frac{\lambda_1}{\lambda_0}\right)^{3-H} . \tag{3.82}$$

Thus the fractal dimension of a connected contour piece,

$$D_h(H) = 3 - H , \quad d = 3 , \tag{3.83}$$

turns out to be the same as of the whole fractional Brownian iso-set $\psi(x, y, z) = h$. (The iso-set of a two-dimensional fractional Brownian function with the fractal dimension (3.78) is a plane cross-section of a three-dimensional iso-set.) This means a fairly good connectedness of 3D contour surfaces: a connected contour piece of the size λ comprises a finite fraction of all the iso-set (with the same level h) in the λ-sized box, for each $\lambda \in [\lambda_0, \lambda_m]$.

The case $-1/\nu < H < 0$, corresponding to the long-range correlated percolation, requires a different approach. To obtain the cluster scaling one has to know the correlated percolation exponents $\tilde{\nu}(H)$ and $\tilde{\beta}(H)$. The first one is given by Eq. (2.28). Here we show that the method of separated scales predicts the beta exponent to be insensitive to correlations and is the same as in the uncorrelated percolation problem (Isichenko and Kalda, 1991b). The following argument refers to any dimensionality d.

Consider the infinite continuum cluster $\psi(\mathbf{x}) < h = h_c + \delta$, where $h_c \equiv h_{c1}$ is the lower critical level of $\psi(\mathbf{x})$ and positive δ satisfies $\psi_{\lambda_m} \ll \delta \ll \psi_{\lambda_0}$. Let us separate scales in the form of Eq. (3.60). Denote λ_δ the solution of the equation $\psi_{\lambda_\delta} = \delta$ and, for brevity, $\lambda_{\delta-1}$, $\lambda_{\delta-2}, \ldots$, λ_0 the shorter separated scales. Since the monoscale potentials $\psi_\lambda(\mathbf{x})$ differ

only by rescaling, their own critical levels are given by the same formula

$$h_c^{(\lambda)} = K\,\psi_\lambda\ , \tag{3.84}$$

with a numerical coefficient K depending on the properties of the ensemble. For example, $K = 0$ for a 2D sign-symmetric potential, but $K < 0$ for $d = 3$. First, consider the infinite connected region (the "λ_δ-cluster") where

$$\psi_{\lambda_\delta}(\mathbf{x}) < K\,\psi_{\lambda_\delta} + \delta\ . \tag{3.85}$$

This cluster is fairly supercritical, hence it occupies the volume fraction

$$P_\infty^{(\lambda_\delta)} \simeq 1\ . \tag{3.86}$$

Now consider the $\lambda_{\delta-1}$-cluster defined by the inequality

$$\psi_{\lambda_{\delta-1}}(\mathbf{x}) < K\,\psi_{\delta-1} + [K\,\psi_{\lambda_\delta} + \delta - \psi_{\lambda_\delta}(\mathbf{x})]\ . \tag{3.87}$$

The second term on the right-hand side of Eq. (3.87) is a slowly varying function which is positive in the λ_δ-cluster. As the local correlation length of the $\lambda_{\delta-1}$-cluster,

$$\xi^{(\lambda_{\delta-1})} \simeq \lambda_{\delta-1}\left(\frac{\psi_{\lambda_\delta}}{\psi_{\lambda_{\delta-1}}}\right)^{-\nu} = \lambda_{\delta-1}\left(\frac{\lambda_\delta}{\lambda_{\delta-1}}\right)^{-\nu H}\ , \tag{3.88}$$

is much less than λ_δ (because $-1/\nu < H < 0$), the infinite $\lambda_{\delta-1}$-cluster lies entirely in the λ_δ-cluster and occupies the volume fraction

$$P_\infty^{(\lambda_{\delta-1})} \simeq P_\infty^{(\lambda_\delta)}\left(\frac{\psi_{\lambda_\delta}}{\psi_{\lambda_{\delta-1}}}\right)^{\beta}\ , \tag{3.89}$$

where β is the infinite-cluster-density exponent of uncorrelated percolation. Similarly, we can consider the $\lambda_{\delta-2}$-cluster where $\psi_{\lambda_{\delta-2}}(\mathbf{x}) < K\,\psi_{\delta-2} + [K\,\psi_{\lambda_{\delta-1}} + K\,\psi_{\lambda_\delta} + \delta - \psi_{\lambda_{\delta-1}}(\mathbf{x}) - \psi_{\lambda_\delta}(\mathbf{x})]$, and so on up to the scale λ_0. This procedure corresponds to a successive increase in the resolution as we view the cluster of $\psi(\mathbf{x}) < h = h_c + \delta$, with $h_c = K(\psi_{\lambda_0} + \ldots + \psi_{\lambda_\delta}) \simeq K\,\psi_0$. Finally we obtain the expression for the density of the correlated infinite cluster,

$$P_\infty(\delta) \equiv P_\infty^{(\lambda_0)} \simeq P_\infty^{(\lambda_\delta)}\left(\frac{\psi_{\lambda_\delta}}{\psi_{\lambda_0}}\right)^{\beta} \simeq \left(\frac{\delta}{\psi_0}\right)^{\beta}\ , \tag{3.90}$$

which means the universality of β for both random and correlated percolation: $\widetilde{\beta}(H) \equiv \beta$.

Notice that the above construction automatically implies $\widetilde{\nu}(H) = -1/H$, because the scale $\lambda_\delta = \lambda_0(\delta/\psi_0)^{1/H}$ is the correlation length ξ_δ of the cluster.

The fractal dimension $D_h(H)$ of a connected isosurface $\psi(x,y,z)$ can be calculated as the correlated hull dimension, which is the same as that of correlated percolation cluster,

$$D_h \equiv \widetilde{d}_h(H) = \widetilde{d}_c(H) = d - \widetilde{\beta}(H)/\widetilde{\nu}(H) = 3 + \beta H \ , \quad d = 3 \ , \quad -1/\nu < H < 0 \ . \quad (3.91)$$

Similarly to the uncorrelated monoscale case, the distribution function of isosurfaces over size a includes a finite $F(\infty)$, with a finite-size component given by a formula similar to (3.48):

$$F(a) \simeq \frac{S(a)w(a)}{a^3} \simeq \left(\frac{\lambda_0}{a}\right)^{(\widetilde{\beta}+1)/\widetilde{\nu}} = \left(\frac{\lambda_0}{a}\right)^{-(\beta+1)H} \ , \quad \lambda_0 < a < \lambda_m \ , \quad -1/\nu < H < 0. \quad (3.92)$$

3. An example

To demonstrate an application of the multiscale topography, let us recall the example of random isopotentials in the quantized Hall conductance or elsewhere. Consider the electrostatic field created by charged impurities randomly distributed in the (x,y) plane ($d = 2$) or in the space ($d = 3$). It might seem that, due to the well-defined scale of the separation of disordered impurities, $\lambda_0 = n_i^{-1/d}$ (where n_i is the average density of impurities), the monoscale continuum percolation model is appropriate (Trugman, 1983). This, however, depends.

The variation ρ_λ of the impurity charge density $\rho(\mathbf{x})$ over scale $\lambda > \lambda_0$ can be estimated using the "$\sqrt{N}$" rule, where $N = n_i\lambda^d$ is the expected number of impurities in the volume λ^d:

$$\lambda^d \rho_\lambda \propto (n_i\lambda^d)^{1/2} \ , \quad (3.93)$$

hence the charge density λ-spectrum is

$$\rho_\lambda \propto \lambda^{-d/2} \ , \quad \lambda \gg \lambda_0 \ . \quad (3.94)$$

Taking into account the effect of Debye screening we describe the electric potential $\Phi(\mathbf{x})$ by the Poisson equation

$$\nabla^2\Phi(x,y,z) - \lambda_D^2\Phi(x,y,z) = \begin{cases} -4\pi\,\delta(z)\,\rho(x,y)\,, & d=2\,, \\ -4\pi\,\rho(x,y,z)\,, & d=3\,, \end{cases} \tag{3.95}$$

where $\lambda_D \gg \lambda_0$ is the Debye length. For two-dimensional impurities, the solution of (3.95) can be found using the Fourier transformation in the (x,y) plane:

$$\Phi_{\mathbf{k}}(z) = \frac{2\pi k}{k^2+\lambda_D^{-2}}\rho_{\mathbf{k}}\,\exp(-k|z|)\,. \tag{3.96}$$

So the electric potential in the plane, $\varphi(x,y) = \Phi(x,y,0)$, has the λ-spectrum

$$\varphi_\lambda \propto \frac{\lambda}{\lambda^2+\lambda_D^2}\rho_\lambda \propto \begin{cases} \text{const}\,, & \lambda_0 \ll \lambda \ll \lambda_D\,, \\ \lambda^{-3}\,, & \lambda \gg \lambda_D\,. \end{cases} \tag{3.97}$$

The $\varphi(x,y)$ spectrum exponent $H = 0$ (for the scaling range $[\lambda_0, \lambda_D]$) falls into the multiscale regime (3.67). Specifically, the fractal dimension (3.72) of an iso-potential line is $D_h = 10/7$. When a small uniform electric field $\mathbf{E}_1$ is applied, the percolating current channels are formed, whose characteristic transverse walk Δ_ε and the width δ_ε are given by formulas (3.57) and (3.58) in the limit $H \to 0$:

$$\Delta_\varepsilon = \lambda_0/\varepsilon\,, \quad \delta_\varepsilon = \lambda_0\,, \quad \varepsilon \equiv E_1/E_0 \ll 1\,. \tag{3.98}$$

In the scaling range above the Debye length, the isopotentials behave in a monoscale manner ($H = -3 < -1/\nu = -3/4$).

In the case of statistically uniform three-dimensional impurities, we similarly obtain

$$\Phi_\lambda \propto \frac{\lambda^2}{\lambda^2+\lambda_D^2}\rho_\lambda \propto \begin{cases} \lambda^{1/2}\,, & \lambda_0 \ll \lambda \ll \lambda_D\,, \\ \lambda^{-3/2}\,, & \lambda \gg \lambda_D\,. \end{cases} \tag{3.99}$$

The unscreened behavior of $\Phi(\mathbf{x})$ with $H = 1/2$ corresponds to a Brownian function, whose 3D isopotentials have the fractal dimension of 5/2, whereas the connected pieces of their planar cross-section have $D_h = 17/14$ and are not subject to any qualitative change when a small constant electric field is applied.

4. Difficulties of the method of separated scales

The method of the separation of scales is a surrogate for an exact solution which is unknown and one should be cautious applying this technique. The calculation of multiscale topographic exponents, such as $D_h(H)$ and $\tilde{\beta}(H)$, involved the estimation of a product of a large number, up to $m = m(\mu) \simeq \log\Lambda/\log\mu$ ($\Lambda = \lambda_m/\lambda_0 \gg 1$, $\mu = \lambda_{i+1}/\lambda_i$), of terms known only by the order of magnitude. To be more exact, Eq. (3.71) at $\lambda = \lambda_m$ should read

$$L(\lambda_m) = \lambda_0 \prod_{i=1}^{m(\mu)} E_i(\mu) \left(\frac{\lambda_i}{\lambda_{i-1}}\right)^{D_h^{(\infty)}} , \tag{3.100}$$

where all $E_i(\mu) \simeq 1$, and $D_h^{(\infty)}$ is given by formula (3.72). If there is a systematic error in the evaluation of the factors in Eq. (3.100), characterized by the geometric mean $E(\mu) \neq 1$ of $E_i(\mu)$, then expression (3.100) can be written as

$$L(\lambda_m) = \lambda_0 \left(\frac{\lambda_m}{\lambda_0}\right)^{D_h^{(\mu)}} , \tag{3.101}$$

where

$$D_h^{(\mu)}(H) = D_h^{(\infty)}(H) + \frac{\log E(\mu)}{\log\mu} . \tag{3.102}$$

While giving a correct value for the fractal dimension of an isoline of a separated-scale potential ($\mu \gg 1$), $D_h^{(\infty)} = (10 - 3H)/7$ may be wrong in the limit $\mu = 2$, if $E(2) \neq 1$.

On the other hand, being applied to the evaluation of the fractal dimension of the fractional Brownian iso-set $\psi(\mathbf{x}) = h$, $0 < H < 1$, the separated scales predict a correct result, $D = d - H$, confirmed by a direct box-counting calculation and the cross-section rule (Sec. B). The correlation-length exponent of the correlated percolaion problem given in the framework of the method of separated scales, $\tilde{\nu}(H) = -1/H$, also agrees with an independent calculation (Weinrib, 1984).

More confusion is added by the comparison of the correlated beta exponent calculated by the method of separated scales ($\tilde{\beta}(d, H) \equiv \beta(d)$ for any dimension d and $H < 0$) and the

renormalization-group (RG) technique. Weinrib (1984) has developed the RG expansion of the exponent $\tilde{\eta}(d,H) = 2 - d + 2\tilde{\beta}(d,H)/\tilde{\nu}(d,H)$ in a series in $(6-d) > 0$ and $(H+2) > 0$ up to linear terms. The η exponent describes the behavior of a cluster correlation function (Shklovskii and Efros, 1984). At $d = 6$ and higher, the uncorrelated percolation exponents take on their effective-medium values $\nu = 1/2$, $\beta = 1$, $\eta = 0$ (Stauffer, 1979), hence the correlated behavior for $d = 6$ takes place at $H < -1/\nu = -2$. The Weinrib result $\tilde{\eta}(d,H) = (2/11)(H+2) - (1/11)(6-d) + \ldots$ corresponds, in terms of the beta exponent, to $\tilde{\beta}(6,H) = 1 + (6/11)(H+2) + \ldots$, whereas the scale-separation prediction is $\tilde{\beta}(6,H) \equiv 1$. Still, the RG expansion method is far from a rigorous calculation, as well as the separation of scales.

So an independent approach is strongly desired to evaluating the exponents of multiscale statistical topography/correlated percolation or, at least, a specially designed numerical code.

F. Statistics of separatrices

To show the existence of arbitrarily large contours we have used two types of argument: "flood-in-the-hills" and the correspondence of the contour problem to a lattice percolation problem. Another approach to generating large-scale contour lines and surfaces is based on a topological construction of "dressing."

Consider a level line of $\psi(x,y)$ or a level surface of $\psi(x,y,z)$. Move outwards from it and explore neighboring level sets which enclose the initial one. The topology of the nested contours will not change until we encounter a separatrix coming through a saddle point of ψ (Fig. 15). For a nondegenerate potential $\psi(\mathbf{x})$, every saddle (hyperbolic) point lies on a *F 15* different level, therefore, every separatrix looks like figure eight (perhaps, self-enclosed), in two dimensions, or a dumbell, in three dimensions. After encountering a separatrix, we go further and construct a nested set of separatrices similar to Russian Matreshkas. Nothing in

this construction prevents from inflating the contours up to infinity.

For a power-spectrum random function with $H < 1$, the density of stationary points (where $\nabla\psi(\mathbf{x}) = 0$) per unit volume is governed by the λ_0-component of the potential because this component dominates the potential gradient. If follows, in particular, that the average density of saddles points per unit volume is of the order of λ_0^{-d}. As on each step of the dressing procedure the closest to the given separatrix saddle point is caught, the gap $s(a)$ between two nearest-neighbor separatrices of the size a is determined from the requirement that the volume between the separatrices be approximately constant (λ_0^d). Thus $s(a)$ decreases with growing size a inversely proportional to the separatrix measure (length or area):

$$s(a) \propto a^{-D_h} . \tag{3.103}$$

Although telling nothing about critical levels, the topological argument can be used to develop the statistics of separatrices (Gruzinov *et al.*, 1990). Each nondegenerate closed separatrix divides the space into three parts: two bounded and one unbounded (Fig. 15). *F 15* Each bounded part contains at least one extremum of ψ. Introduce the index (i, j) of a saddle point as the number of extrema in the two bounded parts of its separatrix. (We can distinguish the order of i and j, assuming, for example, that the first index corresponds to the part located lower.) Let $P(i, j)$ be the number, per unit volume, of saddle points with the corresponding indices. These numbers are related by certain topological constraints. Indeed, each closed separatrix with the index (i, j) is necessarily surrounded by a nearest -separatrix with the index $(i + j, k)$ or $(k, i + j)$, so that

$$\sum_{i=1}^{l-1} P(i, l-i) = \sum_{k=1}^{\infty} [P(l, k) + P(k, l)] + P(l, \infty) + P(\infty, l) . \tag{3.104}$$

In Eq. (3.104), the possibility is taken into account of the presence of finite number of open separatrices (corresponding to the infinite indices), which is the case in three dimensions. In two dimensions, there exists only one unclosed level line, hence $P(l, \infty) = P(\infty, l) =$

$P(\infty, \infty) = 0$.

A corolary of Eq. (3.104) is the well-known *sum rule* for a two-dimensional potential $\psi(x, y)$ (Longuet-Higgins, 1960b),

$$N_{\text{saddle}} = N_{\text{max}} + N_{\text{min}} \ , \tag{3.105}$$

for the number of the saddles, maxima, and minima of ψ. Indeed, there are exactly as many extrema (minima plus maxima) as the number of saddles, one of whose indices is unity (that is, whose separatrix is the closest one to the given extremum). Relating the number of stationary points to unit volume, we write

$$N_{\text{extr}} \equiv N_{\text{max}} + N_{\text{min}} = \sum_{i=1}^{\infty} [P(1,i) + P(i,1)] + P(1,\infty) + P(\infty,1) \ . \tag{3.106}$$

On the other hand, the total number of saddles is

$$N_{\text{saddle}} = \sum_{i=1}^{\infty}\sum_{j=1}^{\infty} P(i,j) + \sum_{i=1}^{\infty} [P(i,\infty) + P(\infty,i)] + P(\infty,\infty) \ . \tag{3.107}$$

Summing Eq. (3.104) over l and using expressions (3.106)–(3.107), we finally infer

$$N_{\text{saddle}} = N_{\text{extr}} + P(\infty,\infty) \ . \tag{3.108}$$

In two dimension, Eq. (3.108) reduces to the sum rule (3.105). The usual proof of this result (Longuet-Higgins, 1960b) uses the correspondence of the saddles, minima, and maxima of a function defined on a torus to the edges, vertices, and faces, respectively, of a polyhedron, and the Euler theorem (Coxeter, 1973), $N_{\text{edge}} = N_{\text{vertex}} + N_{\text{face}}$.

We continue discussing the two-dimensional case. The toplogical restraint (3.104) can be rewritten in terms of a generating function

$$G(x,y) = (1/N_{\text{saddle}}) \sum_{i=1}^{\infty}\sum_{j=1}^{\infty} P(i,j) x^i y^j \ . \tag{3.109}$$

Multiplying Eq. (3.104) by x^l and summing over l, we obtain the functional equation,

$$G(x,x) = 2G(x,1) - x \ , \tag{3.110}$$

where the normalization condition $G(1,1) = 1$ was taken into account.

Sure enough, being exact for any nondegenerate potential, relation (3.110) is insufficient to determine $G(x,y)$ and thereby $P(i,j)$. If we assume, vaguely referring to a "randomness," that two closed parts of each separatrix are independent, $P(i,j) = P(i)P(j)$, then G is also factorized: $G(x,y) = G(x)G(y)$. Under this assumption, Eq. (3.110) immediately yields

$$G(x) = 1 - (1-x)^{1/2} = \sum_{i=1}^{\infty} \frac{(2i-3)!!}{(2i)!!} x^i \,, \tag{3.111}$$

hence

$$P(i,j) = \frac{(2i-3)!!\,(2j-3)!!}{(2i)!!\,(2j)!!} \simeq \frac{1}{4\pi}\, i^{-3/2}\, j^{-3/2} \,, \quad i,j \gg 1 \,. \tag{3.112}$$

It was established (Gruzinov *et al.*, 1990) that such distribution of separatrices is consistent with the long-range behavior of a monoscale uncorrelated potential $\psi(x,y)$. In all other cases, the two parts of a separatrix are not independent.

IV. TRANSPORT IN RANDOM MEDIA

In this section, two wide classes of transport phenomena are discussed: the diffusion of a tracer (impurity, temperature, etc.) in an incompressible flow and the conductivity of a medium with spatially fluctuating properties. Physically, the most interesting are the cases involving large parameters such as Péclet number (the ratio of convective term to molecular diffusion term) or the strength of the fluctuations in microscopic characteristics of the medium. We will try to demonstrate that, in many cases, percolation theory and/or statistical topography provide helpful tools in theoretical studies of such transport processes.

In Sec. A the advective-diffusive transport of a passive tracer is reviewed. In two dimensions, incompressible streamlines are represented by the contour lines of a stream-function, hence the geometry of a random flow is described in terms of the statistical topography. For a bounded stream-function, the passive transport is asymptotically diffusive, and is characterized by a finite effective (turbulent) diffusion coefficient D_{eff} (Tatarinova *et al.*, 1991; Avellaneda and Majda, 1991). When the stream-function (velocity vector potential in 3D) is not bounded, or is characterized by many scales of length, the passive transport may be *superdiffusive* meaning that the average square displacement grows faster than linear with time. For special initial conditions and on limited time-scales, a more exotic *subdiffusive* tracer behavior is also possible.

In Sec. B selected problems of transport in randomly inhomogeneous media are discussed. The simplest example of such system is a random mixture of conducting and insulating phases (random resistor network) described in the framework of standard percolation problem. Two-dimensional systems *at* the percolation threshold have a remarkable symmetry (Keller, 1964; Dykhne, 1970a), which allows to exactly calculate the effective conductivity for arbitrary conductivities of two phases. Other examples include the plasma heat conduction in a stochastic magnetic field and the electrical conductivity of randomly-inhomogeneous media

with the Hall effect.

A. Advective-diffusive transport

Everyone will acknowledge the striking effect a teaspoon stirring exerts on the sugar dissolution in a cup of coffee. A vast variety of processes, ranging from everyday propagation of smell to heat transport in fusion plasmas, can be cast into the simplest form of the advective-diffusive equation

$$\frac{\partial n}{\partial t} + \mathbf{v}(\mathbf{x},t)\nabla n = D_0 \nabla^2 n \ , \tag{4.1}$$

where n is the density of a passively advected agent (concentration of an impurity, temperature, etc.), $\mathbf{v}$ is a velocity field, and D_0 is the molecular diffusion coefficient or thermal conductivity. In most practically applicable cases, velocity $\mathbf{v}(\mathbf{x},t)$ can be considered incompressible: $\nabla\cdot\mathbf{v} = 0$, or $\mathbf{v} = \nabla\times\boldsymbol{\psi}(\mathbf{x},t)$, where $\boldsymbol{\psi}$ is a vector potential. Along with Eq. (4.1), the problem can be equivalently formulated in terms of a random trajectory of tracer particle described by

$$\frac{d\mathbf{x}}{dt} = \mathbf{v}(\mathbf{x},t) + \mathbf{v}_D(t) \ , \tag{4.2}$$

where $\mathbf{v}_D(t)$ is a Gaussian random noise corresponding to the molecular diffusion, so that

$$\langle \mathbf{v}_D(t)\rangle = 0 \ , \quad \langle v_{Di}(t)\, v_{Dj}(t')\rangle = 2D_0\,\delta(t-t')\,\delta_{ij} \ . \tag{4.3}$$

Then the probability distribution function $n(\mathbf{x},t)$ of the particle position evolves according to Eq. (4.1).

In 1921, G. Taylor put forward the hypothesis of "diffusion by continuous movements." According to this hypothesis, the solution of Eq. (4.2), for a turbulent, zero-mean velocity field $\mathbf{v}(\mathbf{x},t)$, behaves diffusively in the long-time limit, so that

$$\lim_{t\to\infty} \frac{\langle (\mathbf{x}_i(t) - \mathbf{x}_i(0))\,(\mathbf{x}_j(t) - \mathbf{x}_j(0))\rangle}{2t} = D^*_{ij} \ , \tag{4.4}$$

where D_{ij}^* is the effective, or turbulent diffusivity tensor. Taylor (1921) related the effective diffusivity, to the Lagrangian velocity correlator $C_{ij}(t) = \langle v_i(\mathbf{x}(t), t)\, v_j(\mathbf{x}(0), 0)\rangle$ as follows:

$$D_{ij}^* = \int_0^\infty C_{ij}(t)dt \ . \tag{4.5}$$

This well-known result, however, is almost a tautology, because in order to obtain $C_{ij}(t)$ one has first to solve the equation of motion (4.2). The Taylor hypothesis of the turbulent diffusion behavior corresponds to a sufficiently fast decay of Lagrangian correlations so that integral (4.5) converges.

Richardson (1926) analyzed then-available experimental data on diffusion in air. Those data varied by twelve orders of magnitude indicating that there is something wrong with the Taylor hypothesis. Richardson phenomenologicallly conjectured that the diffusion coefficient D_λ in turbulent air depended on the scale length λ of the measurement. The Richardson law,

$$D_\lambda \propto \lambda^{4/3} \tag{4.6}$$

was related to the Kolmogorov-Obukhov turbulence spectrum, $v_\lambda \propto \lambda^{1/3}$, by Batchelor (1952). So the effective-diffusion limit (4.4) does not necessarily exist. It is emphasized that the Richardson law (4.6) describes the *relative diffusivity* of suspended particles, that is, the rate of growth of the mean square distance between two fluid elements in the turbulent medium. The *absolute diffusion* in Kolmogorov turbulence is not universal because the boundary-condition-dependent long-scale velocity pulsations govern the absolute motion of a fluid element and make integral (4.5) diverge (Moffatt, 1981).

There exists, however, an important class of incompressible flows, which lead to a finite absolute turbulent diffusion coefficient (4.4); namely, the flows with a bounded velocity vector potential $\psi(\mathbf{x}, t)$. In Sec. 1 recent rigorous results are reviewed concerning such flows. In Sec. 2 certain regular flows are listed, for which the effective diffusivity D^* is known exactly or can be easily estimated by the order of magnitude. Section 3 is devoted to the

problem of turbulent diffusion in random, steady 2D flows, which are described using the statistical topography theory. In Sec. 4 transport properties of time-varying random flows are discussed. The applications of this theory are primarily concerned with the anomalous transport in turbulent plasmas.

Even when the effective diffusivity D^* governs the asymptotic tracer behavior in an advective-diffusive system, this behavior has finite set-in (mixing) time and length scales. On time- and space-scales below the mixing time τ_m, and the mixing scale ξ_m, the passive scalar transport can be "anomalous," meaning the propagation rate

$$\left\langle (\mathbf{x}(t) - \mathbf{x}(0))^2 \right\rangle^{1/2} \propto t^{\zeta} , \tag{4.7}$$

with $\zeta \neq 1/2$, instead of the behavior of Eq. (4.4). For flows with unbounded vector potential $\psi(\mathbf{x})$ the mixing time τ_m may be infinite, with the anomalous diffusion (4.7) featuring the long-time behavior. The mechanisms of the anomalous diffusion, including both the *superdiffusion* ($\zeta > 1/2$) and the *subdiffusion* ($\zeta < 1/2$) are discussed in Sec. 5.

1. When is the effective transport diffusive, and what are the bounds on the effective diffusivity?

This question was addressed in many works, beginning from Zeldovich (1937), who showed that the lower bound for the effective diffusivity D^* is simply the molecular diffusivity D_0. To be more exact, his result was that arbitrary incompressible convection in a fluid necessarily increases (with respect to the absence of convection) the average impurity flux J between two surfaces where the two constant impurity densities, n_1 and n_2, are maintained. The idea of the proof is based on a simple variation principle: Integrate the quantity $(n\mathbf{v} - D_0 \nabla n)\nabla n$ over the volume outside the two closed surfaces. Then the result is

$$J(n_1 - n_2) = D_0 \int (\nabla n)^2 d\mathbf{x} . \tag{4.8}$$

The right-hand side of Eq. (4.8) is minimized by a harmonic function, $\nabla^2 n = 0$, which corresponds to the zero velocity field in time-independent (or time-averaged) Eq. (4.1).

Effective transport in a convective-diffusive system is governed by a dimensionless parameter,

$$P = \frac{\psi_0}{D_0} , \tag{4.9}$$

known as the *Péclet number*, where ψ_0 is some characteristic (for example, root-mean-square) value of the vector potential $\psi(\mathbf{x}, t)$. According to the Zeldovich variation principle, the effective diffusivity, if exists, must expand in a series of even powers of the Péclet number:

$$D^* = D_0 \left(1 + a_2 P^2 + a_4 P^4 + \ldots\right) , \quad P \ll 1 , \tag{4.10}$$

where $a_2 > 0$. In the limit of a large Péclet number, it is natural to expect that the effective diffusivity greatly exceeds the molecular one:

$$D^* \simeq D_0 \, P^\alpha , \quad P \gg 1 , \tag{4.11}$$

where a non-negative exponent α depends on the topology of the flow.

A more difficult question concerns the very realizability of the effective diffusion regime and the upper bounds for the effective diffusivity. Strictly speaking, condition (4.4) yet does not imply the effective diffusion of a tracer. A stronger requirement is that the local-average tracer density $\langle n \rangle$ evolve according to the effective-diffusion equation

$$\frac{\partial \langle n \rangle}{\partial t} = \frac{\partial}{\partial x_i} D^*_{ij} \frac{\partial \langle n \rangle}{\partial x_j} . \tag{4.12}$$

The local average of the density n is taken near the point $(\mathbf{x}, t)$ over such length scale ξ and time scale τ that satisfy

$$\xi_m \ll \xi \ll l^* , \quad \tau_m \ll \tau \ll t^* , \tag{4.13}$$

where ξ_m and τ_m are the flow-dependent *mixing length* and *mixing time*, respectively, and l^* and t^* are the characteristic length- and time-scales of $\langle n \rangle$. As show inequalities (4.13), the

set-in of the effective diffusion takes finite mixing time τ_m, hence Eq. (4.12) becomes valid only asymptotically.

Another approach to the effective diffusion problem is to consider the velocity field $\mathbf{v}(\mathbf{x}, t)$ as a stationary random field and to average the tracer density n over the statistical ensemble of $\mathbf{v}$. Pioneered by Taylor (1921), this approach remains the most popular. Kraichnan (1970) undertook the explicit computation of mean square particle displacement in 2D and 3D Gaussian velocity fields averaging over 2000 realizations for each ensemble. There was no molecular diffusion in this simulation, and both time-dependent and "frozen" velocity fields were tested. In each case, except for the case of two-dimensional time-independent flows, Kraichnan observed well-established turbulent diffusivity (4.4).

Another computational approach proposed in Isichenko *et al.* (1989) used a precribed quasi-periodic stream-function $\psi(x, y)$ (such as the one shown in Fig. 10) as a model of *F 10* random flow. Although not random, the flow has no apparent degeneracies such as periodicity and looks quite generic. However, one still can visually identify a "trace of periodicity," especially for a small number N of harmonics, because the flow pattern is a two-dimensional projection of a N-dimensional periodic structure (In Fig. 10 $N = 25$). Also, the space- *F 10* average correlator $C(\boldsymbol{\rho}) = \langle \psi(\mathbf{x})\psi(\mathbf{x}+\boldsymbol{\rho})\rangle_{\mathbf{x}}$ does not vanish at large scales showing long correlations that are characteristic for quasicrystals (Levine and Steinhardt, 1984; Kalugin *et al.*, 1985; Steinhardt and Ostlund, 1987; Arnold, 1988). These correlations were not found to appreciably affect the advective-diffusive transport for $N > 3$ (Isichenko *et al.*, 1989).

Analytical results regarding the criterion of the transition to effective diffusion were obtained by McLaughlin *et al.* (1985), who proved the following *homogenization property* of time-independent, incompressible, zero-mean, stationary random flow $\mathbf{v}(\mathbf{x})$. If the Fourier transform $C_{ij}(\mathbf{k})$ of the velocity correlator $C_{ij}(\boldsymbol{\rho}) = \langle v_i(\mathbf{x})v_j(\mathbf{x}+\boldsymbol{\rho})\rangle$ is continuous at the origin $\mathbf{k} = 0$, then the ensemble-average solution of Eq. (4.1), $\langle n\rangle = N_\varepsilon(\mathbf{x}, t)$, corresponding to the initial condition $n(\mathbf{x}, 0) = n_0(\varepsilon\mathbf{x})$, becomes very close, as $\varepsilon \to 0$, to $N(\mathbf{x}/\varepsilon, t/\varepsilon^2)$,

where $N(\mathbf{x},t)$ is the solution of the initial-value problem

$$\frac{\partial N}{\partial t} = \frac{\partial}{\partial x_i} D^*_{ij} \frac{\partial N}{\partial x_j} , \quad N(\mathbf{x},0) = n_0(\mathbf{x}) , \tag{4.14}$$

and the effective diffusivity in any direction $\mathbf{n}$ exceeds the molecular diffusivity:

$$D^*(\mathbf{n}) \equiv |\mathbf{n}|^{-2} D^*_{ij} n_i n_j \geq D_0 . \tag{4.15}$$

Battacharya *et al.* (1989) obtained a similar result for arbitrary periodic incompressible flow, without ensemble averaging. Kalugin *et al.* (1990) proved a homogenization theorem for periodic flows using the analytical continuation of $D^*_{ij}(P)$, considered as a function of Péclet number $P = \psi_{\rm rms}/D_0$, to the complex plane of P. Such an approach led to an efficient algorithm of the computation of D^*_{ij} for any periodic flow using continuous fractions.

Avellaneda and Majda (1989, 1991) generalized the McLaughlin *et al.* (1985) result and showed that the finiteness of the Péclet number (4.9) (with ψ_0 understood as the ensemble root-mean-square vector potential) is an essential necessary and sufficient condition to guarantee the homogenization property for time-independent random flows $\mathbf{v}(\mathbf{x}) = \nabla \times \psi(\mathbf{x})$. They also developed a theory of Padé approximants using a Stieltjes measure representation formula for the effective diffusivity. This theory led to a sequence of rigorous bounds on D^*, of which the simplest one is

$$D_0 \leq D^* \leq D_0 \left(1 + \frac{1}{d} P^2\right) , \tag{4.16}$$

where d is the dimension of the problem. Generally, the first two terms in the low-P expansion (4.10) turn out to be an upper bound for D^* at any P.

Independently, Tatarinova *et al.* (1991) considered the most general case of an arbitrary incompressible 3D time-dependent flow. They gave an elegant proof of the following theorem: If the vector potential $\psi(\mathbf{x},t)$ of a given flow is bounded, $|\psi(\mathbf{x},t)| \leq \psi_{\max}$, then the solution of the initial-value problem (4.1) with $n(\mathbf{x},0) = \delta(\mathbf{x} - \mathbf{x}_0)$ behaves as follows. The

mean square displacement,

$$R^2(t,\mathbf{x}_0) \equiv \int (\mathbf{x}-\mathbf{x}_0)^2 n(\mathbf{x},t)d\mathbf{x}\ , \tag{4.17}$$

grows with progressing time not slower and not faster than linearly in the sense that

$$D_0 \le \frac{\langle R^2(t,\mathbf{x}_0)\rangle_{\mathbf{x}_0}}{2td} \le D_0 + \frac{\psi^2_{\max}}{D_0}\ . \tag{4.18}$$

Most likely, the averaging of R^2 over the initial position $\mathbf{x}_0$ is not essential for this result. The comparison of the Tatarinova *et al.* theorem with the Avellaneda-Majda theorem suggests that the boundedness of the vector potential $\boldsymbol{\psi}(\mathbf{x},t)$ is also sufficient for the global transport homogenization, that is, the asymptotic transition from Eq. (4.1) to Eq. (4.12). In such general form, however, the homogenization theorem has not yet been proved.

Thus one may conclude that, in the presence of finite molecular diffusivity, the finite vector potential is sufficient, and "almost necessary" condition for the effective diffusion to be established, with the effective diffusivity satisfying the inequality

$$D_0 \le D^* \le D_0 + \frac{\psi^2_{\max}}{D_0}\ . \tag{4.19}$$

In terms of the scaling exponent α entering expression (4.11), this implies $0 \le \alpha \le 2$.

For the case of anisotropic molecular diffusivity tensor $\widehat{D_0}$ and a possible anisotropy of the flow, following the lines of Tatarinova *et al.* (1991), inequality (4.19) can be generalized as

$$D_{0\mathbf{n}} \le D^*_{\mathbf{n}} \le D_{0\mathbf{n}} + \max_{\mathbf{x},t}\max_{\mathbf{m}} \frac{[\mathbf{m}\times\mathbf{n}\cdot\boldsymbol{\psi}(\mathbf{x},t)]^2}{|\mathbf{m}|^2\,|\mathbf{n}|^2\,D_{0\mathbf{m}}}\ , \tag{4.20}$$

where $D_{\mathbf{n}} \equiv D_{ij}n_in_j/|\mathbf{n}|^2$ denotes the diffusivity in the $\mathbf{n}$ direction. Apparently, inequality (4.19) is a particular case of (4.20). Result (4.20) will be used in Sec. B.3 to establish bounds on the effective conductivity of heterogeneous media.

2. Effective diffusivity: Simple scalings

There exist several classes of flow, whose transport properties can be calculated exactly. As we will see, the rigorous bounds on the effective diffusivity (4.19) are attainable.

The simplest example of a shear flow in a tube was considered by Taylor (1953, 1954), who noticed that the axial dispersion of a solute advected by the Poiseuille flow $v(r) = v_0(1 - r^2/a^2)$ (where $v(r)$ is the axial velocity in a tube of the radius a) is described, in a mean velocity frame of reference, by a diffusive law. For $av_0 \gg D_0$, Taylor found the following expression for the "virtual coefficient of the diffusivity": $D^* = a^2 v_0^2/(192 D_0)$. He proposed to use this result for the investigation of the propagation of salts in blood streams. Aris (1956) has generalized Taylor results to the case of arbitrary Péclet number $P = av_0/D_0$ and different tube cross-sections, where all possibilities are covered by one exact formula

$$D^* = D_0 + K \frac{a^2 v_0^2}{D_0} \tag{4.21}$$

with different values of the numerical constant K.

Zeldovich (1982) considered the periodic time-dependent flow in the (x, y) plane,

$$\mathbf{v} = v_0 \hat{\mathbf{x}} \cos ky \cos \omega t \ , \tag{4.22}$$

and found the effective diffusivity in the x-direction:

$$D^*_{xx} = D_0 \left(1 + \frac{1}{4} \frac{k^2 v_0^2}{\omega^2 + k^4 D_0^2} \right) . \tag{4.23}$$

In the case of a general time-independent shear flow $\mathbf{v} = \hat{\mathbf{x}}\, d\psi(y)/dy$, $\langle \psi(y) \rangle_y = 0$, one has (Avellaneda and Majda, 1990; Isichenko and Kalda, 1991a) $D^*_{yy} = D_0$,

$$D^*_{xx} = D_0 + \frac{\langle \psi^2(y) \rangle_y}{D_0} \ . \tag{4.24}$$

The above results are obtained separating the tracer density n into an oscillating and a smoothed component, a method similar to the technique of multiple-scale expansion (cf. Bender and Orszag, 1978). The physical meaning of result (4.24) is quite simple: Due to the

molecular diffusion in the y-direction, a tracer particle resides in a channel with the same direction of velocity for a characteristic correlation time $\tau_m = \lambda_0^2/D_0$, where λ_0 is the characteristic scale of the flow. The advective displacement experienced by the particle during this time is $\xi_m = v_0\,\tau_m$. The effective diffusivity in the x-direction is then estimated as $D^* \simeq \xi_m^2/\tau_m = \lambda^2\,v_0^2/D_0$, in accordance with (4.24). Quantities ξ_m and τ_m represent the mixing length in the x-direction and the mixing time, respectively.

In terms of the scaling exponent α (see Eq. (4.11)), result (4.24) corresponds to the maximum possible value $\alpha = 2$. This is quite sensible because open (e.g., straight) streamlines promote the best imaginable mixing along their direction. By the way, the exact maximum of D^*_{xx}, given by expression (4.19) is also attained by a shear flow with a step-like stream-function

$$\psi(y) = \psi_0 \operatorname{sign} f(y)\ , \quad \langle \psi(y) \rangle_y = 0\ , \tag{4.25}$$

corresponding to vanishingly narrow velocity jets located at the zero lines of $f(y)$. According to formula (4.24), we have $D^*_{xx} = D_0 + \psi_0^2/D_0 = D_0 + \psi_{\max}^2/D_0$.

The second class of flow with a simple effective diffusion scaling is a periodic array of convection rolls, such as modelled by the stream-function

$$\psi(x,y) = \psi_0 \sin k_x x\, \sin k_y y \tag{4.26}$$

(see Fig. 20). For this, and topologically similar flows, and its simplest generalizations, it *F 20* was noticed (Dykhne, 1981; Moffatt, 1983) that the large-Péclet-number asymptotics of D^* corresponds to the exponent $\alpha = 1/2$:

$$D^* = C\sqrt{D_0\,\psi_0}\ , \quad P \equiv \psi_0/D_0 \gg 1\ . \tag{4.27}$$

It was later in 1987 that flow (4.22) drew much attention (Osipenko *et al.*, 1987; Rosenbluth *et al.*, 1987; Shraiman, 1987; Perkins and Zweibel, 1987; Soward, 1987). Using asymptotic expansion for periodic fields (Bensoussan *et al.*, 1978; Brenner, 1980) or similar in spirit

methods, the problem was reduced to the effectively one-dimensional cross-stream diffusion within one convection cell making it possible to calculate the numerical constant C in expression (4.27). Formula (4.27) was confirmed in a specially designed experiment (Solomon and Gollub, 1988), where passive tracer transport was studied in a periodic system of controlled Rayleigh-Bénard convection rolls.

The $\sqrt{D_0}$ scaling is due to the formation, in the large Péclet number limit, of diffusive boundary layers near the separatrices (Fig. 20) where the tracer density gradients turn out *F 20* to be concentrated. Being of major significance for effective transport, the boundary layer width w_b is determined as the characteristic diffusive displacement a tracer particle undergoes in the course of the advective rotation period:

$$w_b = \sqrt{D_0 \, \lambda_0 / v_0} \; , \tag{4.28}$$

where λ_0 is the cell size and $v_0 = \psi_0/\lambda_0$ the characteristic velocity. Then the effective diffusivity is estimated in terms of a usual random walk expression $\lambda_0^2/(\lambda_0/v_0)$ multiplied by the fraction of "active" particles w_b/λ_0 lying in the boundary layer. This leads to the result

$$D^* \simeq v_0 \, w_b \; , \tag{4.29}$$

revealing expression (4.27).

It is interesting to note that, while the periodic flow (4.26) was generally invoked to model steady Rayleigh-Bénard convection (Chandrasekhar, 1961; Busse, 1978; Haken, 1977), the effective diffusivity in the Rayleigh-Bénard system may behave quite differently from the prediction of formula (4.27) (Dykhne, 1981). There are two principle patterns of steady convection in a fluid heated from below; namely, rolls (Fig. 21(a)) and hexagons (Fig. 21(b); *F 21a* Busse, 1978). The transport properties of rolls are properly modelled by flow (4.26) for the *F 21b* case of "free-slip" boundaries at the bottom of the vessel. In the case of "no-slip" boundary condition, the effective diffusivity D^* scales proportional to $D_0^{2/3}$ (Rosenbluth *et al.*, 1987).

Unlike the roll-convection pattern, the separatrices of Rayleigh-Bénard hexagons include not only the interfaces between the cells but also the cells' axes (Fig. 21(b)). Due to the F. 21b incompressibility of the flow, a near-axis boundary layer is much wider ($W \gg w$) than a corresponding near-interface boundary layer (w). Assuming the same order of magnitude in velocity, the fluid flux conservation yields $v_0 \lambda_0 w = v_0 W^2$, hence

$$W(w) = \sqrt{\lambda_0 w} \ , \tag{4.30}$$

where λ_0 is the horizontal size of the hexagonal cells. For the effective diffusion to be established, the tracer particle has to diffuse all way through the near-axis layer: until then it will just walk between two neighboring cells (Fig. 21(b)). The widths of the diffusive *F 21b* boundary layers are estimated from $W^2(w_b)/D_0 = \lambda_0/v_0$, hence

$$w_b = \frac{D_0}{v_0} \ , \quad W_b = \sqrt{D_0 \, \lambda_0 / v_0} \ . \tag{4.31}$$

The simplest evaluation (4.29) would then give $D^* = D_0$, which is, however, somewhat underestimated. In fact, one must sum the contributions of approximately $\log(\lambda_0/w_b)$ different layers, $w = w_b, 2w_b, 4w_b, \ldots, \lambda_0$, each contribution being $D^*(w) \simeq (w/\lambda_0)\, \lambda_0^2/(W^2(w)/D_0) = D_0$. As a result, for the steady Rayleigh-Bénard convection pattern, the effective diffusivity scales as (Dykhne, 1981)

$$D^* \simeq D_0 \log P \ , \quad P = \frac{\lambda v_0}{D_0} \gg 1 \ , \tag{4.32}$$

showing an anomalously weak transport enhancement.

Smaller yet enhancement, up to the lower bound in Eq. (4.19), is realized for flows with localized, non-overlapped domains of nonvanishing velocity, for sufficiently small fraction of volume occupied by these domains. This becomes quite obvious if one substitutes the advective domains by infinite-diffusivity domains. Well below the percolation threshold, this will not significantly increase the transport properties of the medium, compared to the

background diffusivity D_0. Approaching the percolation threshold for the advective domains, one can in principle construct flows with an arbitrary transport scaling exponent $\alpha \in [0, 2]$. One such example, with $\alpha = 1/2$, was given in Avellaneda and Majda (1991).

The next exactly solvable example is the 2D isotropic system of narrow velocity jets:

$$\psi(x, y) = \psi_0 \operatorname{sign} f(x, y) \ , \quad \langle \psi(x, y) \rangle = 0 \ , \tag{4.33}$$

where the isotropicity of the effective diffusivity D^* is *assumed.* The function $f(x, y)$ may be a checkerboard pattern, $f = \sin kx \sin ky$, or a realization of a random field, such as the one shown in Fig. 10. Using the correspondence between the advective-diffusive problem and the *F 10* effective conductivity of an inhomogeneous medium with Hall-effect (Dreizin and Dykhne, 1972) and the solution of the conductivity problem for a 2D, two-phase system (Dykhne, 1970b; see Sec. IV.B.2), D^* can be calculated exactly. The result is the "Pithagor formula" (Dykhne, 1981; Tatarinova, 1990)

$$D^* = \sqrt{D_0^2 + \psi_0^2} \ , \tag{4.34}$$

corresponding to the scaling exponent $\alpha = 1$. Result (4.34) is valid for arbitrary Péclet number. The mixing length and time are less universal and depend on the details of $\psi(x, y)$.

Regarding time-dependent advecting flows, it is generally believed that, while being of importance for smoothing small-scale tracer density structure (Moffatt, 1981), weak molecular diffusion does not significantly affect the long-range passive transport. In the limit of vanishing molecular diffusivity D_0, the effective diffusivity remains finite, $D^* \simeq \psi$ (Kraichnan, 1970; Pettini *et al.*, 1988; Horton, 1989), that is, $\alpha = 1$. The Zeldovich (1982) result (4.22)–(4.23) is exceptional in this respect, due to the special kind of the flow time-dependence, which preserves the topology of the streamlines. Another special case of preserved topology is the system of localized travelling vortices, which can arise in course of the evolution of two-dimensional turbulence in atmosphere, ocean, or plasmas (Larichev and Reznik, 1976;

Flierl *et al.*, 1980; Hasegawa *et al.*, 1979; Kraichnan and Montgomery, 1980; Petviashvili and Yankov, 1989). The dominant feature of a localized travelling vortex is the presence of a separatrix, inside which the fluid is carried by the vortex (Fig. 22) moving at a constant *F 22* speed **u**. This feature makes vortices efficient mixing agents, so that the scaling exponent α in Eq. (4.11) attains its maximum value, $\alpha = 2$, for a flow presented as a "vortex gas," that is, an ensemble of large number of travelling vortices, whose interaction is unessential. The effective diffusivity of the vortex gas for the large Péclet number limit was calculated in Isichenko *et al.* (1989):

$$D^*_{ij} = \eta \langle s\tau_m u_i u_j \rangle + D_0 \delta_{ij} , \tag{4.35}$$

where η is the number of vortices per unit area, $s \simeq \lambda_0^2$ is the area enclosed by the separatrix of a vortex, $\tau_m \simeq \lambda_0^2/D_0$ is a diffusion time inside the vortex, and the averaging in (4.35) is taken over the vortices. The estimate of the exact result (4.35) can be obtained as follows. A tracer particle is trapped and carried by a vortex for the diffusion time $\tau_m = \lambda_0^2/D_0$ and then released the distance $\xi_m = u\tau_m$ apart from the point of trapping. The effective diffusivity is then obtained as ξ_m^2/τ_m multiplied by the fraction of area, $\eta\lambda_0^2$, where the trapping processes take place. The resulting expression, $D^* \simeq \eta\lambda_0^4 u^2/D_0$, agrees with formula (4.35) for sufficiently high Péclet number, $P = \lambda_0 u/D_0 \gg (\eta\lambda_0^2)^{-1/2} \gg 1$. The effects of vortex collisions (Horton, 1989) and of the inhomogeneity of the vortex-supporting medium (Zabusky and McWilliams, 1982; Nycander and Isichenko, 1990) lead to various regimes of effective diffusion, including those, for which the molecular diffusivity D_0 is unessential.

3. Effective diffusivity in two-dimensional random, steady flows

As we have seen, the behavior of effective diffusivity in the large-Péclet-number limit depends on the topology of flow streamlines. The best mixing properties exhibit flows with extended streamlines, such as a shear flow, where the mixing length ξ_m tends to infinity as $D_0 \to 0$. The geometry of 2D random flows assumes the presence of arbitrarily extended streamlines,

though their share falls out with increasing size. To estimate the effective diffusivity in such a flow, statistical topography must be used for the description of streamlines (Isichenko *et al.*, 1989; Gruzinov *et al.*, 1990; Isichenko and Kalda, 1991c).

It is difficult to imagine a time-independent, or slowly time-dependent, 2D random flow in such traditional 2D objects as atmosphere or ocean, where the characteristic frequency ω is typically of the order of the inverse eddy rotation time, $\omega \simeq v_0/\lambda$. The practical implications of "frozen" 2D random flows involve primarily condense-matter objects, such as quantum diffusion (Kravtsov *et al.*, 1986), quantum Hall effect (Prange and Girvin, 1990), or inhomogeneously doped semiconductors (Dreizin and Dykhne, 1972; Isichenko and Kalda, 1991a).

The first percolation-theory analysis of the effective diffusion in a 2D, random, incompressible, steady flow (Isichenko *et al.*, 1989) was motivated by the observation that the periodic flow pattern (4.26) is structurally unstable: A vanishingly small perturbation of the stream-function will destroy the regular system of elementary convective cells, gather them into various conglomerates, and thereby produce arbitrary length scales in the isolines of $\psi(x,y)$ (see Fig. 11). Although there is no doubt in the existence of a well-defined effective diffusivity D^* for a bounded random stream-function $\psi(x,y)$, there has been developed no formal theory involving the rigorous calculation of D^* for a large Péclet number. The small Péclet number expansion for random flows was developed in Derrida and Luck (1983), Fisher (1984), Kravtsov *et al.* (1986), and Bouchard *et al.* (1987) using path integrals and the renormalization group theory. *F 11*

For a monoscale stream-function $\psi(x,y)$ (Fig. 10) heuristic arguments were used (Isichenko *et al.*, 1989) to derive the $\alpha = 10/13$ scaling *F 10*

$$D^* \simeq D_0 \left(\frac{\psi_0}{D_0}\right)^{10/13} , \quad \psi_0 \equiv \psi_{\rm rms} \gg D_0 , \tag{4.36}$$

where the exponent was expressed through the 2D percolation indices, $\nu = 4/3$ and $d_h = 7/4$:

$$\alpha = \frac{\nu d_h + 1}{\nu d_h + 2} = \frac{10}{13} \,. \tag{4.37}$$

Due to the role of extended streamlines of a random flow, effective diffusivity (4.36) greatly exceeds expression (4.27), valid for finite-size convection cells, at the same Péclet number.

The derivation of result (4.36) employs a hypothesis of broken coherence. This hypothesis assumes that the particle displacements governed by Eq. (4.2) may be considered uncorrelated if the streamlines, on which these displacements are experienced, differ twice or more in size. In this way, one naturally comes to the concept of convection cells being the conglomerates of streamlines with diameter between a and $2a$ ("a-cells" — see Fig. 17). The mixing F 17
length ξ_m is then determined as the size of convection cells producing the most efficient coherent contribution to transport. The calculation is quite similar to that based on the boundary layer argument for a periodic array of vortices (Fig. 20). The difference, however, *F 20*
is that the convection cells of a random flow are diverse, and their size a, width $w(a)$, and perimeter $L(a)$ are coupled in a fashion determined by the statistics of the random field $\psi(x,y)$. For example, for a monoscale (λ_0) flow the relations given by Eqs. (3.41) and (3.43) should be used. Using the standard boundary layer argument, we find the mixing length ξ_m as the cell size where the convection time equals the transverse diffusion time,

$$\frac{L(\xi_m)}{v_0} = \frac{w^2(\xi_m)}{D_0} \,, \tag{4.38}$$

where $v_0 = \psi_0/\lambda_0$ is the characteristic velocity. Substituting expressions (3.41) and (3.43) for the length $L(a)$ and the width $w(a)$ of the convection cell, we find

$$\xi_m = \lambda_0 \, P^{\frac{\nu}{\nu d_h + 2}} \,, \quad P \equiv \frac{\psi_0}{D_0} \gg 1 \,. \tag{4.39}$$

The effective diffusivity is then estimated as

$$D^* \simeq F(\xi_m) \frac{\xi_m^2}{w^2(\xi_m)/D_0} = v_0 \, w(\xi_m) \,, \tag{4.40}$$

where $F(a) = L(a)w(a)/a^2$ is the distribution function (area fraction) of the convection cells over their size. Substituting expression (4.39) into (4.40) we arrive at the result (4.36). The mixing time in a monoscale λ_0-flow is given by the formula

$$\tau_m = \frac{\lambda_0^2}{D_0} , \tag{4.41}$$

corresponding to the time of diffusive sampling of all "undermixing" (that is, with $a < \xi_m$) convection cells.

Expression (4.40) describes the effective diffusion contribution of mixing (ξ_m) convection cells only. Nevertheless, this contribution constitutes of order one half the effective diffusivity thereby yielding a correct estimate of D^*. The contribution of more numerous "undermixing" cells with $\lambda < \xi_m$ can be written similarly to (4.40):

$$D_\lambda \simeq F(\lambda) \frac{\lambda^2}{w^2(\lambda)/D_0} = D_0 \frac{L(\lambda)}{w(\lambda)} , \quad \lambda_0 < \lambda < \xi_m . \tag{4.42}$$

The hypothesis of broken coherence implies that the effective diffusivity can be estimated as the sum of *partial diffusivities* D_λ, for $\lambda = \lambda_0, 2\lambda_0 4\lambda_0, \ldots \xi_m$, that is, [1]

$$D^* \simeq \int_{\lambda_0}^{\xi_m} D_\lambda \frac{d\lambda}{\lambda} . \tag{4.43}$$

The partial diffusivity $D_\lambda \propto \lambda^{d_h+1/\nu}$ increases with the increasing scale λ making expression (4.43) peak near the upper integration limit.

The percolation scaling of the effective diffusivity involving the exponent $\alpha = 10/13$ appears to be as universal as the static exponents of continuum percolation (see Sec. II.E). This implies that the randomness (in the sense of the ensemble averaging) of the velocity field is not really necessary for the result (4.36) to be valid, the *genericity* (absence of exceptional features like periodicity, etc.) of the flow will suffice. The computation of effective diffusion for quasi-periodic flows having extended streamlines showed a fair agreement with the "10/13" scaling (Isichenko *et al.*, 1989).

[1] The contribution of "overmixing" convection cells with diameter $\lambda \gg \xi_m$ is negligible due to both the scarcity of such cells and the particle diffusive decorrelation from them well before sampling their extent.

A similar approach was used to calculate the effective diffusivity in a multiscale random flow, with the stream-function spectrum $\psi_\lambda \propto \lambda^H$, $\lambda_0 < \lambda < \lambda_m$ (Isichenko and Kalda, 1991c). Due to a more sophisticated dependence of $L(a)$ and $w(a)$ (see Eqs. (3.71)), (3.75), and (3.77)), there are several regimes of effective diffusion in this flow. The regimes are depicted in Fig. 23, where the parameter space (H, $\log(\lambda_m/\lambda_0)/\log(\psi_0/D_0)$) is shown. One of these regimes corresponding to the monoscale correlated stream-function (regime B in Fig. 23) is recovered by simple substitution of the random-percolation exponents by their correlated counterparts (see Sec. II.D), F 23 F 23

$$\nu \to -\frac{1}{H}\,, \quad d_h \to D_h\,, \quad -\frac{1}{\nu} < H < 0\,. \tag{4.44}$$

In this case we have from Eq. (4.37)

$$\alpha = \frac{-D_h/H+1}{-D_h/H+2} = \frac{10(1-H)}{10-17H}\,, \quad -\frac{3}{4} < H < 0\,. \tag{4.45}$$

For H tending to zero, α tends to unity and the effective diffusivity D^* becomes independent of D_0. Such independence extends to regime C. Regime A, which is characterized by the monoscale-like scaling $D^* \propto D_0^{3/13}$, is obtained by substituting the partial diffusivity D_{λ_m} (4.42) into the monoscale flow $\psi_{\lambda_m}(x,y)$ and using formula (4.36). In this representation, D_{λ_m} is the "renormalized molecular diffusivity," which accounts for the transport effect of the flow spectral components with $\lambda < \lambda_m$.

4. Diffusion in time-dependent random flows

Thus far, we were concerned with "frozen" random flows, or an "unessential" time-dependence preserving the topology of streamlines. In the case of an "essential" time-dependence, where the topology is changed, effective diffusion can set in even at zero molecular diffusivity.

The general reason for the decay of orbit correlations in (4.5), and hence the transition to the effective diffusion, is Hamiltonian chaos (Lichtenberg and Lieberman, 1983; Sagdeev

et al., 1988). Suppose $D_0 = 0$. Then the equations of fluid element motion,

$$\frac{dx}{dt} = \frac{\partial \psi(x,y,t)}{\partial y} \ , \quad \frac{dy}{dt} = -\frac{\partial \psi(x,y,t)}{\partial x} \ , \tag{4.46}$$

correspond to the Hamiltonian ψ defined in the phase space (x, y). The Liouville theorem is equivalent to the incompressibility of the flow $\mathbf{v} = \nabla\psi \times \hat{\mathbf{z}}$. The one-degree-of-freedom time-dependent Hamiltonian $\psi(x, y, t)$ is equivalent to a two-degree-of-freedom autonomous Hamiltonian in a four-dimensional phase space (Lichtenberg and Lieberman, 1983). Subtracting one dimension for the autonomous Hamiltonian conservation, we get an essentially three-dimensional iso-energetic manyfold, which is the lower critical dimension for the stochastic phase orbits. Indeed, a self-avoiding smooth Hamiltonian orbit can behave chaotically in a 3D space, densely filling whole domains, which is impossible in two dimensions. In fact, the stochastic behavior is a structurally stable property of Hamiltonian systems far from (degenerate) integrable cases, that is, chaos is not eliminated by a small change in the Hamiltonian (Arnold, 1978). The manifestation of the stochasticity is the extreme sensitivity of phase orbits to the initial conditions. Two close trajectories diverge in time exponentially fast. The quantitative characteristic of this exponentiation is the Kolmogorov entropy,

$$K = \lim_{t\to\infty} \lim_{|\delta\mathbf{x}(0)|\to 0} \frac{1}{t} \log \frac{\langle |\delta\mathbf{x}(t)| \rangle}{|\delta\mathbf{x}(0)|} \ , \tag{4.47}$$

where $\delta\mathbf{x}(t)$ designates the distance between two neighboring fluid elements, and average over the initial condition is taken. The case of positive K is usually referred to as chaotic advection (Aref, 1984), or Lagrangian chaos (Dombre *et al.*, 1986).

For a generic 2D fluid motion characterized by the velocity amplitude v_0 and length-scale λ_0, velocity field evolves at the characteristic frequency $\omega = v_0/\lambda_0$. In this case the turbulent diffusivity D^* and the Kolmogorov entropy are estimated from the simplest dimensional consideration: $D^* \simeq \lambda_0 v_0$, $K \simeq v_0/\lambda_0$, because there are no other independent parameters. In thecase of plasma turbulence ω can be independent of λ_0 and v_0. For example, the

drift wave frequency ω_* is determined from a linear dispersion relation, whereas the drift turbulence amplitude is governed by various nonlinear effects (Horton, 1990). The guiding center motion of a charged particle in crossed electric ($\mathbf{E} = -\nabla\varphi(\mathbf{x},t)$) and magnetic ($\mathbf{B} = B_0\,\hat{\mathbf{z}}$) fields is described by

$$\frac{d\mathbf{x}}{dt} = v_{\|}\,\hat{\mathbf{z}} + c\,\frac{\mathbf{E}\times\mathbf{B}}{B^2}\,, \tag{4.48}$$

which corresponds to incompressible motion across the magnetic field with the stream-function

$$\psi(x,y,t) = -\frac{c}{B_0}\,\varphi\left(x,y,z_0 + \int_0^t v_{\|}(t')dt', t\right)\,. \tag{4.49}$$

The characteristic frequency, $\omega = \max(\omega_*, k_{\|}\,v_{\|})$ (where $k_{\|} \simeq |\partial \log\varphi/\partial z|$), is thus decoupled from the amplitude of ψ. This leads to the possibility of both the high-frequency regime ($\omega \gg v_0/\lambda_0$, also known as the quasilinear limit) and the low-frequency ($\omega \ll v_0/\lambda_0$), or percolation regime of turbulent diffusion (Isichenko and Horton, 1991).

Another example is the plasma heat conduction in a magnetic field with a small random component, $\mathbf{B} = B_0\,\hat{\mathbf{z}} + \delta\mathbf{B}_\perp(\mathbf{x})$, $\delta\mathbf{B}_\perp = \nabla A_{\|}(\mathbf{x})\times\hat{\mathbf{z}}$. The equation of a magnetic field line in the form

$$\frac{d\mathbf{x}_\perp}{dz} = \frac{\delta\mathbf{B}_\perp}{B_0} \tag{4.50}$$

is equivalent to Eq. (4.46) with the stream-function $\psi(\mathbf{x}_\perp, z) = A_{\|}(\mathbf{x}_\perp, z)/B_0$ and the coordinate z standing for time. The turbulent diffusivity stemming from Eq. (4.50) is known as the magnetic field line diffusivity D_m (Rosenbluth *et al.*, 1966). This quantity has the dimensionality of length. In a collisionless plasma, the diffusive walk of magnetic lines causes an enhanced electron thermal conductivity across the background magnetic field (Rechester and Rosenbluth, 1978; Kadomtsev and Pogutse, 1979; Krommes, 1978)

$$\chi_\perp^* \simeq D_m\,v_e\,, \tag{4.51}$$

where v_e is the thermal velocity of electrons. Particle transport coefficients are also proportional to D_m (Finn *et al.*, 1991). The processes of heat conduction in a collisional plasma

are more complicated, the expression for χ^* involving both the magnetic line diffusivity D_m and the Kolmogorov entropy K (see Sec. B.2).

Gruzinov *et al.* (1990) studied turbulent diffusion in two dimensions, with the characteristic flow frequency ω considered a free parameter. In the high-frequency limit, $\omega \gg v_0/\lambda_0$, the effective diffusivity is insensitive to the topology of the streamlines because the flow is changed in the correlation time ω^{-1}, that is, well before a tracer particle is displaced to the distance λ_0. This leads to the following *quasilinear* expression for the diffusivity (Kadomtsev and Pogutse, 1979):

$$D^* \simeq \frac{v_0^2}{\omega}\,, \quad \omega \gg \frac{v_0}{\lambda_0}\,. \tag{4.52}$$

In the low-frequency (percolation) limit, $\omega \ll v_0/\lambda_0$, a tracer particle can traverse along an almost steady streamline to a large distance before the flow pattern has appreciably changed. The mixing length ξ_m is defined as the maximum coherent particle displacement, which occurs in the life-time $\tau(\xi_m)$ of the convection cell:

$$L(\xi_m) = v_0\,\tau(\xi_m) \tag{4.53}$$

(compare with (4.38)). The life-time $\tau(a)$ of an a-cell is the time of unrecognizable change (for example, twice in diameter) in the contour $\psi(x,y,t) = h$ with the initial diameter a. Such a change is undergone through the contour reconnection process (Fig. 24). The F 24
reconnection takes place when the saddles corresponding to neighboring separatrices come through the same level. An essential change in the shape of the convection cell occurs when the saddles pass the level difference $\delta\psi = \psi_0 w(a)/\lambda_0$ corresponding to the width of the cell. Since the level of a saddle point changes at the characteristic rate $\psi_0\omega$, one finds the life-time of the convection cell,

$$\tau(a) = \frac{\delta\psi}{\psi_0\omega} = \frac{w(a)}{\lambda_0\,\omega}\,. \tag{4.54}$$

Substituting Eq. (4.54) into (4.53), we find the mixing scale

$$\xi_m = \lambda_0 \left(\frac{v_0}{\lambda_0 \omega} \right)^{\frac{\nu}{\nu d_h + 1}} . \tag{4.55}$$

The turbulent diffusivity is then estimated similarly to (4.40),

$$D^* \simeq F(\xi_m) \frac{\xi_m^2}{\tau(\xi_m)} = v_0 \, w(\xi_m) . \tag{4.56}$$

So the percolation scaling of the turbulent diffusivity is given by

$$D^* = \psi_0 \left(\frac{\omega \lambda_0}{v_0} \right)^{\frac{1}{\nu d_h + 1}} = \psi_0 \left(\frac{\omega \lambda_0}{v_0} \right)^{3/10} , \quad \omega \ll \frac{v_0}{\lambda_0} . \tag{4.57}$$

Ottaviani (1991) studied the effective diffusion in a slowly varying 2D flow numerically. He used a quasiperiodic stream-function with $N = 64$ standing waves modulated by random Gaussian amplitudes with a long correlation time ω^{-1}. The observed scaling of the turbulent diffusivity, $D^* \propto \psi_0^{0.8}$ was close to the one predicted by formula (4.57) ($D^* \propto \psi_0^{7/10}$).

The Kolmogorov entropy in a fast-oscillating random flow was calculated by Kadomtsev and Pogutse (1978):

$$K \simeq \frac{v_0^2}{\lambda_0^2 \omega} , \quad \omega \gg \frac{v_0}{\lambda_0} . \tag{4.58}$$

The quasilinear result (4.58) can be obtained by averaging the second-order moments of linearized Eq. (4.46) (Krommes *et al.*, 1983; Isichenko, 1991a).

This method does not work in the percolation limit $\omega \ll v_0/\lambda_0$, again implying the necessity of using geometrical tricks. Berry *et al.* (1979) proposed to study mappings of curves rather than points. They described two principal types of convolution of a "liquid curve:" "whorls" and "tendrils" (Fig. 25). The advantage of the liquid curve representation F 25
lies in that at any time the curve consists of close points, hence the rate of the curve elongation provides a natural measure of the average stochastic exponentiation of neighboring orbits. Gruzinov *et al.* (1990) studied the exponentiating tendrils in a monoscale 2D random flow that occur due to the elementary reconnections of the separatrices (Fig. 26). The most *F 26*

efficient contribution to the liquid curve elongation is done by convection cells where the convective revolution time is balanced by the reconnection time of two neighboring separatrices. Consider a monoscale random flow changing with the characteristic frequency $\omega \ll v_0/\lambda_0$. As the distance $s(a)$ between two neighboring separatrices is inversely proportional to the length $L(a)$ of the streamline (see Eq. (3.103)), the reconnection occurs in the characteristic time $\tau_s(a) = \omega^{-1}s(a)/\lambda_0 = \omega^{-1}\lambda_0/L(a)$ corresponding to the level difference $\psi_0 s(a)/\lambda_0$ passed by a saddle at the velocity $\psi_0\omega$. The rate of exponentiation is dominated by such streamlines (diameter a_K) that reconnect in the advective revolution time: $\tau_s(a_K) = L(a_K)/v_0$). Hence we find $L(a_K) = (\lambda_0 v_0/\omega)^{1/2}$, and the Kolmogorov entropy is estimated as $K \propto v_0/L(a_K)$. The multiplicity of separatrices inside one a_K-cell leads to a logarithmic correction in K, so that

$$K \simeq \left(\frac{\omega\, v_0}{\lambda_0}\right)^{1/2} \log \frac{v_0}{\lambda_0\,\omega}\,, \quad \omega \ll \frac{v_0}{\lambda_0}\,. \tag{4.59}$$

The low-frequency/large Péclet number turbulent diffusion theory, which employs the statistical topography analysis, was extended in several directions. Kalda (1991) studied the general case of multiscale, time-dependent, incompressible 2D flow, including the effect of molecular diffusion, where numerous effective diffusion regimes have been identified.

Gruzinov (1991) considered the effective diffusion in a weakly compressible random flow

$$\mathbf{v} = \boldsymbol{\nabla}\psi(x,y,t) \times \hat{\mathbf{z}} + \varepsilon \boldsymbol{\nabla}\psi(x,y,t)\,. \tag{4.60}$$

The last term in (4.60), which models a non-Hamiltonian friction experienced by a drifting guiding center, makes particles move at a small angle $\varepsilon \ll 1$ with respect to the contours of ψ. Random walk in fields with finite divergence was also discussed in respect of random-hopping models in disordered solids (Derrida and Luck, 1983; Fisher, 1984; Kravtsov *et al.*, 1986). The compressibility of advecting flow results in the occurrence of limit cycles and stable foci, which attract and trap tracer particles (Fig. 27) until they are released due to molecular diffusion or flow time-dependence destroying the traps. So the diffusion process F 27

results from the particle flights from one trap to another. In the low-frequency limit, these flights are approximately along the contours of $\psi(x,y,t)$ and may be long enough (Lévy flights, cf. Shlesinger *et al.*, 1987). For the monoscale compressible flow (4.60), the effective diffusivity scales as

$$D^* \simeq \lambda_0^2 \omega \varepsilon^{-\frac{\nu d_h}{\nu d_h + 1}} , \quad \frac{\lambda_0 \omega}{v_0} \ll \varepsilon \ll 1 . \tag{4.61}$$

For smaller ε, the effect of compressibility is unimportant and D^* is given by formula (4.57). In the case of time-independent compressible flow with finite molecular diffusivity D_0, the effect of traps can result in an exponentially small effective diffusivity D^*.

Yushmanov (1991) studied the neoclassical diffusion in a turbulent plasma. Mathematically, this problem was reduced to the chaotic advection in a random 2D flow with a temporally varying average component. The average velocity component in an equation similar to (4.48) results from bounce oscillations of particle guiding center due to the toroidal geometry of a tokamak. Causing alternating opening and closing of random streamlines, such effect leads to the onset of effective diffusion at zero molecular diffusivity.

5. Anomalous diffusion

Effective diffusion in an advective-diffusive system results from asymptotically decaying correlations in the particle trajectory. This "loss of memory," which is due to the molecular diffusion, or the Lagrangian chaos, or both, occurs in a finite mixing time τ_m. On time-scale $t < \tau_m$ the advective-diffusive transport can exhibit more sophisticated, "anomalous" behavior. In particular, the root-mean-square particle displacement can scale differently from the standard square root of time,

$$\lambda(t) = \left\langle (\mathbf{x}(t) - \mathbf{x}(0))^2 \right\rangle^{1/2} \propto t^{\zeta} , \tag{4.62}$$

where $\zeta \neq 1/2$ is the exponent of *anomalous diffusion.*

Anomalous diffusion can also take place in nonintegrable Hamiltonian systems where the velocity field is the phase-space flux (Swägerl and Krug, 1991).

One might suppose that the coordinates $\mathbf{x}(t)$ of a particle undergoing an anomalous diffusion (4.62) can be modelled by a fractional Brownian function $\mathbf{B}_\zeta(t)$. In general case, however, this is not true as the increments of $\mathbf{x}(t)$ may not be Gaussian (Bouchard *et al.*, 1990). The probability distribution function $n(\mathbf{x},t)$ of $\mathbf{x}$, for $n(\mathbf{x},0) = \delta(\mathbf{x})$, is given by the solution of the complete advective-diffusive equation. In the long-time limit, one can expect a self-similar behavior in the form

$$n(\mathbf{x},t) = Ct^{-\zeta d} f(|\mathbf{x}|/t^\zeta) , \tag{4.63}$$

where an isotropic transport is assumed. In the Fisher (1966) model of a random self-avoiding walk (which may not be the case for the advective-diffusive transport),

$$f(u) \propto \exp(-u^{1/(1-\zeta)}) , \tag{4.64}$$

which becomes Gaussian only in the case of a standard Brownian motion ($\zeta = 1/2$). Still, for a sufficiently fast decresing $f(u)$, distribution (4.63) is qualitatively similar to the Gaussian probability distribution function, so that a fractional Brownian motion can serve a reasonable model for anomalous diffusion. Specifically, the fractal dimension D of the particle trail is given by formula (3.33), whose derivation is not hinged on the Gaussianity of $\mathbf{x}(t)$:

$$D = \min(1/\zeta, d) , \tag{4.65}$$

where d is the corresponding space-dimension.

Two physically different regimes of anomalous diffusion should be distinguished: the superdiffusion ($\zeta > 1/2$) and the subdiffusion ($\zeta < 1/2$).

a. Superdiffusion

One can imagine flows with long-range velocity correlations resulting in a "persistent" particle orbit, whose at least partial memory of the previous history lasts forever: $\tau_m = \infty$.

According to the Tatarinova *et al.* (1991) and the Avellaneda and Majda (1991) theorems, in the presence of finite molecular diffusivity such flows should have an unbounded vector potential $\psi(\mathbf{x}, t)$. The simplest example of superdiffusion was described by Dreizin and Dykhne (1972). Consider a shear flow with the velocity taking at random two constant values, $v = v_x(y) = \pm v_0$, in the strips of the width λ_0 (Fig. 28). The average velocity for *F 28* almost each realization of this flow is zero, while the stream-function $\psi(y) = \int_0^y v_x(y')dy'$ is unbounded at $y \to \infty$. By time t, a tracer particle gets quasi-uniformly dispersed in the y-direction over the distance $\lambda_y = (D_0\, t)^{1/2}$ covering approximately $N = \lambda_y/\lambda_0$ flow strips. Given the random distribution of velocity directions, one can expect approximately $N^{1/2}$, say, left-directed strips in excess of right-directed ones. The fraction of time the particle spends in these excessive (left-directed) strips is of order $N^{1/2}/N = N^{-1/2}$. Hence the expected (rms) particle displacement in the x-direction is given by

$$\lambda_x \simeq v_0\, t\, N^{-1/2} = v_0 \left(\frac{\lambda_0^2}{D_0}\right)^{1/4} t^{3/4}\,, \tag{4.66}$$

a superdiffusive behavior ($\zeta = 3/4 > 1/2$).

A continuum generalization of this step-like flow is one-dimensional random stream-function $\psi = \psi(y)$, with the spectrum $\psi_\lambda = \psi_0(\lambda/\lambda_0)^H$, $\lambda > \lambda_0$, $0 < H < 1$. (The example of Dreizin and Dykhne, 1972, corresponds to $H = 1/2$.) The velocity spectrum of such flow, $v_\lambda = v_0(\lambda/\lambda_0)^{H-1}$, also implies zero mean velocity: $\langle v \rangle = v_{\lambda=\infty} = 0$. The superdiffusion law is similarly obtained as

$$\lambda_y(t) = \sqrt{D_0\, t}\,, \quad \lambda_x(t) = v_{\lambda_y(t)}\, t = v_0 \left(\frac{\lambda_0^2}{D_0}\right)^{\frac{1-H}{2}} t^{\frac{1+H}{2}}\,, \quad t > \frac{\lambda_0^2}{D_0}\,. \tag{4.67}$$

The averaged transport equation describing superdiffusion (4.67) cannot be cast into a local form, however, the average tracer density $\langle n \rangle$ may be asymptotically represented as the ensemble average of solution of the simple equation

$$\partial n/\partial t = \mathcal{R}\, t^H \partial^2 n/\partial x^2\,, \tag{4.68}$$

where $\mathcal{R}$ is a random coefficient with known distribution (Avellaneda and Majda, 1990).

Bouchard *et al.* (1990) considered an isotropic 2D generalization of the random-directional shear flow — the "Manhattan system"

$$\psi(x,y) = \psi_1(x) + \psi_2(y) \tag{4.69}$$

(see Fig. 29). Suppose each component of the stream-function (4.69) has a power spectrum *F 29* with the exponent $H > 0$: $\psi_\lambda \propto \lambda^H$. Anomalous diffusion in such flow can be obtained similarly to Eq. (4.67). Due to the statistical isotropicity of the system, the rms displacement $\lambda(t)$ is self-consistently coupled to the result:

$$\lambda(t) = v_{\lambda(t)}\, t\ . \tag{4.70}$$

It follows,

$$\lambda(t) = \lambda_0 \left(\frac{v_0\, t}{\lambda_0}\right)^{\frac{1}{2-H}}\ , \quad t > \frac{\lambda_0^2}{D_0}\ . \tag{4.71}$$

At $H = 1/2$ one has the superdiffusion exponent $\zeta = 1/(2-H) = 2/3$ (Bouchard *et al.*, 1990).

The way result (4.71) has been derived, one can expect its wider generality. In fact, superdiffusive law (4.71) is valid not only for a Manhattan flow, but also for an arbitrary random stream-function with the isotropic power spectrum $\psi_\lambda \propto \lambda^H$ (Isichenko and Kalda, 1991c). The validity of (4.71) for a two-dimensional random flow, however, is restricted by the inequality $0 < H < 10/17$ (region C in Fig. 23). Formula (4.71) also extends *F 23* to three-dimensional random time-independent flows. Koch and Brady (1989; see also Brady, 1990) considered random 3D flows with algebraically decaying velocity covariance $\langle v_i(\mathbf{x}) v_j(\mathbf{x}+\boldsymbol{\rho})\rangle \propto \delta_{ij}|\boldsymbol{\rho}|^{-\gamma}$ and found the superdiffusive tracer dispersion (4.62) with the exponent

$$\zeta = \frac{2}{(\gamma+2)}\ , \quad 0 < \gamma < 2\ . \tag{4.72}$$

The velocity covariance $\propto |\boldsymbol{\rho}|^{-\gamma}$ corresponds to the spectrum $v_\lambda \propto \lambda^{-\gamma/2}$ (see Eqs. (3.9)–(3.13)) and hence to the vector potential $\boldsymbol{\psi}(\mathbf{x})$ λ-spectrum exponent $H = 1 - \gamma/2$. Then Eq. (4.72) is equivalent to $\zeta = 1/(2 - H)$, in accordance with Eq. (4.71).

The superdiffusive law (4.71) does not exhaust all anomalous regimes in 2D, random, power-spectrum flows. Another superdiffusive regime in a multiscale flow corresponds to the random walk with the self-consistently determined partial diffusivity (4.42):

$$\lambda^2(t) = D_{\lambda(t)}\, t \; . \tag{4.73}$$

Substituting formulas (3.71) and (3.77a) into the expression $D_\lambda = D_0\, L(\lambda)/w(\lambda)$, we obtain $D_\lambda \propto \lambda^{D_h - H}$, hence (Isichenko and Kalda, 1991c)

$$\lambda(t) = \lambda_0 \left(\frac{D_0\, t}{\lambda_0^2} \right)^{\frac{1}{2+H-D_h}} \; , \quad \lambda_0 < \lambda(t) < \min(\xi, \lambda_m) \; , \tag{4.74}$$

where ξ is the solution of Eq. (4.38). For $H < 1$ we have

$$\zeta = \frac{1}{2 + H - D_h} = \frac{7}{10H + 4} > \frac{1}{2} \; . \tag{4.75}$$

This superdiffusive regime is possible for $H > -\frac{2}{5}$. It is interesting to note that, for $-\frac{2}{5} < H < \frac{3}{10}$, Eq. (4.57) predicts the root-mean-square particle displacement faster than linear with time ($\zeta > 1$), that is, with an acceleration.

Perhaps, more important implications of the anomalous diffusion concern real turbulent (time-dependent) flows. The Richardson law (4.6) means, by definition of D_λ, that the root-mean-square *relative* displacement of advected particles behaves as $\lambda(t) = (D_{\lambda(t)}\, t)^{1/2}$, hence

$$\lambda(t) \propto t^{3/2} \; . \tag{4.76}$$

The Richardson superdiffusion (4.76) is naturally obtained from the Kolmogorov-Obukhov spectrum[2] (Kolmogorov, 1941; Monin and Yaglom, 1971, 1975; Rose and Sulem, 1978; Batchelor, 1982) $v_\lambda \propto \lambda^{1/3}$ using the relation $\lambda(t) = v_{\lambda(t)}\, t$. Indeed, v_λ is the characteristic velocity

[2]The standard form for this spectrum is usually given in terms of the energy spectral density, $E(k) \propto k^{-5/3}$. The relation between $E(k)$ and $E_\lambda \propto v_\lambda^2$ is given by $E_\lambda = \int_{1/(2\lambda)}^{1/\lambda} E(k)dk \propto \lambda^{2/3}$.

difference in two points, which are the distance λ apart from each other. Superdiffusion law (4.76) was derived by Obukhov (1941) from a dimensional analysis similar to the one that led Kolmogorov (1941) to the $\lambda^{1/3}$ ($H = 4/3$) velocity spectrum. A detailed discussion of the relation between the Kolmogorov spectrum and the Richardson dispersion was given by Batchelor (1952).

In the case of a decreasing velocity spectrum, $v_\lambda \propto \lambda^{H-1}$, $H < 1$, a nontrivial *absolute* superdiffusion is also possible. Time-dependence can be introduced in the form of the characteristic frequency ω_λ, at which the λ-component $v_\lambda(\mathbf{x}, t)$ of the velocity field is evolved:

$$\omega_\lambda = \omega_0 \left(\frac{\lambda}{\lambda_0}\right)^{-G} , \quad \lambda_0 < \lambda < \lambda_m . \tag{4.77}$$

In a pure fluid turbulence one would have $\omega_\lambda = v_\lambda/\lambda$, that is, $G = 2 - H$. For the turbulence of Rossby waves in a rotating fluid and drift waves in plasmas (Hasegawa and Mima, 1978; Hasegawa *et al.*, 1979), or other systems having a characteristic velocity V such as the phase velocity of linear waves, regimes with $\omega_\lambda = V/\lambda$ are possible, that is, $G = 1$. The superdiffusive law for arbitrary $G > 0$ and $H < 1$ can be obtained as follows. The displacement of a tracer particle, released in the flow at $t = 0$, is governed, by time t, by the flow component with $\lambda = \lambda^*(t)$ determined from the equation $\omega_{\lambda^*(t)}\, t = 1$. Indeed, at $H < 1$ longer scales ($\lambda \gg \lambda^*(t)$) have smaller velocity, whereas shorter scales ($\lambda \ll \lambda^*(t)$) have fast-oscillation velocity components: $\omega_\lambda t \gg 1$. In the absence of other scales, these oscillations would lead to the turbulent diffusivity given by formula (4.52): $D_\lambda = v_\lambda^2/\omega_\lambda \propto \lambda^{G+2H-2}$. If D_λ increases with growing λ, that is, $G > 2 - 2H$, then the $\lambda^*(t)$ velocity scale dominates the tracer motion. In this case, we can write the root-mean-square displacement $\lambda(t)$ in two equivalent forms, $\lambda(t) = v_{\lambda^*(t)}\, t = \left(D_{\lambda^*(t)}\, t\right)^{1/2}$. Thus we obtain

$$\lambda(t) = \frac{v_0}{\omega_0} (\omega_0 t)^{\frac{G+H-1}{G}} , \quad G > 2 - 2H > 0 . \tag{4.78}$$

In the opposite case, $G < 2 - 2H$, the small-scale velocity pulsation dominates the particle motion leading to the turbulent diffusivity $D^* \simeq v_0^2/\omega_0$. The validity of result (4.78) in two

dimensions is further restricted by the inequality $G \leq 2 - H$ to ensure the absence of an additional integral of motion — the adiabatic invariant of the stream-function $\psi(x(t), y(t), t)$, which is approximately conserved at $\omega_\lambda \ll v_\lambda/\lambda$. The low-frequency transport in a two-dimensional multiscale time-dependent flow is more complicated and requires the statistical-topography analysis of particle orbits (Kalda, 1991).

Osborne and Caponio (1990) studied passive transport in a 2D time-dependent random flow with spectral exponents $G = 1$, $1/2 < H < 1$. They found numerically that in this interval of H the superdiffusion exponent ζ behaves as $\zeta = H$, in accordance with Eq. (4.78).

Notice that in the case of a turbulence with the eddy-revolution characteristic frequency $\omega_\lambda = v_\lambda/\lambda$, that is, $G = 2-H$, Eq. (4.78) leads to the superdiffusive exponent $\zeta = 1/(2-H)$, the same as in Eq. (4.71) describing the superdiffusion in steady flows.

Avellaneda and Majda (1990) considered anomalous diffusion in random unsteady shear flows, $v = v_x(y, t)$. They identified several regimes of the tracer behavior and established the equations describing the average density $\langle n \rangle$.

The anomalous diffusion scalings, such as in Eqs. (4.71), (4.74), and (4.78), can be used to recover turbulent spectra from the observed tracer motion, such as satellite-tracked buoys deployed in the ocean (Osborne *et al.*, 1986; Brown and Smith, 1991). To do so, one can use either complete time-coordinate records $\{t_i, x_i, y_i\}$ or only the trail $\{x_i, y_i\}$, whose fractal dimension D is related to the anomalous diffusion exponent ζ by formula (4.65). However, for deciphering turbulence spectra $\psi_\lambda \propto \lambda^H$ with $H > 1$, the information stored in the relative particle dispersion has to be used.

Another manifestation of a self-similar (power-spectrum) turbulence is the fractal structure of the isoscalar surfaces, that is, the surfaces where the density of a passive scalar takes constant value. Constantin *et al.* (1991) give theoretical expressions for the fractal dimension of isoscalar surfaces, $D_{\text{in}} = 2 + H/2$, in the internal region of a turbulent spot, and $D_{\text{ex}} = 1 + H$, near the boundary of a turbulent jet, where $v_\lambda \propto \lambda^{H-1}$ is the velocity

spectrum. These predictions agree with experimental data (Sreenivasan and Prasad, 1989; Sreenivasan *et al.*, 1989; Constantin *et al.*, 1991). Recent experiments on turbulent diffusion, superdiffusion, and fractal behavior also include Swinney and Tam (1987), Ramshankar *et al.* (1990), and Ramshankar and Gollub (1991). Some other fractal and multifractal properties of passive scalars are discussed in Mandelbrot (1975b), Hentschel and Procaccia (1983a), Ott and Antonsen (1988), Voss (1989), Vulpiani (1989), Fung and Vassilicos (1991), and Városi *et al.* (1991).

b. Subdiffusion

The superdiffusive ("persistent") random walk does not exhaust the variety of anomalous diffusion regimes in incompressible flows. The subdiffusive ("antipersistent") tracer motion with $\zeta < 1/2$ is also possible (Young, 1988; Pomeau *et al.*, 1988; Young *et al.*, 1989). In a time-independent flow, such behavior arises from the tracer particles resting in closed pockets of recirculation. Getting to such a region of closed streamlines, the particle resides there for some (random) time before proceeding with its further propagation. The resulting retarded ($\zeta < 1/2$) dispersion is quite similar to the diffusion on loopless structures (Havlin and Ben-Avraham, 1987), such as a "comb" (Fig. 30). The system of regular convection rolls (Fig. 20) is equivalent to a comb, whose base represents the diffusive boundary layers, and the teeth correspond to the inner area of the convection cells. To complete this analogy, one should position the teeth, λ_0 long, the distance $w_b = \lambda_0 P^{-1/2}$ ($P \equiv \psi_0/D_0 \gg 1$) apart from each other and to ascribe the diffusion coefficient of the order of the molecular diffusivity D_0 to the whole structure. Such a representation of the transport properties of flow (4.22) is valid on time-scale $t \gg \lambda_0/v_0$, when (a) the boundary layer structure of transport is set in and (b) the tracer dispersion inside the convection rolls can be described by averaged

F 30 F 20

one-dimensional cross-stream diffusion equation

$$\frac{\partial n(J,t)}{\partial t} = \frac{\partial}{\partial J} D(J) \frac{\partial n(J,t)}{\partial J} , \tag{4.79}$$

instead of the full 2D advective-diffusive equation (4.1). In Eq. (4.79), $n(J,t)$ designates the tracer density averaged over a streamline $\psi(x,y) = \text{const.}$ with the area J inside it. The idea of such averaging stems from the perturbation theory of nearly integrable Hamiltonian systems (Arnold, 1978), where one switches from the phase space variables (x,y) to the action-angle variables (J,ϕ) of the unperturbed (integrable) motion. The action-diffusion coefficient $D(J)$ is given by

$$D(J) = D_0 \oint |\nabla\psi| d\ell \oint |\nabla\psi|^{-1} d\ell , \tag{4.80}$$

where integrals are taken around the streamline (Young *et al.*, 1989; Isichenko *et al.*, 1989).

Suppose a small spot of dye (passive tracer) is deposited at $t = 0$ close to the separatrix mesh of a periodic array of vortices (Fig. 20) corresponding to the base of the comb (Fig. 30). *F 20* *F 30*
Consider time-scales $\lambda_0/v_0 \ll t \ll \lambda_0^2/D_0$. Then the dye invades the distance $(D_0\, t)^{1/2}$ along the teeth. The fraction $F(t)$ of "active" particles, that is, those residing on the base and determining the long-range tracer dispersion, decreases with time as

$$F(t) = \frac{w_b}{(D_0\, t)^{1/2}} . \tag{4.81}$$

In terms of the random walk of a single particle, expression (4.81) yields the fraction of time spent on the comb base. Then the propagation rate along the base coordinate b is given by

$$b^2(t) = F(t)\, D_0\, t = w_b (D_0\, t)^{1/2} . \tag{4.82}$$

This corresponds to the root-mean-square displacement in real space (Havlin and Ben-Avraham, 1987; Pomeau *et al.*, 1988; Young *et al.*, 1989)

$$\lambda(t) = b(t) \frac{\lambda_0}{w_b} = (\lambda_0^2\, D_0\, t)^{1/4} , \tag{4.83}$$

a subdiffusive law ($\zeta = 1/4$) sometimes referred to as "double diffusion" (Krommes *et al.*, 1983). Such tracer behavior is valid for nonvanishing velocity on the separatrix mesh ("free slip" boundary condition). For "no slip" (rigid) boundary, where the velocity turns linearly to zero, one has $\zeta = 1/3$ (Pomeau *et al.*, 1988; Young *et al.*, 1989).

Not only the rms displacement scaling can be established for periodic flows but also the governing equation for the tracer envelope. The general form of this equation was derived by Young *et al.* (1989):

$$\frac{\partial}{\partial t} \int_0^t K(t-\tau) f(\mathbf{x},\tau) d\tau = D^* \nabla^2 f(\mathbf{x},t) \ , \tag{4.84}$$

where f is the tracer density on a separatrix considered as a function of "slow" coordinate $\mathbf{x}$, D^* is the effective diffusivity, and $K(\tau)$ is an integral kernel satisfying the matching relation

$$\int_0^\infty K(\tau) d\tau = 1 \ . \tag{4.85}$$

The sense of Eq. (4.84) is that the tracer flux is determined solely by the density f in the diffusive boundary layers and the effective diffusivity D^* (rhs), while lhs specifies the change in the average tracer density $\langle n \rangle = \int_0^t K(t-\tau) f(\mathbf{x},\tau) d\tau$. The latter is obtained from f via a linear integral operator describing the tracer invasion in a convection cell. In the limiting case $t \gg \tau_m$, where the mixing time $\tau_m \simeq \lambda_0^2/D_0$ is the characteristic time of the convergence of integral (4.85), the kernel K can be substituted by a delta-function, hence $\langle n \rangle = f$, and the effective-diffusion equation is recovered from (4.84). In the opposite case, $\lambda_0/v_0 \ll t \ll \tau_m$, the kernel behaves as a power, $K(\tau) = (\tau_m \tau)^{-1/2}$, and the operator on the left-hand side of Eq. (4.84) becomes the operator of fractional differentiation (see Eq. (3.34)):

$$\sqrt{\frac{\pi}{\tau_m} \frac{\partial}{\partial t}} \, f = D^* \nabla^2 f \ . \tag{4.86}$$

As the nonlocal time-operator $\sqrt{\partial/\partial t}$ is commutant with the space-operator ∇^2, one can write a consequence of Eq. (4.86) in a local differential form,

$$\frac{\partial f}{\partial t} = \frac{\tau_m D^{*2}}{\pi} \nabla^4 f \ , \tag{4.87}$$

which emphasizes the term "double diffusion." The simplicity of (4.87) is, nevertheless, deceptive: while including all solutions of the nonlocal equation (4.86), the local double-diffusion equation (4.87) has many (*much*, to be more correct) extraneous solutions, [3] which well manifests itself in a strongly unstable behavior of Eq. (4.87): A monochromatic solution $f \propto \exp(-i\omega t + i\mathbf{kx})$ grows with time exponentially, $\omega = ik^4 \tau_m D^{*2}/\pi$, whereas our intuitive conception of (sub)diffusion suggests a behavior of f that smoothes out initial inhomogeneities.

Subdiffusive behavior is also possible in random flows (Isichenko and Kalda, 1991c). Like in regular convection cells, this behavior is transient ($t < \tau_m$) and takes place for special initial conditions, namely, for the initial tracer spot deposited in a mixing convection cell. (Remember that the mixing convection cells of the size ξ_m play the role of boundary layers.) The difference between random flows and regular flows lies in the appearance of their equivalent loopless structures. Due to the presence of numerous separatrices in a random flow, tracer fills up the holes in a ξ_m-cell topologically nontrivially as on each separatrix the converging diffusion front breaks into two (in a nondegenerate case — see Fig. 31). Hence *F 31* the equivalent "diffusion comb" of a random flow has branching teeth (Fig. 32). The rate F 32 of filling up the branches of these trees can be found using the topographic properties of random flows.

Introduce the "action distance" x_J across the streamlines according to $dJ = \pm\mathcal{L}(x_J)dx_J$, where $\mathcal{L}(x_J)$ is the length of a closed streamline and J the area inside this line. The action-diffusion coefficient (4.80) being estimated as $D(J) \simeq D_0\,\mathcal{L}^2(x_J)$, one can rewrite Eq. (4.79) in terms of the action distance x_J:

$$\frac{\partial n}{\partial t} = \frac{1}{\mathcal{L}(x_J)} \frac{\partial}{\partial x_J} \left(D_0\,\mathcal{L}(x_J) \frac{\partial n}{\partial x_J} \right) . \tag{4.88}$$

Hence the segments of the "diffusion tree" (Fig. 31) can be measured in the action-distance *F 31*

[3] Those of Eq. (4.86) with D^* substituted by $-D^*$.

units, with the diffusivity along the branches of order D_0.

Consider a monoscale uncorrelated, random, steady flow with the characteristic scale λ_0. The action distance between the external boundary of an a-cell and the innermost point of a hole in the cell can be calculated as the sum of the widths (3.43) of the nested cells of diameter $\lambda_0, 2\lambda_0, \ldots, a$. For any $a \gg \lambda_0$, this sum is estimated as λ_0. It follows, in particular, that the action distance between two arbitrary points on the (x, y) plane is bounded by a constant of the order of λ_0. Hence the mixing time in the monoscale flow equals

$$\tau_m = \frac{\lambda_0^2}{D_0} \,. \tag{4.89}$$

Consider time-scales $w^2(\xi_m)/D_0 \ll t \ll \tau_m$. Then diffusion front invades the action distance $x_J(t) = \sqrt{D_0\, t}$ along each branch of the diffusion tree. To calculate the total area $S(x_J)$ (in physical space) covered by the invaded region inside one ξ_m-cell, introduce a new topographic exponent δ, which can be called "dimension of the diffusion tree": $S(x_J) \propto x_J^\delta$. Using the matching conditions $S(w(\xi_m)) = L(\xi_m) w(\xi_m)$ (where $L(\xi_m)$ is the perimeter (3.41) of the ξ_m-cell) and $S(\lambda_0) = \xi_m^2$ (all the holes are filled up by $t = \tau_m$, when $x_J = \lambda_0$) we find

$$\delta = 1 + \nu(2 - d_h) = \frac{4}{3} \,. \tag{4.90}$$

The fractional value of the tree dimension δ between 1 and 2 indicates that, while complete 2D description (4.1) is redundant, purely one-dimensional action-diffusion oversimplifies the transport in topologically complex flows.

The rest of the calculation essentially repeats that for the simplest nonbranching diffusion comb, whose dimension δ is unity. The fraction of active particles lying on the base of the comb is

$$F(t) = \frac{S(w(\xi_m))}{S(\sqrt{D_0\, t})} \propto t^{-\delta/2} \,. \tag{4.91}$$

The tracer propagation along the comb base is given by $b^2(t) = F(t)\, D_0\, t$, and as the distance $w(\xi_m)$ between the tree-like teeth of the comb corresponds to the physical distance ξ_m, we

obtain

$$\lambda(t) = b(t)\,\frac{\xi_m}{w(\xi_m)} = \xi_m \left(\frac{D_0\,t}{w^2(\xi_m)}\right)^{\zeta}, \quad \frac{w^2(\xi_m)}{D_0} < t < \tau_m\ , \tag{4.92}$$

where the subdiffusion exponent for 2D monoscale random flow equals

$$\zeta = \frac{1}{2} - \frac{\delta}{4} = \frac{1}{6}\ . \tag{4.93}$$

The "triple diffusion" (4.92)–(4.93) can also be described by a nonlocal integro-differential equation involving the operator $(\partial/\partial t)^{1/3}$.

The generalization of the above result to the case of multiscale flows is easily done for the "monoscale correlated" spectrum with the exponent $-1/\nu < H < 0$. In this case one simply substitutes the percolation exponents ν and d_h in expression (4.90) by their correlated-percolation counterparts (4.44). As a result, we have the dimension of the diffusion tree

$$\delta = \frac{H + D_h - 2}{H}\ , \quad -1/\nu < H < 0\ , \tag{4.94}$$

and the subdiffusion exponent

$$\zeta = \frac{1}{2} - \frac{\delta}{4} = \frac{2 + H - D_h}{4H} = \frac{5H + 2}{14H}\ . \tag{4.95}$$

The subdiffusion law (4.92)–(4.95) is valid for $-3/4 \le H < -2/5$, where $0 < \zeta \le 1/6$.

B. Conductivity of inhomogeneous media

The problem of average characteristics of spatially fluctuating dielectrics and conductors is as old as the electrodynamics itself (Maxwell, 1873). The review of early work by Clausius, Mossotti, Lorentz, and others on polarizability of geterogeneous media was given by Landauer (1978). Up to now, there is no general solution of this classical problem, which is mathematically formulated as follows. Denote $\mathbf{e}(\mathbf{x})$ the microscopic electric field and $\mathbf{j}(\mathbf{x})$ the microscopic current density in a medium with a nonuniform conductivity tensor $\widehat{\sigma}(\mathbf{x})$:

$$\mathbf{j}(\mathbf{x}) = \widehat{\sigma}(\mathbf{x})\,\mathbf{e}(\mathbf{x}) \ . \tag{4.96}$$

To satisfy time-independent Maxwell's equations, the electric field should be irrotational and the current density solenoidal:

$$\nabla \times \mathbf{e} = 0 \ , \qquad \nabla \cdot \mathbf{j} = 0 \ . \tag{4.97}$$

Given a deterministic (or statistical) description of fluctuating conductivity $\widehat{\sigma}(\mathbf{x})$, what is the space (or ensemble) average conductivity $\widehat{\sigma}^*$? By definition, the effective conductivity is the proportionality coefficient (in general, tensor) between the average electric field $\mathbf{E} = \langle \mathbf{e}(\mathbf{x}) \rangle$ and the average current density $\mathbf{J} = \langle \mathbf{j}(\mathbf{x}) \rangle$:

$$\mathbf{J} = \widehat{\sigma}^* \mathbf{E} \ . \tag{4.98}$$

Similarly to the advective-diffusive problem, one can introduce the mixing length ξ_m characterizing the minimum scale of the effective-conduction behavior (4.98).

Not only the problem of electrical conductivity is described by Eqs. (4.96)–(4.98). Mathematically equivalent are the problems of averaging of dielectric constant $\widehat{\varepsilon}$ (where $\mathbf{j}$ is substituted by the electric induction $\mathbf{D}$), diffusivity $\widehat{D}$ (where $\mathbf{E}$ is substituted by the density gradient of a diffusing substance and $\mathbf{j}$ is its flux), and thermal conduction tensor $\widehat{\chi}$ (with $\mathbf{E}$ standing for the temperature gradient and $\mathbf{j}$ for the thermal flux). Among versatile transport

processes occurring in heterogeneous media, we discuss primarily those involving a large parameter, such as the strength of fluctuations of $\widehat{\sigma}(\mathbf{x})$, or the strength of its anisotropy. It is believed that a qualitative analysis of scaling relations for the effective conductivity σ^* is most important for the physical understanding of the problem. Nevertheless, not numerous available examples of nontrivial exact solution will be also reviewed.

The extreme case of binary mixture of an ideal insulator with a conducting phase was discussed in Sec. II in the framework of the percolation theory. The behavior of such a mixture involves a sharp transition from an insulator to a conductor. However, due to the reasons discussed in Sec. II.E, the behavior of three-dimensional effective conductivity σ^* near the continuum percolation threshold may not be quite universal. In Sec. 1 we discuss the special case of a two-dimensional, two-phase system, which is *exactly at the percolation threshold.* For an arbitrary ratio of the phase conductivities, it turns out to be possible to calculate the effective conductivity using a reciprocity relation discovered by Keller (1964) and Dykhne (1970a; Sec. 1). This method is also applicable to polycrystals and heat conduction in anisotropic plasmas (Sec. 2). In Sec. 3 the anomalous magnetoresistance taking place in inhomogeneous conductors with the Hall effect is discussed.

1. Keller-Dykhne reciprocity relations

One of very few exact results on the conductivity of composite materials was obtained for a two-dimensional binary mixture. Once again we notice the remarkable (and exceptional) feature of two dimensions favoring successful analytical advance. In the long run, the availability of exact percolation exponents, as well as of results discussed below, stems from the highly nontrivial fact of the existence of complex numbers and resulting conformal maps. (Indeed, it is not easy to expect that a vector algebra can be introduced, including the operation of division, similar to the algebra of real numbers. And such an algebra cannot be naturally introduced in three dimensions.)

Originally, Keller (1964, see also 1987) considered a composite medium consisting of a rectangular lattice of identical parallel cylinders of any cross-section, having electrical conductivity σ_2, embedded in a medium of conductivity σ_1. Using the theory of harmonic functions, Keller proved the following relation for the principal values of the effective conductivity tensor $\hat{\sigma}^*(\sigma_1, \sigma_2)$:

$$\sigma^*_{xx}(\sigma_1, \sigma_2)\, \sigma^*_{yy}(\sigma_2, \sigma_1) = \sigma_1 \sigma_2 \ , \tag{4.99}$$

where the x and y axes lie along the axes of the lattice. The second factor on the left-hand side of Eq. (4.99) refers to the conductivity of a *reciprocal medium*, that is, the medium of the same geometry but with interchanged phases σ_1 and σ_2.

Independently, Dykhne (1970a) derived formula (4.99) under more general assumptions using an elegant reciprocity transformation. Following his work, consider new vector fields

$$\mathbf{j}'(\mathbf{x}) = \sigma_* \hat{R}\, \mathbf{e}(\mathbf{x}) \ , \qquad \mathbf{e}'(\mathbf{x}) = \frac{1}{\sigma_*} \hat{R}\, \mathbf{j}(\mathbf{x}) \ , \tag{4.100}$$

where σ_* is a constant and $\hat{R} = \hat{\mathbf{z}} \times \ldots$ is the operator of rotation in the plane (x, y) at the angle of 90°. The choice of $\mathbf{j}'$ and $\mathbf{e}'$ is designed to satisfy the relations

$$\nabla \cdot \mathbf{j}' = 0 \ , \qquad \nabla \times \mathbf{e}' = 0 \ , \tag{4.101}$$

following from (4.97). Comparing the Ohm's law (4.96) with Eqs. (4.100), one easily finds the relation between the "primed" vector fields:

$$\mathbf{j}'(x) = \hat{\sigma}'(\mathbf{x})\, \mathbf{e}'(\mathbf{x}) \ , \qquad \hat{\sigma}'(\mathbf{x}) = \sigma_*^2 \hat{R}\, \hat{\sigma}^{-1}(\mathbf{x}) \hat{R}^{-1} \ . \tag{4.102}$$

For the case of an isotropic tensor $\sigma_{ij}(\mathbf{x}) = \sigma(\mathbf{x})\, \delta_{ij}$, and $\sigma(\mathbf{x})$ taking on only two values, σ_1 and σ_2, in the regions I and II, respectively, it is convenient to choose $\sigma_*^2 = \det \hat{\sigma} = \sigma_1 \sigma_2$, so that $\sigma'_{ij} = \sigma'(\mathbf{x})\, \delta_{ij}$, and

$$\sigma'(\mathbf{x}) = \frac{\sigma_1 \sigma_2}{\sigma(\mathbf{x})} = \begin{cases} \sigma_2 \ , & \text{in I} \ , \\ \sigma_1 \ , & \text{in II} \ . \end{cases} \tag{4.103}$$

Thus the system of equations (4.101)–(4.102) becomes quite similar to (4.96)–(4.97) and describes the current flow in a new two-dimensional system differing from the old one by the interchange of the conductivities σ_1 and σ_2. Once, by assumption, from (4.96) and (4.97) follows relation (4.98) for the average current and electric field, with the effective conductivity $\hat{\sigma}^*(\sigma_1, \sigma_2)$ being a definite function of σ_1 and σ_2, then we conclude on the existence of an effective conductivity, $\hat{\sigma}^{*\prime}$, of the "primed" system:

$$\mathbf{J}' = \hat{\sigma}^{*\prime}\mathbf{E}' \,, \tag{4.104}$$

where

$$\hat{\sigma}^{*\prime} = \hat{\sigma}^*(\sigma_2, \sigma_1) \,. \tag{4.105}$$

In Eq. (4.104), $\mathbf{J}'$ and $\mathbf{E}'$ denote the average values of $\mathbf{j}'(\mathbf{x})$ and $\mathbf{e}'(\mathbf{x})$, respectively. According to (4.100), we have

$$\mathbf{J}' = (\sigma_1\sigma_2)^{1/2}\hat{R}\,\mathbf{E} \,, \qquad \mathbf{E}' = (\sigma_1\sigma_2)^{-1/2}\hat{R}\,\mathbf{J} \,. \tag{4.106}$$

The final result comes from the comparison of Eq. (4.98) with Eq. (4.104). With constraint (4.106), they are compatible for any $\mathbf{E}$ only if the tensor operator $(\sigma_1\sigma_2)^{-1}\hat{R}^{-1}\hat{\sigma}^{*\prime}\hat{R}\,\hat{\sigma}^*$ is identity. In terms of the principal values, $\sigma^*_{xx}(\sigma_1, \sigma_2)$ and $\sigma^*_{yy}(\sigma_1, \sigma_2)$, of the effective conductivity $\hat{\sigma}^*(\sigma_1, \sigma_2)$, this results in the reciprocity relation (4.99).

Now consider a composite medium, which is macroscopically isotropic: $\sigma^*_{xx}(\sigma_1, \sigma_2) = \sigma^*_{yy}(\sigma_1, \sigma_2) = \sigma^*(\sigma_1, \sigma_2)$. Then Eq. (4.99) reads

$$\sigma^*(\sigma_1, \sigma_2)\,\sigma^*(\sigma_2, \sigma_1) = \sigma_1\sigma_2 \,. \tag{4.107}$$

In the case of statistically equivalent distributions of two phases, which implies, however not reduces to, a split 50/50 area occupation, the function $\sigma^*(\sigma_1, \sigma_2)$ becomes a symmetric function of σ_1 and σ_2. Then it follows (Dykhne, 1970a),

$$\sigma^* = (\sigma_1\sigma_2)^{1/2} \,. \tag{4.108}$$

This exact result is valid for arbitrary values of σ_1 and σ_2. Specifically, if σ_1 tends to infinity and σ_2 to zero, the effective conductivity σ^* still *may* remain finite. Such a behavior is possible only *exactly at the percolation threshold.* (Here we mean the continuum percolation through the high-conducting phase σ_1.) Indeed, below the threshold, σ^* *should* tend to zero at $\sigma_2 \to 0$, whatever be σ_1, while above the threshold, σ^* *should* tend to infinity even at $\sigma_2 = 0$. Thus, for isotropic random mixtures in two dimensions, the critical fraction of volume (percolation threshold) equals one half, the same value as in the potential continuum percolation with a sign-symmetric potential (see Sec. II.E).

It is noteworthy that, for any σ_1 and σ_2, the symmetry leading to Eq. (4.108) extends to the equipartition of Ohmic dissipation in phases I and II (Dykhne, 1970a):

$$\frac{1}{\sigma_1}\left\langle \mathbf{j}^2(\mathbf{x})\right\rangle_I = \frac{1}{\sigma_2}\left\langle \mathbf{j}^2(\mathbf{x})\right\rangle_{II} = \frac{\mathbf{J}^2}{\sigma^*} \,. \tag{4.109}$$

There exist no universal formula for the effective conductivity of a material with unequal amount of randomly distributed phases, or with more than two phases, because the information about the volume fractions and the conductivities of phases is not enough to determine the effective conductivity. The result will also depend on the spatial distribution of phases. Specifically, the conductivity behavior near the percolation threshold may crucially depend on the presence of long-range correlations in the distribution. In addition, the percolation conductivity exponent μ (see Eq. (2.10)) is not exactly known even for the uncorrelated lattice model. Schulgasser (1976) showed the nonexistence of a Keller-Dykhne-type theorem in three dimensions. Instead, using the classical variation principle (cf. Dykhne, 1967), that the electric current distribution minimize the integral Ohmic heat under appropriate constraints, Schulgasser established the inequality

$$\sigma^*_{xx}(\sigma_1,\sigma_2)\,\sigma^*_{yy}(\sigma_2,\sigma_1) \geq \sigma_1\sigma_2 \,, \tag{4.110}$$

which is valid for arbitrary 3D two-phase composite. Some other inequalities were obtained in

Bergman (1978), Milton (1982), and Golden and Papanicolaou (1983), where the analytical continuation of $\widehat{\sigma}^*/\sigma_1$, considered as a function of σ_1/σ_2, was used.

2. Systems with inhomogeneous anisotropy

a. Polycrystals

Another classical example of a heterogeneous medium is a polycrystal consisting of multiple grains (crystallites) of an identical anisotropic material with random orientations (Fig. 33). *F 33* The importance of the problem of electrical and heat conduction in such media is emphasized by the fact that all metals are typically polycrystals.

In two dimensions, the effective conductivity of a macroscopically isotropic polycrystal is also amenable to the Keller-Dykhne approach. Let σ_1 and σ_2 be the principal values of the microscopic conductivity tensor

$$\widehat{\sigma}(\mathbf{x}) = \widehat{\theta}(\mathbf{x}) \begin{pmatrix} \sigma_1 & 0 \\ 0 & \sigma_2 \end{pmatrix} \widehat{\theta}^{-1}(\mathbf{x}) \,, \tag{4.111}$$

and $\widehat{\theta}(\mathbf{x})$ be the rotation matrix at the angle $\theta(\mathbf{x})$, which varies from one crystallite to another. Again introducing primed fields (4.100), we obtain the reciprocal Ohm's law with a new conductivity as shown in Eq. (4.102). Using formula (4.111) and taking into account the commutity of the rotation matrices $\widehat{R}$ and $\widehat{\theta}$, we find

$$\widehat{\sigma}'(\mathbf{x}) = \frac{1}{\sigma_*^2}\, \widehat{\theta}(\mathbf{x}) \begin{pmatrix} \sigma_2 & 0 \\ 0 & \sigma_1 \end{pmatrix} \widehat{\theta}^{-1}(\mathbf{x}) \,. \tag{4.112}$$

Under the choice of $\sigma_*^2 = \sigma_1\sigma_2$, $\widehat{\sigma}'(\mathbf{x})$ becomes identically equal to $\widehat{\sigma}(\mathbf{x})$. Hence, for the effective conductivity $\widehat{\sigma}^*(\sigma_1, \sigma_2)$ of the considered system, instead of Eq. (4.99), the reciprocity relation reads

$$\sigma_{xx}^*(\sigma_1, \sigma_2)\, \sigma_{yy}^*(\sigma_1, \sigma_2) = \sigma_1\sigma_2 \,, \tag{4.113}$$

where x and y are the principal axes of $\widehat{\sigma}^*$. Thus, for a macroscopically isotropic 2D polycrystal, formula (4.13) yields an exact result (Dykhne, 1970a). Unlike the case of a two-phase

system, the polycrystal result does not require the equipartition of phases (which is quite a strong limitation on the two-phase result) since both principal axes, σ_1 and σ_2, are naturally "equally represented" in each crystallite.

To understand the meaning of the Dykhne formula (4.13), it is instructive to consider the extreme of a strong anisotropy, $\sigma_1 \gg \sigma_2$ (Dreizin and Dykhne, 1983). Then, in most places, the current flows along the axes of a high conductivity (σ_1). These paths, however, terminate in "traps" in the form of foci (Fig. 34(a)) or limit cycles (Fig. 34(b)). To escape these traps, *F 34a* *F 34b* the current is forced to flow across the well-conducting lines, where the conductivity is σ_2. To make the dissipation smaller, this is better to do close enough to the trap. Denote l_1 the characteristic length and l_2 the characteristic width of the bundle of high-conductivity lines near a focus where the main resistance r occurs. Then r can be estimated as the sum of the high-conductivity path (along the bundle) and that of the low-conductivity path (across the bundle):

$$r = \frac{1}{\sigma_1}\frac{l_1}{l_2} + \frac{1}{\sigma_2}\frac{l_2}{l_1} \,. \tag{4.114}$$

Expression (4.114) is minimized at $l_1/l_2 \simeq (\sigma_1/\sigma_2)^{1/2}$ where it takes on the value $r_{\min} \simeq (\sigma_1\sigma_2)^{-1/2}$. Thus the conducting properties of the polycrystal can be represented by an equivalent network of resistors with the characteristic resistivity $r_{\min}$ connected by well-conducting (σ_1) wires. This network is similar to the field shown in Fig. 27. Such a network *F 27* has the macroscopic conductivity of the order of $(\sigma_1\sigma_2)^{1/2}$, in accordance with exact result (4.108). The above argument also shows that main Ohmic dissipation is released in the traps occupying a small fraction of area, of the order of $(\sigma_2/\sigma_1)^{1/2} \ll 1$.

For three-dimensional polycrystals, no exact results are known. A set of rigorous inequalities on the effective conductivity $\hat{\sigma}^*$ was obtained in Hashin and Shtrikman (1963), Schulgasser (1982), and Avellaneda *et al.* (1988). The scaling behavior of σ^* for the case of a strong anisotropy can be predicted by a qualitative theory (Dreizin and Dykhne, 1983).

Let $\sigma_1 \gg \sigma_2 \gg \sigma_3$ be the principal values of the microscopic conductivity tensor. Then

the high-conductivity (σ_1) lines terminate in several type of traps. In addition to foci and limit cycles, a generic 3D compressible vector field (the paths along σ_1 axes) can form "strange attractors" (Lorenz, 1963). Such a name received the fractal attracting sets of low-dimensional non-Hamiltonian dynamical systems that exhibit exponentiation of close orbits and are characterized by finite size but zero volume in the configuration space. Along with foci, saddles, and limit cycles, strange attractors represent a typical invariant set of a 3D vector field. The fractal dimension of an attractor given by formula (1.16) is not universal as the Lyapunov exponents Λ_1 and Λ_3 change from one attractor to another being everywhere of order λ_0^{-1} (reciprocal crystallite size) thus introducing a peculiar "multifractality" of the problem.

One can estimate the resistance of a trap formed by a strange attractor of high-conductivity lines. Similar to the calculation in Eq. (4.114), we can write

$$r(l) = \frac{1}{\sigma_1} \frac{l}{l_1(l)\, l_3(l)} + \frac{1}{\sigma_2} \frac{l_3(l)}{l\, l_1(l)} , \tag{4.115}$$

where l is the distance along the high-conductivity (σ_1) axes, the subscripts of $l_i(l) \simeq \lambda_0 \exp(\Lambda_i l)$ correspond to the Lyapunov exponents ordering, and the fact was used that, generically, the projection of the σ_2 conductivity axis onto the shrinking direction (l_3) is not zero. Expression (4.115) is minimized by $l \simeq (1/|2\Lambda_3|) \log(\sigma_1/\sigma_2)$, which results in

$$\sigma_D^* \equiv (\lambda_0 r_{\min})^{-1} \simeq \sigma_1 \left(\frac{\sigma_2}{\sigma_1}\right)^{\frac{\Lambda_1+\Lambda_3}{\Lambda_3}} \log^{-1}\left(\frac{\sigma_1}{\sigma_2}\right) . \tag{4.116}$$

Using formula (1.16) for the fractal dimension D of the attractor, expression (4.116) can be rewritten as

$$\sigma_D^* \simeq \sigma_1^{(D-1)/2}\, \sigma_2^{(3-D)/2} \log^{-1}(\sigma_1/\sigma_2) . \tag{4.117}$$

So the equivalent network of a 3D polycrystal includes several kinds of resistors with a broad distribution of resistances. Due to the inequality $2 < D < 3$, the conductivity of a strange attractor (4.117) is much larger than that of a focus or a limit cycle ($\simeq \sigma_1^{1/2}\sigma_2^{1/2}$). This

is the play of a number, whether a generic polycrystalline configuration admits percolation through higher-conductivity (strange attractor) traps or not. Preliminary numerical results (Dykhne and Marianer, 1991) indicate that the concentration of such traps is well below the percolation threshold, so that foci seem to govern the asymptotics of the effective conductivity, which thus scales similarly to the two-dimensional case, $\sigma^* \simeq (\sigma_1\sigma_2)^{1/2}$. In both two and three dimensions, the mixing length ξ_m is of the order of the crystallite size λ.

b. Plasma heat condution in a stochastic magnetic field

While being somewhat artificial, the problem of conductance in a strongly anisotropic polycrystal invokes the geometry of generic (random, in particular) compressible fields in a rather instructive manner. The approximation of highly anisotropic transport, however, is quite natural for the heat conduction in a magnetized high-temperature plasma, where the longitudinal (with respect to the magnetic field $\mathbf{B}(\mathbf{x})$) heat conductivity $\chi_{||}$ can exceed the transverse conductivity $\chi_\perp$ by many orders of magnitude (cf. White, 1989).

The idea of magnetic confinement fusion is to organize such a geometry of the magnetic field (e.g., nested toroidal magnetic surfaces) that $\chi_\perp$ controls the heat losses from plasma. In reality, however, there may arise irregularities of $\mathbf{B}(\mathbf{x})$, which, due to the triggering of the large longitudinal conductivity $\chi_{||}$, can significantly increase the effective heat conductivity $\chi_\perp^*$ across the unperturbed magnetic field (Rechester and Rosenbluth, 1978; Kadomtsev and Pogutse, 1979). In the approximation of frequent collisions, the problem of the effective heat conductivity belongs to the same category as polycrystals. The difference is that the high-conduction lines in a magnetized plasma are the magnetic field lines, which are incompressible ($\nabla \cdot \mathbf{B}(\mathbf{x}) = 0$) and hence cannot terminate in traps.

In a two-dimensional magnetic field, $\mathbf{B}(\mathbf{x}) = \nabla\psi(x,y)\times\hat{\mathbf{z}}$, the reciprocity theorem (4.113) is still valid since in its proof nothing was assumed on the type of the local anisotropy field $\mathbf{B}(\mathbf{x})$. Hence, in the macroscopically isotropic case, the effective heat conductivity is given

by (Kadomtsev and Pogutse, 1979)

$$\chi^* = (\chi_{\|}\chi_{\perp})^{1/2} . \tag{4.118}$$

Having the same scaling as the conductivity of a 2D polycrystal, expression (4.118) originates from quite a different heat conduction pattern (Isichenko, 1991b). Consider the case of a random 2D magnetic field with the monoscale (λ_0) flux potential $\psi(x,y)$. Since the magnetic lines (contours of $\psi(x,y)$) are not trapped, one can expect a significant role played by extended magnetic lines, so that the mixing length ξ_m is much greater than the characteristic scale λ_0. To establish the transition to the effective heat conduction, it is more convenient to argue in terms of the diffusion of "caloric" (the heat substance), whose particles diffuse at the diffusivity $\chi_{\|}$ along the magnetic lines and at the diffusivity $\chi_{\perp}$ across them. The mixing length ξ_m can be estimated as the size of a cell formed by magnetic lines, such that a caloric particle is decorrelated from it in the time of the longitudinal diffusion:

$$\tau_m = \frac{w^2(\xi_m)}{\chi_{\perp}} = \frac{L^2(\xi_m)}{\chi_{\|}} , \tag{4.119}$$

where $w(\xi_m)$ and $L(\xi_m)$ denote the width and the length of the bundle of magnetic lines with diameters of the order of ξ_m. Using formulas (3.41) and (3.43), we find from (4.119)

$$\xi_m = \lambda_0 \left(\frac{\chi_{\|}}{\chi_{\perp}}\right)^{\frac{1}{2(d_h+1/\nu)}} = \lambda_0 \left(\frac{\chi_{\|}}{\chi_{\perp}}\right)^{1/5} \gg \lambda_0 . \tag{4.120}$$

The effective heat conductivity can be estimated in a "diffusive manner" as follows:

$$\chi^* \simeq F(\xi_m)\frac{\xi_m^2}{\tau_m} , \tag{4.121}$$

where $F(\xi_m) = L(\xi_m)w(\xi_m)\xi_m^{-2}$ is the fraction of area covered by the ξ_m-cells where most of the transport takes place. Taking into account Eq. (4.119), formula (4.121) reduces to Eq. (4.118).

In the case when a strong background magnetic field $\mathbf{B}_0 = B_0\,\hat{\mathbf{z}}$ is present, result (4.118) is modified by the substitution $\chi_{\|} \to \chi_{\|}(\delta B/B_0)^2$, which is simply a projection of the

longitudinal conductivity onto the (x, y) plane, where $\delta\mathbf{B} = \nabla\psi(x, y) \times \hat{\mathbf{z}}$ is a 2D magnetic fluctuation (Kadomtsev and Pogutse, 1979):

$$\chi_\perp^* \simeq \frac{\delta B}{B_0} (\chi_\perp \chi_\parallel)^{1/2} , \quad \chi_\parallel \left(\frac{\delta B}{B_0}\right)^2 > \chi_\perp . \tag{4.122}$$

In a more realistic model of a general three-dimensional magnetic perturbation, $\mathbf{B}(\mathbf{x}) = B_0 \hat{\mathbf{z}} + \delta\mathbf{B}(x, y, z)$, the magnetic lines exhibit a stochastic exponentiation. Indeed, the equation of a magnetic line,

$$\frac{d\mathbf{x}_\perp}{dz} = \frac{\delta\mathbf{B}_\perp(\mathbf{x}_\perp, z)}{B_0} , \tag{4.123}$$

is similar to that of a particle orbit in a nearly incompressible, 2D, time-dependent flow, if the coordinate z is treated as time. In the *quasilinear limit*, corresponding to the high-frequency limit of passive advection, the length l_K of the exponentiation can be estimated as the inverse Kolmogorov entropy in Eq. (4.58). In terms of the magnetic field, this results in

$$l_K \simeq \lambda_\parallel \cdot R^{-2} , \qquad R \equiv \frac{\delta B}{B_0} \frac{\lambda_\parallel}{\lambda_\perp} \ll 1 , \tag{4.124}$$

where $\lambda_\parallel$ and $\lambda_\perp$ denote the characteristic scales of $\delta\mathbf{B}(\mathbf{x}_\perp, z)$ along and across the background magnetic field, respectively. The exponentiation of magnetic lines leads to a convoluted geometry of magnetic flux tubes (Fig. 35). *F 35*

To estimate the effective heat conductivity in a stochastic magnetic field, we again argue in terms of diffusion. A "caloric" particle can be believed to have decorrelated from a given magnetic line when the particle leaves a magnetic flux tube encompassing this line, with the initial radius $\lambda_\perp$. At sufficiently small transverse diffusivity $\chi_\perp$, this is easier to do by first longitudinally diffusing to a distance z of several exponentiation lengths l_K, where the magnetic tube gets strongly convoluted and then undertaking a short transverse diffusion to a distance

$$w(z) \simeq \lambda_\perp \exp\left(-\frac{|z|}{l_K}\right) , \tag{4.125}$$

which is the characteristic width of the flux tube wall (Fig. 35). The optimum value of *F 35*

$z = l_m$ (the longitudinal mixing length) is obtained from the comparison of longitudinal and transverse diffusion times:

$$\tau_m = \frac{l_m^2}{\chi_{\|}} = \frac{w^2(l_m)}{\chi_{\perp}} \ . \tag{4.126}$$

Substituting Eq. (4.125) into (4.126), we find

$$l_m \simeq l_K \log\left(\frac{\chi_{\|}}{\chi_{\perp}} \frac{\lambda_{\perp}^2}{l_K^2}\right) \ . \tag{4.127}$$

This result is valid if the expression under logarithm is large.

During the decorrelation time τ_m, the transverse particle displacement ξ_m is given by the diffusion of magnetic lines, $\xi_m \simeq (D_m\, l_m)^{1/2}$, where

$$D_m \simeq \lambda_{\|} \left(\frac{\delta B}{B_0}\right)^2 \tag{4.128}$$

is the magnetic line diffusivity (compare with Eq. (4.52)). Finally, the effective cross-field heat conductivity is given by the formula (Rechester and Rosenbluth, 1978; Kadomtsev and Pogutse, 1979)

$$\chi^* \simeq \frac{\xi_m^2}{\tau_m} = \chi_{\|} \frac{D_m}{l_m} = \chi_{\|} \frac{D_m}{l_K} \log^{-1}\left(\frac{\chi_{\|}}{\chi_{\perp}} \frac{\lambda_{\perp}^2}{l_K^2}\right) \ . \tag{4.129}$$

In the case of stronger magnetic perturbations, $R \equiv \frac{\delta B}{B_0} \frac{\lambda_{\|}}{\lambda_{\perp}} \gg 1$, magnetic diffusivity is given by percolation scaling (4.57),

$$D_m \simeq \lambda_{\perp} \frac{\delta B}{B_0} R^{-1/(\nu d_h + 1)} \propto \left(\frac{\delta B}{B_0}\right)^{7/10} \ , \tag{4.130}$$

and there are several regimes of the effective heat conductivity (Isichenko, 1991b), one of which reduces to the Kadomtsev-Pogutse regime (4.122) in the 2D limit $R \to \infty$.

3. Magnetoresistance of inhomogeneous media with the Hall effect

Thus far we were concerned with the conductance in media that were either microscopically isotropic (Sec. 1) or anisotropic with a symmetric conductivity tensor (Sec. 2). Here we

consider inhomogeneous anisotropic media with unchanged direction of anisotropy (given, for example, by an external magnetic field), but with a conductivity tensor having an essential antisymmetric part $\widehat{\sigma}^a$ associated with the Hall effect:

$$\sigma_{ij}(\mathbf{x}) = \sigma^s_{ij}(\mathbf{x}) + \sigma^a_{ij}(\mathbf{x}) \ , \tag{4.131}$$

where $\sigma^s_{ij} = \sigma^s_{ji}$ and $\sigma^a_{ij} = -\sigma^a_{ji}$. This is a noticeable feature of such media that the conductivity processes are related to the advective-diffusive transport in an incompressible steady flow, which problem is amenable to a more or less clear qualitative analysis. The correspondence between the two problems (Dreizin and Dykhne, 1972, Dykhne, 1984) follows from the microscopic Ohm's law, $\mathbf{j}(x) = \widehat{\sigma}(\mathbf{x})\,\mathbf{e}(\mathbf{x})$, $\mathbf{e}(\mathbf{x}) = \boldsymbol{\nabla}\varphi(\mathbf{x})$, and the requirement that the current density $\mathbf{j}(\mathbf{x})$ be divergence-free:

$$\frac{\partial}{\partial x_i}\,\sigma_{ij}(\mathbf{x})\,\frac{\partial \varphi}{\partial x_j} = 0 \ . \tag{4.132}$$

Substituting expression (4.131) into (4.132), we obtain

$$\mathbf{v}\boldsymbol{\nabla}\varphi = \boldsymbol{\nabla}(\widehat{\sigma}^s \boldsymbol{\nabla}\varphi) \ , \tag{4.133}$$

where

$$v_i(\mathbf{x}) = \frac{\partial \sigma^a_{ij}(\mathbf{x})}{\partial x_j} \tag{4.134}$$

is an incompressible ($\boldsymbol{\nabla}\cdot\mathbf{v} = \nabla_i\nabla_j\sigma^a_{ij} = 0$) field. Equation (4.133) can be thought of to describe the steady distribution of a tracer with the density φ advected by the velocity field $\mathbf{v}(\mathbf{x})$ and subject to the molecular diffusion $\widehat{\sigma}^s(\mathbf{x})$ (perhaps, anisotropic). Notice that the vector potential $\boldsymbol{\psi}(\mathbf{x})$ of the incompressible flow $\mathbf{v}(\mathbf{x})$ is given by

$$\psi_i = \frac{1}{2}\,\varepsilon_{ijk}\,\sigma^a_{jk} \ , \qquad \sigma^a_{ij} = \varepsilon_{ijk}\,\psi_k \ , \tag{4.135}$$

where ε_{ijk} is the Levi-Cevita tensor. For bounded perturbations in the antisymmetric conductivity $\widehat{\sigma}^a(\mathbf{x})$, the vector potential $\boldsymbol{\psi}(\mathbf{x})$ is also bounded leading to the existence of a finite

effective diffusivity $\widehat{D}^*$ (see Sec. IV.A.1). In terms of steady tracer distribution, this means that the average flux is proportional to the average density gradient:

$$\langle \mathbf{v}\varphi - \hat{\sigma}^s \nabla\varphi \rangle = -\widehat{D}^* \langle \nabla\varphi \rangle \ , \tag{4.136}$$

where the angular brackets denote spatial average over scale much larger than a mixing scale ξ_m. Integrating the left-hand side of Eq. (4.136) by parts one finds

$$\langle \hat{\sigma} \nabla\varphi \rangle = \widehat{D}^* \langle \nabla\varphi \rangle + \langle \psi \rangle \times \langle \nabla\varphi \rangle \ . \tag{4.137}$$

Since the left-hand side of Eq. (4.137) is the average current density, we recover the average Ohm's law with the effective conductivity tensor (Dreizin and Dykhne, 1972)

$$\hat{\sigma}^* = \widehat{D}^* + \langle \hat{\sigma}^a(\mathbf{x}) \rangle \ . \tag{4.138}$$

Thus, if one is able to determine the effective diffusivity $= \widehat{D}^*$ in flow (4.134) with the molecular diffusivity $\hat{\sigma}^s$, formula (4.138) yields the result for the effective conductivity of the inhomogeneous medium with Hall effect.

Another approach, which is restricted to a two-dimensional, two-phase system, is based on reciprocity relations (Dykhne, 1970b; Balagurov, 1978, 1986, Bozhokin and Bykov, 1990). Consider the microscopic Ohm's law

$$\mathbf{j} + \mathbf{j} \times \beta(\mathbf{x}) = \sigma_0(\mathbf{x})\, \mathbf{e} \ , \tag{4.139}$$

where $\beta(\mathbf{x}) = \beta(\mathbf{x})\, \hat{\mathbf{z}}$ is the Hall parameter proportional to the external magnetic field $\mathbf{B}$. The conductivity tensor corresponding to (4.139) is

$$\hat{\sigma}(\mathbf{x}) = \frac{\sigma_0(\mathbf{x})}{1+\beta^2(\mathbf{x})} \begin{pmatrix} 1 & -\beta(\mathbf{x}) & 0 \\ \beta(\mathbf{x}) & 1 & 0 \\ 0 & 0 & 1+\beta^2(\mathbf{x}) \end{pmatrix} \ . \tag{4.140}$$

This tensor is a good model of conductance in plasmas (Kingsep *et al.*, 1990) and in non-compensated metals and semiconductors (Lifshitz and Pitaevskii, 1981). Let the parameters

$\sigma_0(\mathbf{x})$ and $\beta(\mathbf{x})$ fluctuate, each taking on only two values, σ_1 and σ_2 (for $\sigma_0(\mathbf{x})$) and β_1 and β_2 (for $\beta(\mathbf{x})$), in the phases I and II, respectively. The idea of the approach (Dykhne, 1970b) is to use linear transformations from $\mathbf{j}$ and $\mathbf{e}$ to new fields $\mathbf{j}'$ and $\mathbf{e}'$ such that the macroscopic properties of the new system are equivalent to those of the original system. In the presence of the Hall-effect, one such transformation is not sufficient to calculate the effective conductivity tensor; however, there exist two independent linear transformations satisfying the desired conditions. Of course, the result can be achieved only for a statistically equivalent and isotropic distribution of the phases I and II. Dykhne (1970b) considered the case when only $\sigma_0(\mathbf{x})$ fluctuates ($\sigma_1 \neq \sigma_2, \beta_1 = \beta_2$). Balagurov (1978) generalized the result for the more general case $\beta_1 \neq \beta_2$. The effective conductivity tensor $\hat{\sigma}^*$ can be written similarly to expression (4.140) with the substitution $\sigma_0(\mathbf{x}) \to \sigma_0^*, \beta(\mathbf{x}) \to \beta^*$, where

$$\sigma_0^* = \left[\frac{\sigma_1\sigma_2}{1 + (\sigma_1\beta_2 - \sigma_2\beta_1)^2/(\sigma_1 + \sigma_2)^2}\right]^{1/2}, \tag{4.141}$$

$$\beta^* = \sigma_0^* \frac{\beta_1 + \beta_2}{\sigma_1 + \sigma_2}. \tag{4.142}$$

In the absence of magnetic field ($\beta_1 = \beta_2 = 0$), formula (4.141) reproduces result (4.108).

In the limit of a strong magnetic field ($\beta \equiv (|\beta_1| + |\beta_2|)/2 \gg 1$) and strong fluctuations of the Hall conductance ($\beta\Delta \equiv |\sigma_1\beta_2 - \sigma_2\beta_1|/(\sigma_1 + \sigma_2) \gg 1$) the effective conductivity (4.141) becomes anomalously low:

$$\sigma_0^* \simeq \sigma_0(\beta\Delta)^{-1}. \tag{4.143}$$

This anomalous resistance is caused by strongly nonuniform flow of electric current in the presence of the fluctuations. The linear dependence of the transverse magnetoresistance $\rho^*(B) \equiv 1/\sigma_0^*(B) \propto B$ on the external magnetic field $\mathbf{B}$ ($\beta \propto B$) is not an exceptional property of the exact solution (4.141). Such behavior extends to generic 3D *sharp* inhomogeneities of the medium, such as voids or cracks (Herring, 1960; Pippard, 1989). A similar magnetoresistance behavior can also result from the effect of the sample boundaries (Rendell

and Girvin, 1981; Chukbar and Yankov, 1988; Isichenko and Kalda, 1992). It is interesting that in the first measurements of the magnetoresistance in metals in strong magnetic fields (Kapitza, 1928, 1929) a linear dependence $\rho^*(B) \propto B$ was observed even for monocrystalline samples. Such a pronounced effect was not reproduced in later experiments (for review see Pippard, 1989). The polycrystalline structure of metals would lead either to the saturation of the transverse magnetoresistance $\rho^*(B)$ or to its growth as $B^{2/3}$, $B^{4/3}$, or B^2, depending on the topology of the metal Fermi surface (Dreizin and Dykhne, 1972; Stachowiak, 1978). The explanation (Isichenko and Kalda, 1992) of the linear Kapitza law $\rho^*(B) \propto B$ is that in Kapitza's experiments (unlike later works) no separate potential leads were used and both the potential and power leads were (improperly) brought from the same electrodes thus introducing the boundary effect of a sharp interface. In the case of smooth inhomogeneities the behavior of the magnetoresistance is different (see below).

It is interesting to identify the implication of exact result (4.141)–(4.142) in terms of the advective-diffusive analogy (4.133)–(4.138). To do so, put $\sigma_1 = \sigma_2 = \sigma_0$ and $\beta_1 = -\beta_2 = \beta_0$. Then the symmetric part of tensor (4.140) becomes homogeneous, corresponding to the "molecular diffusivity" in the (x, y) plane

$$D_0 = \frac{\sigma_0}{1 + \beta_0^2} , \tag{4.144}$$

and flow (4.134) becomes two-dimensional with the stream-function

$$\psi(x, y) = \begin{cases} -\psi_0 , & \text{in I} , \\ \psi_0 , & \text{in II} , \end{cases} \tag{4.145}$$

where

$$\psi_0 = \frac{\sigma_0 \beta_0}{1 + \beta_0^2} . \tag{4.146}$$

According to Eq. (4.141), the effective conductivity, or the diffusivity in flow (4.144), is equal to

$$\sigma^* = D^* = \sigma_0 (1 + \beta_0^2)^{-1/2} = (D_0^2 + \psi_0^2)^{1/2} . \tag{4.147}$$

Thus one concludes (Dykhne, 1981; Tatarinova, 1990) that "Pithagor formula" (4.147) exactly describes the effective diffusivity in the isotropic system of narrow jets separating statistically equivalent regions I and II. For results (4.141), (4.142), and (4.147) to be valid, the width w of the jets (in the advective-diffusive system), or of the transition layer between the phases I and II must be small not only in comparison with the characteristic inhomogeneity scale λ_0, but also in comparison with the width of a diffusive boundary layer: $w \ll (D_0\lambda_0/v_0)^{1/2}$, where $v_0 = \psi_0/w$ is the characteristic velocity in the jets. Hence we obtain $w \ll \lambda_0/P_0$, where $P_0 = \psi_0/D_0 = \beta\Delta \gg 1$ is the Péclet number.

Usually, the advective-diffusive analogy serves in the opposite direction: to calculate the effective conductivity of a Hall medium using presumably known effective diffusivity in a corresponding velocity field (Dreizin and Dykhne, 1972; Isichenko and Kalda, 1991a). In the case of monoscale isotropic 3D fluctuations of the off-diagonal conductivity $\sigma_{xy}(x,y,z)$ with the correlation length λ_0, one has the velocity field (4.134),

$$\mathbf{v}(\mathbf{x}) = -\nabla\sigma_{xy}(x,y,z) \times \hat{\mathbf{z}} \,, \tag{4.148}$$

representing a two-dimensional incompressible random flow in each plane $z = \text{const.}$, with the stream-function $\psi(x,y,z) = -\sigma_{xy}$ smoothly varying with z. The characteristic velocity in the flow is $v_0 = \sigma_0\Delta/(\beta\lambda_0)$, where σ_0 and $\beta \gg 1$ are the average values of $\sigma_0(\mathbf{x})$ and $\beta(\mathbf{x})$, respectively, and Δ is the relative fluctuation amplitude of $\sigma_{xy} = \sigma_0(\mathbf{x})/\beta(\mathbf{x})$. The "molecular diffusivity" $\hat{\sigma}^s$ in this flow is anisotropic. At $\beta \gg 1$, the diffusivity in the (x,y) plane ($\sigma_{xx} = \sigma_{yy} = \sigma_0\beta^{-2}$) is much smaller than that in the z-direction ($\sigma_{zz} = \sigma_0$). If the fluctuations of σ_{xx} and σ_{zz} are not too large, they may be neglected in comparison with the effect of the fluctuations in the Hall conductivity σ_{xy}. In the considered case the long-range topography of the stream-function $\psi(x,y,z)$ in a plane $z = \text{const.}$ is irrelevant, because the tracer particle diffuses the correlation length λ_0 in the z-direction long before the flow shows an inhomogeneity in the (x,y) plane: $v_0\lambda_0^2/\sigma_0 = \lambda_0\Delta/\beta \ll \lambda_0$. This means that on the

time-scale[1] $t \gtrsim \lambda_0^2/\sigma_0$, the velocity field can be substituted by a 3D shear flow $\mathbf{v} = \mathbf{v}_\perp(z)$ with randomly changed (on the correlation scale λ_0) direction of $\mathbf{v}_\perp$. For this situation, formula (4.66) predicts a superdiffusive particle displacement in the (x, y) plane,

$$x_\perp(t) \simeq v_0 \left(\frac{\lambda_0^2}{\sigma_0}\right)^{1/4} t^{3/4} , \tag{4.149}$$

while the effect of the transverse molecular diffusivity $\sigma_0\beta^{-2}$ may be neglected. Superdiffusion (4.149) takes place until the transverse displacement $x_\perp(t)$ attains the correlation length λ_0; after that a crossover to effective diffusion occurs. Denote t_c the crossover, or correlation time: $x_\perp(t_c) = \lambda_0$. Then the effective transverse diffusivity, and thereby the effective transverse conductivity, is estimated as

$$D_\perp^* = \sigma_\perp^* \equiv \frac{\sigma_0^*}{\beta^{*2}} \simeq \frac{x_\perp^2(t_c)}{t_c} \simeq \sigma_0 \left(\frac{\Delta}{\beta}\right)^{4/3} . \tag{4.150}$$

The effective Hall parameter β^* is calculated using formula (4.138): $\sigma_{xy}^* \equiv -\sigma_0^*/\beta^* = \langle\sigma_{xy}(\mathbf{x})\rangle \simeq -\sigma_0/\beta$, hence we have (Dreizin and Dykhne, 1972)

$$\sigma_0^* \simeq \sigma_0(\beta\Delta^2)^{-2/3} , \tag{4.151}$$

$$\beta^* \simeq \beta^{1/3}\Delta^{-4/3} . \tag{4.152}$$

Formula (4.151) describes the anomalous resistance, $\rho^*(B) \propto B^{2/3}$, which is much smaller than that in Eq. (4.143), $\rho^*(B) \propto B$, in the limit of a strong magnetic field B. The difference between two mechanisms of the anomalous resistance lies in the geometry of the current streamlines in media with sharp and smooth inhomogeneities. In the case of sharp interfaces main Ohmic dissipation is released in narrow boundary. For isotropic smooth inhomogeneities, the anomalous resistance results from a long ($\xi_z = (\sigma_0 t_c)^{1/2} = \lambda_0(\beta/\Delta)^{2/3} \gg \lambda_0$) walk of current streamlines in the direction of the magnetic field (Fig. 36). In the gen- *F 36*

[1]Notice that in the employed advective-diffusive analogy the dimensionalities of v_0 and σ_0 are different from those of a velocity and a diffusivity. Only final results expressed in terms of the effective conductivity will be dimensionally correct.

eral case of anisotropic fluctuations in microscopic conductivity $\hat{\sigma}(\mathbf{x})$, both mechanisms of anomalous resistance (contraction in boundary layers and tangled walk of current streamlines) can coexist leading to the fractal geometry of both individual current streamlines and the dissipation-containing region (Isichenko and Kalda, 1991a).

The extreme situation of a very strong anisotropy of fluctuations, corresponding to a two-dimensional geometry ($\partial/\partial z = 0$) can realize in a magnetized plasma. Here, flow (4.148) becomes purely two-dimensional, with the molecular diffusivity $D_0 = \sigma_0\beta^{-2}$. The Péclet number in this flow is estimated as

$$P = \frac{\lambda_0 v_0}{D_0} = \beta\Delta \ . \tag{4.153}$$

For monoscale fluctuations of $\sigma_0(\mathbf{x})/\beta(\mathbf{x})$ with a sufficiently large amplitude, $\beta\Delta \gg 1$, the effective diffusivity, and thereby conductivity across the magnetic field is given by formula (4.36),

$$\sigma_\perp^* \equiv \frac{\sigma_0^*}{\beta^{*2}} \simeq D_0 P^{10/13} = \frac{\sigma_0}{\beta^2}\,(\beta\Delta)^{10/13} \ , \tag{4.154}$$

which corresponds to (Isichenko *et al.*, 1989)

$$\sigma_0^* \simeq \sigma_0(\beta\Delta)^{-10/13} \ , \tag{4.155}$$

$$\beta^* \simeq \beta^{3/13}\Delta^{-10/13} \ . \tag{4.156}$$

The behavior of conductivity (4.155) is an intermediate one between the case of sharp boundaries (4.143) and isotropic 3D fluctuations (4.151).

Inequality (4.20) specifying the allowed range of the effective diffusivity in an advective-diffusive system can be translated into the bounds on the effective conductivity of an inhomogeneous medium with the Hall-effect. Using the above notation this results in the following inequalities:

$$C_1\,\sigma_0/(1+\beta^2\Delta^2) \le \sigma_0^* \le C_2\,\sigma_0 \ , \tag{4.157}$$

$$C_3\,\beta/(1+\beta^2\Delta^2) \le \beta^* \le C_4\,\beta \ , \tag{4.158}$$

where parameters C_i accounting for moderate variation of the symmetric part of $\widehat{\sigma}(\mathbf{x})$ are of the order of unity. The limiting case of the anomalous resistance described by the left-hand side of inequality (4.157) is attained in the direction across the for layer-shaped inhomogeneities, $\sigma_{xy}(\mathbf{x}) = \sigma_{xy}(x)$ (Chukbar and Yankov, 1988).

V. Concluding remarks

Throughout this paper, a general idea was pursued about the usefulness of the geometrical images of physical phenomena. Geometry unifies and interconnects very different physical problems enriching methods of their solution. For phenomena involving many scales of length (usually associated with the presence of a large parameter), the fractal geometry provides sensible guidelines for qualitative analysis.

The quantitative description of random media in terms of the scaling behavior of effective transport coefficients involves a set of power exponents, to which the large parameters of the problem are to be raised. We tried to demonstrate that in many cases these exponents form certain universality classes, that is, depend on the system parameters in a piecewise constant manner. The universality class of random percolation covers a variety of lattice and continuum models including the contour lines and surfaces of a monoscale random potential. The latter problem is particularly relevant for two-dimensional incompressible flows, which describe the advective-diffusive transport of a tracer, the guiding center drift in a turbulent plasma, or the geometry of stochastic magnetic field lines. Some other problems including the averaging of randomly-inhomogeneous conductance can be related to the percolation model in more or less direct ways.

In addition to the discrete universality classes, there exists a continuum universality, whose characteristic exponents continuously depend on a spectral parameter H. An example of a continuous universality class is the long-range correlated percolation with H being an exponent of the algebraic decay of lattice correlations. An extension of this problem to continuum is the statistical topography of potentials with algebraic spectra. I hope that this classical geometrical problem will see further development and new areas of application.

Acknowledgements

It is a pleasure to acknowledge many discussions and exchange of ideas with Jaan Kalda. I am grateful to M. Avellaneda, A.M. Dykhne, M. Ottaviani, and E.B. Tatarinova for communicating their work, including unpublished results, and to A.D. Beklemishev for helping in computer simulations. Special thanks to Tanya Isichenko who generated pictures on a computer and provided necessary support.

This work was supported by U.S. Department of Energy under Contract No. DE-FG05-80ET53088.

References

1. Abrikosov, A.A., 1980, *Spin glasses with short range interaction.* Adv. Phys. **29**, 869.

2. Adler, R.J., 1981, *The geometry of random fields* (Wiley, New York).

3. Adler, J., Y. Meir, A. Aharony, and A.B. Harris, 1990, *Series study of percolation moments in general dimension.* Phys. Rev. **B 41**, 9183.

4. Aharony, A., 1984, *Dynamics of fractal structures.* J. Stat. Phys. **34**, 735.

5. Alexandrowicz, Z., 1980, *Critically branched chains and percolation clusters.* Phys. Lett. **A 80**, 284.

6. Anderson, P.W., 1958 *Absence of diffusion in certain random lattices.* Phys. Rev. **109**, 1492.

7. Aref, H., 1984, *Stirring by chaotic advection.* J. Fluid Mech. **143**, 1.

8. Aris, R., 1956, *On the dispersion of a solute in a fluid flowing through a tube.* Proc. R. Soc. London, Ser. A **235**, 67.

9. Arnold, V.I., 1978, *Mathematical methods in classical mechanics* (Springer, Heidelberg).

10. Arnold, V.I., 1983, *Singularities, bifurcations and catastrophes.* Usp. Fiz. Nauk (SSSR) **141**, 569 [Sov. Phys. Usp. **26**, 1025 (1983)].

11. Arnold, V.I., 1988, *Remarks on quasisrystallic symmetries.* Physica **D 33**, 21.

12. Avellaneda, M., A.V. Cherkaev, K.A. Lurie, and G.M. Milton, 1988, *On the effective conductivity of polycrystals and three-dimensional phase-interchange inequality.* J. Appl. Phys. **63**, 4989.

13. Avellaneda, M., and A.J. Majda, 1989, *Stieltjes integral representation and effective diffusivity bounds for turbulent transport.* Phys. Rev. Lett. **62**, 753.

14. Avellaneda, M., and A.J. Majda, 1990, *Mathematical models with exact renormalization for turbulent transport.* Commun. Math. Phys. **131**, 381.

15. Avellaneda, M., and A.J. Majda, 1991, *An integral representation and bounds on the effective diffusivity in passive advection by laminar and turbulent flows.* Commun. Math. Phys. **138**, 339.

16. Balagurov, B.Ya., 1978, *Galvanomagnetic properties of thin inhomogeneous films.* Fiz. Tverd. Tela **20**, 3332 [Sov. Phys. Solid State **20**, 1922 (1978)].

17. Balagurov, B.Ya., 1986, *Thermogalvanomagnetic properties of two-dimensional two-component systems.* Fiz. Tverd. Tela **28**, 2068 [Sov. Phys. Solid State **28**, 1156 (1986)].

18. Balberg, I., 1987, *Recent developments in continuum percolation.* Phil. Mag. **B 56**, 991.

19. Batchelor, G.K., 1952, *Diffusion in a field of homogeneous turbulence II. The relative motion of particles.* Proc. Cambridge Philos. Soc. **48**, 345.

20. Batchelor, G.K., 1982, *The theory of homogeneous turbulence* (Cambridge University Press, Cambridge).

21. Battacharya, R., V. Gupta, and H.F. Walker, 1989, *Asymptotics of solute dispersion in periodic porous media.* SIAM J. Appl. Math. **49**, 86.

22. Baxter, R.J., 1982, *Exactly solved models in statistical mechanics* (Academic, London).

23. Belavin, A.A., A.M. Polyakov, and A.B. Zamolodchikov, 1984, *Infinite conformal symmetry of critical fluctuations in two dimensions.* J. Stat. Phys. **34**, 763.

24. Bender, C.M., and S.A. Orszag, 1978, *Advanced mathematical methods for scientists and engineers* (McGrow-Hill, New York).

25. Bensoussan, A., J.L. Lions, and G. Papanicolaou, 1978, *Asymptotic analysis for periodic structures* (North-Holland, Amsterdam).

26. Benzi, R., L. Biferale, G. Paladin, A. Vulpiani, and M. Vergassola, 1991, *Multifractality in the statistics of the velocity gradients in turbulence.* Phys. Rev. Lett. **67**, 2299.

27. Bergman, D.J., and Y. Imry, 1977, *Critical behavior of the complex dielectric constant near the percolation threshold of a heterogeneous material.* Phys. Rev. Lett. **39**, 1222.

28. Bergman, D.J., 1978, *The dielectric constant of a composite material – a problem in classical physics.* Phys. Rep. **43**, 377.

29. Berry, M.V., N.C. Balazs, M. Tabor, and A. Voroz, 1979, *Quantum maps.* Ann. Phys. **122**, 26 (1979).

30. Berry, M.V., and J.H. Hannay, 1978, *Topography of random surfaces.* Nature **273**, 573.

31. Berry, M.V., and Z.V. Lewis, 1980, *On the Weierstrass-Mandelbrot fractal function.* Proc. Roy. Soc. London **A370**, 459.

32. Besicovitch, A.S., 1929, *On linear sets of points of fractional dimensions.* Math. Annalen **101**, 161.

33. Besicovitch, A.S., 1935a, *On the sum of digits of real numbers represented in the diadic system. (On linear sets of points of fractional dimensions II.)* Math. Annalen **110**, 321.

34. Besicovitch, A.S., 1935b, *Sets of points of non-differentiability of absolutely continuous functions and of divergence of Fejér sums. (On linear sets of points of fractional dimensions III).* Math. Annalen **110**, 331.

35. Bouchard, J.-P., A. Comete, A. Georges, and P. Le Doussal, 1987, *Anomalous diffusion in random media at any dimensionality.* J. Physique **48**, 1455.

36. Bouchard, J.-P., A. Georges, J. Koplik, A. Provata, and S. Redner, 1990, *Superdiffusion in random velocity fields.* Phys. Rev. Lett. **64**, 2503.

37. Bozhokin, S.V., and A.M. Bykov, 1990, *Transport processes in a randomly inhomogeneous plasma in a magnetic field.* Fizika Plasmy **16**, 717 [Sov. J. Plasma Phys. **16**, 415 (1990)].

38. Brady, J.F., 1990, *Dispersion in heterogeneous media.* In *Hydrodynamics of dispersed media*, edited by J.P. Hulin, A.M. Cazabat, E Guyon, and F. Carmona (Elsevier Science Publishers B.V., North-Holland), p. 271.

39. Brenner, H., 1980, *Dispersion resulting from flow through spatially periodic porous media.* Phil. Trans. R. Soc. Lond. **A 297**, 81.

40. Broadbent, S.R., and J.M. Hammersley, 1957, *Percolation processes, I. Crystals and mazes.* Proc. Cambridge Phil. Soc. **53**, 629.

41. Brown, M.G., and K.B. Smith, 1991, *Ocean stirring and chaotic low-order dynamics.* Phys. Fluids **A 3**, 1186.

42. Bug, A.L.R., S.A. Safran, G.S. Grest, and I. Webman, 1985, *Do interactions raise or lower a percolation threshold?* Phys. Rev. Lett. **55**, 1896.

43. Bunde, A., and J.F. Gouyet, 1985, *On scaling relations in growth models for percolation clusters and diffusion fronts.* J. Phys. **A18**, L285.

44. Bunde, A., H. Harder, and S. Havlin, 1986, *Nonuniversality of diffusion exponents in percolation systems.* Phys. Rev. **B 34**, 3540.

45. Burrough, P.A., 1981, *Fractal dimensions of landscapes and other environmental data.* Nature **234**, 240.

46. Busse, F.H., 1978, *Non-linear properties of thermal convection.* Rep. Prog. Phys. **41**, 1929.

47. Chandrasekhar, S., 1961, *Hydrodynamic and hydromagnetic stability* (Dover, New York).

48. Chukbar, K.V., and V.V. Yankov, 1988, *Evolution of the magnetic field in plasma opening switches.* Zh. Tekhn. Fiz. **58**, 2130 [Sov. Tech. Phys. **33**, 1293 (1988)].

49. Clerc, J.P., G. Giraud, S. Alexander, and E. Guyon, 1980, *Conductivity of a mixture of conducting and insulating grains: Dimensionality effects.* Phys. Rev. **B 22**, 2489.

50. Coniglio, A., 1981, *Thermal phase transition of the dilute s-state Potts and n-vector models at the percolation threshold.* Phys. Rev. Lett. **46**, 250.

51. Coniglio, A., C.R. Nappi, F. Peruggi, and L. Russo, 1977, *Percolation points and critical point of the Ising model.* J. Phys. **A10**, 205.

52. Constantin, P., I. Procaccia, and K.R. Sreenivasan, 1991, *Fractal geometry of isoscalar surfaces in turbulence: Theory and experiments.* Phys. Rev. Lett. **67**, 1739.

53. Coxeter, H.S.M., 1973, *Regular polytopes* (Dover, New York).

54. Dean, P., and N.F. Bird, 1967, *Monte Carlo estimates of critical percolation probabilities.* Proc. Cambridge Phil. Soc. **63**, 477.

55. Derrida, B., and J.M. Luck, 1983, *Diffusion on a random lattice: Weak-disorder expansion in arbitrary dimension.* Phys. Rev. **B28**, 7183.

56. Derrida, B., and J. Vannimenus, 1982, *A transfer-matrix approach to random resistor network.* J. Phys. **A 15**, L557.

57. Deutscher, G., R. Zallen, and J. Adler, 1983, Eds. *Percolation structures and processes.* (Hilger, Bristol).

58. Domb, C., M.S. Green, and J.L. Lebowitz, 1972-1987, Eds. *Phase transitions and critical phenomena,* vols. 1 to 11, (Academic, London).

59. Domb, C., and M.F. Sykes, 1960, *Cluster size in random mixtures and percolation processes.* Phys. Rev. **122**, 77.

60. Dombre, T., U. Frish, J.M. Greene, M. Hénon, A. Mehr, and A.M. Soward, 1986, *Chaotic streamlines in the ABC flows.* J. Fluid Mech. **167**, 353.

61. Dotsenko, Vl.S., and V.A. Fateev, 1984, *Conformal algebra and multipoint correlation functions in 2D statistical models.* Nucl. Phys. **B 240**[FS12], 312.

62. Dreizin, Yu.A., and A.M. Dykhne, 1972, *Anomalous conductivity of inhomogeneous media in a strong magnetic field.* Zh. Eksp. Teor. Fiz. **63**, 242 [Sov. Phys. JETP **36**, 127 (1973)].

63. Dreizin, Yu.A., and A.M. Dykhne, 1983, *A qualitative theory of the effective conductivity of polycrystals.* Zh. Eksp. Teor. Fiz. **84**, 1756 [Sov. Phys. JETP **57**, 1024 (1983)].

64. Dunn, A.G., J.W. Essam, and D.S. Ritchie, 1975, *Series expansion study of the pair connectedness in bond percolation models.* J. Phys. **C 8**, 4219.

65. Duplantier, B., and H. Saleur, 1987, *Exact tricritical exponents for polymers at the* Θ *point in two dimensions.* Phys. Rev. Lett. **58**, 539.

66. Dykhne, A.M., 1967, *Calculation of the kinetic coefficients of media with random inhomogeneities.* Zh. Eksp. Teor. Fiz. **52**, 264 [Sov. Phys. JETP **25**, 170 (1967)].

67. Dykhne, A.M., 1970a, *Conductivity of a two-dimensional two-phase system.* Zh. Eksp. Teor. Fiz. **59**, 110 [Sov. Phys. JETP **32**, 63 (1971)].

68. Dykhne, A.M., 1970b, *Anomalous plasma resistance in a strong magnetic field.* Zh. Eksp. Teor. Fiz. **59**, 641 [Sov. Phys. JETP **32**, 348 (1971)].

69. Dykhne, A.M., 1981, unpublished.

70. Dykhne, A.M., 1984, *Physical models reducible to the problem of random walks in randomly inhomogeneous media.* In *Nonlinear and Turbulent Processes in Physics*, edited by R.Z. Sagdeev (Harwood, New York), vol. 3, p. 1323.

71. Dykhne, A.M., and S. Marianer, 1991, private communication.

72. Edwards, B.F., and A.R. Kerstein, 1985, *Is there a lower critical dimension for chemical distance?* J. Phys. **A 18**, L1081.

73. Elan, W.T., A.R. Kerstein, and J.J. Rehr, 1984, *Critical exponents of the void percolation problem for spheres.* Phys. Rev. Lett. **52**, 1516.

74. Essam, J.W., 1972, *Percolation and cluster size.* In *Phase transitions and critical phenomena,* edited by C. Domb, M.S. Green, and J.L. Lebowitz (Academic, London), vol. 2, p. 197.

75. Essam, J.W., 1980, *Percolation theory.* Rep. Prog. Phys. **43**, 833.

76. Farmer, J.D, E. Ott, and J.A. Yorke, 1983, *The dimension of chaotic attractors.* Physica **D 7**, 153.

77. Feder, J., 1988, *Fractals* (Plenum, New York).

78. Feng, S., B.I. Halperin, and P.N. Sen, 1987, *Transport properties of continuum systems near the percolation threshold.* Phys. Rev. **B 35**, 197.

79. Finn, J.M., P.N. Guzdar, and A.A. Chernikov, 1991, *Particle transport and rotation damping due to stochastic magnetic field lines.* Preprint UMLPR 91-050, University of Maryland, College Park, submitted to Phys. Fluids **B**.

80. Fisher, D.S., 1984, *Random walks in random environments.* Phys. Rev. **A 30**, 960.

81. Fisher, M.E., 1966, *Shape of a self-avoiding walk or polymer chain.* J. Chem. Phys. **44**, 616.

82. Flierl, G.R., V.D. Larichev, J.C. McWilliams, and G.M. Reznik, 1980, *The dynamics of baroclinic and barotropic solitary eddies.* Dynamics of Atm. Oceans **5**, 1.

83. Fogelholm, R., 1980, *The conductivity of large percolation network samples.* J. Phys. **C 13**, L571.

84. Fortuin, C.M., and P.W. Kasteleyn, 1972, *On the random cluster model I. Introduction and relation to other models.* Physica (Utrecht) **57**, 536.

85. Frish, U., and G. Parisi, 1985, *On the singularity structure of fully developed turbulence.* In *Turbulence and predictability in geophysical fluid dynamics and climate dynamics*, edited by M. Ghil, R. Benzi, and G. Parisi (North-Holland, New York), p. 84.

86. Fung, J.C.H., and J.C. Vassilicos, 1991, *Fractal dimension of lines in chaotic advection.* Phys. Fluids **A3**, 2725.

87. Garland, J.C., and D.B. Tanner, 1978, Eds. *Electrical transport and optical properties of inhomogeneous media* (AIP, New York).

88. Gaunt, D.S., and M.F. Sykes, 1983, *Series study of random percolation in three dimensions.* J. Phys. **A 16**, 783.

89. Gawlinski, E.T., and S. Redner, 1983, *Monte Carlo renormalization group for continuum percolation with exluded-volume interaction.* J. Phys. **A 16**, 1063.

90. Gawlinski, E.T., and H.E. Stanley, 1977, *Continuum percolation in two dimensions: Monte Carlo tests of scaling and universality for non-interacting discs.* J. Phys. **A 10**, 205.

91. Gefen, Y., A. Aharony, B.B. Mandelbrot, and S. Kirkpatrick, 1981, *Solvable fractal family, and its possible relation to the backbone of percolation.* Phys. Rev. Lett. **47**, 1771.

92. Geiger, A., and H.E. Stanley, 1982, *Test of universality of percolation exponents for a three-dimensional continuum system for interacting water-like particles.* Phys. Rev. Lett. **49**, 1895.

93. de Gennes, P.G., 1979a, *Scaling concepts in polymer physics* (Cornell University Press, Ithaca, NY).

94. de Gennes, P.G., 1979b, *Incoherent scattering near a sol gel transition.* J. Physique Lett. **40**, L198.

95. de Gennes, P.G., P. Lafore and J. Millot, 1959, *Amas accidentels dan les solutions solides désordonnées.* J. Phys. Chem. Sol. **11**, 105.

96. Golden, K., and G.C. Papanicolaou, 1983, *Bounds for effective parameters of heterogeneous media by analytic continuation.* J. Math. Phys. **90**, 473.

97. Good, I.J., 1941, *The fractional dimensional theory of continuous fractions.* Proc. Camb. Phil. Soc. **37**, 199.

98. Gouyet, J.-F., M. Rosso, and B. Sapoval, 1988, *Fractal structure of diffusion and invasion fronts in three-dimensional lattices through the gradient percolation approach.* Phys. Rev. **B 37**, 1832.

99. Grassberger, P., 1983a, *On the critical behavior of the general epidemic processes and dynamical percolation.* Math. Biosci. **62**, 157.

100. Grassberger, P., 1983b, *Generalized dimensions of strange attractors.* Phys. Lett. **A 97**, 227.

101. Grassberger, P., 1985, *On the spreading of two-dimensional percolation.* J. Phys. **A 18**, L215.

102. Grassberger, P., 1986a, *Spreading of percolation in three and four dimensions.* J. Phys. **A 19**, 1681.

103. Grassberger, P., 1986b *On the hull of two-dimensional percolation clusters.* J. Phys. **A 19**, 2675.

104. Grassberger, P., and I. Procaccia, 1983, *Measuring the strangeness of strange attractors.* Physica **D 9**, 189.

105. Grossman, T., and A. Aharony, 1986, *Structure and perimeters of percolation clusters.* J. Phys. **A 19**, L745.

106. Grossman, T., and A. Aharony, 1987, *Accessible external perimeters of percolation clusters.* J. Phys. **A 20**, L1193.

107. Gruzinov, A.V., 1991, *Percolational diffusion of a Larmor radius.* Kurchatov Report # IAE-5331/6, Moscow.

108. Gruzinov, A.V., M.B. Isichenko, and J. Kalda, 1990, *Two-dimensional turbulent diffusion.* Zh. Eksp. Teor. Fiz. **97**, 476 [Sov. Phys. JETP **70**, 263 (1990)].

109. Gurevich, M.I., E.Z. Meilikhov, O.V. Telkovskaya, and V.V. Yankov, 1988, *A computation of the voltage–current characteristics of three-dimensional Josephson contact networks with random parameters.* Sverkhprovodimost: Fizika, Khimiya, Tekhnika (Superconductivity: Physics, Chemistry, Engineering) **4**, 80 [In Russian].

110. Haken, H., 1977, *Cooperative phenomena in systems far from thermal equilibrium and in nonphysical systems.* Rev. Mod. Phys. **47**, 67.

111. Halperin, B.I., S. Feng, and P.N. Sen, 1985, *Difference between lattice and continuum percolation transport exponents.* Phys. Rev. Lett. **54**, 2391.

112. Halperin, B.I., and M. Lax, 1966, *Impurity-band tails in the high-density limit. I. Minimum counting methods.* Phys. Rev. **148**, 722.

113. Halsey, T.C., M.H. Jensen, L.P. Kadanoff, I. Procaccia, and B.I. Shraiman, 1986, *Fractal measures and their singularities: the characterization of strange sets.* Phys. Rev. **A 33**, 1141.

114. Hans, J.W., and K.W. Kehr, 1987, *Diffusion in regular and disordered lattices.* Phys. Rep. **150**, 263.

115. Harris, A.B., 1974, *Effect of random defects on the critical behavior of Ising models.* J. Phys. **C 7**, 1671.

116. Harris, A.B., 1983, *Field-theoretic approach to biconnectedness in percolating systems.* Phys. Rev. **B 28**, 2614.

117. Harris, A.B., 1987, *Resistance correlations in random structures.* Phil. Mag. **B 56**, 833.

118. Hausdorff, F., 1918, *Dimension und äußeres Maß.* Math. Annalen **79**, 157.

119. Hasegawa, A., C.G. Maclennan, and Y. Kodama, 1979, *Nonlinear behavior and turbulence spectra of drift waves and Rossby waves.* Phys. Fluids **22**, 2122.

120. Hasegawa, A., and K. Mima, 1978, *Pseudo-three-dimensional turbulence in magnetized nonuniform plasma.* Phys. Fluids **21**, 87.

121. Hashin, Z., and S. Shtrikman, 1963, *Conductivity of polycrystals.* Phys. Rev. **130**, 129.

122. Havlin, S., and D. Ben-Avraham, 1987, *Diffusion in disordered media.* Adv. Phys. **36**, 695.

123. Heermann, D.W., and D. Stauffer, 1981, *Phase diagram for three-dimensional correlated site-bond percolation.* Z. Phys. **44B**, 339.

124. Hentschel, H.G.E., and I. Procaccia, 1983a, *Fractal nature of turbulence as manifested in turbulent diffusion.* Phys. Rev. **A 27**, 1266.

125. Hentschel, H.G.E., and I. Procaccia, 1983b, *The infinite number of generalized dimensions of fractals and strange attractors.* Physica **D 8**, 435.

126. Herring, C., 1960, *Effect of random inhomogeneities on electrical and galvanomagnetic measurements.* J. Appl. Phys. **31**, 1939.

127. Herrmann, H.J., D.C. Hong, and H.E. Stanley, 1984, *Backbone and elastic backbone of percolation clusters obtained by the new method of 'burning.'* J. Phys. **A 17**, L261.

128. Herrmann, H.J., and H.E. Stanley, 1984, *Building blocks of percolation.* Phys. Rev. Lett. **53**, 1121.

129. Horton, W., 1989, *Drift wave vortices and anomalous transport.* Phys. Fluids **B 1**, 524.

130. Horton, W., 1990, *Nonlinear drift waves and transport in magnetized plasmas.* Phys. Rep. **192**, 1.

131. Hoshen, J., R. Kopelman, and E.M. Monberg, 1978, *Percolation and critical distribution II. Layers, variable range interactions, and exciton cluster model.* J. Stat. Phys. **19**, 219.

132. Hui, P.M., and D. Stroud, 1985, *Anomalous frequency-dependent transport in composites.* Phys. Rev. **B 32**, 7728.

133. Isichenko, M.B., 1991a, *Effective plasma heat conductivity in a "braided" magnetic field–I. Quasi-linear limit.* Plasma Phys. Contr. Fusion **33**, 795.

134. Isichenko, M.B., 1991b, *Effective plasma heat conductivity in a "braided" magnetic field–II. Percolation limit.* Plasma Phys. Contr. Fusion **33**, 809.

135. Isichenko, M.B., and W. Horton, 1991, *Scaling laws of stochastic* $\mathbf{E} \times \mathbf{B}$ *plasma transport.* Comments on Plasma Phys. Contr. Fusion, in press.

136. Isichenko, M.B., and J. Kalda, 1991a, *Anomalous resistance of randomly inhomogeneous media with Hall effect.* Zh. Eksp. Teor. Fiz. **91**, 224 [Sov. Phys. JETP (1991)].

137. Isichenko, M.B., and J. Kalda, 1991b, *Statistical topography I. Fractal dimension of coastlines and number-area rule for islands.* J. Nonlinear Science **1**(3).

138. Isichenko, M.B., and J. Kalda, 1991c, *Statistical topography II. 2D transport of a passive scalar.* J. Nonlinear Science **1**(4).

139. Isichenko, M.B., and J. Kalda, 1992, *Geometrical effects in magnetoresistance.* J. Moscow Phys. Soc., No. 1.

140. Isichenko, M.B., J. Kalda, E.B. Tatarinova, O.V. Telkovskaya, and V.V. Yankov, 1989, *Diffusion in a medium with vortex flow.* Zh. Eksp. Teor. Fiz. **96**, 913 [Sov. Phys. JETP **69**, 517 (1989)].

141. Ising, E., 1925, *Beitrag zur Theorie des Ferromagnetismus.* Z. Phys. **31**, 252.

142. Jensen, M.H., L.P. Kadanoff, A. Lichaber, I. Procaccia, and I. Stavans, 1985, *Global universality at the onset of chaos: results of a forced Rayleigh-Bénard experiment.* Phys. Rev. Lett. **55**, 2798.

143. Jensen, M.H., G. Paladin, and A. Vulpiani, 1991, *Multiscaling in multifractals.* Phys. Rev. Lett. **67**, 208 (1991).

144. Kac, V.G., 1979, *Contravariant form for infinite-demensional Lie algebras and super-algebras.* Lecture Notes in Physics **94**, 441 (Springer, Berlin).

145. Kadanoff, L.P., 1978, *Lattice Coulomb gas representation of two-dimensional problems.* J. Phys. **A 11**, 1399.

146. Kadomtsev, B.B., and O.P. Pogutse, 1979, *Electron heat conductivity of the plasma across a "braided" magnetic field.* In *Plasma Physics and Controlled Nuclear Fusion Research,* Proc. 7th Int. Conf., Innsbruck, 1978 (IAEA, Vienna), vol. I, p. 649.

147. Kalda, J., 1991, *On transport of a passive scalar in 2D turbulent flow*, to be published.

148. Kalugin, P.A., A.Yu. Kitaev, and L.S. Levitov, 1985, *$Al_{0.86}Mn_{0.14}$: A six-dimensional crystal.* Pis'ma v Zh. Eksp. Teor. Fiz. **41**, 119 [JETP Lett. **41**, 148 (1985)].

149. Kalugin, P.A., A.V. Sokol, and E.B. Tatarinova, 1990, *Analytical properties of the effective-diffusion coefficient in periodic flows.* Europhys. Lett. **13**, 417.

150. Kapitulnik, A., A. Aharony, G. Deutscher, and D. Stauffer, 1984, *Self-similarity and correlations in percolation.* J. Phys. **A 16**, L269.

151. Kapitza, P.L., 1928, *The study of the specific resistance of bismuth crystals and its change in strong magnetic fields and some allied problems.* Proc. Roy. Soc. **A 119**, 358.

152. Kapitza, P.L., 1929, *The change of electrical conductivity in strong magnetic fields. Part I.–Experimental results.* Proc. Roy. Soc. **A 123**, 292.

153. Kaplan, J.L., and J.A. Yorke, 1979, *Chaotic behavior of multidimensional difference equations.* Lecture Notes in Mathematics **730**, 204 (Springer, New York).

154. Keller, J., 1964, *A theorem on the conductivity of a composite material.* J. Math. Phys. **5**, 548.

155. Keller, J., 1987, *Effective conductivity of reciprocal media.* In *Random media*, edited by G. Papanicolaou (Springer, New York), p. 183.

156. Kertész, J., 1986, *Extrapolation of transfer matrix data for percolation and lattice animals by the Romberg-Beleznay algorithm.* J. Phys. **A 19**, 599.

157. Kertész, J., B.K. Chakrabarti, and J.A.M.S. Duarte, 1982, *Threshold and scaling in percolation with restricted valence.* J. Phys. **A 15**, L13.

158. Kesten, H., 1982, *Percolation theory for mathematicians* (Birkhauser, Boston).

159. Kikuchi, R., 1970, *Concept of the long-range order in percolation problem.* J. Chem. Phys. **53**, 2713.

160. Kingsep, A.S., K.V. Chukbar, and V.V. Yankov, 1990, *Electron magnetohydrodynamics.* In *Reviews of Plasma Physics*, edited by B.B. Kadomtsev (Consultants Bureau, New York), vol. 16, p. 243.

161. Kirkpatrick, S., 1973, *Percolation and conduction.* Rev. Mod. Phys. **45**, 574.

162. von Klitzing, K., G. Dorda, and M. Pepper, 1980, *New method for high-accuracy determination of the fine-structure constant based on quantized Hall resistance.* Phys. Rev. Lett. **45**, 494.

163. Koch, D.L., and J.F. Brady,, 1989, *Anomalous diffusion due to long-range velocity fluctuations in the absence of a mean flow.* Phys. Fluids **A 1**, 47.

164. Kolmogorov, A.N., 1941, *Local structure of turbulence in an incompressible viscous fluid at very high Reynolds numbers.* Dokl. Akad. Nauk SSSR **30**, 299 [in Russian]. Reprinted in Usp. Fiz. Nauk **93**, 476 (1967) [Sov. Phys. Usp. **10**, 734 (1968)].

165. Kolmogorov, A.N., 1958, *A new invariant for transitive dynamical systems.* Dokl. Akad. Nauk SSSR **119**, 861 [in Russian].

166. Korčak, J., 1938, *Deux types fondamentaux de distribution statistique.* Bulletin de l'Institut International de Statistique **111**, 295.

167. Kraichnan, R.H., 1970, *Diffusion by a random velocity field.* Phys. Fluids **13**, 22.

168. Kraichnan, R.H., and D. Montgomery, 1980, *Two-dimensional turbulence.* Rep. Prog. Phys. **43**, 547.

169. Kravtsov, V.E., I.V. Lerner, and V.I. Yudson, 1986, *Classical diffusion in media with weak disorder.* Zh. Eksp. Teor. Fiz. **91**, 569 [Sov. Phys. JETP **64**, 336 (1986)].

170. Krommes, J.A., 1978, *Plasma transport in stochastic magnetic fields. II. Principles and problems of test electron transport.* Prog. Theoret. Phys. Suppl. **64**, 137.

171. Krommes, J.A., C. Oberman, and R.G. Kleva, 1983, *Plasma transport in stochastic magnetic fields. Part 3. Kinetics of test particle diffusion.* J. Plasma Phys. **30**, 11.

172. Laidlaw, D., J. MacKay, and N. Jan, 1987, *Some fractal properties of percolating backbone in two dimensions.* J. Stat. Phys. **46**, 507.

173. Landauer, R., 1978, *Electrical conductivity of inhomogeneous media.* In *Electrical transport and optical properties of inhomogeneous media*, edited by J.C. Garland and D.B. Tanner, (AIP, New York), p. 2.

174. Larichev, V.D., and G.M. Reznik, 1976, *On two-dimensional solitary Rossby waves.* Dokl. Akad. Nauk SSSR **231**, 1077 [in Russian].

175. Larsson, T.A., 1987, *Possibly exact fractal dimensions from conformal invariance.* J. Phys. **A 20**, L291.

176. Laughlin, R.B., 1981, *Quantized Hall conductivity in two dimensions.* Phys. Rev. **B 23**, 5632.

177. Lee, S.B., 1990, *Universality of continuum percolation.* Phys. Rev. **B 42**, 4877.

178. Levine, I.D., and S. Sarbach, 1985, *Theory of tricritical points.* In *Phase transitions and critical phenomena,* edited by C. Domb, M.S. Green, and J.L. Lebowitz, (Academic, London), vol. 9.

179. Levine, D., and P. Steinhardt, 1984, *Quasicrystals: A new class of ordered structures.* Phys. Rev. Lett. **53**, 2477.

180. Li, P.S., and W. Strieder, 1982, *Critical exponents for conduction in a honeycomb random site lattice.* J. Phys. **C 15**, L1235.

181. Lichtenberg, A., and M. Lieberman, 1983, *Regular and stochastic motion* (Springer, New York).

182. Lifshitz, E.M., and L.P. Pitaevskii, 1981, *Physical kinetics* (Pergamon, New York).

183. Longuet-Higgins, M.S., 1957a, *The statistical analysis of a random, moving surface.* Phil. Trans. Roy. Soc. (London) **A 249**, 321.

184. Longuet-Higgins, M.S., 1957b, *Statistical properties of an isotropic random surface.* Phil. Trans. Roy. Soc. (London) **A 250**, 157.

185. Longuet-Higgins, M.S., 1957c, *On the velocity of the maxima in a moving wave-form.* Proc. Camb. Phil. Soc. **52**, 230.

186. Longuet-Higgins, M.S., 1957d, *Statistical properties of a moving wave-form.* Proc. Camb. Phil. Soc. **52**, 234.

187. Longuet-Higgins, M.S., 1960a, *Reflection and refraction at a random moving surface. I. Pattern and paths of specular points.* J. Opt. Soc. Am. **50**, 838.

188. Longuet-Higgins, M.S., 1960b, *Reflection and refraction at a random moving surface. II. Number of specular points in a Gaussian surface.* J. Opt. Soc. Am. **50**, 845.

189. Longuet-Higgins, M.S., 1960c, *Reflection and refraction at a random moving surface. III. Frequency of twinkling in a Gaussian surface.* J. Opt. Soc. Am. **50**, 851.

190. Lorenz, E.N., 1963, *Deterministic nonperiodic flow.* J. Atmos. Sci. **20**, 130.

191. Lubensky, T.C., and A.M.J. Tremblay, 1986, *ε-expansion of transport exponents of continuum percolating systems.* Phys. Rev. **B34**, 3408.

192. Ma, S.-K., 1976, *Modern theory of critical phenomena* (Benjamin, London).

193. Machta, J., R.A. Guyer, and S.M. Moore, 1986, *Conductivity in percolation networks with broad distributions of resistances.* Phys. Rev. **B 33**, 4818.

194. MacKay, G., and N. Jan, 1984, *Forest fires as critical phenomena.* J. Phys. **A 17**, L757.

195. Mandelbrot, B.B., 1967, *How long is the coast of Britain? Statistical self-similarity and fractional dimension.* Science **155**, 636.

196. Mandelbrot, B.B., 1975a, *Les objects fractal: forme, hasarde et dimension* (Flammarion, Paris).

197. Mandelbrot, B.B., 1975b, *Stochastic models for the Earth's relief, the shape and the fractal dimension of the coastlines, and the number-area rule for islands.* Proc. Natl. Acad. Sci. (USA) **72**, 3825.

198. Mandelbrot, B.B., 1975c, *On the geometry of homogeneous turbulence, with stress on the fractal dimension of the iso-sets of scalars.* J. Fluid. Mech. **72**, 401.

199. Mandelbrot, B.B., 1977, *Fractals: form, chance, and dimension* (Freeman, San Francisco).

200. Mandelbrot, B.B., 1982, 1983, *The fractal geometry of nature* (Freeman, San Francisco).

201. Mandelbrot, B.B., 1984, *Fractals in physics: squig clusters, diffusions, fractal measures, and the unicity of fractal dimensionality.* J. Stat. Phys. **34**, 895.

202. Mandelbrot, B.B., 1985, *Self-affine fractals and fractal dimension.* Phys. Scr. **32**, 257 (1985).

203. Mandelbrot, B.B., and J.A. Given, 1984, *Physical properties of a new fractal model of percolation clusters.* Phys. Rev. Lett. **52**, 1853.

204. Mandelbrot, B.B., and J.W. Van Ness, 1968, *Fractional Brownian motion, fractional noises and applications.* SIAM Review **10**, 422.

205. Margolina, A., H.J. Herrmann, and D. Stauffer, 1982, *Size of largest and second largest cluster in random percolation.* Phys. Lett. **93A**, 73.

206. Martin, J.L., 1974, *Computer techniques for evaluating lattice constants.* In *Phase transitions and critical phenomena,* edited by C. Domb, M.S. Green, and J.L. Lebowitz (Academic, London), vol. 3, p. 97.

207. Maxwell, J.C., 1873, *A treatise on electricity and magnetism* (Reprint: Dover, New York, 1954).

208. McLaughlin, D., G.C. Papanicolaou, and O. Pironneau, 1985, *Convection of microstructure and related problems.* SIAM J. Appl. Math. **45**, 780.

209. Meakin, P., and F. Family, 1986, *Diverging length scales in diffusion-limited aggregation.* Phys. Rev. **A 34**, 2558.

210. Milton, G.W., 1982, *Bounds on the complex permittivity of a two-component composite material.* J. Appl. Phys. **52**, 5286.

211. Mitescu, C.D., M. Allain, E. Guyon, and J.P. Clerc, 1982, *Electrical conductivity of finite-size percolation networks.* J. Phys. **A 15**, 2523.

212. Moffatt, H.K., 1981, *Some developments in the theory of turbulence.* J. Fluid Mech. **106**, 27.

213. Moffatt, H.K., 1983, *Transport effects associated with turbulence with particular attention to the influence of helicity.* Rep. Prog. Phys. **46**, 621.

214. Monin, A.S., and A.M. Yaglom, 1971, 1975, *Statistical fluid mechanics of turbulence* (MIT Press, Cambridge), vols. I and II.

215. Mori, H., 1980, *Fractal dimensions of chaotic flows of autonomous dissipative systems.* Prog. Theor. Phys. **63**, 1044.

216. Murat, M., S. Marianer, and D.J. Bergman, 1986, *A transfer matrix study of conductivity and permeability exponents in continuum percolation.* J. Phys. **A 19**, L275.

217. Nagatani, T., 1986, *A monte Carlo renormalization approach to fractal dimensions of infinite clusters, backbone, and cutting bonds for percolation.* J. Phys. **A 19**, L275.

218. Newman, C.M., and L.S. Schulman, 1981, *Number and density of percolation clusters.* J. Phys. **A 14**, 1735.

219. Nienhuis, B., 1982, *Exact critical point and critical exponents of $O(n)$ models in two dimensions.* Phys. Rev. Lett. **49**, 1062.

220. Nienhuis, B., 1984, *Critical behavior of two-dimensional spin models and charge assymetry in the Coulomb gas.* J. Stat. Phys. **34**, 731.

221. Nienhuis, B., A.N. Berker, E.K. Riedel, and M. Schick, 1979, *First- and second-order phase transitions in Potts models: Renormalization-group solutions.* Phys. Rev. Lett. **43**, 737.

222. den Nijs, M.P.M., 1979, *A relation between the temperature exponents of the eight-vertex and q-state Potts model.* J. Phys. **A12**, 1857.

223. Nycander. J., and M.B. Isichenko, 1990, *Motion of dipole vortices in a weakly inhomogeneous medium and related convective transport.* Phys. Fluids **B 2**, 2042.

224. Obukhov, A.M., 1941, *On the distribution of energy in the spectrum of turbulent flow.* Izv. Akad. Nauk SSSR Ser. Geogr. Geofiz. **5**, 453 [C.R. Acad. Sci. U.R.S.S. **32**, 19 (1941)].

225. Onizuka, K., 1975, *Computer experiment on a 3D site percolation model of porous material – its connectivity and conductivity.* J. Phys. Soc. Japan **39**, 527.

226. Onsager, L., 1944, *Crystal statistics. I. A two-dimensional model with an order-disorder transition.* Phys. Rev. **65**, 117.

227. Orbach, R., 1984, *Percolation, fractals, and anomalous diffusion.* J. Stat. Phys. **34**, 931.

228. Osborne, A.R., and R. Caponio, 1990, *Fractal trajectories and anomalous diffusion for chaotic particle motions in 2D turbulence.* Phys. Rev. Lett. **64**, 1733.

229. Osborne, A.R., A.D. Kirwan, Jr., A. Provenzale, and L. Bergamasco, 1986, *A search for chaotic behavior in large and mesoscale motions in the Pacific Ocean.* Physica **D 23**, 75.

230. O'Shaughnessy, B., and I. Procaccia, 1985a, *Analytical solutions for diffusion on fractal sets.* Phys. Rev. Lett. **54**, 455.

231. O'Shaughnessy, B., and I. Procaccia, 1985b, *Diffusion on fractas.* Phys. Rev.**A 32**, 3073.

232. Osipenko, M.V., O.P. Pogutse, and N.V.Chudin, 1987, *Plasma diffusion in an array of vortices.* Fiz. Plazmy **13**, 953 [Sov. J. Plasma Phys. **13**, 550 (1987)].

233. Ott, E. and T.M. Antonsen, 1988, *Chaotic fluid convection and the fractal nature of passive scalar gradients.* Phys. Rev. Lett. **61**, 2839.

234. Ottaviani, M., 1991, private communication.

235. Paladin, G., and A. Vulpiani, 1987, *Anomalous scaling laws in multifractal objects.* Phys. Rep. **156**, 147.

236. Pearson, R.B., 1980, *Conjecture for the extended Potts model magnetic eigenvalue.* Phys. Rev. **B 22**, 2579.

237. Peitgen, H.-O., and D. Saupe, 1988, Eds. *The science of fractal images* (Springer, Berlin).

238. Penrose, O., J.L. Lebowitz, J. Marro, M.H. Kalos, and A. Sur, 1978, *Growth of clusters in a first-order phase transition.* J. Stat. Phys. **19**, 243.

239. Perkins, F.W., and E.G. Zweibel, 1987, *A high magnetic Reynolds number dynamo.* Phys. Fluids **30**, 1079.

240. Pettini, M., A. Vulpiani, J.H. Misguich, M. De Leener, J. Orban, and R. Balescu, 1988, *Chaotic diffusion across a magnetic field in a model of electrostatic turbulent plasma.* Phys. Rev. **A 38**, 344.

241. Petviashvili, V.I., and V.V. Yankov, 1989, *Solitons and turbulence.* In *Reviews of plasma physics*, edited by B.B. Kadomtsev (Consultants Bureau, New York), vol. 14, p. 1.

242. Pietronero, L., and E. Tosatti, 1986, Eds. *Fractals in physics*, (North-Holland, Amsterdam).

243. Pike, G.E., and C.H. Seager, 1974, *Percolation and conductivity: A computer study, I.* Phys. Rev. **B 10**, 1421.

244. Pike, R., and H.E. Stanley, 1981, *Order propagation near the percolation threshold.* J. Phys. **A 14**, L169.

245. Pippard, A.B., 1989, *Magnetoresistance in metals* (Cambridge University Press, New York).

246. Polyakov, A.M., 1970, *Conformal symmetry of critical fluctuations.* Pis'ma v Zh. Eksp. Teor. Fis. **12**, 538 [JETP Lett. **12**, 381 (1970)].

247. Pomeau, Y., A. Pumir, and W.R. Young, 1988, *Transitoires dans l'advection-diffusion d'impuretes.* C. R. Acad. Sci. (Paris) **306 II**, 741.

248. Poston, T., and I. Stewart, 1978, *Catastrophe theory and its applications* (Pitman, London).

249. Potts, R.B., 1952, *Some generalized order-disorder transformations.* Proc. Cambridge Philos. Soc. **48**, 106.

250. Prange, R.E., and S.M. Girvin, 1990, Eds. *The quantum Hall effect* (Springer, New York).

251. Procaccia, I., 1984, *Fractal structures in turbulence.* J. Stat. Phys.**36**, 649.

252. Quinn, G.P., G.H. Bishop, and R.J. Harrison, 1976, *On the cluster size distribution for critical percolation.* J. Phys. **A 9**, L9.

253. Rammal, R., 1984, *Random walk statistics on fractal structures.* J. Stat. Phys. **34**, 547.

254. Ramshankar, R., D. Berlin, and J.P. Gollub, 1990, *Transport by capillary waves. Part I. Particle trajectories.* Phys. Fluids **A 2**, 1955.

255. Ramshankar, R., and J.P. Gollub, 1991, *Transport by capillary waves. Part II. Scalar dispersion and structure of the concentration field.* Phys. Fluids **A 3**, 1344.

256. Rechester, A.B., and M.N. Rosenbluth, 1978, *Electron heat transport in a tokamak with destroyed magnetic surfaces.* Phys. Rev. Lett. **40**, 38.

257. Rechester, A.B., M.N. Rosenbluth, and R.B. White, 1979, *Calculation of the Kolmogorov entropy for motion along a stochastic magnetic field.* Phys. Rev. Lett. **42**, 1247.

258. Reich, G.R., and P.L. Leath, 1978, *The ramification of large clusters near percolation threshold.* J. Phys. **C 11**, 1155.

259. Rendell, R.W., and S.M. Girvin, 1981, *Hall voltage dependence on inversion-layer geometry in the quantum Hall-effect regime.* Phys. Rev. **B 23**, 6610.

260. Rice, S.D., 1944, 1945, *Mathematical analysis of random noise.* Bell System Tech. J. **23**, 282 (1944); 24, 46 (1945).

261. Richardson, L.F., 1926, *Atmospheric diffusion shown on a distance-neighbour graph.* Proc. R. Soc. London, Ser. A **110**, 709.

262. Rosenbluth, M.N., H.L. Berk, I. Doxas, and W. Horton, 1987, *Effective diffusion in laminar convective flows.* Phys. Fluids **30**, 2636.

263. Rosenbluth, M.N., R.Z. Sagdeev, J.B. Taylor, and G.M. Zaslavsky, 1966, *Destruction of magnetic surfaces by magnetic field irregularities.* Nucl. Fusion **6**, 297.

264. Ross, B., 1975, Ed. *Fractional calculus and its applications.* Lecture Notes in Mathematics, No. 457 (Springer, Berlin).

265. Rose, H.A., and P.-L. Sulem, 1978, *Fully developed turbulence and statistical mechanics.* J. Physique **39**, 441.

266. Ruelle, D., and F. Takens, 1971, *On the nature of turbulence.* Comm. Math. Phys. **20**, 167.

267. Safran, S.A., I. Webman, and G.S. Grest, 1985, *Percolation in interacting colloids.* Phys. Rev. **A 32**, 506.

268. Sagdeev, R.Z., D.A. Usikov, and G.M. Zaslavsky, 1988, *Nonlinear physics* (Harwood, New York).

269. Saleur, H., 1987, *Conformal invariance for polymers and percolation.* J. Phys. **A 20**, 457.

270. Saleur, H., and B. Duplantier, 1987, *Exact determination of the percolation hull exponent in two dimensions.* Phys. Rev. Lett. **58**, 2325.

271. Sapoval, B., M. Rosso, and J.F. Gouyet, 1985, *The fractal nature of a diffusion front and the relation to percolation.* J. Phys. Lett. **46**, L149.

272. Scher, H., and R. Zallen, 1970, *Critical density in percolation processes.* J. Chem. Phys. **53**, 3759.

273. Schulgasser, K., 1976, *On a phase interchange relationship for composite materials.* J. Math. Phys. **17**, 378.

274. Schulgasser, K., 1882, *Sphere assemblage model for polycrystals and symmetric materials.* J. Appl. Phys. **54**, 1380.

275. Seager, C.H., and G.E. Pike, 1974, *Percolation and conductivity: A computer study. II.* Phys. Rev. **B 10**, 1435.

276. Sen, P.N., J.N. Roberts, and B.I. Halperin, 1984, *Nonuniversal critical exponents for transport in percolating systems with a distribution of bond strengths.* Phys. Rev. **B 32**, 3306.

277. Shante, V.K.S., and S. Kirkpatrick, 1971, *An introduction to percolation theory.* Adv. Phys. **20**, 325.

278. Shklovskii, B.I., and A.L. Efros, 1984, *Electronic properties of doped semiconductors* (Springer, New York).

279. Shlesinger, M.F., B.J. West, and J. Klafter, 1987, *Lévi dynamics of enhanced diffusion: Application to turbulence.* Phys. Rev. Lett. **58**, 1100.

280. Shraiman, B., 1987, *Diffusive transport in a Rayleigh-Bénard convection cell.* Phys. Rev. **A 36**, 261.

281. Skal, A.S., and B.I. Shklovskii, 1973, *Influence of impurity concentration on the hopping conduction in semiconductors.* Fiz. Tekhn. Poluprov. **7**, 1589 [Sov. Phys. Semicond. **7**, 1058 (1973)].

282. Skal, A.S., and B.I. Shklovskii, 1974, *Topology of an infinite cluster in the theory of percolation and its relation to the theory of hopping conduction.* Fiz. Tekhn. Poluprov. **8**, 1586 [Sov. Phys. Semicond. **8**, 1029 (1975)].

283. Skal, A.S., B.I. Shklovskii, and A.L. Efros, 1973, *Percolation level in a three-dimensional random potential.* Pis'ma v. Zh. Eksp. Teor. Fiz. **17**, 522 [JETP Lett. **17**, 377 (1973)].

284. Smith, L.N., and C.J. Lobb, 1979, *Percolation in two-dimensional conductor-insulator networks with controllable anisotropy.* Phys. Rev. **B 20**, 3653.

285. Sokolov, I.M., 1986, *Dimensionalities and other geometric critical exponents in percolation theory.* Usp. Fiz. Nauk **150**, 221 [Sov. Phys. Usp. **29**, 924 (1986)].

286. Solomon, T.H., and J.P. Gollub, 1988, *Passive transport in steady Rayleigh-Bénard convection.* Phys. Fluids **31**, 1372.

287. Soward, A.M., 1987, *Fast dynamo action in a steady flow.* J. Fluid Mech. **180**, 267.

288. Sreenivasan, K.R., and C. Meneveau, 1986 *The fractal facets of turbulence.* Physica **D 38**, 322.

289. Sreenivasan, K.R., and R.R. Prasad, 1989, *New results on the fractal and multifractal structure of the large Schmidt number passive scalars in fully turbulent flows.* Physica **D 38**, 322.

290. Sreenivasan, K.R., R. Ramshankar, and C. Meneveau, 1989, *Mixing, entrainment, and fractal dimensions of surfaces in turbulent flows.* Proc. Roy. Soc. London **A 421**, 79.

291. Stachowiak, H., 1978, *Calculation of the magnetoresistance of polycrystalline metals.* In *Electrical transport and optical properties of inhomogeneous media*, edited by J.C. Garland and D.B. Tanner (AIP, New York), p. 156.

292. Stanley, H.E., 1968, *Dependence of critical properties on dimensionality of spins.* Phys. Rev. Lett. **20**, 589.

293. Stanley, H.E., 1977, *Cluster shapes at the percolation threshold: an effective cluster dimensionality and its connection with critical-point exponents.* J. Phys. **A 10**, L211.

294. Stanley, H.E., 1984, *Application of fractal concepts to polymer statistics and to anomalous transport in randomly porous media.* J. Stat. Phys. **34**, 843.

295. Stanley, H.E., and N. Ostrowsky, 1986, Eds. *On growth and form* (Martinus Nijhoff).

296. Stauffer, D., 1979, *Scaling theory of percolation clusters.* Phys. Rep. **54**, 2.

297. Stauffer, D., 1985, *Introduction to percolation theory* (Taylor and Francis, London).

298. Steinhardt, P., and S. Ostlund, 1987, Eds. *The physics of quasicrystals* (World Scientific, Singapore).

299. Stiassnie, M., Y. Agnon, and L. Shemer, 1991, *Fractal dimensions of random water surfaces.* Physica **D 47**, 341.

300. Straley, J.P., 1977, *Critical exponents for the conductivity of random resistor lattices.* Phys. Rev. **B 15**, 5733.

301. Strenski, P.N., R.M. Bradley, and J.-M. Debierre, 1991, *Scaling behavior of percolation surfaces in three dimensions.* Phys. Rev. Lett. **66**, 1330.

302. Suzuki, M., 1983, *Phase transition and fractals.* Prog. Theor. Phys. **69**, 65.

303. Schwägerl, M., and J. Krug, 1991, *Subdiffusive transport in stochastic webs.* Physica **D 52**, 143.

304. Swerling, P., 1962, *Statistical properties of the contours of random surfaces.* IRE Trans. Information Theory **IT-8**, 315.

305. Swinney, H., and W.Y. Tam, 1987, *Mass transport in turbulent Couette-Taylor flow.* Phys. Rev. **A 36**, 1374.

306. Sykes, M.F., and J.W. Essam, 1963, *Some exact critical percolation probabilities for bond and site problems in two dimensions.* Phys. Rev. Lett. **10**, 3.

307. Sykes, M.F., and J.W. Essam, 1964a, *Critical probabilities by series methods.* Phys. Rev. **A 133**, 310.

308. Sykes, M.F., and J.W. Essam, 1964b, *Exact critical percolation probabilities for site and bond problems in two dimensions.* J. Math. Phys. **5**, 1117.

309. Sykes, M.F., and M. Glen, 1976, *Percolation process in two dimensions I. Low-density series expansion.* J. Phys. **A 9**, 87.

310. Sykes, M.F., D.S. Gaunt, and M. Glen, 1976a, *Percolation process in two dimensions II. Critical concentrations and the mean size index.* J. Phys. **A 9**, 97.

311. Sykes, M.F., D.S. Gaunt, and M. Glen, 1976b, *Percolation process in two dimensions III. High density series expansions.* J. Phys. **A 9**, 715.

312. Sykes, M.F., D.S. Gaunt, and M. Glen, 1976c, *Percolation process in two dimensions IV. Percolation probability.* J. Phys. **A 9**, 725.

313. Tatarinova, E.B., 1990, unpublished.

314. Tatarinova, E.B., P.A. Kalugin, and A.V. Sokol, 1991, *What is the propagation rate of the passive component in turbulent flows limited by?* Europhys. Lett. **14**, 773.

315. Taylor, G.I., 1921, *Diffusion by continuous movements.* Proc. Lond. Math. Soc., Ser. 2, **20**, 196.

316. Taylor, G.I., 1953, *Dispersion of soluble matter in solvent flowing slowly through a tube.* Proc. R. Soc. London, Ser. A **219**, 186 (1953).

317. Taylor, G.I., 1954, *Conditions under which dispersion of solute in a stream of solvent can be used to measure molecular diffusion.* Proc. R. Soc. London, Ser. A **225**, 473.

318. Thompson, A.H., A.J. Katz, and C.E. Krohn, 1987, *The microgeometry and transport properties of sedimentary rock.* Adv. Phys. **36**, 625.

319. Thouless, D.J., 1974, *Electrons in disordered systems and the theory of localization.* Phys. Rep. **13**, 93.

320. Trugman, S.A., 1983, *Percolation, localization, and quantum Hall effect.* Phys. Rev. **B 27**, 7539.

321. Trugman, S.A., and A. Weinrib, 1985, *Percolation with a threshold at zero: A new universality class.* Phys. Rev. **B 31**, 2794.

322. Városi, F., T.M. Antonsen, and E. Ott, 1991, *The spectrum of fractal dimensions of passively convected scalar gradients in chaotic fluid flows.* Phys. Fluids **A 3**, 1017.

323. Vicsek, T., and J. Kertész, 1981, *Monte Carlo renormalization-group approach to percolation on a continuum: test of universality.* J. Phys. **A 14**, L31.

324. Voss, R.F., 1984, *The fractal dimension of percolation cluster hulls.* J. Phys. **A 17**, L373.

325. Voss, R.F., 1989, *Random fractals: self-affinity in noise, music, mountains, and clouds.* Physica **D 38**, 362.

326. Vulpiani, A., 1989, *Lagrangian chaos and small-scale structure of passive scalars.* Physica **D 38**, 372.

327. Webman, I., J. Jortner, and M.H. Cohen, 1976, *Numerical simulation of continuous percolation conductivity.* Phys. Rev. **B 14**, 4737.

328. Weinrib, A., 1982, *Percolation threshold of a two-dimensional continuum system.* Phys. Rev. **B 26**, 1352.

329. Weinrib, A., 1984, *Long-range correlated percolation.* Phys. Rev. **B 29**, 387.

330. Weinrib, A., and B.I. Halperin, 1982, *Distribution of maxima, minima, and saddle points of the intensity of laser speckle patterns.* Phys. Rev. **B 26**, 1362.

331. Weinrib, A., and B.I. Halperin, 1983, *Critical phenomena in systems with long-range correlated quenched disorder.* Phys. Rev. **B27**, 413.

332. Weinrib, A., and S. Trugman, 1985, *A new kinetic walk and percolation perimeter.* Phys. Rev. **B 31**, 2993.

333. White, R.B., 1989, *Theory of tokamak plasmas* (North-Holland, Amsterdam).

334. Wilson, K.G., 1971a, *Renormalization group and critical phenomena. I. Renormalization group and Kadanoff scaling picture.* Phys. Rev. **B 4**, 3174.

335. Wilson, K.G., 1971b, *Renormalization group and critical phenomena. II. Phase-space cell analysis of critical behavior.* Phys. Rev. **B 4**, 3184.

336. Wilson, K.G., 1975, *The renormalization group: critical phenomena and the Kondo problem.* Rev. Mod. Phys. **47**, 773.

337. Yoon, C.S., and S.-I. Lee, 1990, *Measurements of the ac conductivity and dielectric constant in a two-dimensional percolation system.* Phys. Rev. **B 42**, 4594.

338. Young, L.-S., 1982, *Dimension, entropy and Lyapunov exponents.* Ergodic Theory and Dynamical Systems **2**, 109.

339. Young, W.R., 1988, *Arrested shear dispersion and other models of anomalous diffusion.* J. Fluid Mech. **193**, 129.

340. Young, W., A. Pumir, and Y. Pomeau, 1989, *Anomalous diffusion of tracer in convection rolls.* Phys. Fluids **A 1**, 462.

341. Yushmanov, P.N., 1990, *Two-dimensional diffusion in a shear system.* Pis'ma v Zh. Eksp. Teor. Fiz. **52**, 848 (1990) [JETP Lett. **52**, 217 (1990)].

342. Yushmanov, P.N., 1991, *Neoclassical diffusion in turbulent plasmas.* Comments on Plasma Phys. Contr. Fusion, in press.

343. Zabusky, N.J., and J.C. McWilliams, 1982, *A modulated point-vortex model for geostrophic, β-plane dynamics.* Phys. Fluids **25**, 2175.

344. Zakharov, V.E., 1984, *Kolmogorov spectra of weak turbulence.* In *Basic Plasma Physics*, edited by A.A. Galeev and R.N. Sudan (North-Holland, New York), vol. II, p. 3.

345. Zallen, R., 1983, *The physics of amorphous solids* (Wiley, New York).

346. Zallen, R., and H. Scher, 1971, *Percolation on a continuum and the localization-delocalization transition in amorphous semiconductors.* Phys. Rev. **B 4**, 4471.

347. Zeilinger, A., and Svozil, 1985, *Measuring the dimension of space-time.* Phys. Rev. Lett. **54**, 2553.

348. Ziff, R.M., 1986, *Test of scaling exponents for percolation-cluster perimeters.* Phys. Rev. Lett. **56**, 545.

349. Ziff, R.M., 1989, *Hull-generating walks.* Physica **D 38**, 377.

350. Ziff, R.M., P.T. Cummings, and G. Stell, 1984, *Generation of percolation cluster perimeters by a random walk.* J. Phys. **A 17**, 3009.

351. Ziff, R.M., and B. Sapoval, 1987, *The efficient determination of the percolation threshold by a frontier-generating walk in a gradient.* J. Phys. **A 19**, L1169.

352. Ziman, J.M., 1969, *The localization of electrons in ordered and disordered systems, I. Percolation of classical particles.* J. Phys. **C 1**, 1532.

353. Ziman, J.M., 1979, *Models of disorder* (Cambridge University Press, New York).

354. Zeldovich, Ya.B., 1937, *Limiling laws for free upwelling convective flows.* Dokl. Akad. Nauk SSSR **7**, 1466 [in Russian].

355. Zeldovich, Ya.B., 1982, *Exact solution of the problem of diffusion in a periodic velocity field, and turbulent diffusion.* Dokl. Akad. Nauk SSSR **266**, 821 [Sov. Phys. Dokl. **27**, 797 (1982)].

356. Zeldovich, Ya.B., 1983, *Percolation properties of a random two-dimensional stationary magnetic field.* Pis'ma v. Zh. Eksp. Teor. Fiz. **38**, 51 [JETP Lett. **38**, 57 (1983)].

Figure captions

1. Sierpinski carpet is produced by removing from a square its central part with the size one third the square edge. Then the procedure is repeated with each of eight remaining parts, and so on *ad infinitum*. At the nth step of the procedure, it takes $N_n = 8^n$ squares of the size $\lambda_n = 3^{-n}$ to cover the remaining set, leading to the fractal dimension $D = -\log N_n / \log \lambda_n = \log_3 8$.

2. Computer-generated trail of a Brownian particle. At any resolution of the trajectory, it asymptotically covers a finite area on the plane, because the fractal dimension $D = 2$.

3. Site percolation clusters on a 2D square lattice at $p = 0.45$ (a), $p = 0.5927 = p_c$ (b), and $p = 0.7$ (c).

4. Bond percolation clusters on a 2D triangular lattice at $p = 0.25$ (a), $p = 0.3473 = p_c$ (b), and $p = 0.45$ (c).

5. Pairs of two-dimensional matching lattices, one shown by solid lines (for bonds) and filled circles (for sites) and the other by dashed lines and empty circles.
   (a) Square lattice bond problem is self-matching;
   (b) Honeycomb and triangular lattices are bond-matching;
   (c) Square bonds match triangular sites.

6. Schematic of an infinite bond cluster on a 2D square lattice. The backbone is shown in heavy, and the dangling ends in light lines. Markers denote a minimum path on the backbone.

7. Finite cluster (dashed lines), its external hull (heavy curve), and the unscreened perimeter (light curve).

8. (a) The problem of circular voids in a background 2D transport medium (the "Swiss-cheese" model). The sites of the equivalent lattice lie in the vertices of the Voronoi polyhedra (the sets of points, from which a given void center is the closest one). The edges of the polyhedra represent bonds (solid lines).

   (b) A "neck" lying between three spherical voids.

9. The problem of random sites (overlapping discs).

10. Potential continuum percolation model in two dimensions.

    (a) Undercritical level $h < h_c$;

    (b) Critical level $h = 0 = h_c$;

    (c) Overcritical level $h > h_c$;

    (d) The equivalent lattice of the potential $\psi(x, y)$. Squares and circles denote maxima and minima of ψ, respectively. The steepest descent/ascent paths, connecting the maxima and the minima, cross in the saddle points (shown by +). Bonds on the equivalent lattice connect adjacent minima and are "conducting" (shown heavy) if the corresponding saddle point lies below $h = h_c = 0$.

    To model a random potential, the quasi-periodic function $\psi(\mathbf{x}) = \sum_{i=1}^{N} \sin(\mathbf{k}_i\mathbf{x} + \theta_i)$ was taken, where $N = 25$, $\mathbf{k}_i = (\cos\alpha_i, \sin\alpha_i)$, and α_i and θ_i are random numbers uniformly distributed in $[0, 2\pi]$. The window size is 100×100 (a–c) and 45×45 (d). (Notice that this stream-function satisfies time-independent 2D Euler equation for incompressible ideal fluid: $\partial(\psi, \nabla^2\psi)/\partial(x, y) = 0$.)

11. Level lines $\psi(x, y) = h$ of the potential $\psi(x, y) = \sin x \sin y + \epsilon\psi_1(x, y)$, $\epsilon \ll 1$, $|h| \leq \epsilon$, where ψ_1 takes on independent random values with zero mean and unit variance in the unperturbed saddle points (where $\sin x \sin y = 0$). The contours of this potential represent the external and internal hulls of bond percolation clusters ($p(h) = 1/2 + h/\epsilon$) on a 2D square lattice with the sites $\{(x, y) : \sin x \sin y = -1\}$. At $h = 0$ there exists

an infinite contour corresponding to the external hull of the critical infinite cluster ($p(0) = 1/2 = p_c$).

12. The graphs of several realizations of line-to-line fractional Brownian functions (a–c).

    (a) $H = 0.3$ (antipersistent function);

    (b) $H = 0.5$ (standard Brownian function);

    (c) $H = 0.7$ (persistent function);

    (d) The graph of a stationary Gaussian random process $y = \psi(x)$, $\psi_\lambda \propto \lambda^H$ with $H = -0.2$.

    The following model function was used in all four cases: $\psi(x) = \sum_{k=1}^{1000} \psi_k \sin(kx + \theta_k)$, with $\psi_k = k^{-(H+1/2)}$, and θ_k random numbers uniformly distributed in $[0, 2\pi]$. The scaling range of these graphs is $[10^{-3}, 1]$.

13. Several realizations of fractional Brownian surfaces (a–c).

    (a) $H = 0.3$;

    (b) $H = 0.5$;

    (c) $H = 0.7$;

    (d) The graph of a stationary Gaussian random function $y = \psi(x, y)$, $\psi_\lambda \propto \lambda^H$ with $H = -0.2$.

    The vertical cross-sections of these surfaces are similar to the corresponding graphs in Fig. 12. The following model potential was used in all four cases: $\psi(x, y) =$ *F 12*
    $\sum_{k_x=1}^{100} \sum_{k_y=1}^{100} \psi_k \sin(k_x x + k_y y + \theta_k)$, with $\psi_k = (k_x^2 + k_y^2)^{-(H+1)}$, and θ_k random numbers uniformly distributed in $[0, 2\pi]$. The scaling range is $[10^{-2}, 1]$.

14. Zero-level contour lines of the surfaces shown in Fig. 13. *F 13*

15. The procedure of "contour dressing." Separatrices (self-intersecting lines) come through saddle points. Extrema (maxima and minima) are shown by circles.

16. The set of contours with linear size larger than a: the a-web.

17. (a) The set of contours with linear size between a and $2a$ consists of a-cells.
    (b) Typical a-cell.

18. (a) The set of unclosed contour lines on a tilted relief (3.51) forms a network of channels. For the simulation $\psi_0(x, y)$ was taken the same as in Fig. 10, and $\mathbf{v}_1 = 0.1\,\hat{\mathbf{x}}$. F 10
    The window size is 40×40.
    (b) Unclosed contour line of the horizontal size 200.

19. The interaction of scales in terms of the behavior of a percolating isoline of separated-scale potential (3.60).

20. Periodic system of convection rolls described by stream-function (4.26). The hatched region denotes diffusive boundary layers near the separatrices, where the tracer density gradients are localized in the high-Péclet-number limit.

21. Two types of steady Rayleigh-Bénard convection pattern: Rolls (a) and hexagons (b). Axes AA′ and BB′ of the hexagons act on streamlines as "free-slip" rigid boundaries. The hatched region shows the cross-section of a diffusive boundary layer by the plane AA′BB′. To leave the trap of these two hexagons, a tracer particle has to diffuse (radially or azimuthally) all the way across the wider (near axis) boundary layer (W).

22. Typical pattern of streamlines in a travelling dipole vortex, shown in the frame of reference moving together with the vortex. The hatched region surrounded by a separatrix (heavy line) represents the trapped fluid transported by the vortex.

23. Regimes of effective diffusion in a multiscale, steady, random 2D flow (Isichenko and Kalda, 1991c) shown in the parameter space $(H, \log P_0/\log\Lambda)$, where $P_0 = \psi_{\lambda_0}/D_0$ is the short-scale Péclet number and $\Lambda = \lambda_m/\lambda_0$ is the width of the flow spectrum.

Expression $D^* \simeq \psi_0 P_0^\alpha \Lambda^\gamma$ for the effective diffusivity includes the following exponents in regimes (A–D):

$$\begin{array}{lll} \text{(A)} & \alpha = -1/(\nu d_h + 2)\,, & \gamma = (\nu H d_h + D_h)/(\nu d_h + 2)\,; \\ \text{(B)} & \alpha = H/(D_h - 2H)\,, & \gamma = 0\,; \\ \text{(C)} & \alpha = 0\,, & \gamma = H\,; \\ \text{(D)} & \alpha = (2 - D_h/H)/(\nu d_h + 2)\,, & \gamma = (\nu H d_h + D_h)/(\nu d_h + 2)\,. \end{array}$$

Regimes (0) and (m) correspond to diffusion in monoscale flows $\psi_{\lambda_0}(\mathbf{x})$ and $\psi_{\lambda_m}(\mathbf{x})$, respectively. In the hatched region D^* is of the order of D_0.

24. The reconnection of separatrices takes place when two saddles, 1 and 2, cross the same level of the stream-function.

25. The principal morphology of an incompressible map is the liquid curve convolution of two types: "whorls" (a) and "tendrils" (b) (Berry *et al.*, 1979). Whorls are generated by velocity fields of unchanged topology and lead to asymptotically linear with time elongation of a passively advected curve. Tendrils are created by essentially time-dependent flows and lead to an exponential elongation of a liquid curve. For the simulation a stream-function was chosen of the kind shown in Fig. 10, with $N = 5$ *F 10* frozen (a) or travelling (b) waves.

26. Liquid curve elongation in a slowly time-varying 2D flow. Dashes denote separaterices, which are shown for simplicity straight and open (imagine a periodic boundary condition along the vertical direction). The curve catches slowly moving saddle points 1, 2, and 3 and is rapidly stretched in the channel between the separatrices. The exponential behavior results from intersection of separatrices causing multiple folding of the curve.

27. Streamlines of weakly-compressible flow (4.60) with $\varepsilon = 0.1$ and $\psi(x, y)$ the same as in Fig. 10. *F 10*

28. Randomly-directed shear flow with zero mean velocity.

29. Isotropic random flow of the "Manhattan grid" type is the superposition of two mutually perpendicular random shear flows.

30. Diffusion comb corresponding to a periodic array of convection rolls.

31. Diffusion tree (branches shown in heavy lines) corresponding to passive transport in a topologically complex flow. For a nondegenerate flow each separatrix divides the plane into two inner regions and one outer region, hence all branching points on the tree are Y-points.

32. Diffusion comb of a random flow looks like a "thicket." The subdiffusive propagation along the "ground" (network of mixing convection cells) stems from the delay caused by random walk in the "bushes."

33. Schematic of a polycrystal. The hatches indicate main axes of the crystallites' conductivity tensors.

34. Electric current streamlines in a strongly anisotropic polycrystal terminate in two types of traps: a focus (a) and a limit cycle (b).

35. Magnetic flux tube in a magnetic field with a 3D random component is convoluted due to the exponentiation of neighboring magnetic lines. Because of the magnetic flux conservation within the tube the exponentiation of the lines leads to exponentially decreasing thickness w of the flux tube wall.

36. Schematic of a current streamline corresponding to steady flow of electric current across the magnetic field $\mathbf{B}$ in a conducting medium with three-dimensional fluctuations.

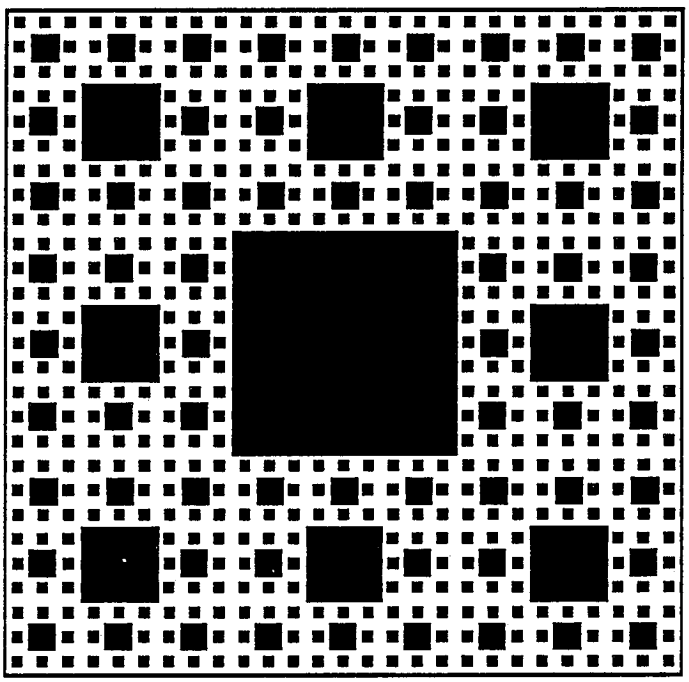

Fig. 1

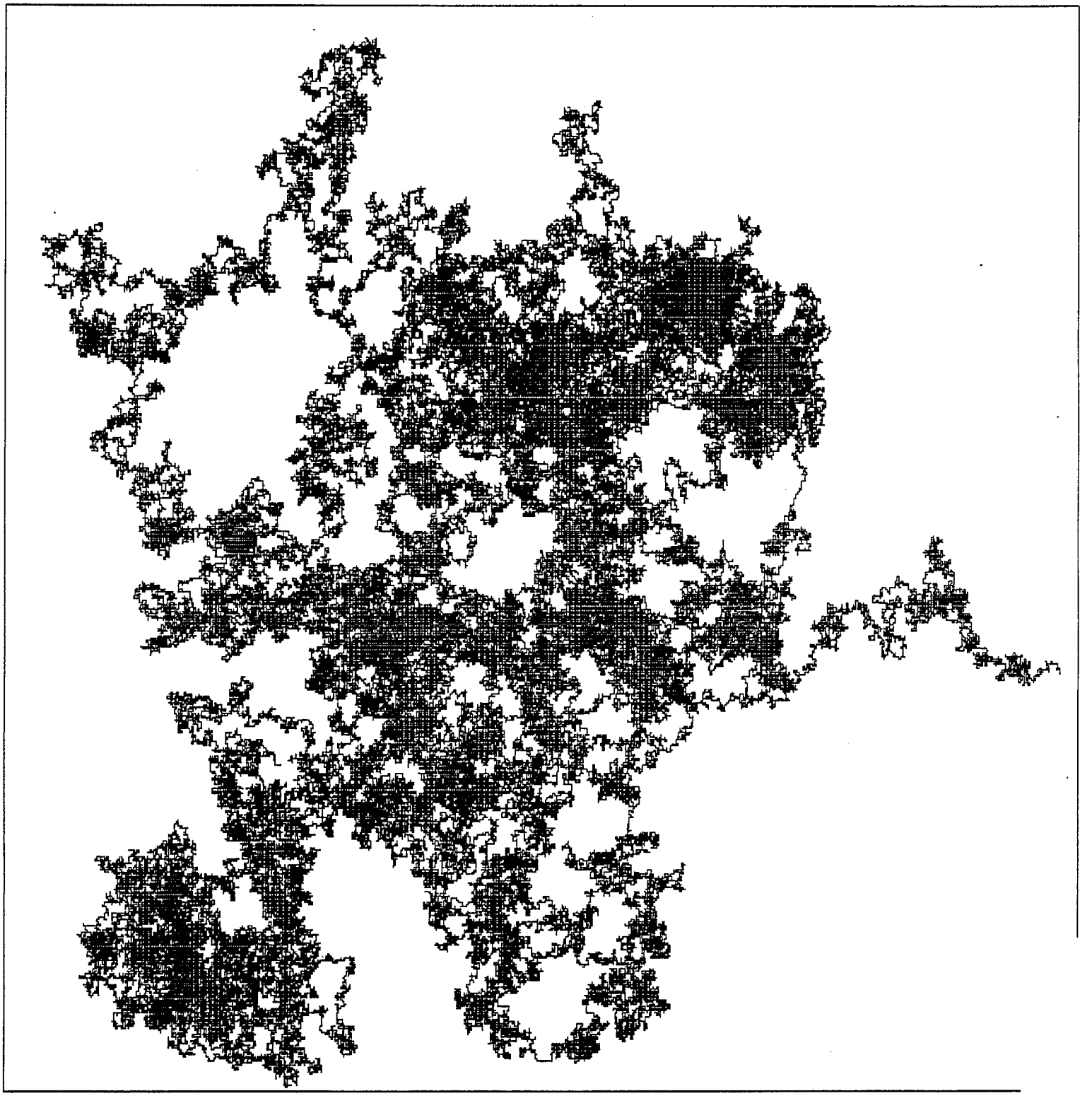

Fig. 2

a

b

c

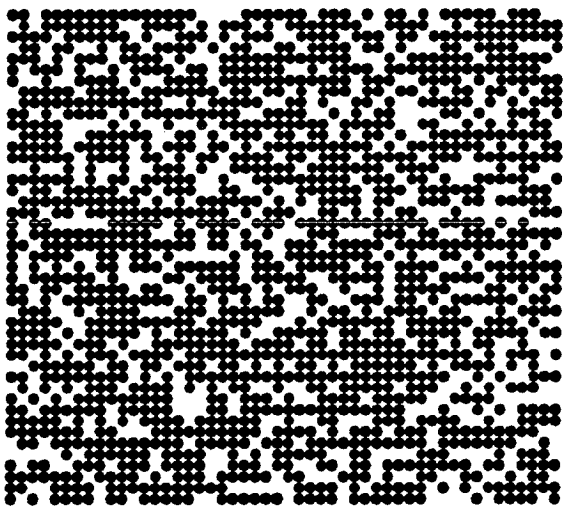

Fig. 3

a

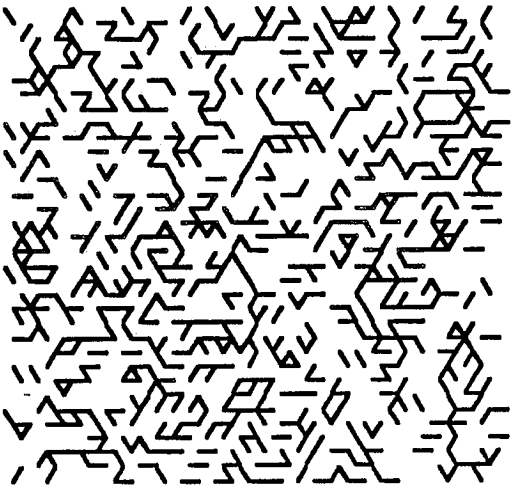

b

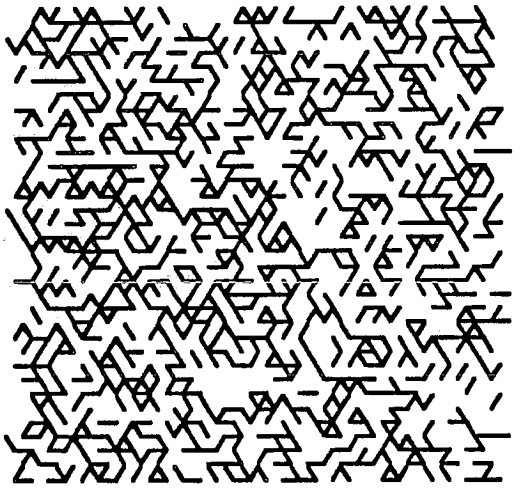

c

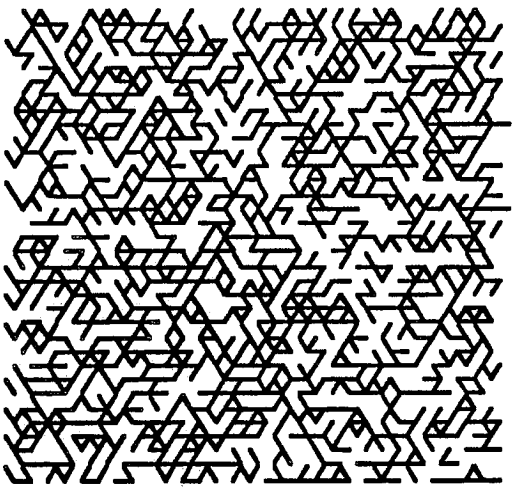

Fig. 4

a

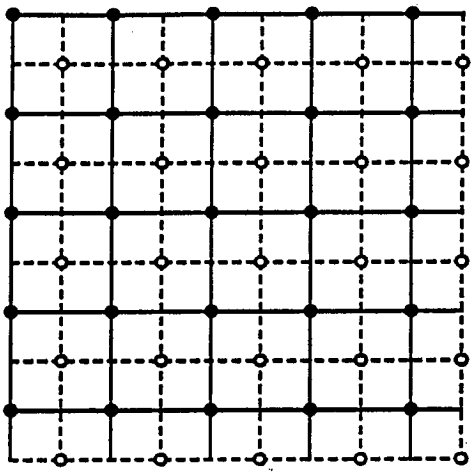

b

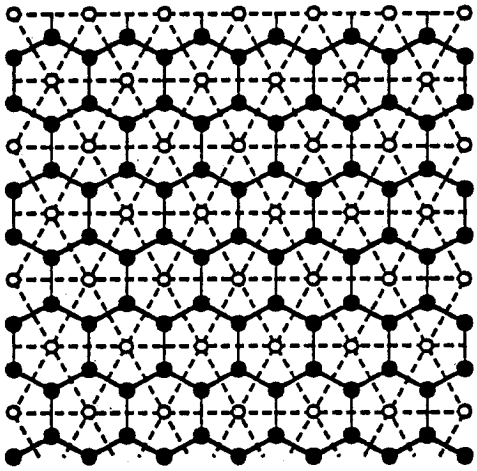

c

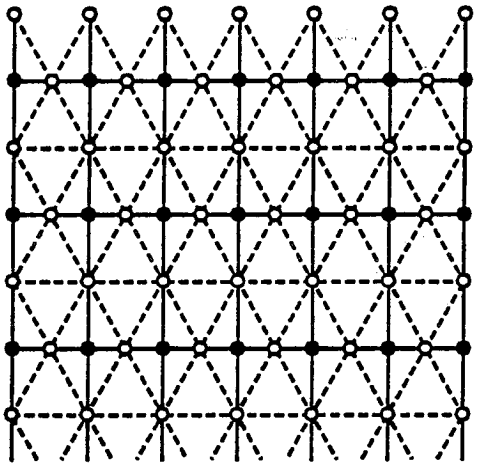

Fig. 5

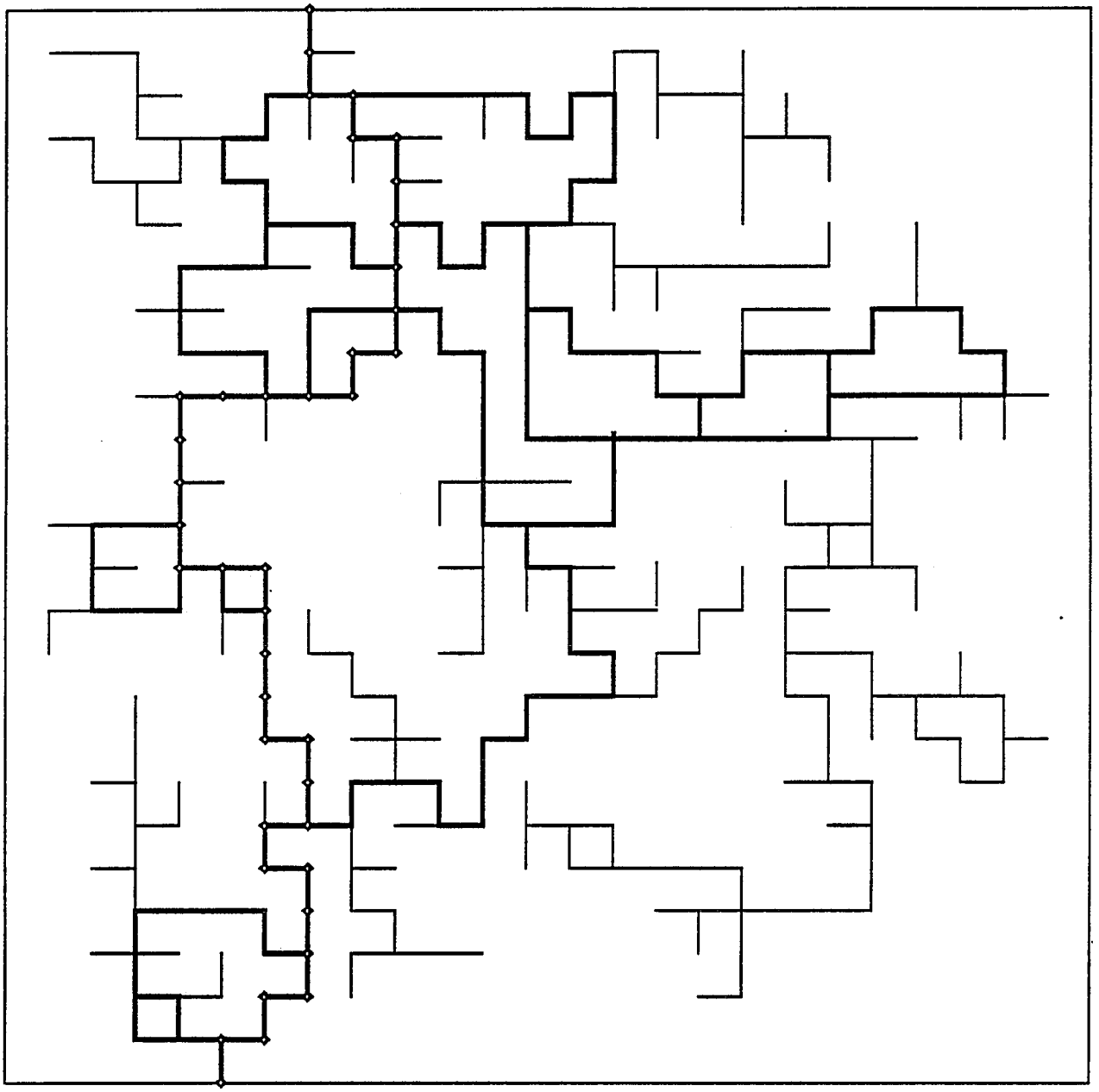

Fig. 6

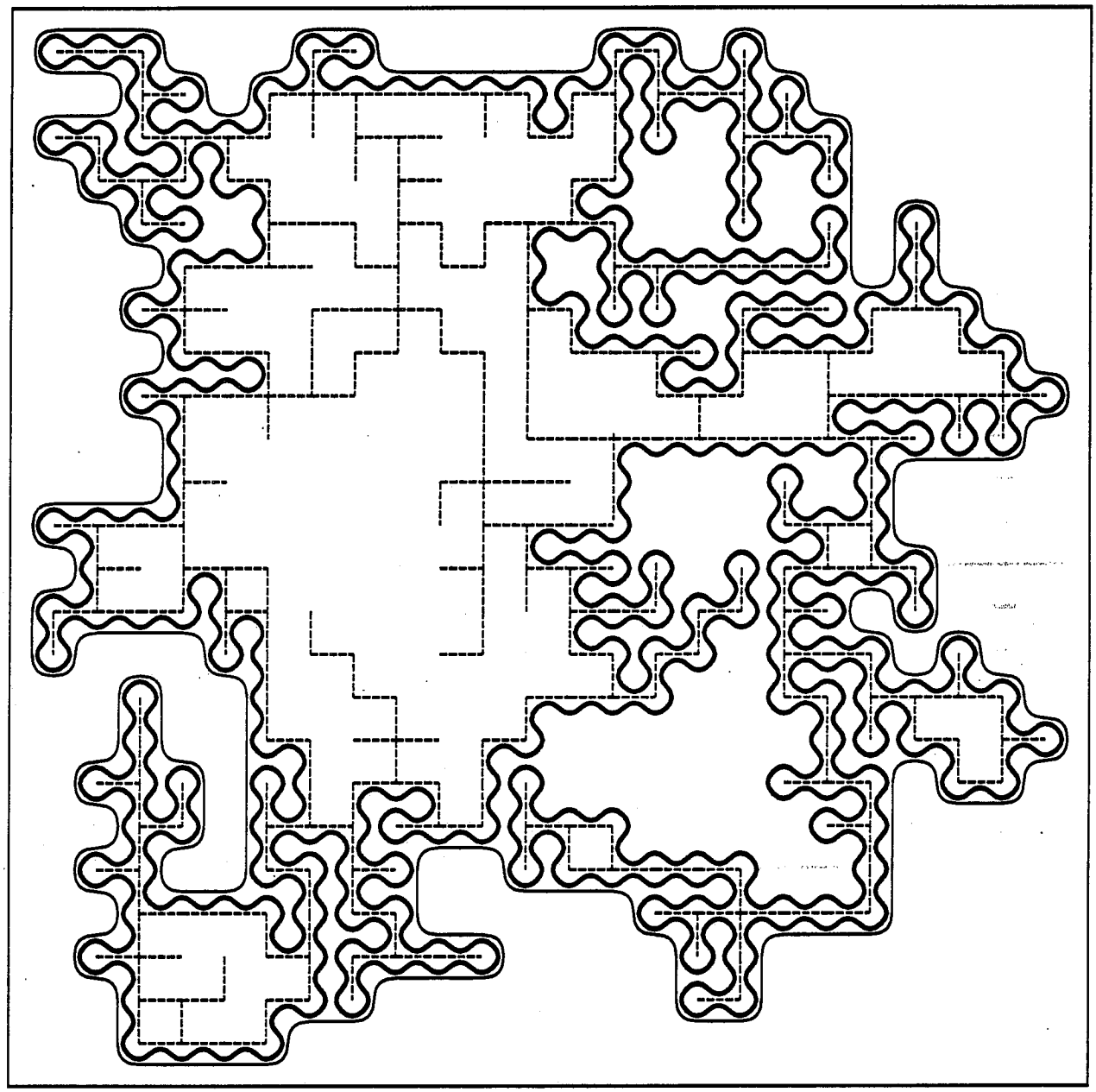

Fig. 7

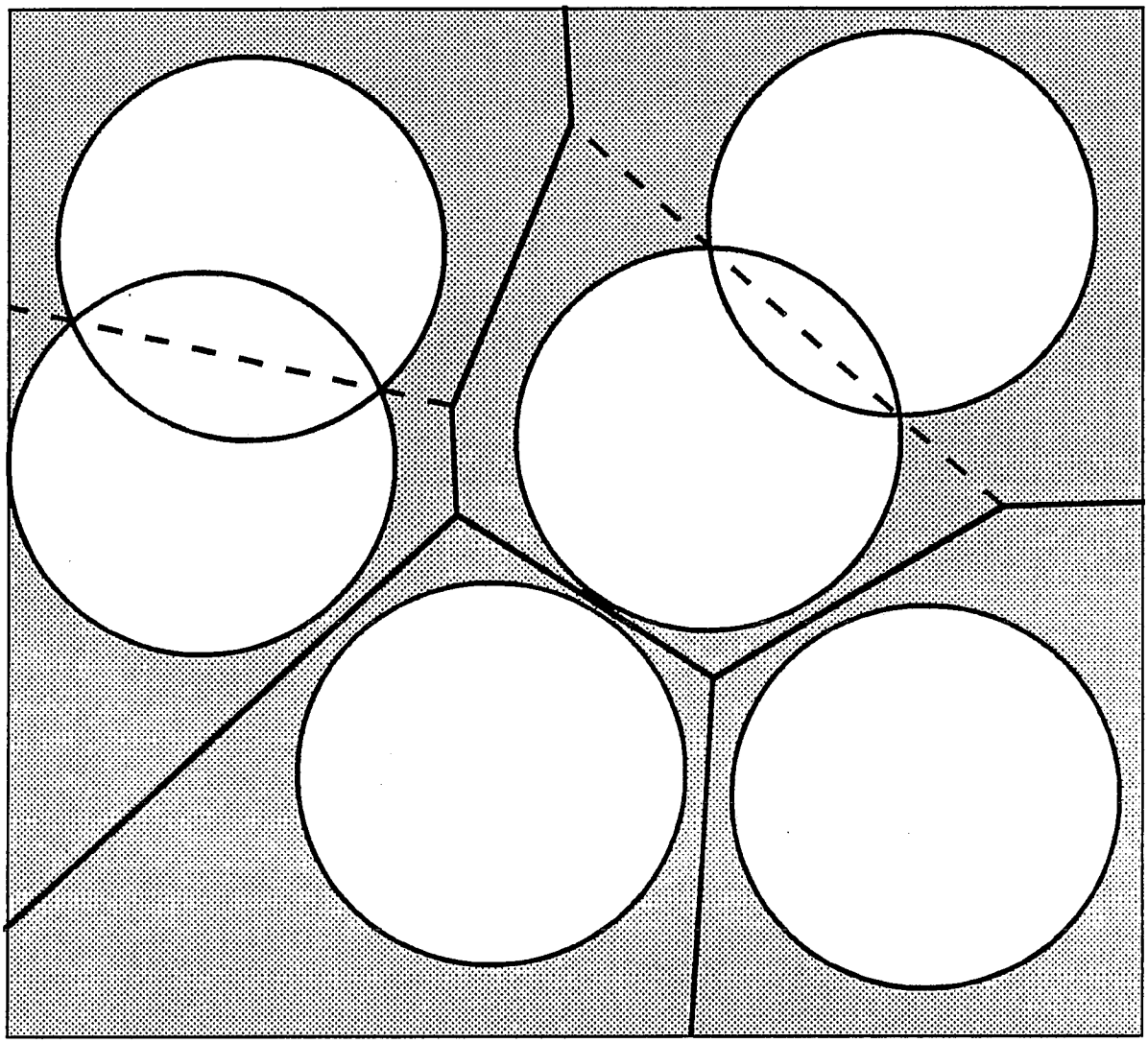

a

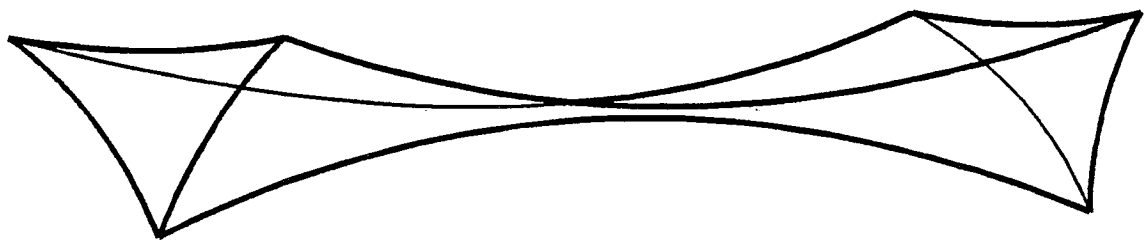

b

Fig. 8

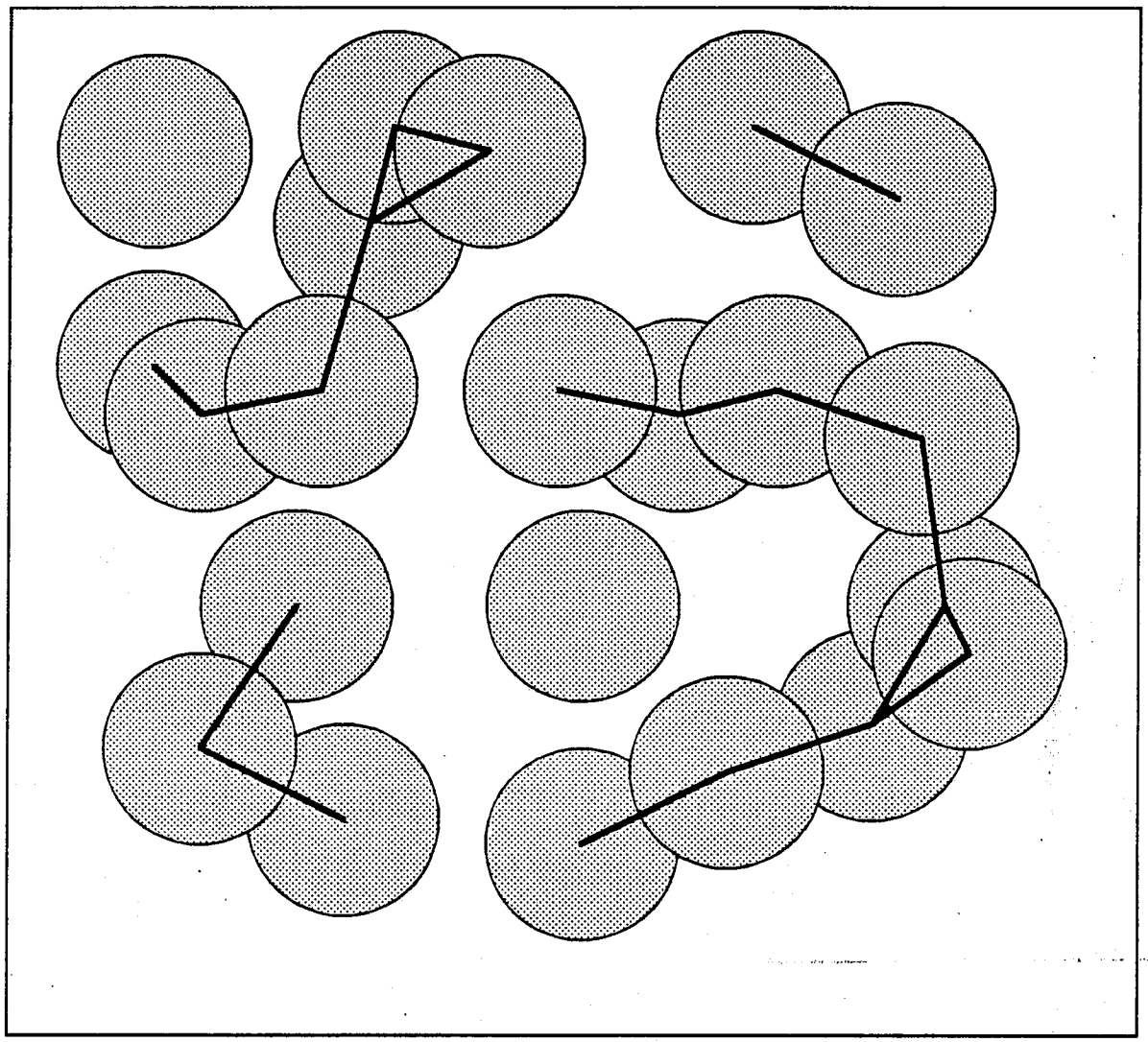

Fig. 9

h = −2

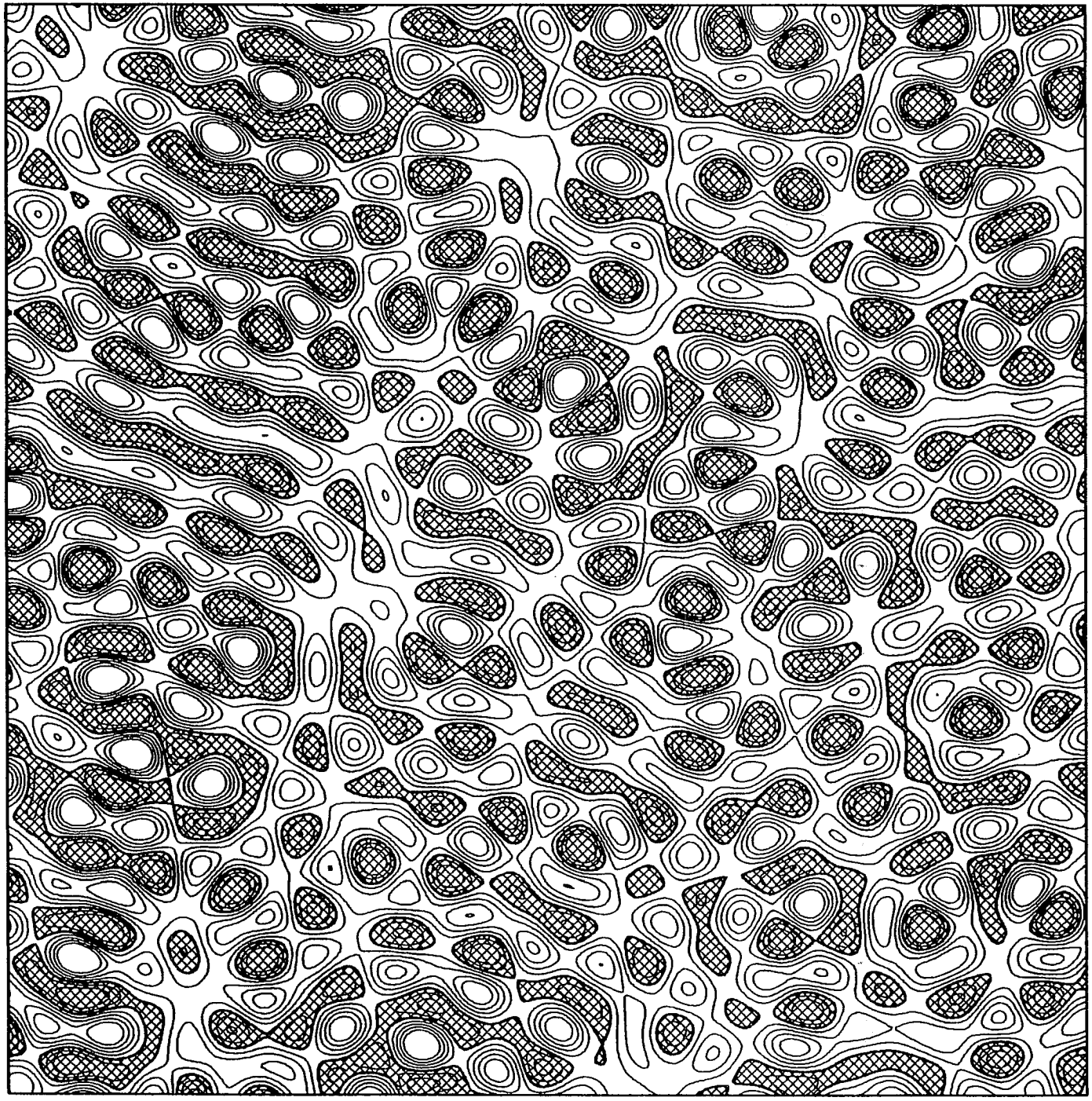

Fig. 10(a)

h = 0

Fig. 10(b)

h = 2

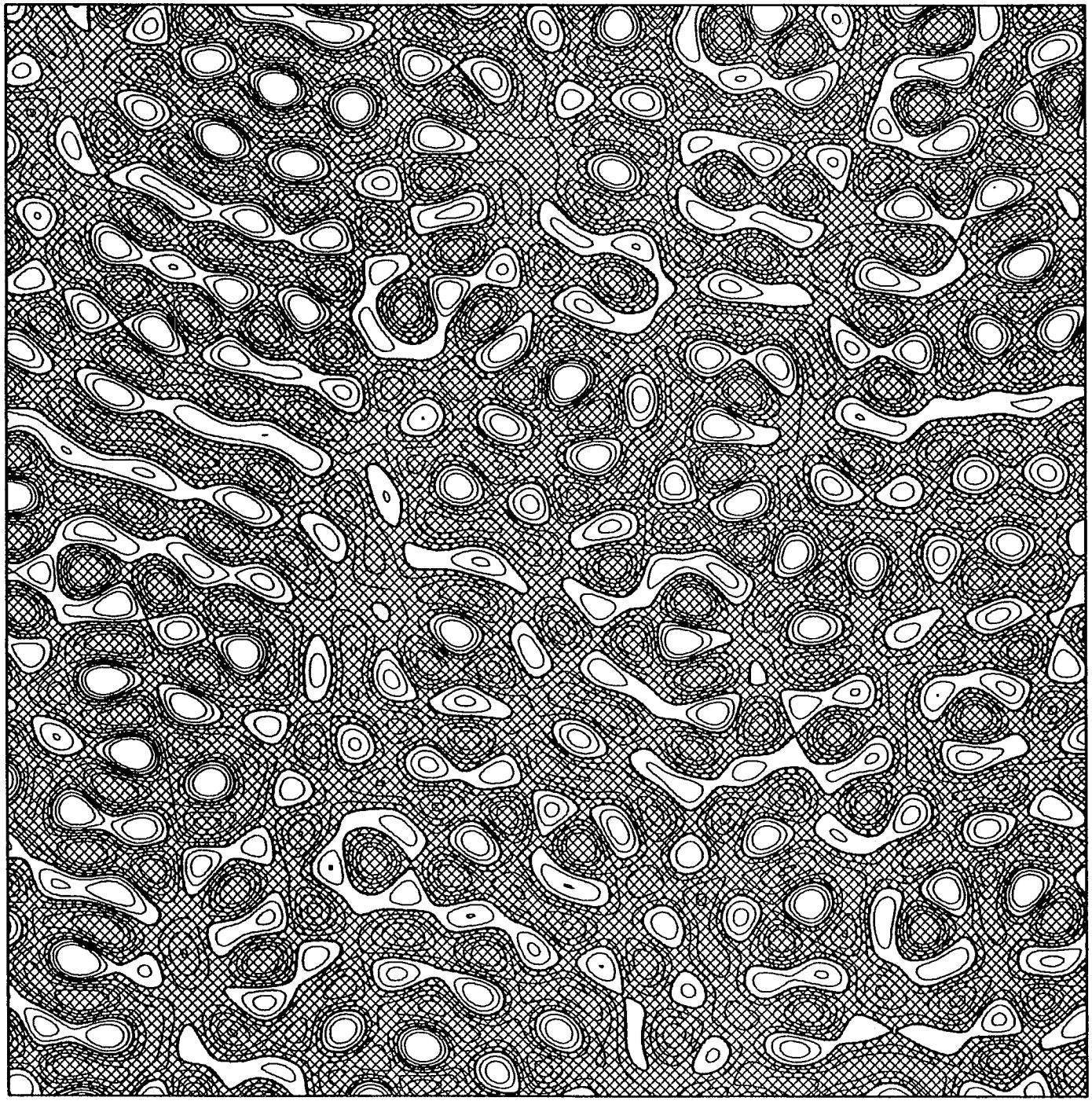

Fig. 10 (c)

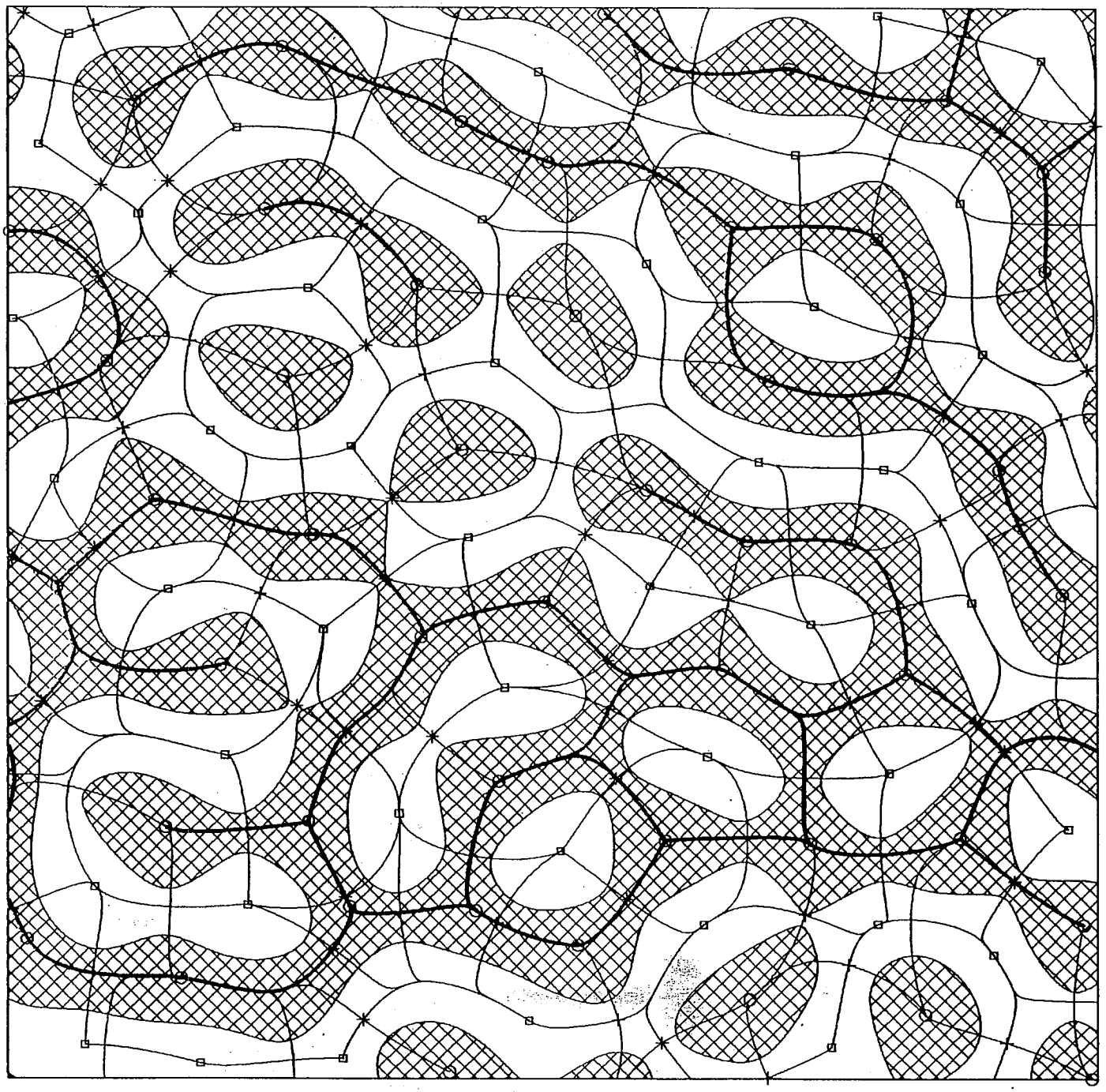

Fig. 10(d)

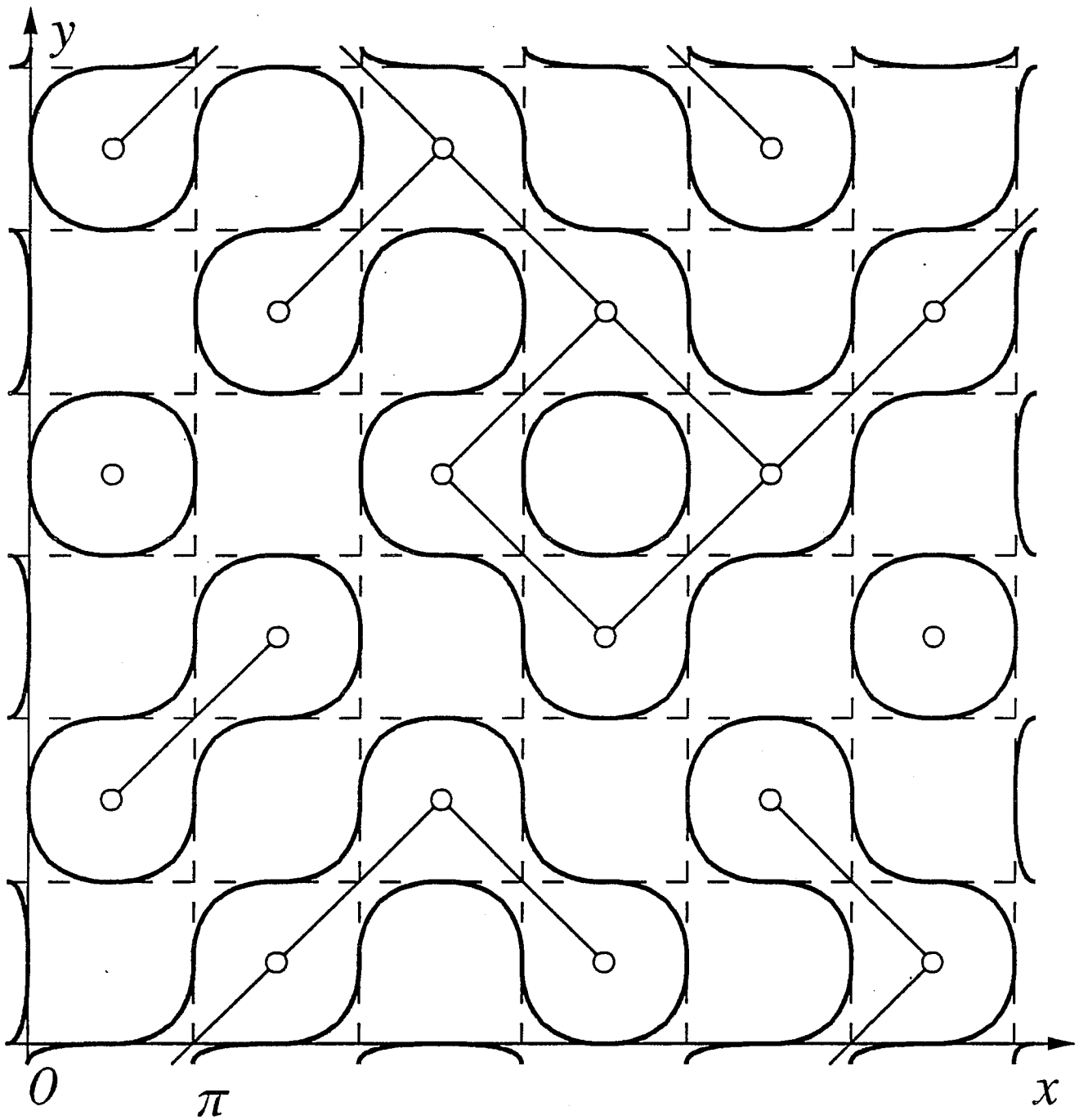

Fig. 11

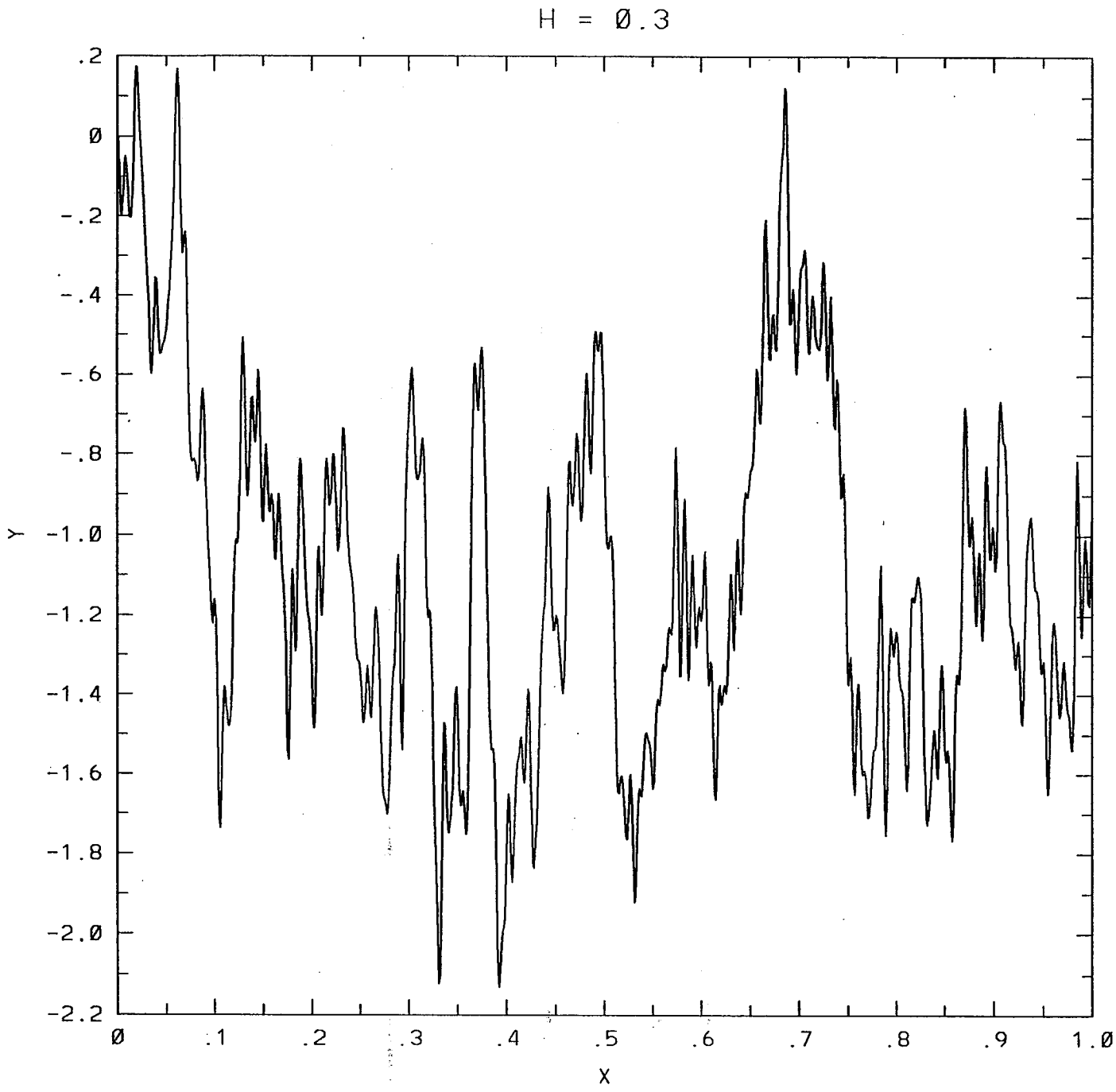

Fig. 12(a)

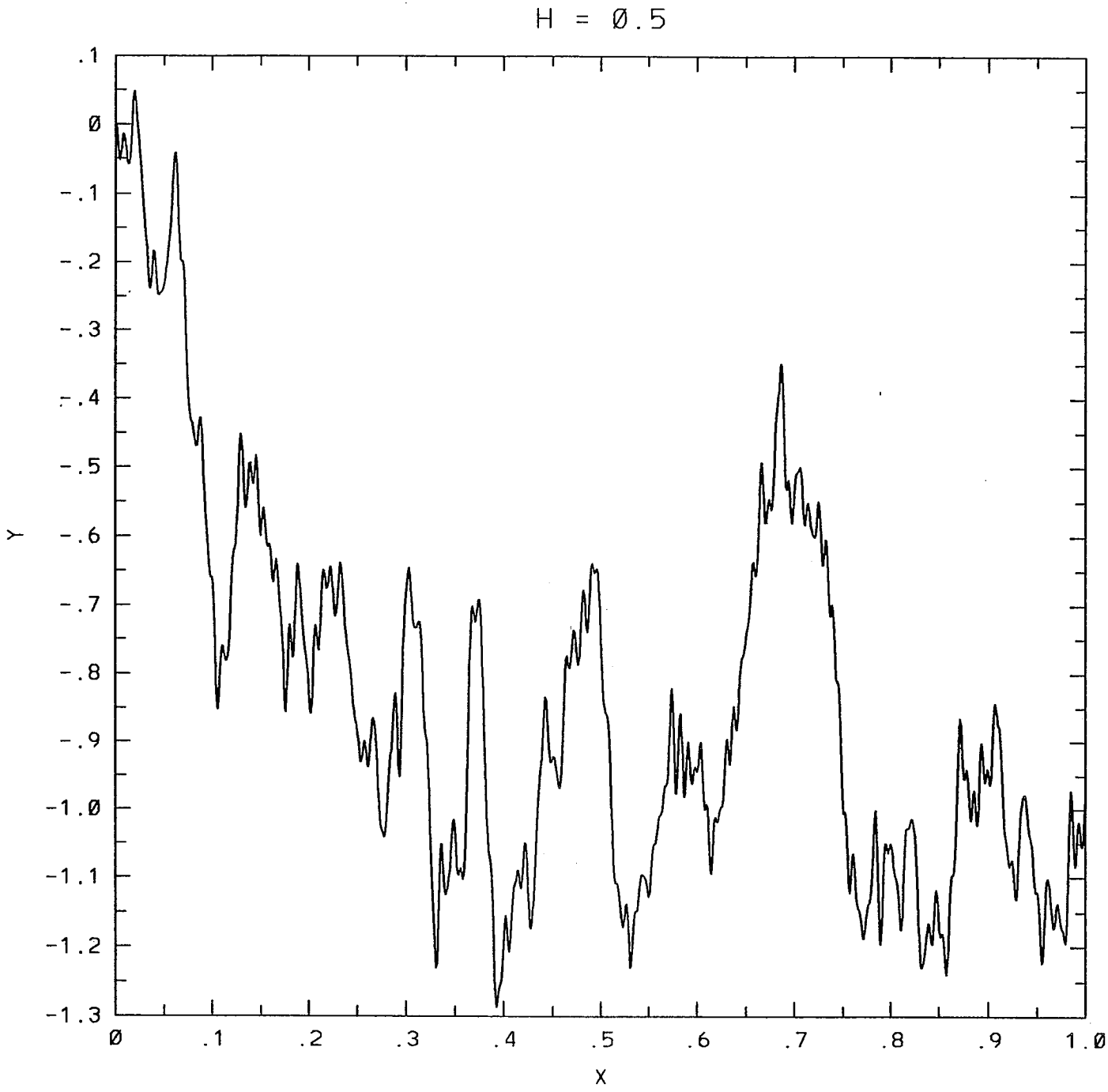

Fig. 12(b)

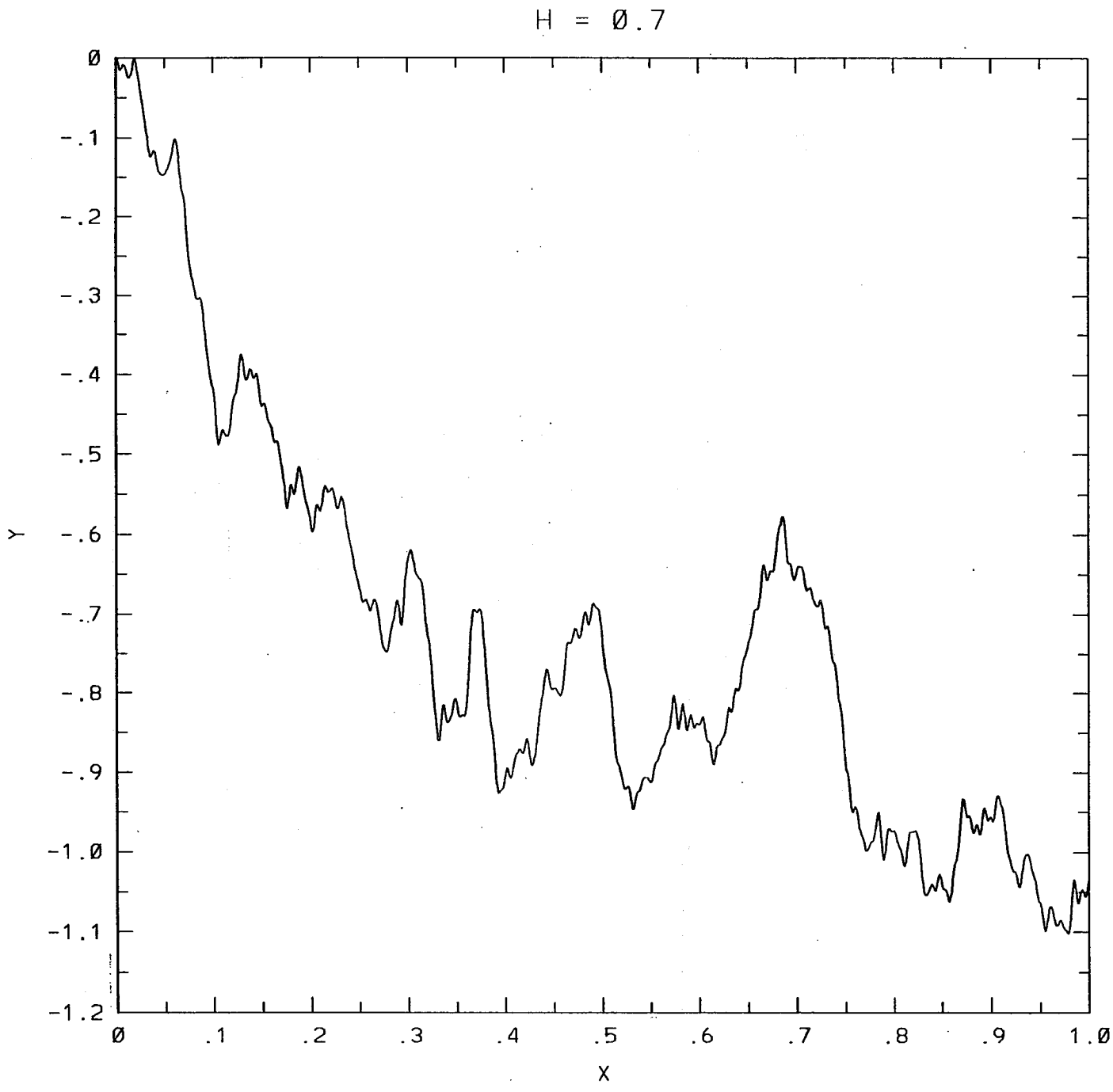

Fig. 12(c)

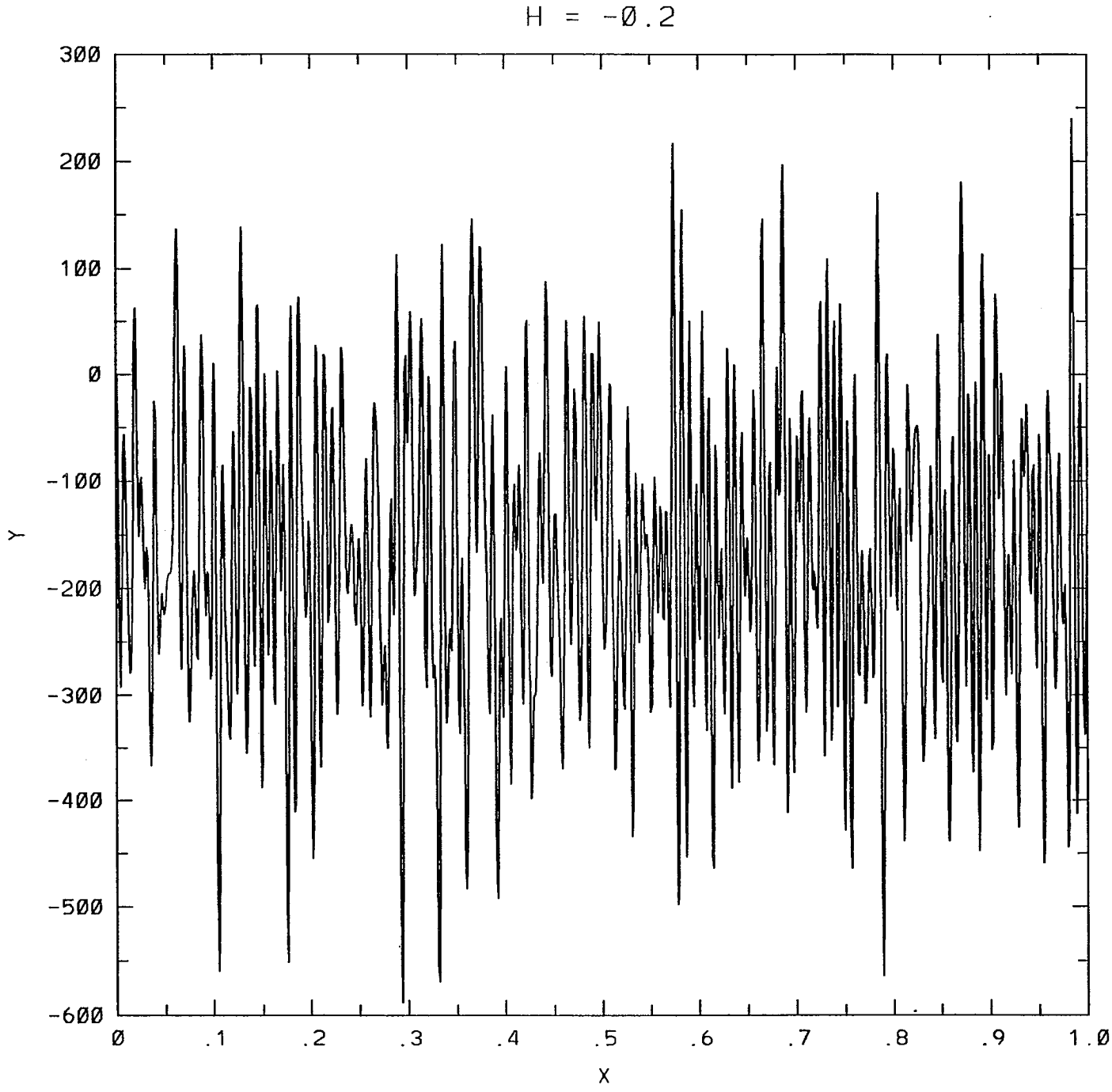

Fig. 12(d)

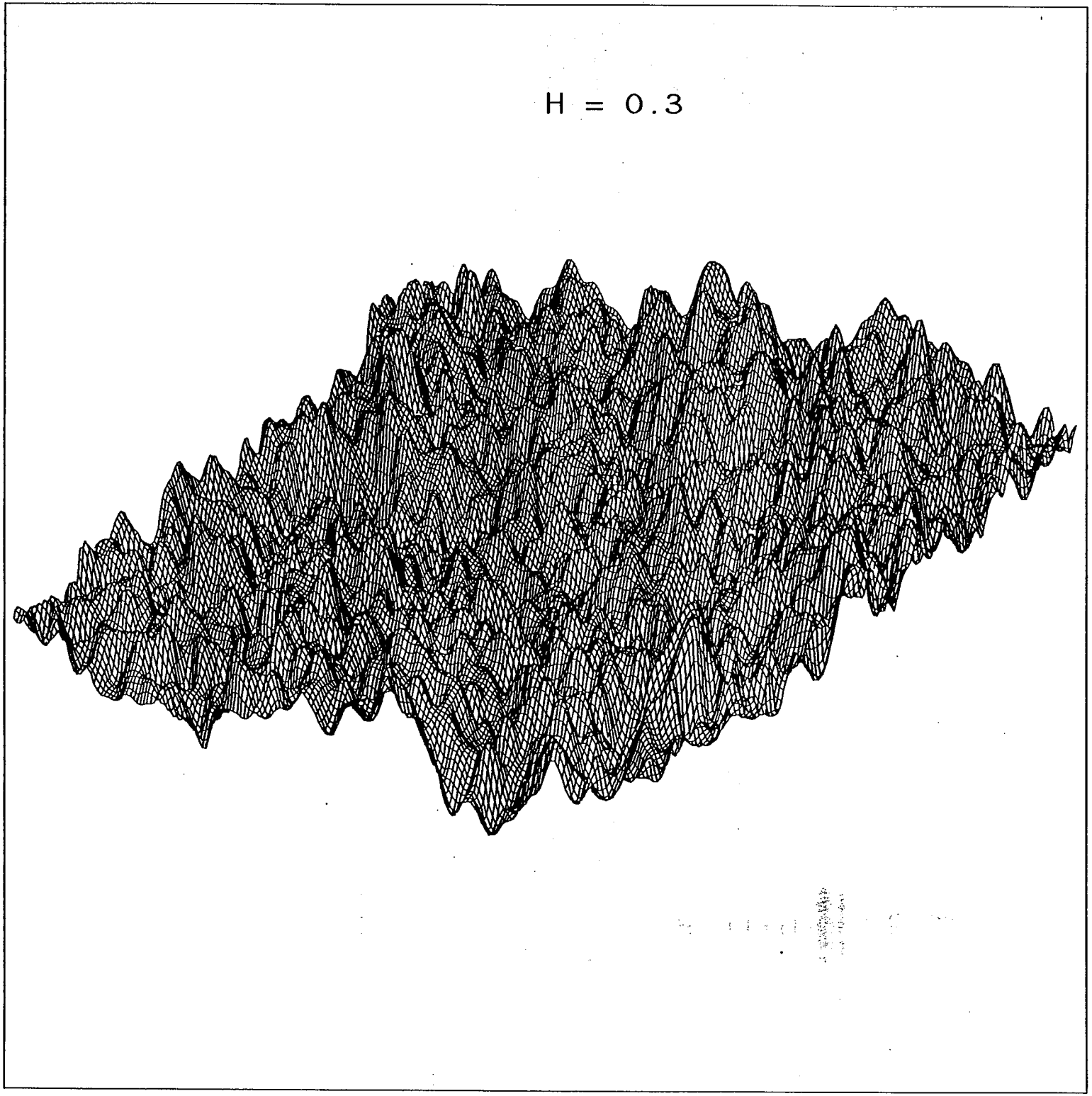

Fig. 13(a)

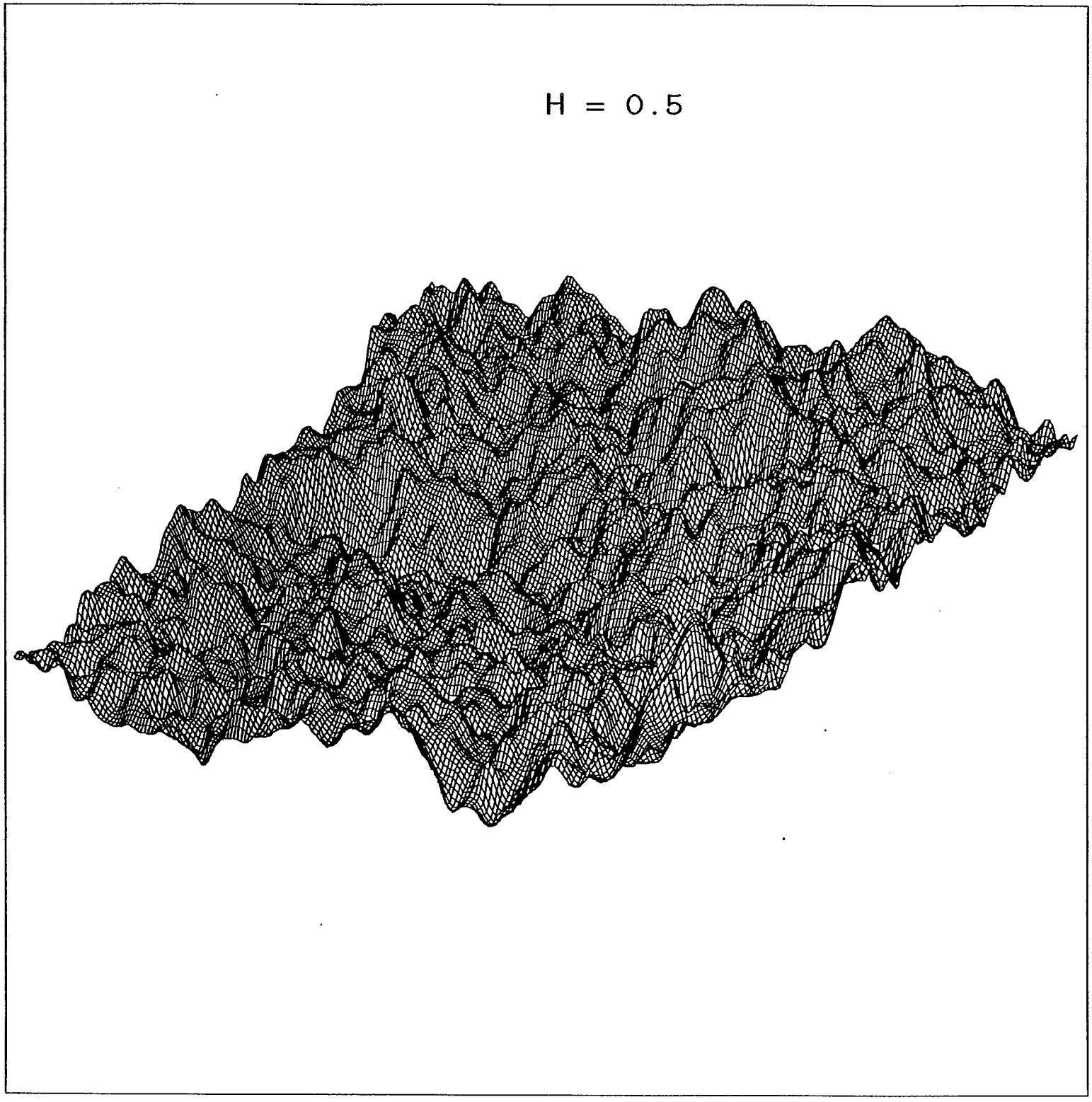

Fig. 13(b)

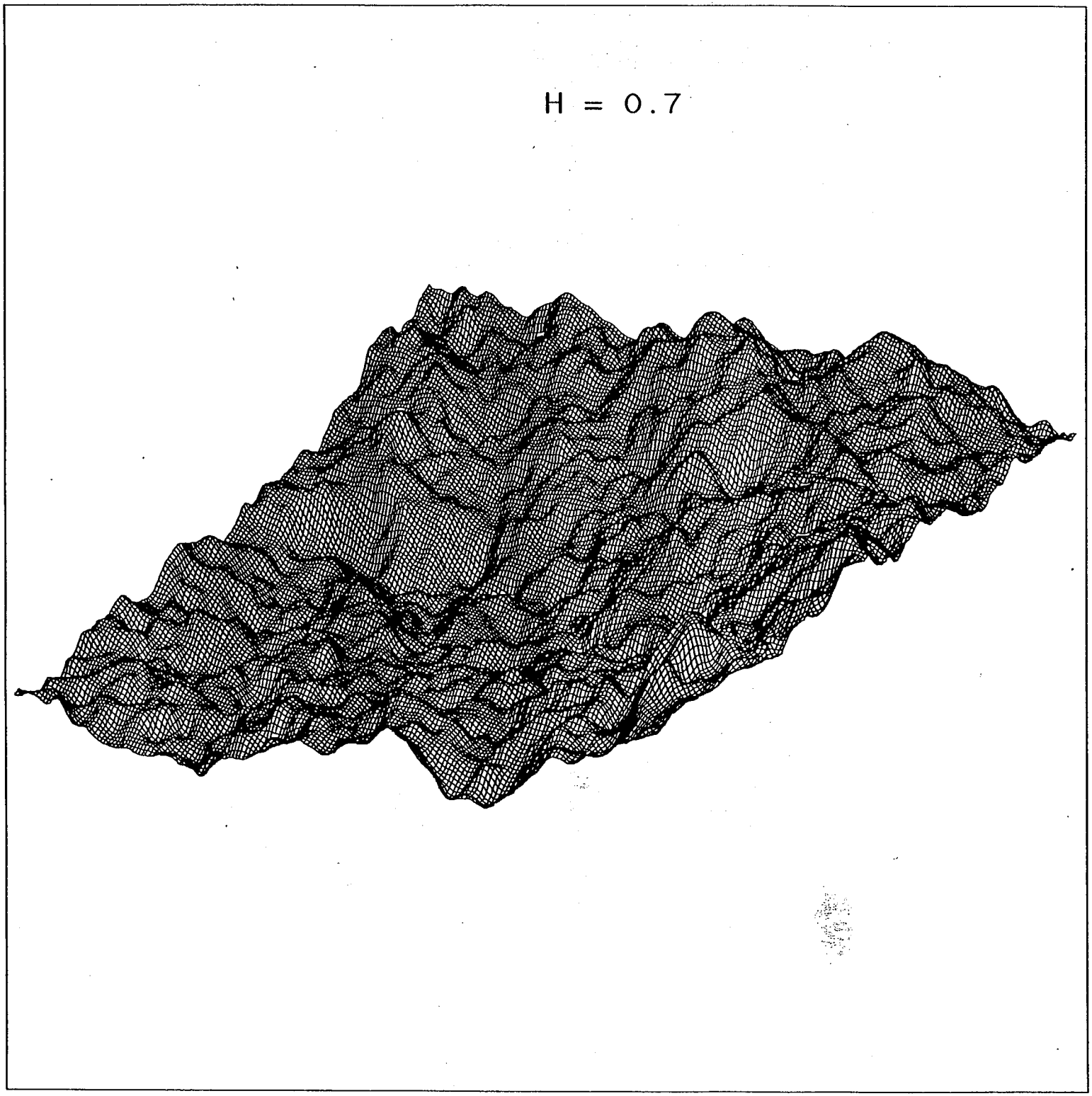

Fig. 13(c)

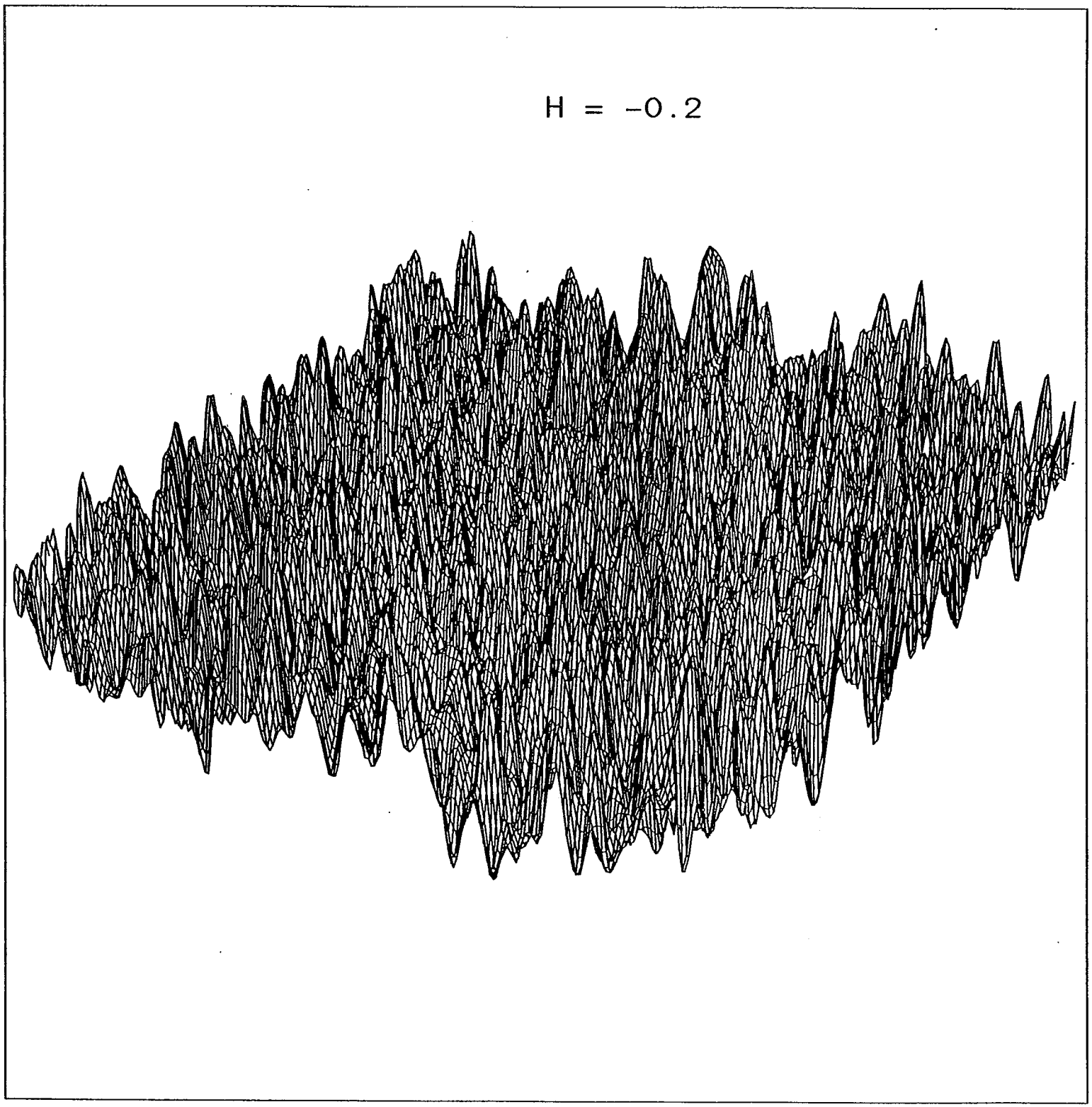

Fig.13(d)

H = 0.3

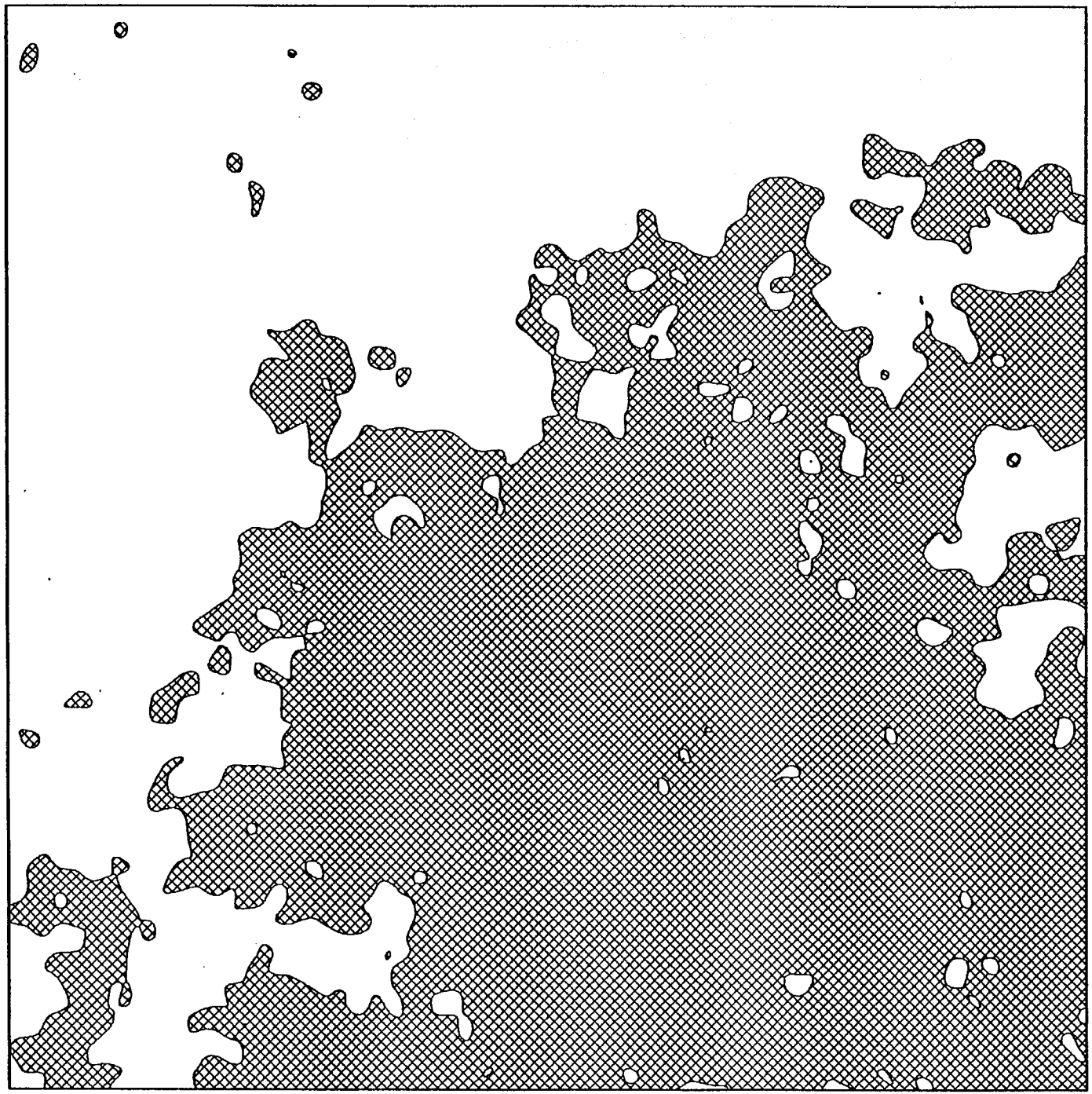

Fig. 14(a)

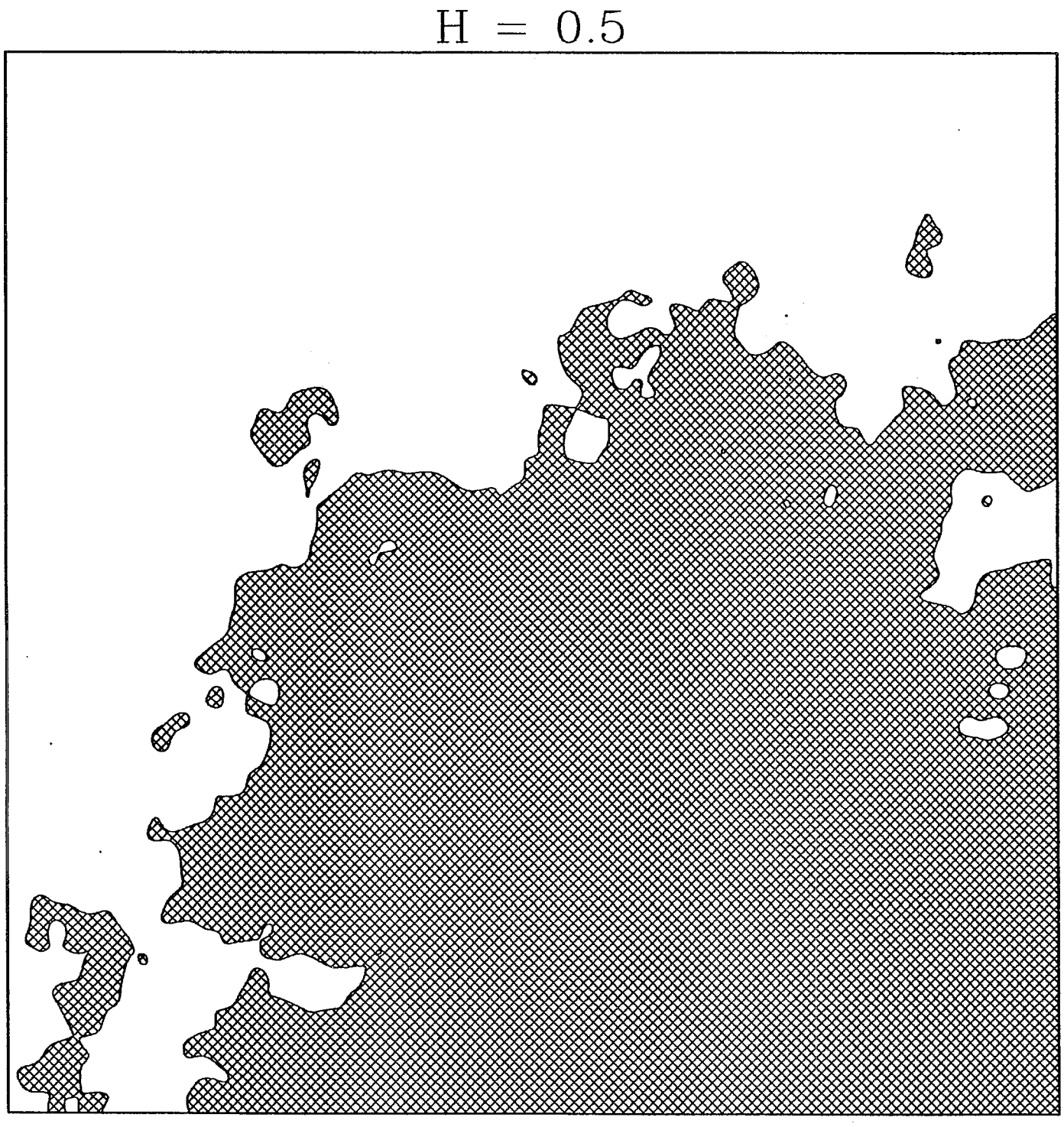

Fig. 14(b)

H = 0.7

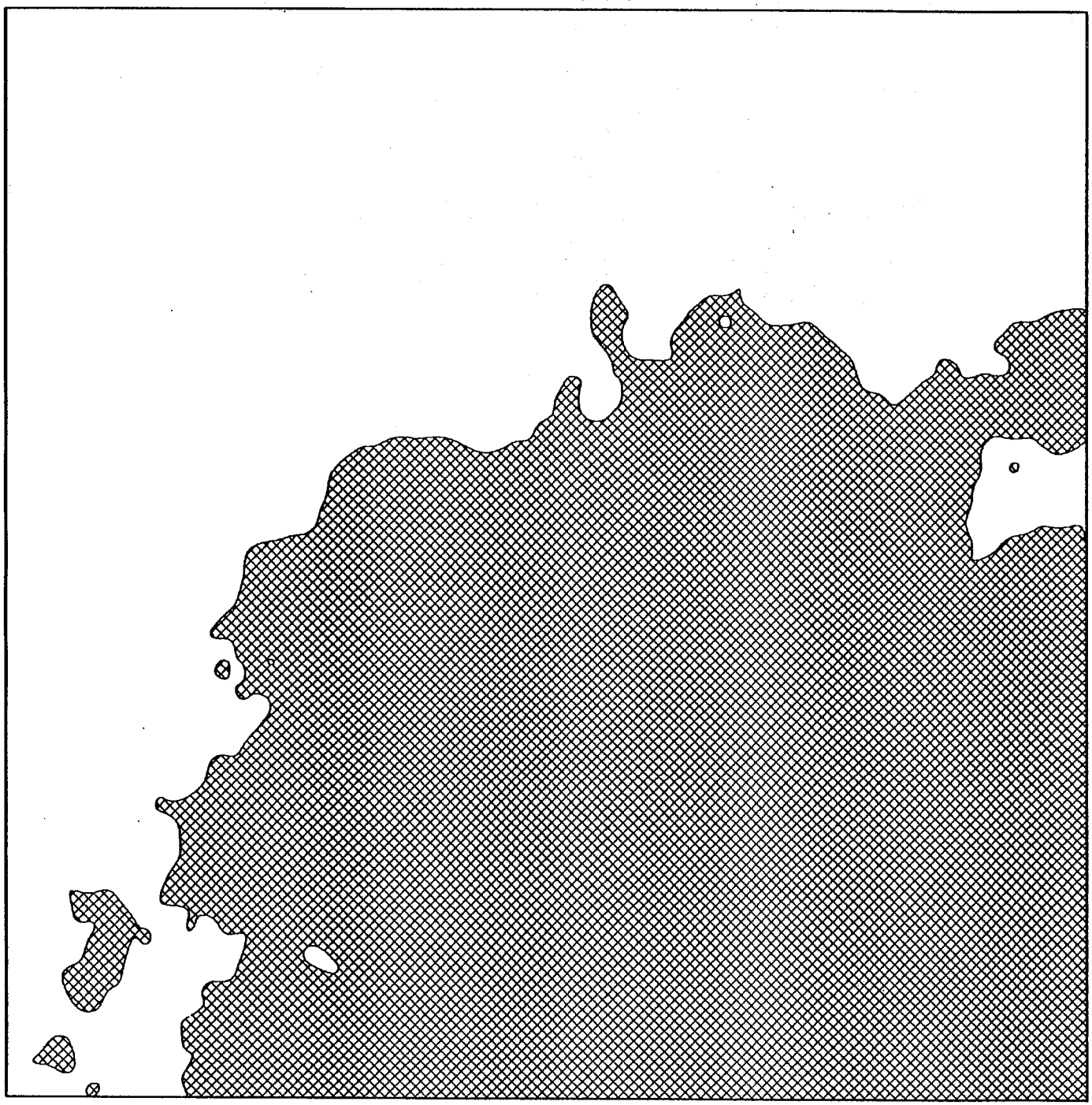

Fig. 14(c)

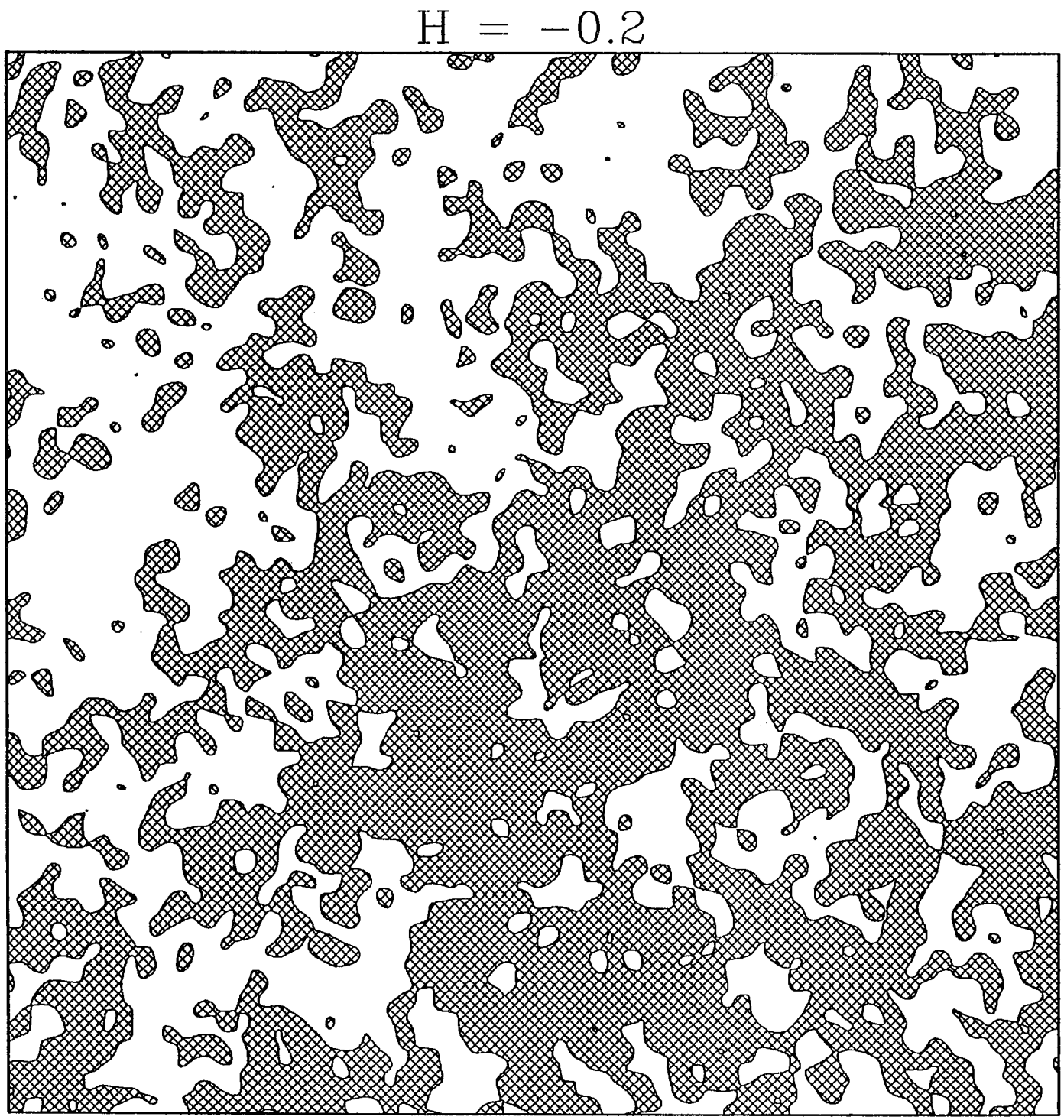

Fig. 14(d)

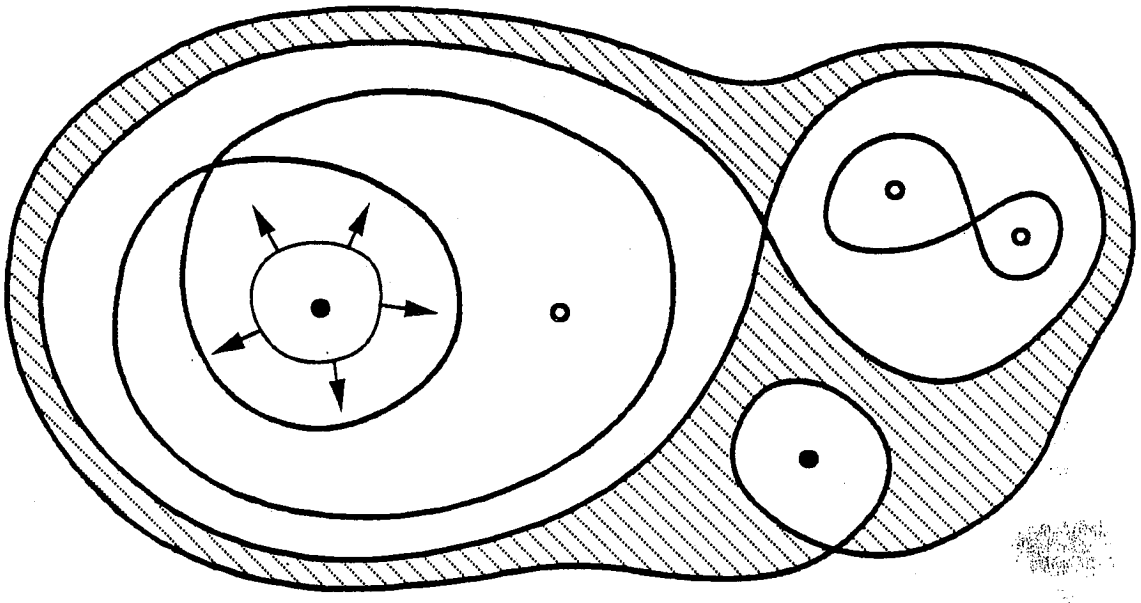

Fig. 15

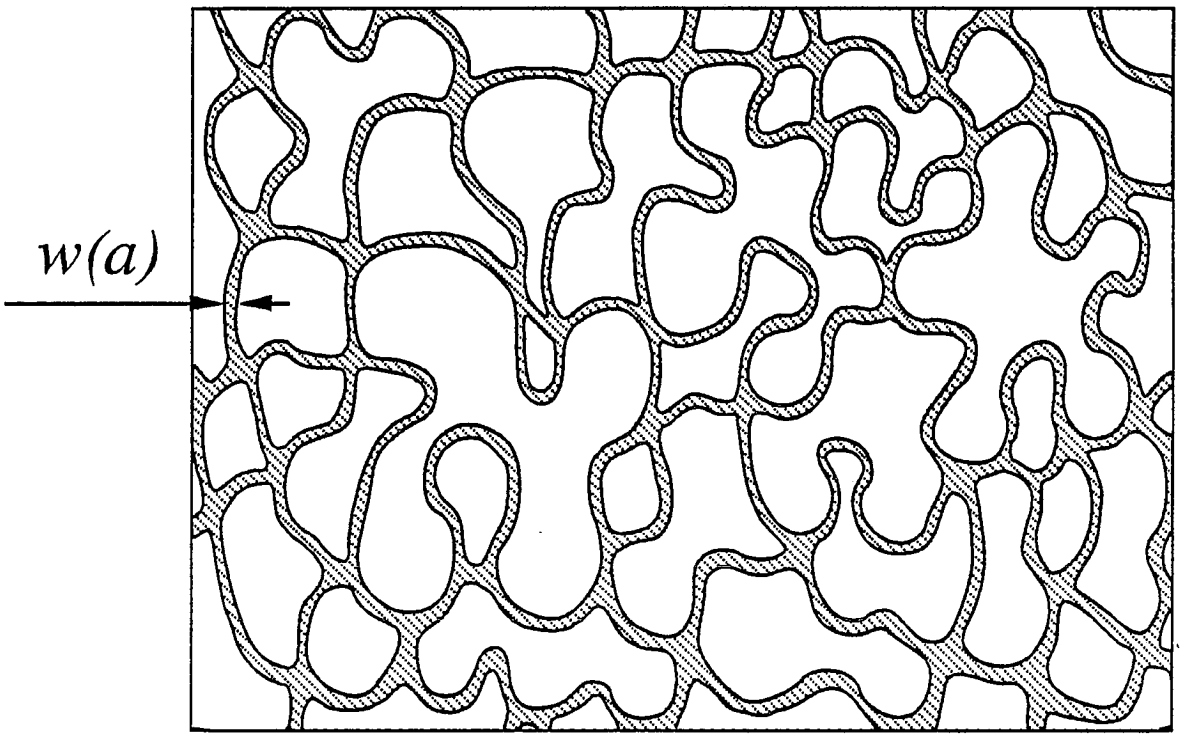

Fig. 16

a

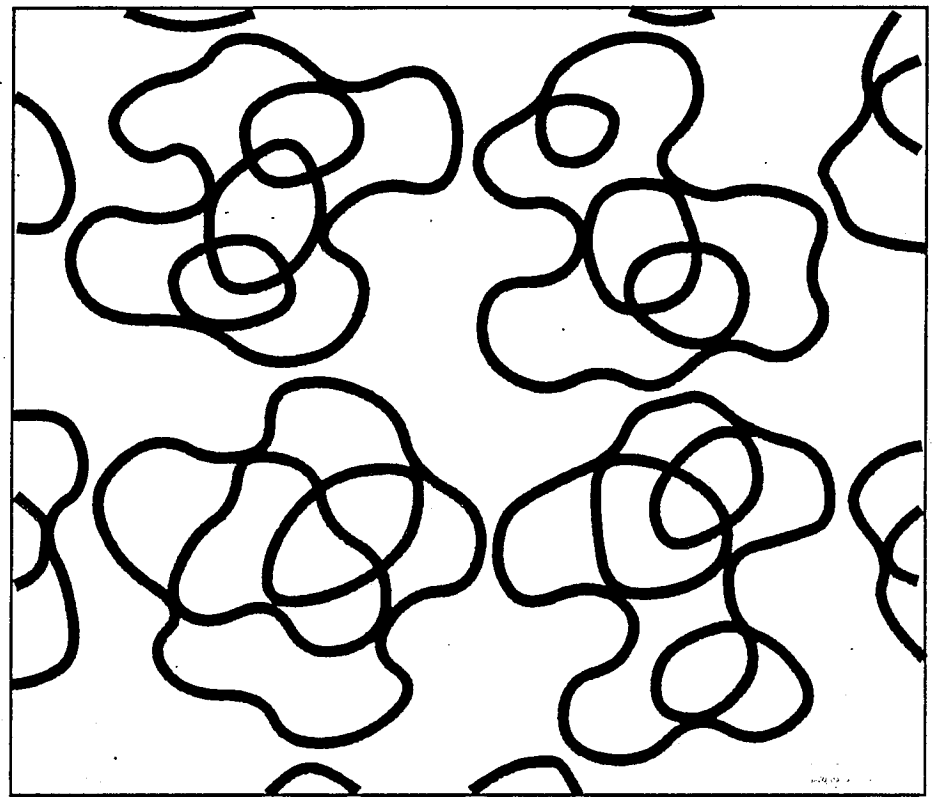

b

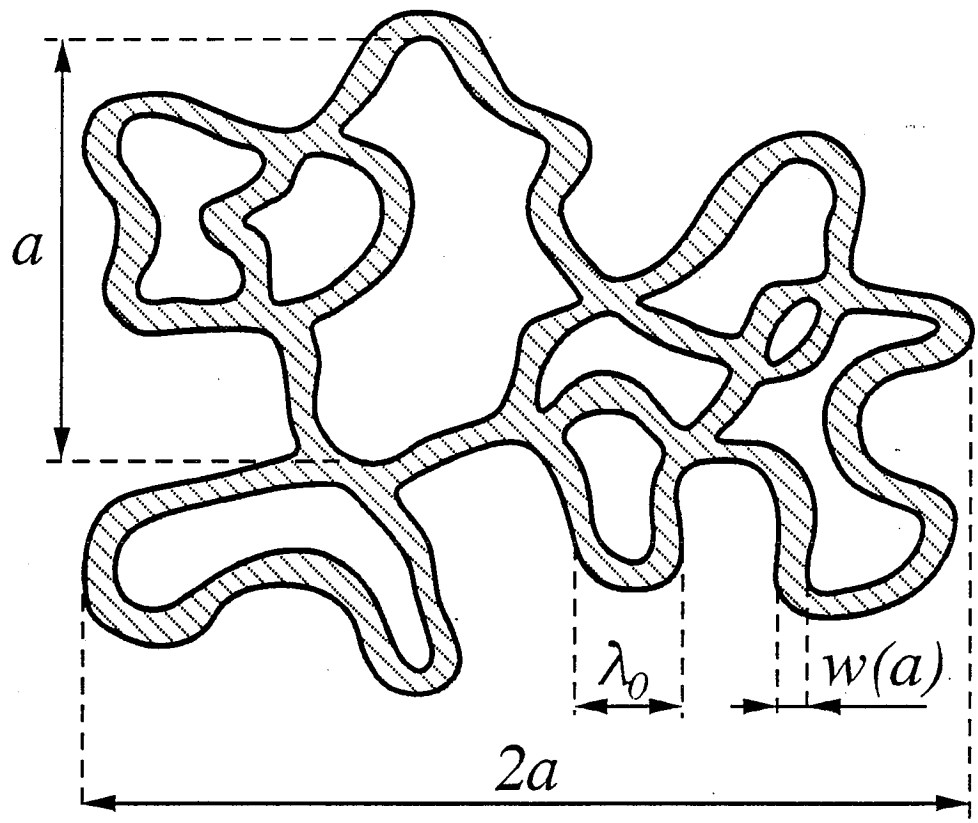

Fig. 17

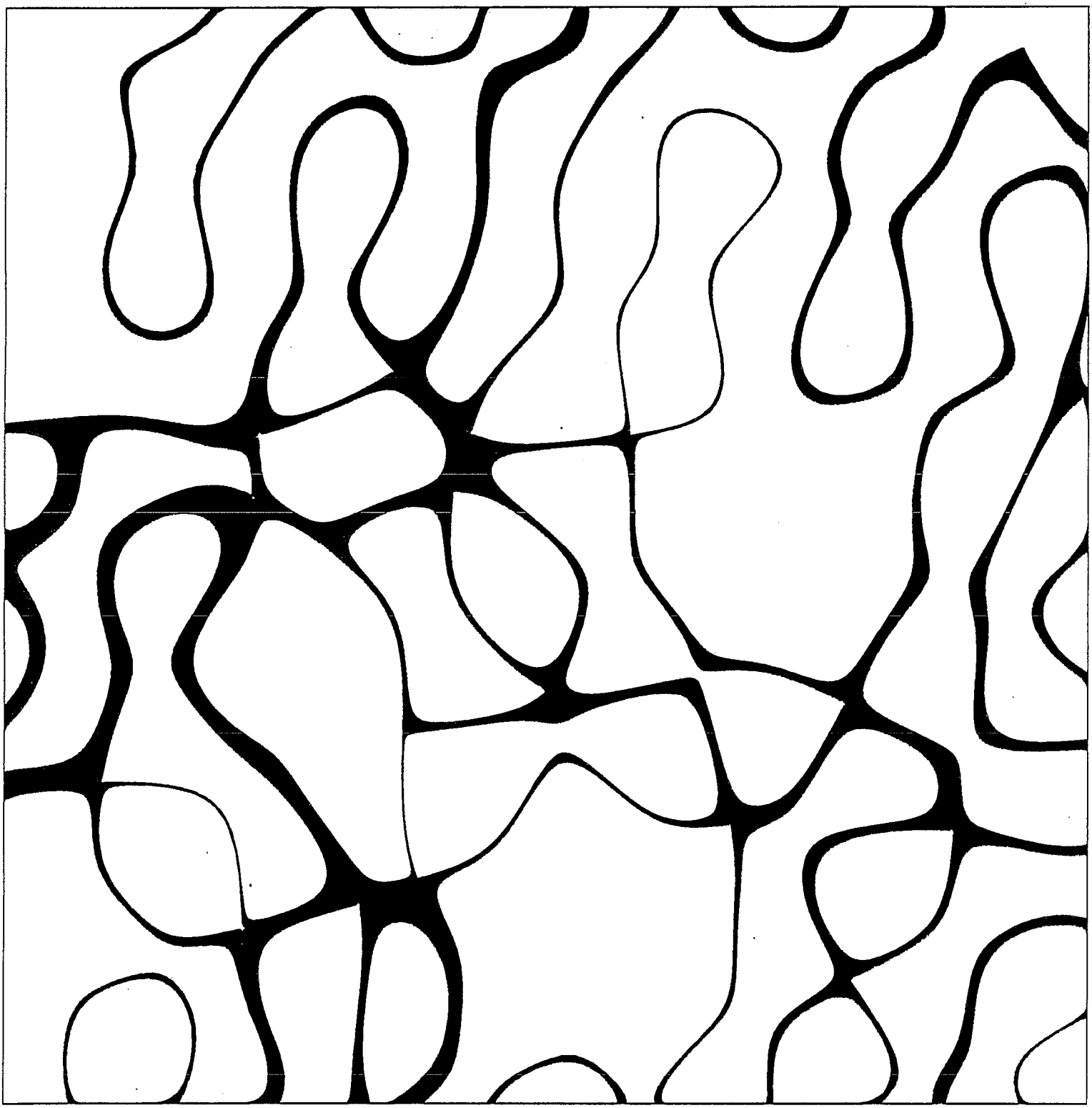

Fig. 18(a)

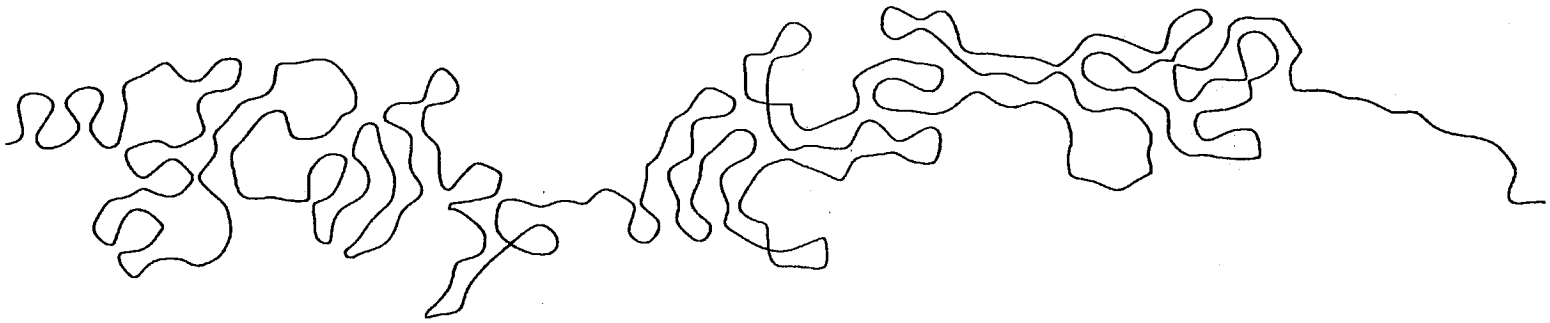

Fig. 18 (b)

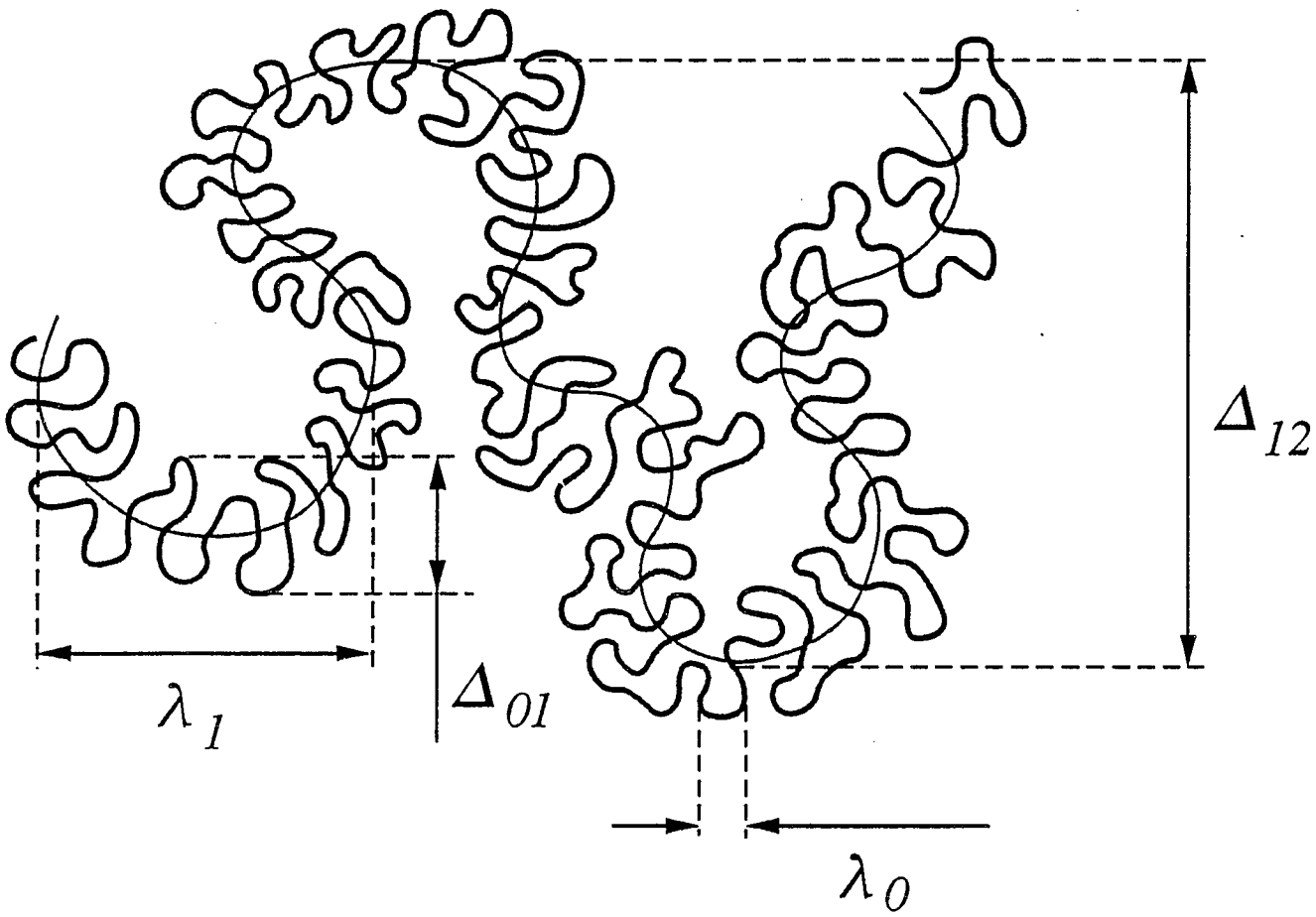

Fig. 19

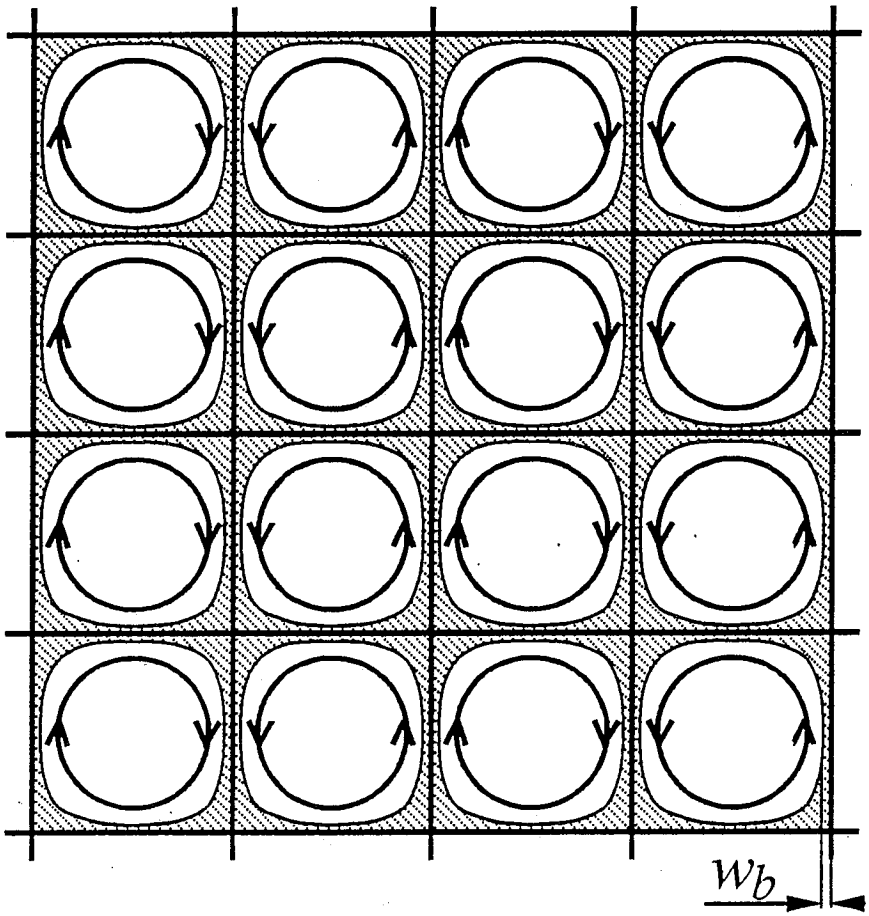

Fig. 20

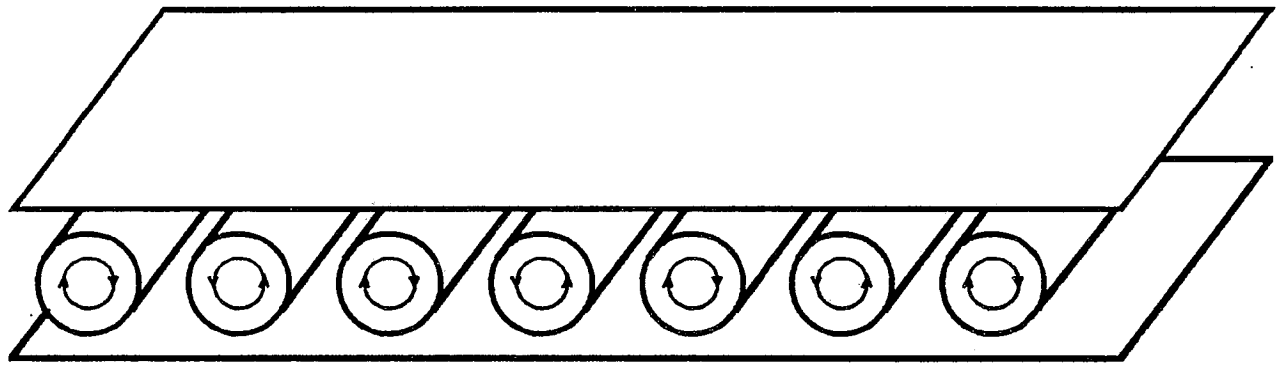

a

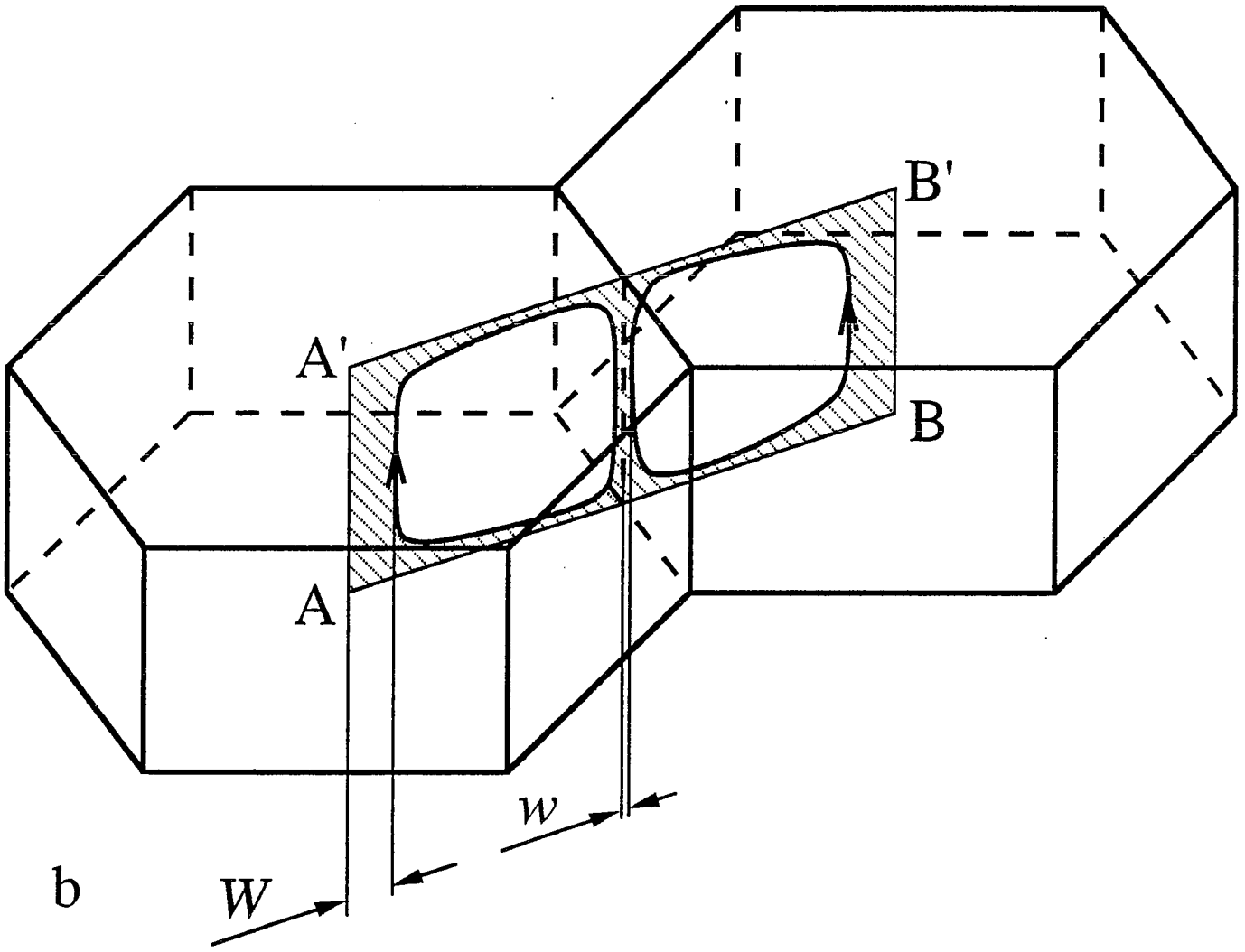

b

Fig. 21

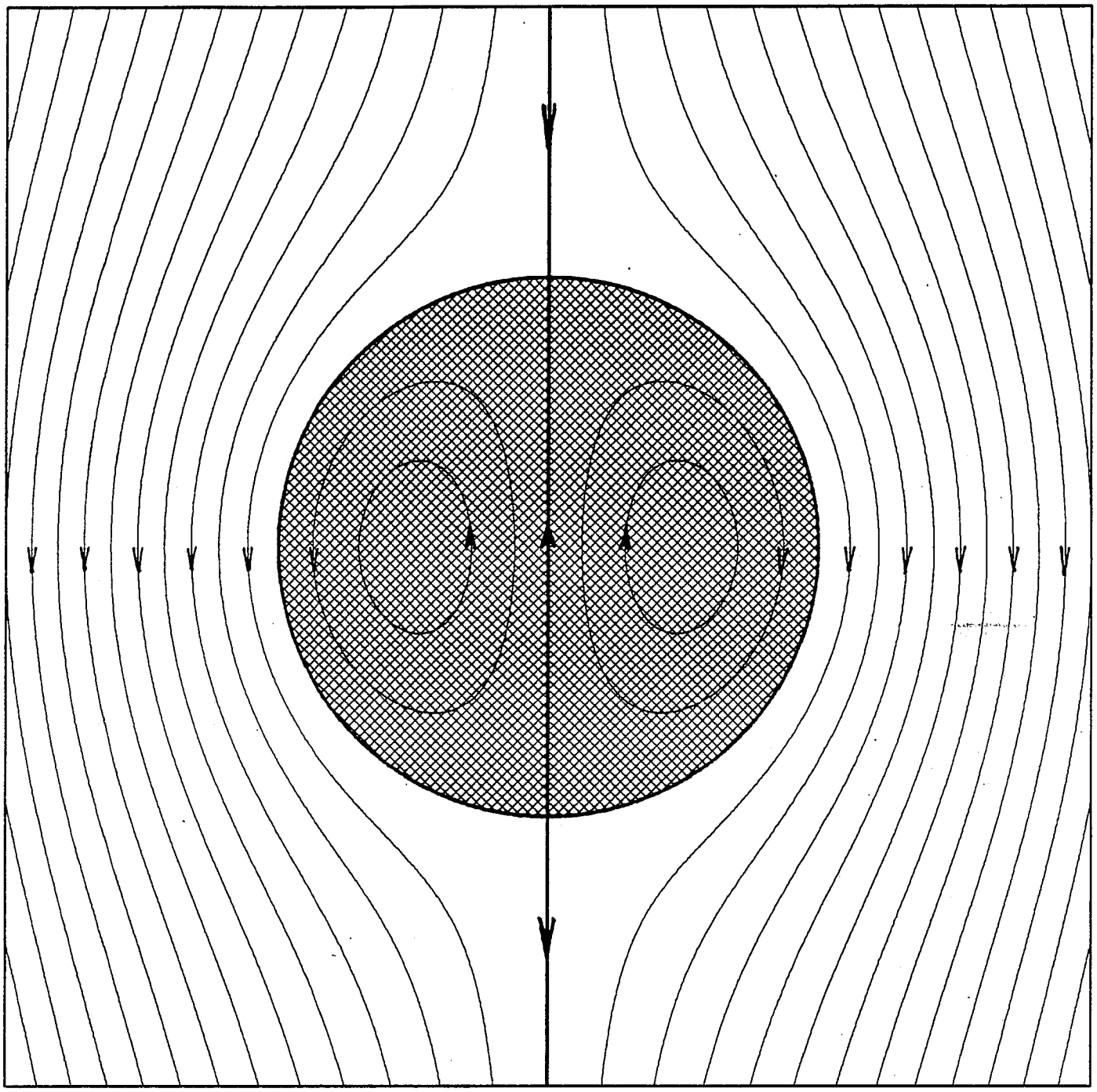

Fig. 22

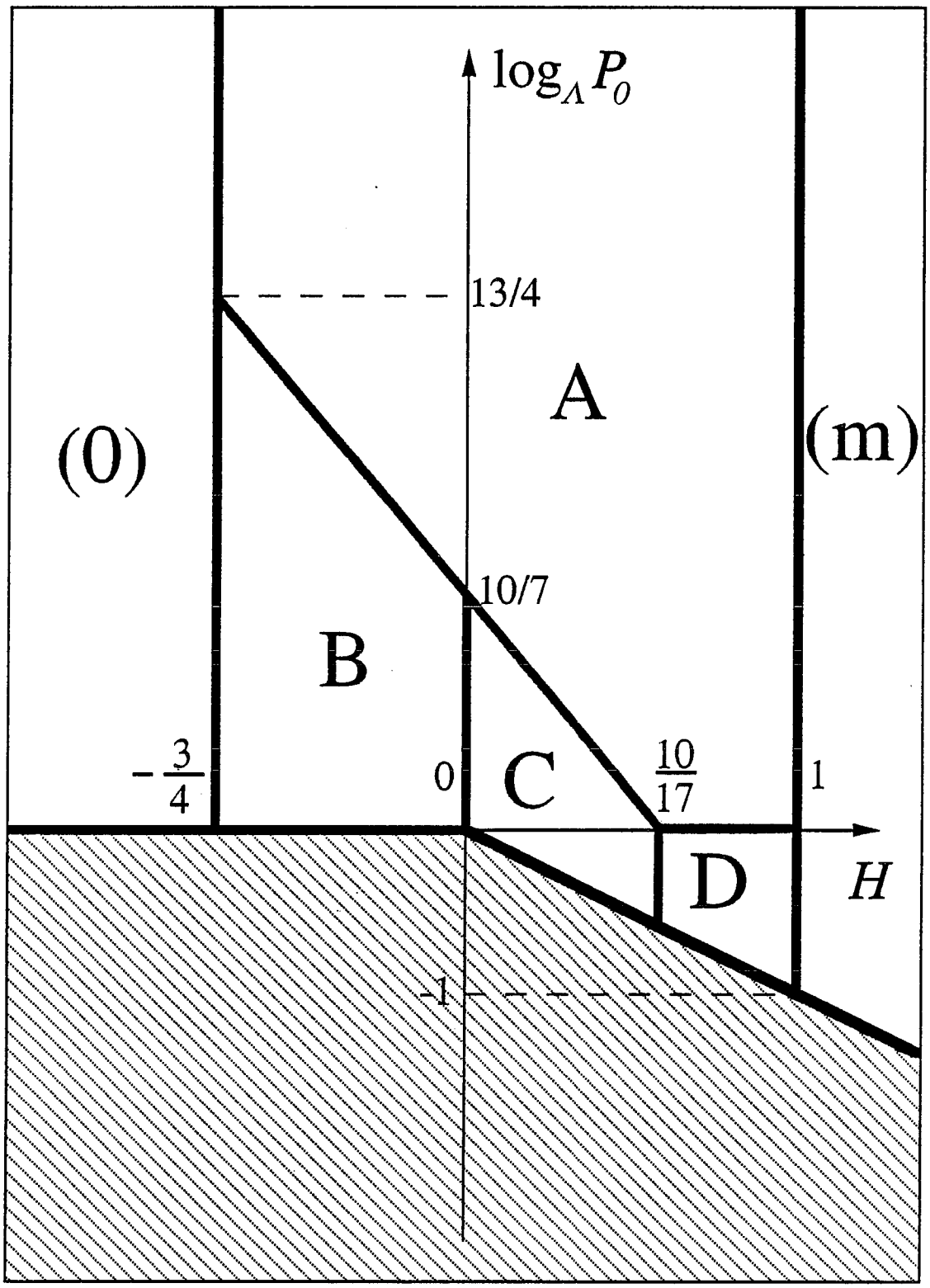

Fig. 23

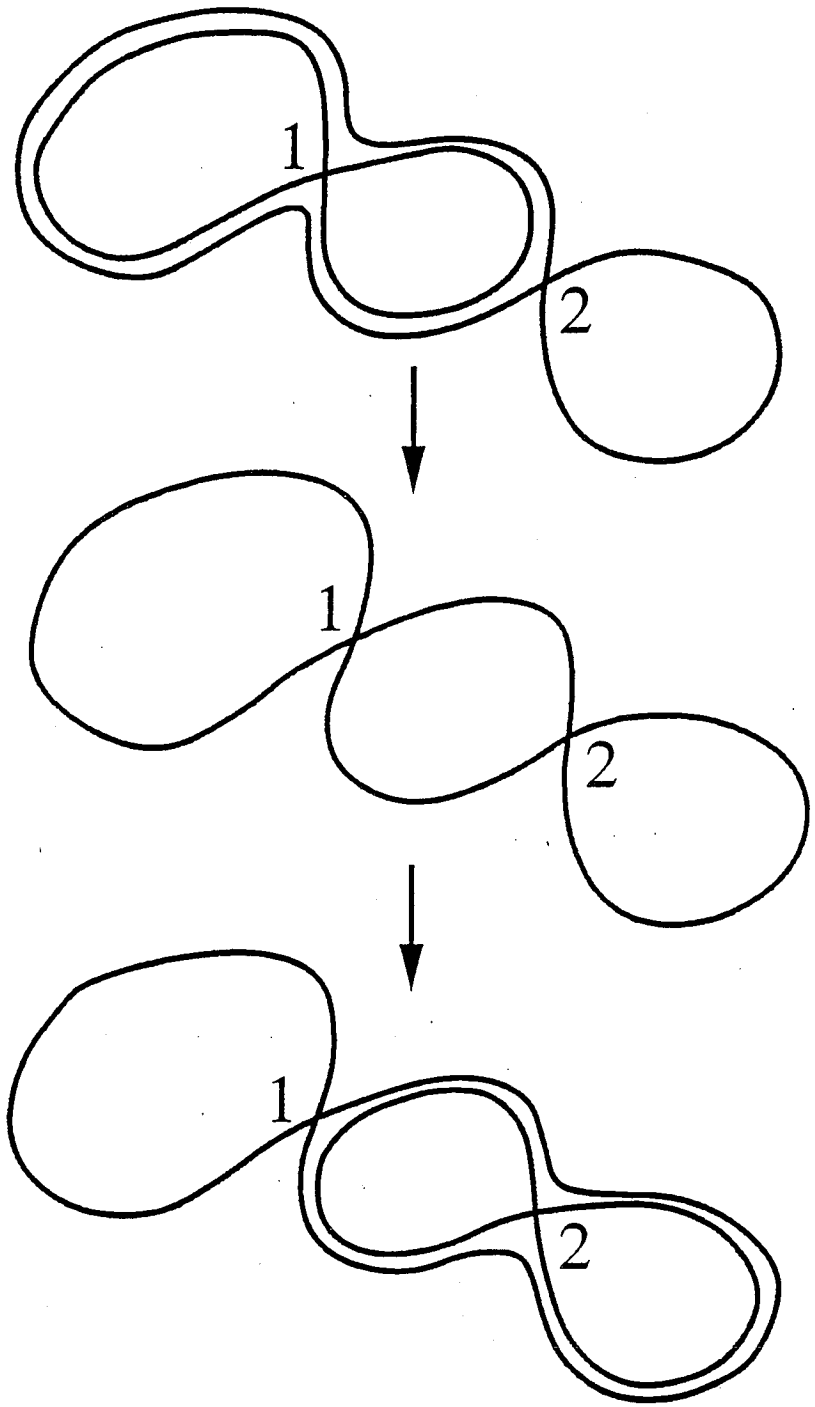

Fig. 24

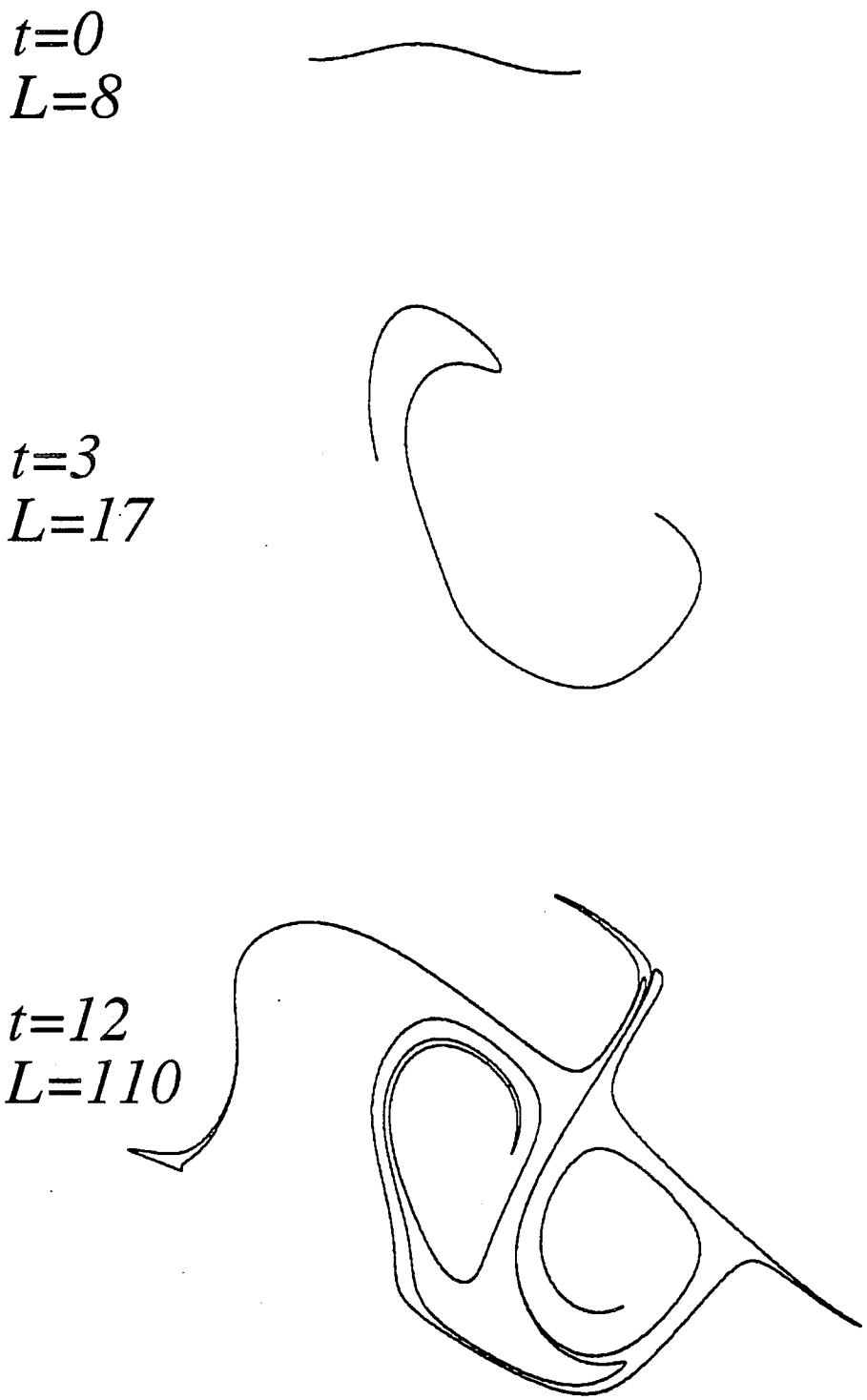

Fig. 25(a)

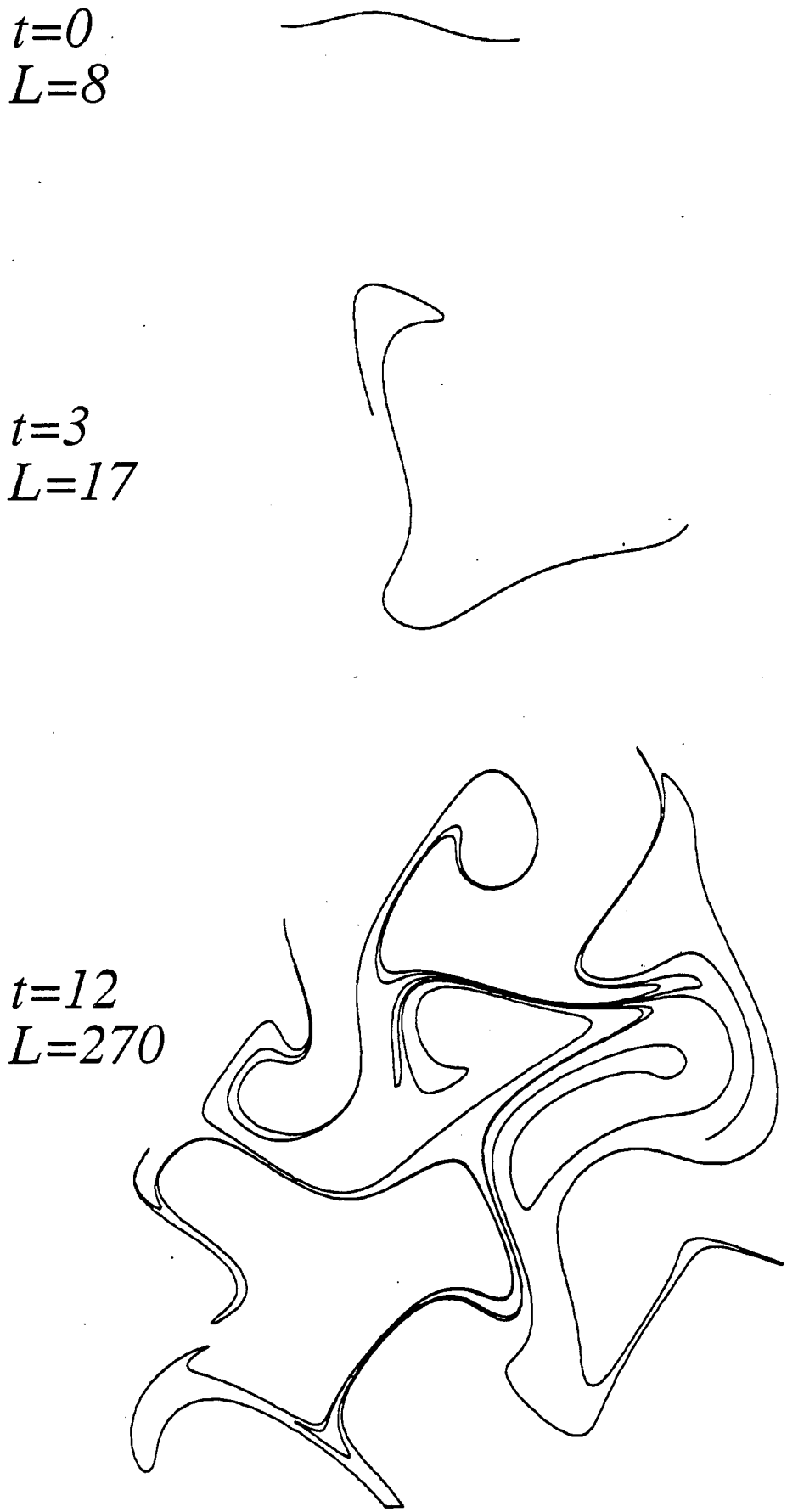

Fig. 25(b)

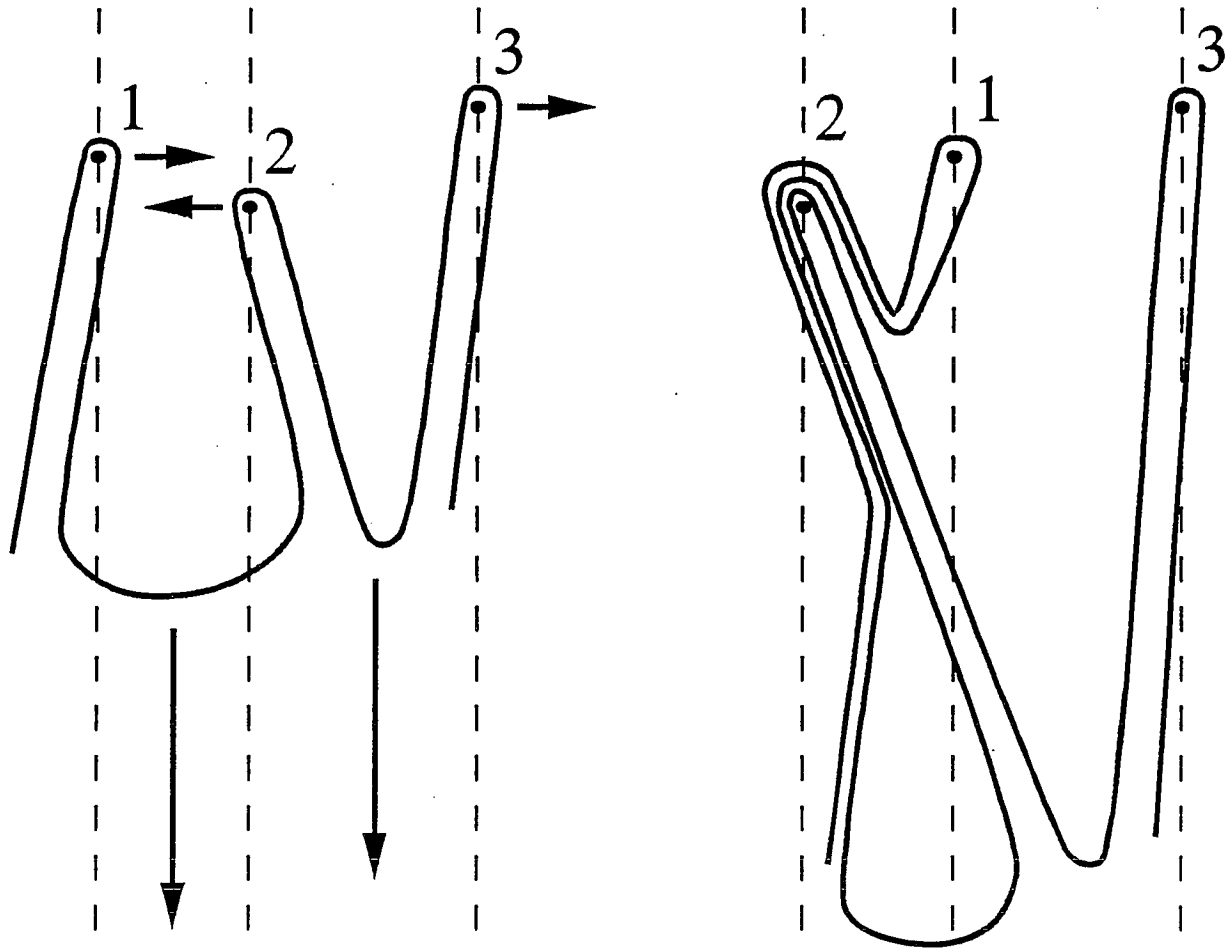

Fig. 26

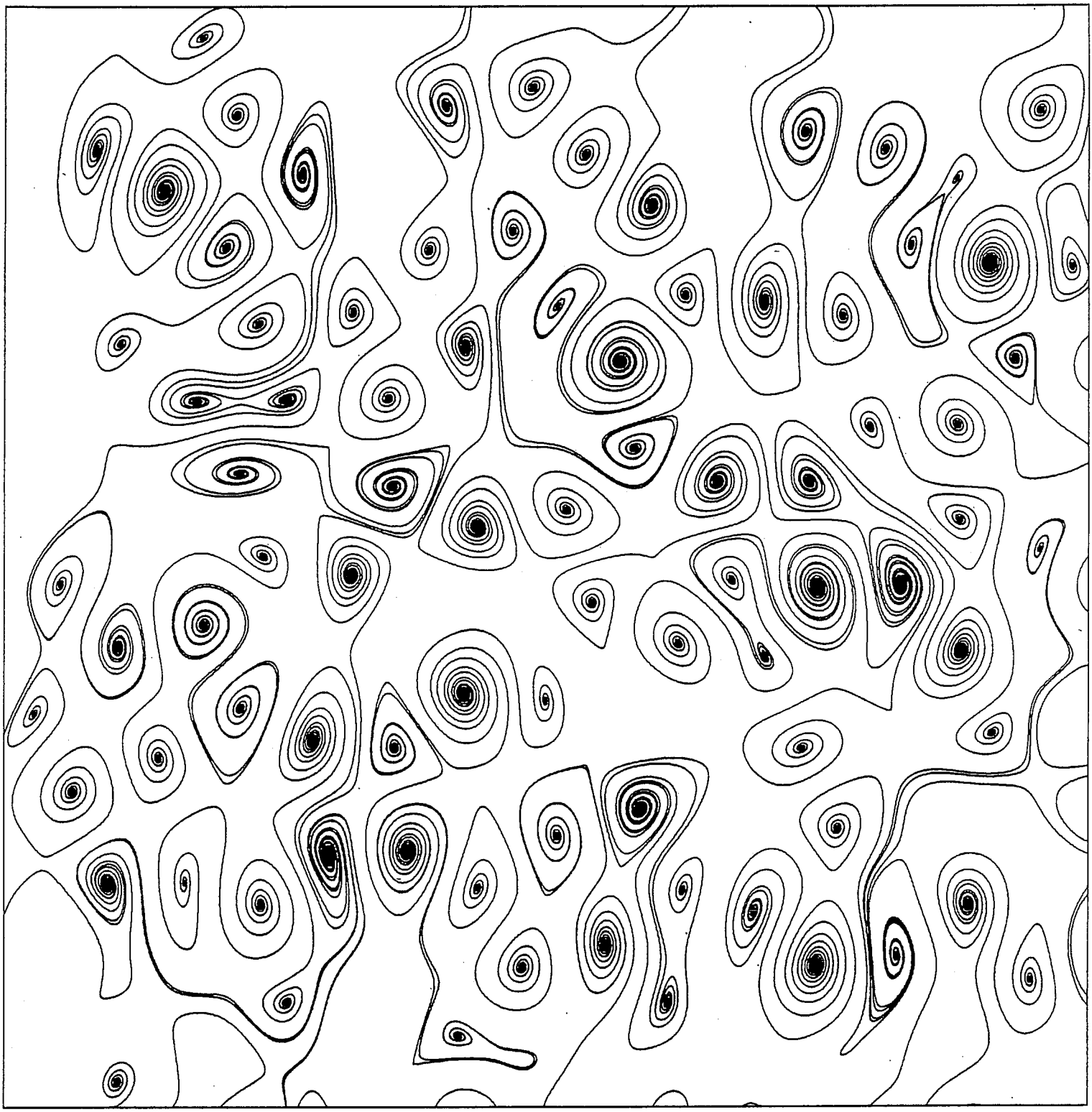

Fig. 27

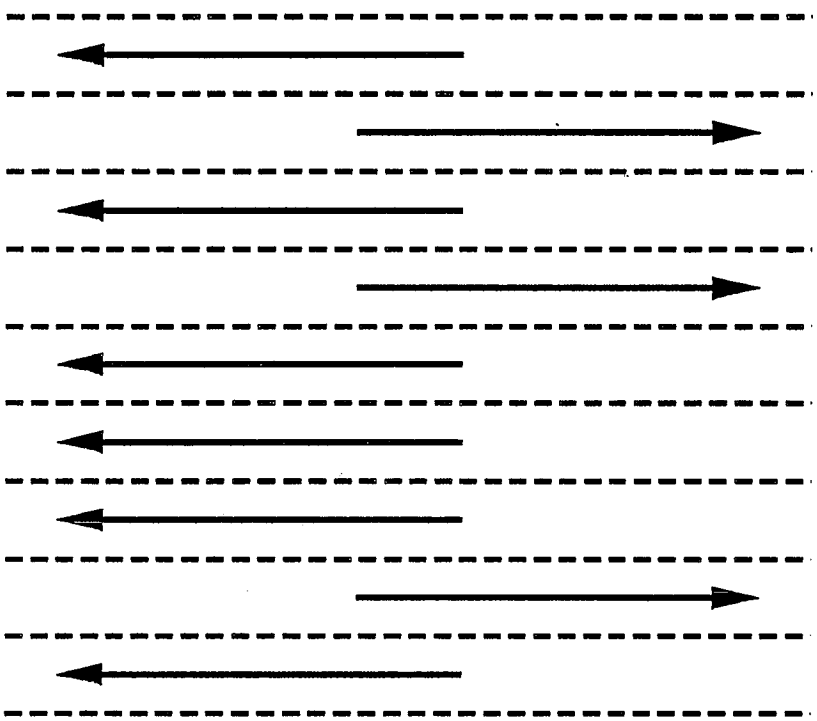

Fig. 28

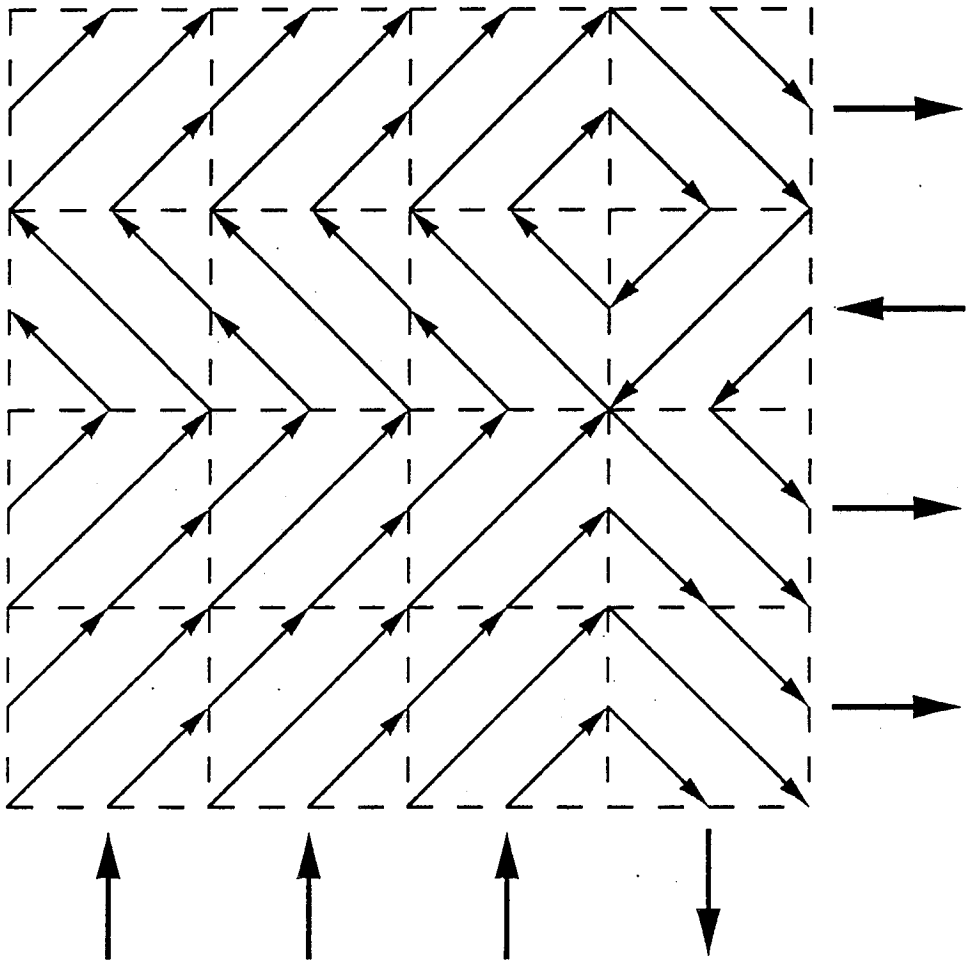

Fig. 29

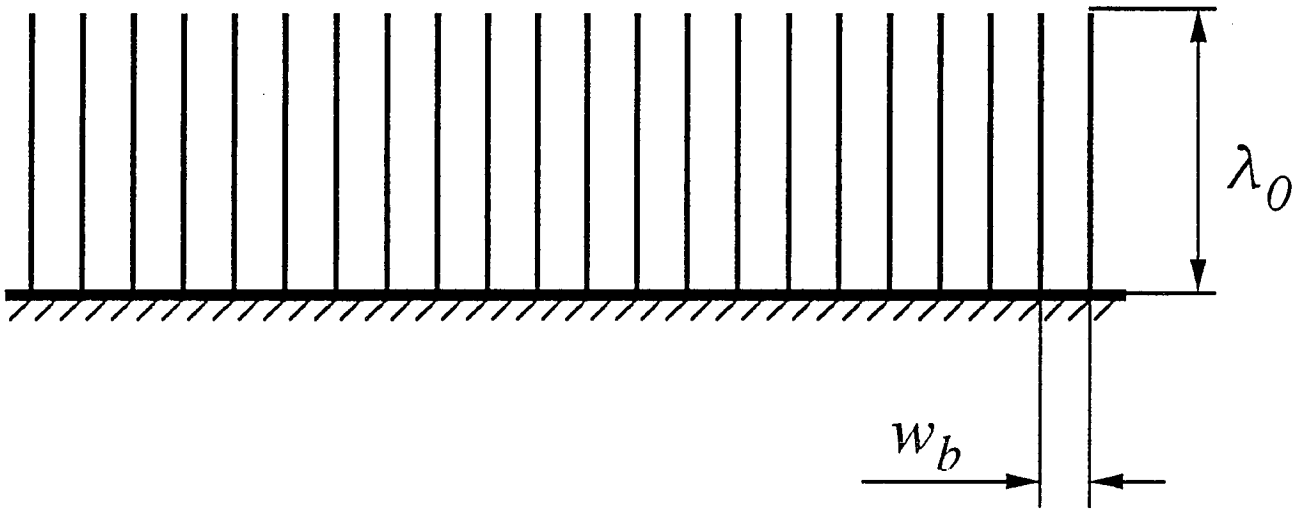

Fig. 30

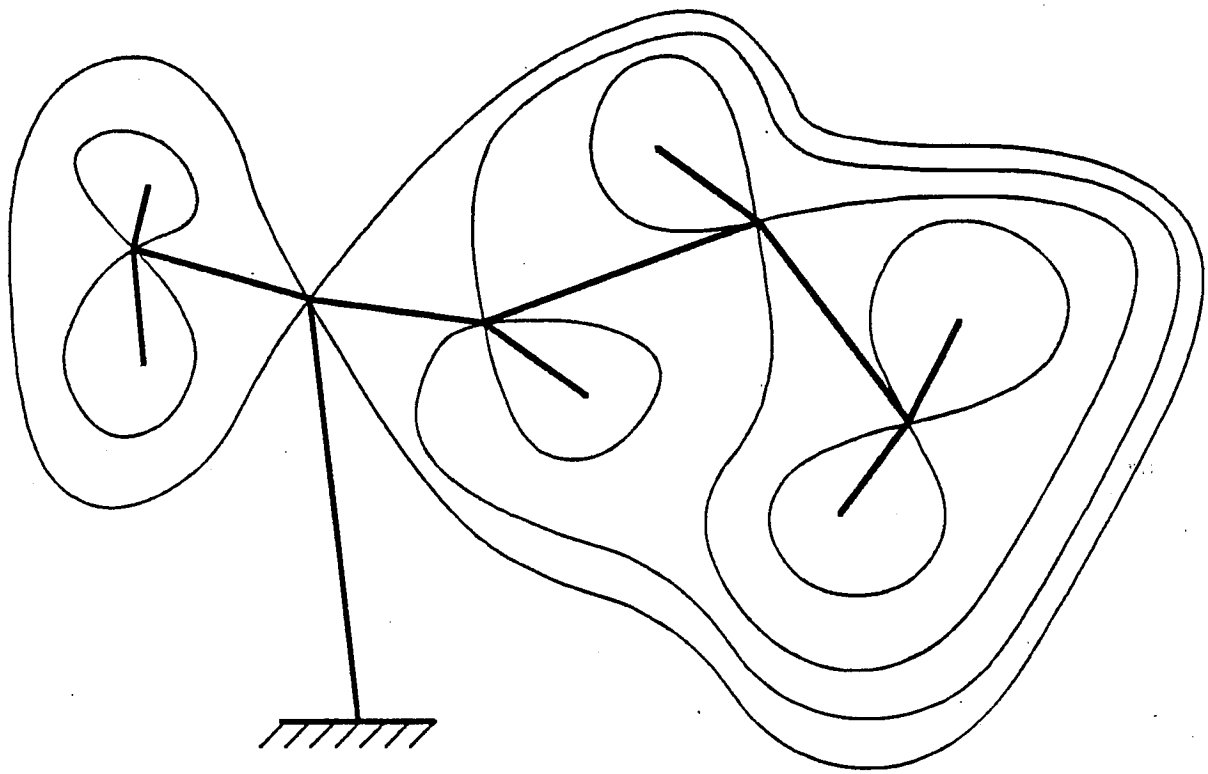

Fig. 31

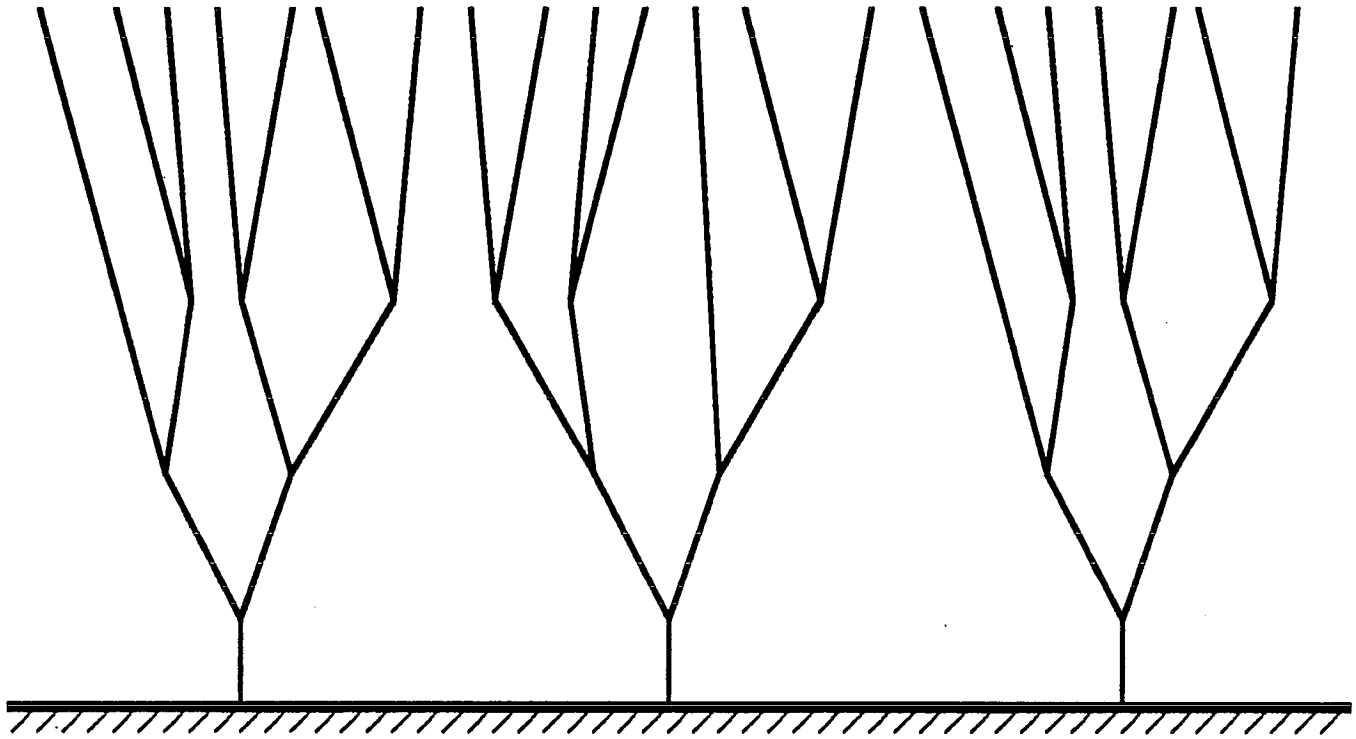

Fig. 32

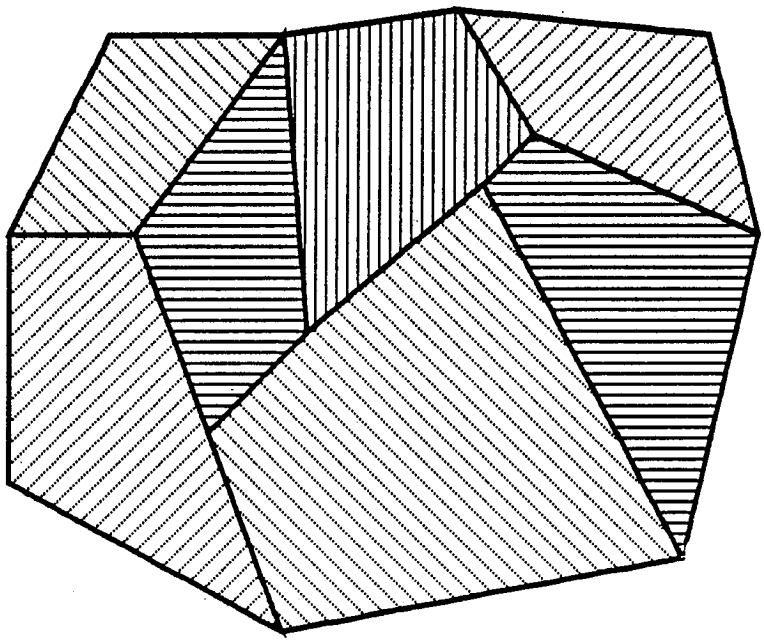

Fig. 33

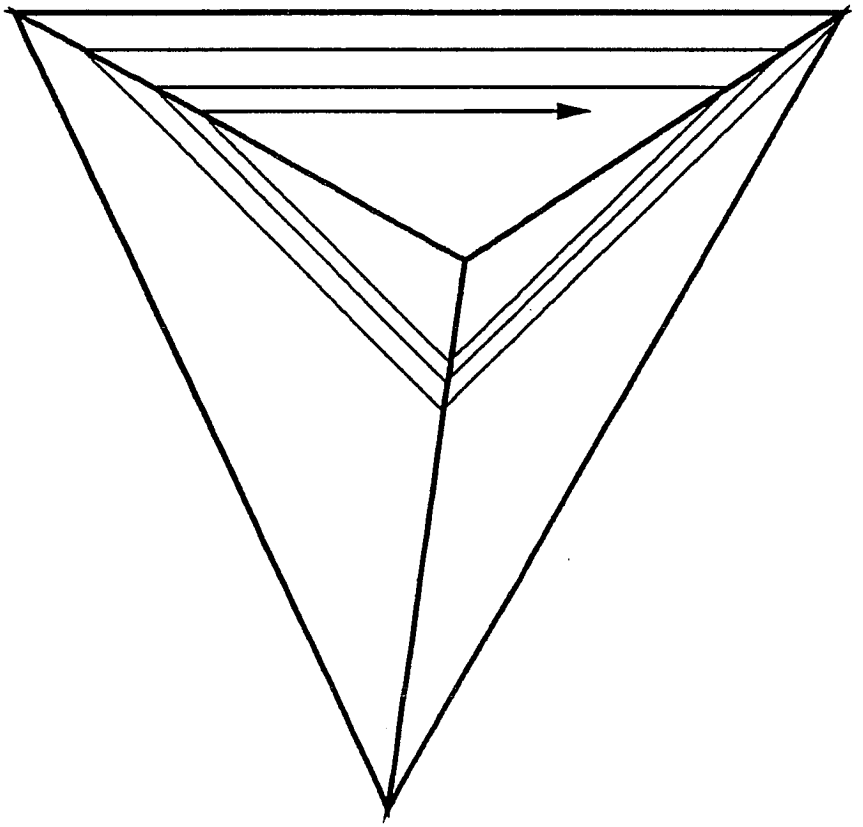

a

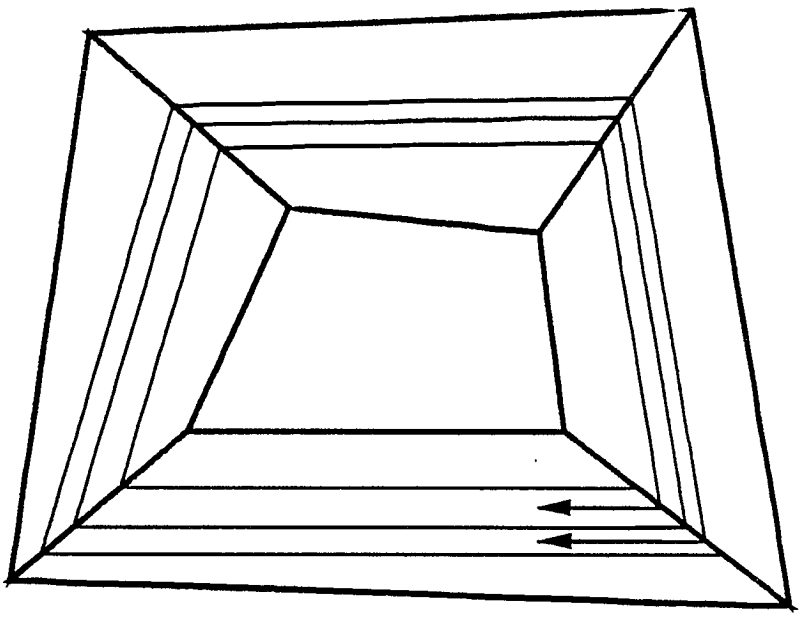

b

Fig. 34

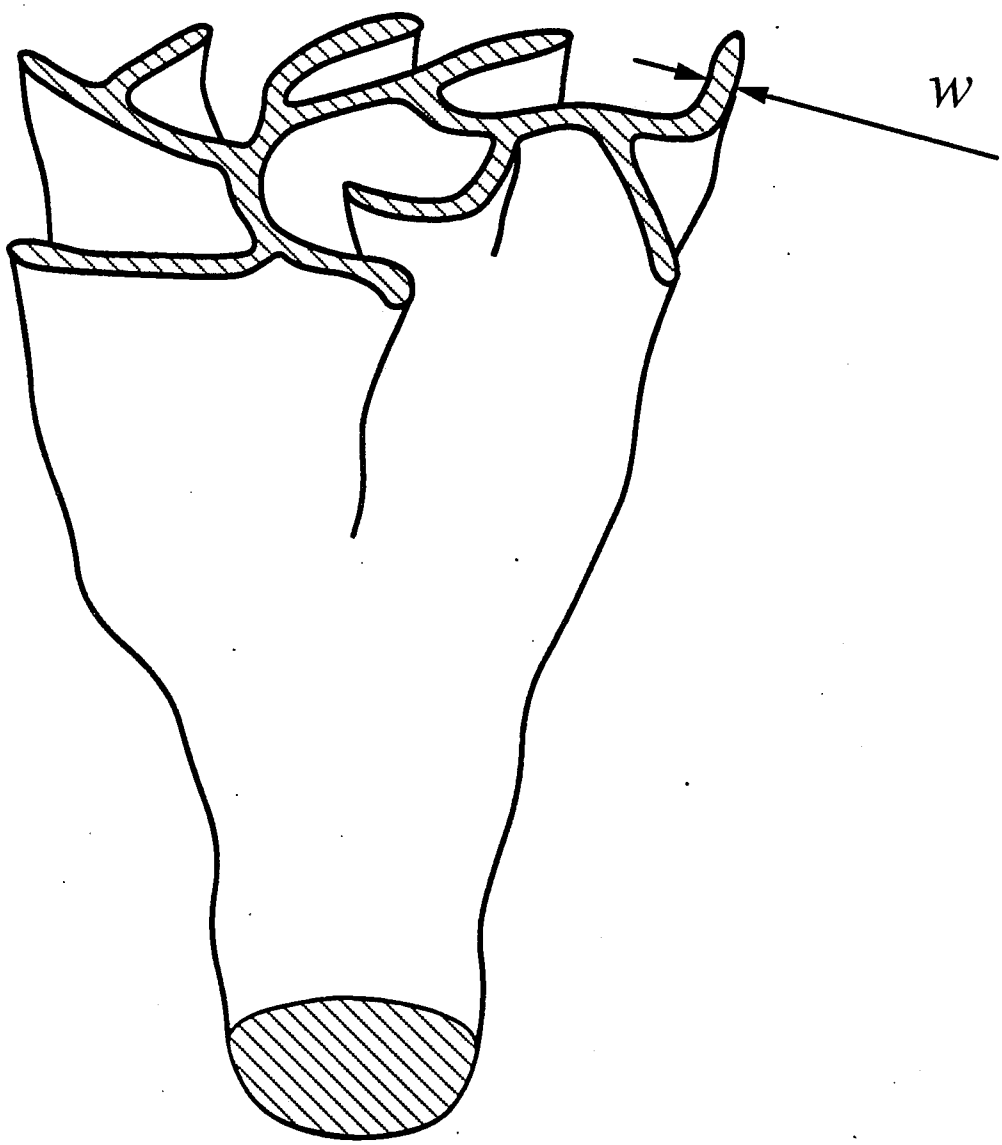

Fig. 35

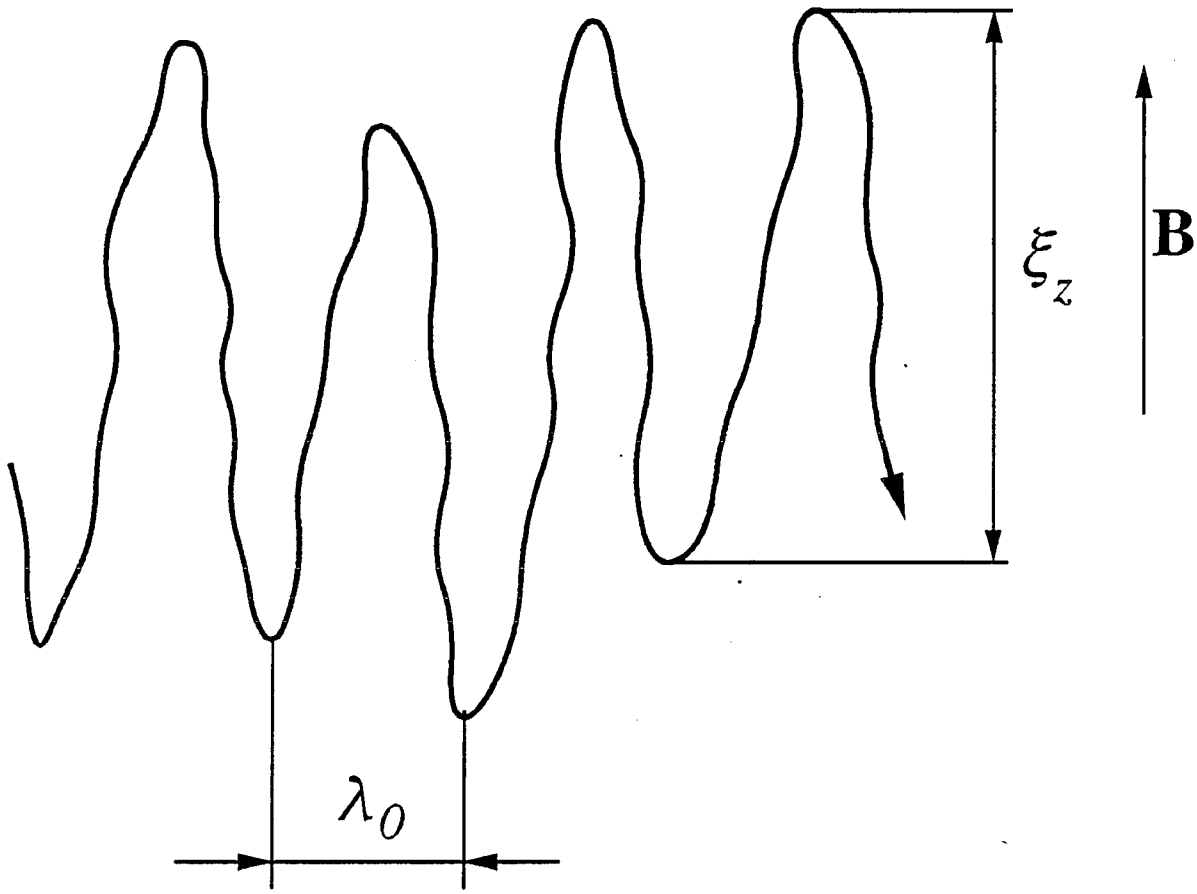

Fig. 36

TABLE I. Fractal dimensions and scaling ranges of some geometrical sets

Object	Fractal dimension	Scaling range	Section
Fractional Brownian hypersurface* $\{\mathbf{x}, B_H(\mathbf{x})\}$ in a $(d+1)$-space, $\langle (B_H(\mathbf{x}_1) - B_H(\mathbf{x}_2))^2 \rangle^{1/2} = b\,\lvert\mathbf{x}_1 - \mathbf{x}_2\rvert^H$, $0 < H < 1$	$d+1-H$ d	$[0, b^{1/(1-H)}]$ $[b^{1/(1-H)}, \infty]$	III.B
Zero-set of the fractional Brownian function: $\{\mathbf{x}\colon\ B_H(\mathbf{x}) = 0\}$	$d-H$	$[0, \infty]$	III.B
Connected piece of the above isoset with the diameter a	$\begin{cases} (10-3H)/7, & d=2 \\ d-H, & d \geq 3 \end{cases}$	$[0, a]$	III.E
Fractional Brownian trail $\{\mathbf{x}(t) = \mathbf{B}_H(t)\}$ in d dimensions	$\min(1/H, d)$	$[0, \infty]$	III.B
Connected contour piece (diameter a) of a monoscale (λ_0) random potential	$7/4$	$[\lambda_0, a]$	III.C
Finite percolation cluster (size $a \gg \lambda_0$) on a lattice with the period λ_0 in d dimensions	$d - \frac{\beta}{\nu} = \begin{cases} 91/48, & d=2 \\ \simeq 2.50, & d=3 \end{cases}$	$[\lambda_0, a]$	II.A

TABLE I (continued)

Object	Fractal dimension	Scaling range	Section
Infinite cluster near the percolation threshold with the correlation length $\xi \gg \lambda_0$	$d - \beta/\nu$ d	$[\lambda_0, \xi]$ $[\xi, \infty]$	II.A
Backbone of an infinite cluster	$\simeq \begin{cases} 1.6, & d = 2 \\ 1.7, & d = 3 \end{cases}$	$[\lambda_0, \xi]$	II.A
External hull of a finite percolation cluster	$\begin{cases} 7/4, & d = 2 \\ d - \beta/\nu, & d \geq 3 \end{cases}$	$[\lambda_0, a]$	II.A
Red bonds of an incipient ($\xi = \infty$) infinite cluster	$1/\nu$	$[\lambda_0, \infty]$	II.A
Unclosed self-avoiding random walk (SAW) on a 2D lattice with the period λ_0	$4/3$	$[\lambda_0, \infty]$	II.A
Unclosed smart kinetic walk (SKW) on the same lattice	$7/4$	$[\lambda_0, \infty]$	II.A
Correlated percolation cluster ($-1/\nu < H < 0$) with the diameter a	$d + \beta H$	$[\lambda_0, a]$	II.D
External hull of a correlated percolation cluster ($-1/\nu < H < 0$)	$\begin{cases} (10 - 3H)/7, & d = 2 \\ d + \beta H\ , & d \geq 3 \end{cases}$	$[\lambda_0, a]$	II.D
Chaotic attractor (size a) of a three-dimensional dynamical system with Lyapunov exponents $-\Lambda_3 > \Lambda_1 > \Lambda_2 = 0$	$2 + \Lambda_1/\lvert\Lambda_3\rvert$	$[0, a]$	I.B, IV.B.2

* Self-affine fractal. The box-counting dimension is shown.

TABLE II. Percolation thresholds for some lattices

d	Lattice	Bond	Site
2	Square	$0.50^{1(a)}$ $1/2^{3(c)}$ $0.499 \pm 0.004^{4(b)}$ $0.499^{6(b)}$	$0.590 \pm 0.010^{2(a)}$ $0.591 \pm 0.005^{4(b)}$ $0.53 \pm 0.002^{5(a)}$ $0.5927 \pm 0.00003^{7(b)}$ $0.59273(6)^{8(b)}$
	Triangular	$0.33^{1(a)}$ $2\sin(\pi/18) = 0.347296^{3(c)}$	$1/2^{3(c)}$ $0.500 \pm 0.005^{4(b)}$
	Honeycomb	$0.66^{1(a)}$ $1 - 2\sin(\pi/18) = 0.6527014^{3(c)}$	$0.70 \pm 0.01^{2(a)}$ $0.697 \pm 0.004^{4(b)}$ $0.698 \pm 0.003^{5(a)}$
3	Simple Cubic	$0.24^{1(a)}$ $0.247 \pm 0.005^{2(a)}$ $0.248 \pm 0.001^{9(b)}$ $0.2479 \pm 0004^{11(a)}$ $0.2488 \pm 0.0002^{12(a)}$	$0.307 \pm 0.010^{2(a)}$ $0.320 \pm 0.004^{4(b)}$ $0.318 \pm 0.002^{10(b)}$ $0.3117 \pm 0.0003^{9,13(b),11(a)}$
	Body-Centered Cubic	$0.178 \pm 0.005^{2(a)}$ $0.1795 \pm 0.0003^{11(a)}$ $0.18025 \pm 0.00015^{12(a)}$	$0.243 \pm 0.010^{2(a)}$ $0.254 \pm 0.004^{4(b)}$ $0.2464 \pm 0.0007^{11(a)}$
	Face-Centered Cubic	$0.119 \pm 0.002^{2(a)}$ $0.1190 \pm 0.0005^{14(a)}$ $0.1198 \pm 0.0003^{11(a)}$	$0.195 \pm 0.005^{2(a)}$ $0.208 \pm 0.0035^{4(b)}$ $0.1998 \pm 0.0006^{11(a)}$
	Diamond	$0.388 \pm 0.05^{2(a)}$ $0.3886 \pm 0.0005^{11(a)}$	$0.425 \pm 0.012^{2(a)}$ $0.4299 \pm 0.0008^{11(a)}$

TABLE II (continued)

[1] Domb and Sykes (1960)
[2] Sykes and Essam (1964a)
[3] Sykes and Essam (1963,1964b)
[4] Dean and Bird (1967)
[5] Sykes *et al.* (1976a, 1976b, 1976c)
[6] Fogelholm (1980)
[7] Ziff (1986)
[8] Kertész (1986)
[9] Heermann and Stauffer (1981)
[10] Onizuka (1975)
[11] Gaunt and Sykes (1983)
[12] Adler *et al.* (1990)
[13] Kertész *et al.* (1982)
[14] Dunn *et al.* (1975)

(*a*) From series expansion
(*b*) Monte Carlo simulation
(*c*) Exact

TABLE III. Percolation critical exponents

Exponent	$d = 2$	$d = 3$
$\alpha = 2 - \nu d$	$-2/3$[d,e]	-0.64 ± 0.05[4(a)]
β	$5/36 = 0.13888$[1,2,3(d)] 0.15 ± 0.03[5(e)] 0.138 ± 0.007[6(a)] 0.14 ± 0.02[8(c)]	0.39 ± 0.07[5(e)] 0.454 ± 0.008[4(a)] 0.45 ± 0.2[7(c)] 0.43 ± 0.04[9(b)] 0.405 ± 0.025[10(a)]
$\gamma = \nu d - 2\beta$	$43/18 = 2.3888$[1,2,3(d)] 2.38 ± 0.02[5(a)] 2.43 ± 0.03[6(a)] 2.43 ± 0.04[8(c)] 2.39 ± 0.02[11(c)]	1.70 ± 0.11[5(a)] 1.73 ± 0.03[4(a)] 1.63 ± 0.2[7(c)] 1.91 ± 0.01[11(c)] 1.805 ± 0.02[10(a)] 1.77 ± 0.02[12(b)]
$\delta = \nu d/\beta - 1$	$91/5 = 18.2$[d,e]	4.81 ± 0.14[4(e)]
ν	$4/3$[1,2,3(d)] 1.34 ± 0.02[5(a)] 1.343 ± 0.019[8(c)] 1.33 ± 0.07[15(c)] 1.35 ± 0.03[14(b)] 1.35 ± 0.06[16(b)] $1.3330(7)$[17(b)]	0.82 ± 0.05[5(a)] 0.89 ± 0.01[13(b)] 0.91 ± 0.08[14(b)] 0.88 ± 0.02[4(e)] 0.94 ± 0.02[7(c)] 0.88 ± 0.05[9(b)] 0.905 ± 0.023[10(e)]
μ	1.25 ± 0.05[18(b)] 1.10 ± 0.05[18(b)] 1.30[21(f)] 1.25 ± 0.1[23(f)] 1.28 ± 0.03[24(b)] 1.27 ± 0.04[25(b)] 1.31 ± 0.04[26(b)] 1.22 ± 0.08[16(b)] 1.24 ± 0.05[27(b)] 1.32 ± 0.05[27(c)]	1.6 ± 0.1[19(b)] 1.725 ± 0.005[20(b)] 1.4[22(c)] 1.70 ± 0.05[18(b)] 1.75 ± 0.1[18(b)] 1.50 ± 0.10[23(f)] 1.95 ± 0.1[27(b)] 2.46 ± 0.1[27(c)]

TABLE III (continued)

Exponent	$d = 2$	$d = 3$
$\tau = (2\nu d - \beta)/(\nu d - \beta)$	$187/91 = 2.0549$[d,e] 2.0 ± 0.1[8(c)]	2.19 ± 0.01[12(b)]
$d_c = d - \beta/\nu$	$91/48 = 1.89583$[d,e] 1.88 ± 0.02[28(b)] $91/48 \pm 1\%$[29(b)]	2.484 ± 0.012[4(e)] 2.51 ± 0.025[9(b)] 2.5 ± 0.05[30(b)] 2.529 ± 0.016[12(b)] 2.49[29(b)]
d_h	$7/4 = 1.75$[31(d)] 1.75 ± 0.05[33(b)] 1.74 ± 0.02[34,35(b)] 1.76 ± 0.01[34(b)] 1.751 ± 0.002[36(b)] 1.750 ± 0.002[37(b)]	$d_h = d_c$[32,30,12(d)] 2.548 ± 0.014[12(b)]
d_b	1.60 ± 0.05[38(b)] 1.62 ± 0.02[39,28(b)] 1.61 ± 0.01[40(b)]	1.77 ± 0.07[38(b)] 1.74 ± 0.04[39(b)]
$d_{rb} = 1/\nu$[41]	$d_{rb} = 3/4$[(d)] 0.75 ± 0.01[28(b)] 0.75 ± 0.07[42(b)]	
$d_{\min}$	1.18 ± 0.08[43(b)] 1.17 ± 0.015[42(b)] 1.10 ± 0.05[38(b)] 1.132 ± 0.003[45(b)] 1.021 ± 0.005[44(b)] 1.15 ± 0.02[40(b)]	1.35 ± 0.05[38(b)] 1.26 ± 0.06[44(b)]

TABLE III (continued)

[1] den Nijs (1979)
[2] Pearson (1980)
[3] Nienhuis (1982)
[4] Gaunt and Sykes (1983)
[5] Dunn *et al.* (1975)
[6] Sykes *et al.* (1976a,1976b,1976c)
[7] Elan *et al.* (1984)
[8] Gawlinski and Stanley (1977)
[9] Grassberger (1986a)
[10] Adler *et al.* (1990)
[11] Lee (1990)
[12] Strenski *et al.* (1991)
[13] Heermann and Stauffer (1981)
[14] Kertész *et al.* (1982)
[15] Vicsek and Kertész (1981)
[16] Mitescu *et al.* (1982)
[17] Kertész (1986)
[18] Straley (1977)
[19] Kirkpatrick (1973)
[20] Onizuka (1975)
[21] Smith and Lobb (1979)
[22] Webman *et al.* (1976)
[23] Clerc *et al.* (1980)
[24] Derrida and Vannimenus (1982)
[25] Li and Strieder (1982)
[26] Fogelholm (1980)
[27] Murat *et al.* (1986)
[28] Nagatani (1986)
[29] Margolina *et al.* (1982)
[30] Gouyet *et al.* (1988)
[31] Saleur and Duplantier (1987)
[32] Stauffer (1979)
[33] MacKay and Jan (1984)
[34] Voss (1984)
[35] Grossman and Aharony (1986)
[36] Ziff (1986)
[37] Grassberger (1986b)
[38] Herrmann *et al.* (1984)
[39] Herrmann and Stanley (1984)
[40] Laidlaw *et al.* (1987)
[41] Coniglio (1981)
[42] Pike and Stanley (1981)
[43] Alexandrowicz (1980)
[44] Edwards and Kerstein (1985)
[45] Grassberger (1985)

(*a*) From series expansion
(*b*) Monte Carlo lattice simulation
(*c*) Monte Carlo continuum simulation
(*d*) Exact
(*e*) From scaling relations
(*f*) Experiment

TABLE IV. Exactly known fractal dimensions of 2D objects and their correspondence to the conformal series

Object	Fractal dimension= $(100 - x^2)/48$	x
Percolation cluster	$91/48$[1]	3
Hull	$7/4$[2]	4
SKW	$7/4$[3]	4
Unscreened perimeter	$4/3$[4,2,5]	6
SAW	$4/3$[6]	6
Red bonds	$3/4$[7]	8

(1) Kapitulnik *et al.* (1984)
(2) Saleur and Duplantier (1987)
(3) Weinrib and Trugman (1985)
(4) Grossman and Aharony (1986,1987)
(5) Duplantier and Saleur (1987)
(6) Nienhuis (1982)
(7) Coniglio (1981)

TABLE V. Critical exponents of correlated percolation $(-1/\nu < H < 0)$

Exponent	$d = 2$	$d = 3$
$\tilde{\beta}$	$\beta = 5/36$	$\beta \simeq 0.4$
$\tilde{\nu}$	$-1/H$	$-1/H$
$\tilde{d}_h$	$(10 - 3H)/7$	$d - \tilde{\beta}/\tilde{\nu} = 3 + \beta H$